University of Zagreb

Faculty of Science

Department of Biology

Katarina Matković

IMPACT OF AIR POLLUTION ON BIOMARKERS OF EXPOSURE AND EFFECT IN HUMANS

DOCTORAL THESIS

Zagreb, 2025

University of Zagreb

Faculty of Science

Department of Biology

Katarina Matković

IMPACT OF AIR POLLUTION ON BIOMARKERS OF EXPOSURE AND EFFECT IN HUMANS

DOCTORAL THESIS

Mentor: Marko Gerić, PhD

Zagreb, 2025

Sveučilište u Zagrebu

Prirodoslovno-matematički fakultet

Biološki odsjek

Katarina Matković

UTJECAJ ONEČIŠĆENJA ZRAKA NA BIOMARKERE IZLOŽENOSTI I UČINKA KOD LJUDI

DOKTORSKI RAD

Mentor: dr. sc. Marko Gerić

Zagreb, 2025.

This doctoral thesis was conducted at the Institute for Medical Research and Occupational Health, under the supervision of Marko Gerić, PhD, Senior Scientific Associate, as part of the University Postgraduate Doctoral Study Program in Biology at the Department of Biology, Faculty of Science, University of Zagreb.

INFORMATION ABOUT THE MENTOR

Marko Gerić, PhD, has been employed at the Institute for Medical Research and Occupational Health since 2010, where he currently holds the position of Senior Scientific Associate. His academic training was completed at the Faculty of Science, University of Zagreb, with a bachelor's and master's degree in biology and a doctorate in natural sciences – biology. Over the course of his career, his research has been focused on genotoxicology, oxidative stress, and human biomonitoring, with a strong emphasis on the toxicological effects of environmental pollutants, cytostatics, and metals.

More than 60 peer-reviewed scientific articles, four book chapters, and over 50 conference abstracts have been published under his authorship, with a Scopus *h*-index of 21. His scientific contributions have been recognized with multiple national and international awards, including the *National Science Award for Junior Researchers* and *the Early Career Award* from the European Environmental Mutagenesis and Genomics Society (EEMGS).

He has actively participated in numerous national and European research projects and has served as principal investigator and mentor on studies addressing the cytogenotoxic effects of air pollution. He has also contributed to the scientific community through his roles on editorial and organizational boards of international conferences and professional societies, including the EEMGS and the Croatian Radiation Protection Association (CRPA). His methodological expertise spans a wide range of cellular and molecular toxicology techniques, as well as advanced biomonitoring approaches.

ACKNOWLEDGMENTS

First and foremost, I would like to thank Marko, my mentor, for his continuous support, patience, and for always believing in me. I truly appreciate the freedom he gave me to find my own pace and direction, even when it may not have been the most straightforward route. His encouragement and guidance helped me navigate the many challenges along the way, and I'm grateful we faced them together.

I would also like to thank Goran Gajski, the project leader, whose ideas and input played a significant role in shaping this thesis. His help with publications, generous support in opening up new collaborations, and encouragement to present my work at conferences greatly enriched my experience and contributed to both my scientific and professional development. Special thanks go to Maja, our lab technician, for all her help with the experimental work. I am also very grateful to colleagues from the department—Vilena, Mirta, Nevenka, and Andreja—for their help and for always being there with advice, support, or just a kind word when it was needed.

I owe a heartfelt thank you to my office mate and dear friend Luka❁. Sharing an office during the intense writing period of a PhD is no small feat, and I couldn't have asked for a better person to go through it with. From shared frustrations to shared laughter (and even a few tears), he has been a huge emotional support and a true teammate—both in the lab and outside of it.

I would also like to thank our collaborators from Unisanté, especially Pascal Wild, for his expertise in statistics and his willingness to share knowledge so generously. I learned a great deal from him, and his support throughout the project was of great importance.

I'm deeply thankful to my friends who stood by me during this process. Special thanks to Paula, Dorotea, Marin, and Robi, who knew exactly what I was going through, having been through it themselves. And to my best friend Ivan—thank you for being by my side ever since high school and for always encouraging me to keep going, even when it got tough.

Finally, to my family—thank you for everything. To my mother, who inspired my love for science and whose example guided me through this journey, and to my father, who taught me to stay strong, stand up for myself, and never give up. Your support means more to me than words can say.

I would like to express my deepest gratitude to all the institutions and collaborators whose support and expertise have been invaluable to the successful completion of this thesis:

Unisanté – University Center for General Medicine and Public Health, Lausanne, Switzerland, for their contributions to cytogenetic analyses, particularly for providing me with training on the Metafer System. Also, to the Lausanne University Hospital (CHUV) for facilitating the quantification and analysis of polycyclic aromatic hydrocarbons (PAHs);

Genos Glycoscience Research Laboratory and the University of Zagreb, Faculty of Science, for facilitating DNA methylation analysis, which significantly informed the interpretation of molecular response patterns;

Teaching Institute of Public Health "Dr. Andrija Štampar" and the Zagreb City Office for Social Protection, Health, War Veterans and People with Disabilities, who provided access to high-resolution pollen data, essential for modeling allergenic exposure;

The University of Zagreb, Faculty of Pharmacy and Biochemistry, is acknowledged for its collaboration in the measurements and analysis of oxidative stress biomarkers, contributing to the oxidative stress assessment in the studied cohorts;

PW Statistical Consulting for their expertise in statistical methodology, model validation, and data interpretation, which ensured the analytical rigor of this study;

The National Institute of Biology, Ljubljana, Slovenia, for further Metafer System training;

Colleagues from the Division of Environmental Hygiene for providing air quality data.

The interdisciplinary and multi-institutional nature of this project has been vital to its scientific depth, and I am sincerely grateful to all partners for their dedicated contributions.

The research was carried out within the project "HUMNap – Air Pollution and Biomarkers of Effect in Humans," HrZZ-IP-2020-02-1192, funded by the Croatian Science Foundation. Additional financial support was provided by the European Regional Development Fund through the project "Research and Education Centre of Environmental Health and Radiation Protection" (KK.01.1.1.02.0007), and by the European Union – Next Generation EU through the projects BioMolTox and EnvironPollutHealth (Reg. no. 533-03-23-0006).

The work of doctoral student Katarina Matković was fully supported by the "Young researchers' career development project – training of doctoral students" of the Croatian Science Foundation. Any opinions, findings, and conclusions or recommendations expressed in this material are those of the author(s) and do not necessarily reflect the views of Croatian Science Foundation.

Sveučilište u Zagrebu
Prirodoslovno-matematički fakultet
Biološki odsjek

Doktorski rad

UTJECAJ ONEČIŠĆENJA ZRAKA NA BIOMARKERE IZLOŽENOSTI I UČINKA KOD LJUDI

KATARINA MATKOVIĆ

Institut za medicinska istraživanja i medicinu rada
Zagreb, Hrvatska

Složenost smjesa onečišćenja zraka u urbanim sredinama predstavlja izazov za procjenu njihovih kombiniranih bioloških učinaka. U ovom su istraživanju razine izloženosti onečišćenju zraka povezane s biomarkerima izloženosti i učinka u populaciji odraslih osoba grada Zagreba, uzorkovanih tijekom hladnije i toplije sezone. Kompozitni klasteri izloženosti onečišćenju zraka dobiveni su hijerarhijskim grupiranjem radi smanjenja dimenzionalnosti, dok je unutarnja izloženost procijenjena mjerenjem razina benzena, toluena, etilbenzena, ksilena, metabolita policikličkih aromatskih ugljikovodika te metala u krvi, plazmi ili urinu. Biomarkeri učinka uključivali su parametre oksidacijskog stresa, metilaciju FOXP3 gena, frakciju izdahnutog dušikovog oksida te citogenetičke i molekularno-biološke testove. Statistički značajne povezanosti utvrđene su između pojedinih klastera onečišćenja i oksidacijskih te imunoloških biomarkera. Citogenetički ishodi bili su snažnije povezani sa životnim stilom, demografskim karakteristikama te izloženošću metalima iz zraka, nego s onečišćenjem zraka unutar promatranog vremenskog okvira. Dobiveni rezultati naglašavaju vrijednost integriranih biomonitoring pristupa temeljenih na naprednim statističkim metodama u istraživanju urbane zdravstvene ekologije.

163 stranica, 38 slika, 6 tablica, 6 slika u prilogu, 351 literaturnih navoda, jezik izvornika engleski

Ključne riječi: onečišćenje zraka, biomonitoring, genotoksičnost, oksidacijski stres, FOXP3, klasteriranje, medijacijska analiza

Mentor: dr. sc. Marko Gerić, viši znanstveni suradnik

Ocjenjivači: prof. dr. sc. Mirjana Pavlica, Prirodoslovno-matematički fakultet, Sveučilišta u Zagrebu
izv. prof. dr. sc. Rosa Karlić, Prirodoslovno-matematički fakultet, Sveučilišta u Zagrebu
dr. sc. Nevenka Kopjar, znanstveni savjetnik u trajnom izboru, Institut za medicinska istraživanja i medicinu rada, Zagreb

University of Zagreb
Faculty of Science
Department of Biology

Doctoral thesis

IMPACT OF AIR POLLUTION ON BIOMARKERS OF EXPOSURE AND EFFECT IN HUMANS

KATARINA MATKOVIĆ
Institute for Medical Research and Occupational Health
Zagreb, Croatia

The complexity of urban air pollution mixtures poses a challenge for assessing their combined biological effects. In this study, air pollution levels were linked to exposure and effect biomarkers in a cohort of adults from the city of Zagreb, sampled during colder and warmer seasons. Composite air pollution exposure clusters were derived using hierarchical clustering to reduce dimensionality, and internal exposure was assessed through measurements of benzene, toluene, ethylbenzene, xylenes, polycyclic aromatic hydrocarbon metabolites, and metals in blood, plasma or urine. Effect biomarkers included oxidative stress parameters, FOXP3 gene methylation, fractional exhaled nitric oxide, as well as cytogenetic and molecular-biological assays. Statistically significant associations were observed between specific pollutant clusters and oxidative and immune biomarkers. Cytogenetic outcomes were more strongly associated with lifestyle, demographic and metal-related variables than with air pollution in observed time frames. These findings highlight the value of integrative, statistically guided biomonitoring approaches in urban environmental health research.

163 pages, 38 figures, 6 tables, 6 supplementary figures, 351 references, original in English

Keywords: Air pollution, Biomonitoring, Genotoxicity, Oxidative stress, FOXP3, Clustering, Mediation analysis

Supervisor: Senior Scientific Associate Marko Gerić, PhD

Reviewers: Full Professor Mirjana Pavlica, PhD, Faculty of Science, University of Zagreb
Associate Professor Rosa Karlić, PhD, Faculty of Science, University of Zagreb
Permanent Scientific Advisor Nevenka Kopjar, PhD, Institute for Medical Research and Occupational Health

TABLE OF CONTENTS

1. INTRODUCTION

Ambient air pollution remains one of the most pervasive environmental threats to human health. Pollutants such as particulate matter (PM), nitrogen dioxide (NO_2), ozone (O_3), volatile organic compounds (VOCs), and polycyclic aromatic hydrocarbons (PAHs) have been consistently linked to adverse health outcomes, including respiratory and cardiovascular disease, cancer, and neurodevelopmental impairment (de Bont et al., 2022; Låg et al., 2020; Lelieveld et al., 2023; Serafini et al., 2022). However, traditional epidemiological approaches often focus on end-stage clinical outcomes rather than the early biological processes that precede them. In response, research has increasingly shifted toward uncovering early biological effects—molecular and cellular alterations that occur before disease onset. These include oxidative stress pathways, DNA integrity, and epigenetic patterns, which serve as critical early indicators of environmental toxicity (Delfino et al., 2011; Kazensky et al., 2024; Lodovici and Bigagli, 2011; Prunicki et al., 2021). However, linking complex environmental exposures to early biological responses presents several methodological challenges. First, air pollution is not a single agent but a dynamic mixture of co-occurring pollutants that often vary by source, season, and spatial scale (Pehnec et al., 2020; Račić et al., 2025). Many of these pollutants are strongly correlated, complicating efforts to disentangle their individual contributions. Second, these complexities introduce substantial statistical challenges. Correlated exposures increase multicollinearity, reduce model stability, and limit the interpretability of single-pollutant associations. Moreover, subtle effects may be masked by noise, and traditional models are often not equipped to detect indirect or mediated relationships (Wang et al., 2020). Finally, exposure–response relationships may be modulated by a range of demographic, behavioral, and environmental factors, complicating interpretation.

Understanding how these diverse pollutants interact biologically requires an integrative approach that considers not only external exposures but also internal markers of exposure, physiological response, and early biological effects (Brucker et al., 2020). This is particularly relevant in urban settings, where individuals are exposed to complex combinations of pollutants from traffic, residential heating, and industrial activity—each with distinct chemical signatures and biological implications (Jakovljević et al., 2018; Piracha and Chaudhary, 2022). Although human biomonitoring (HBM) has significantly advanced the measurement of various biomarkers, comprehensive studies that integrate air pollution exposure with both exposure and effect

biomarkers using statistically robust frameworks remain limited. In particular, population-level biomonitoring studies have yet to fully leverage advanced statistical methods—such as clustering methods, composite score generation, and multivariate and mediation modeling—which offer powerful tools to address challenges like multicollinearity, variable redundancy, and indirect pathways of association.

1.1. Study Objectives

To address these limitations, this study was designed to integrate air pollution exposure monitoring with biomarker-based assessments in an urban cohort, sampled during two contrasting seasons. The study pursued the following core objectives:

1. Characterize exposure to ambient air pollution using clustering techniques
    - Capture temporal and seasonal structure in pollutant behavior.
    - Apply hierarchical clustering to ambient pollutant data to reduce dimensionality and define composite exposure clusters.
    - Examine the influence of meteorological parameters on pollutant cluster behavior to better understand environmental drivers of exposure.
2. Assess internal exposure using biomonitoring approaches
    - Measure internal levels of: benzene, toluene, ethylbenzene, and xylene (BTEX) in blood, PAH metabolites in urine, essential and toxic metals in blood and plasma.
    - Evaluate seasonal variation and pollutant-specific correlations between internal and external exposure.
3. Assess associations between exposure and early biological effect biomarkers
    - Measure biomarkers of:
        - Local airway inflammation,
        - Oxidative stress: panel of pro-oxidant products and antioxidant defense markers,
        - Genotoxicity: DNA damage and genomic instability.
    - Apply multivariate regression and mediation models to:
        - Identify associations between exposure and effect biomarkers,
        - Assess airway inflammation and oxidative stress scores as mediators,
        - Control for demographic, meteorological, and lifestyle confounders.

By integrating external pollutant profiles, internal exposure biomarkers, and biological effect markers within a statistically robust framework, this thesis provides a multidimensional view of how complex urban exposures influence early biological responses. Through the combined use of hierarchical clustering, composite score generation, and mediation modeling—still rarely applied in population-based biomonitoring—this work advances methodological and mechanistic understanding in environmental health and strengthens the link between exposure science and human risk assessment.

2. LITERATURE REVIEW

2.1 Air pollution

Air pollution is one of the largest environmental health risks in Europe and a significant global concern, affecting both human health and ecosystems. Although air pollution emissions have declined over the past two decades, leading to improved air quality, it remains a persistent threat. Between 2005 and 2022, deaths in the EU attributable to fine particulate matter ($PM_{2.5}$) decreased by 45%, bringing the EU closer to its goal of a 55% reduction by 2030, as outlined in the Zero Pollution Action Plan, a key component of the EU Green Deal (EEA, 2024). This broader strategy aims to minimize pollution's impact on health and the environment through stricter regulations and cleaner energy transitions (EU, 2021). Despite this progress, exposure to pollutants such as $PM_{2.5}$, O_3, and NO_2 at levels exceeding World Health Organization (WHO) recommendations was responsible for an estimated 239,000, 70,000, and 48,000 premature deaths, respectively, in 2022 (EEA 2024). Globally, the estimates are even more alarming, indicating that air pollution causes 8.34 million premature deaths annually (Lelieveld et al., 2023), with more than 90% of the world's population living in areas where air quality does not meet WHO standards (WHO, 2021). Over 50% of the global population resides in urban areas, where pollution levels are highest due to the extensive combustion of fossil fuels (EEA, 2021). In addition to human activities, natural factors such as humidity, temperature, seasonal variations, and geographical location influence the dispersion, transformation, and persistence of air pollutants in the atmosphere, ultimately shaping local air quality (Liu et al., 2020). Air pollution affects multiple human organ systems (Figure 1). One of the most significant health impacts is its negative effect on the respiratory system. Individuals chronically exposed to polluted air are at an increased risk of developing various respiratory diseases or exacerbating pre-existing conditions, including asthma, bronchitis, emphysema, and chronic obstructive pulmonary disease (COPD) (Liu et al., 2020). Additionally, long-term exposure to air pollution can increase the risk of cardiovascular diseases such as heart attack, stroke, high blood pressure, and arrhythmias (de Bont et al., 2022). According to WHO estimates, air pollution is responsible for approximately 29% of lung cancer deaths, 43% of COPD-related deaths, about 25% of deaths from ischemic heart disease, and 24% of stroke-related deaths (WHO 2024).

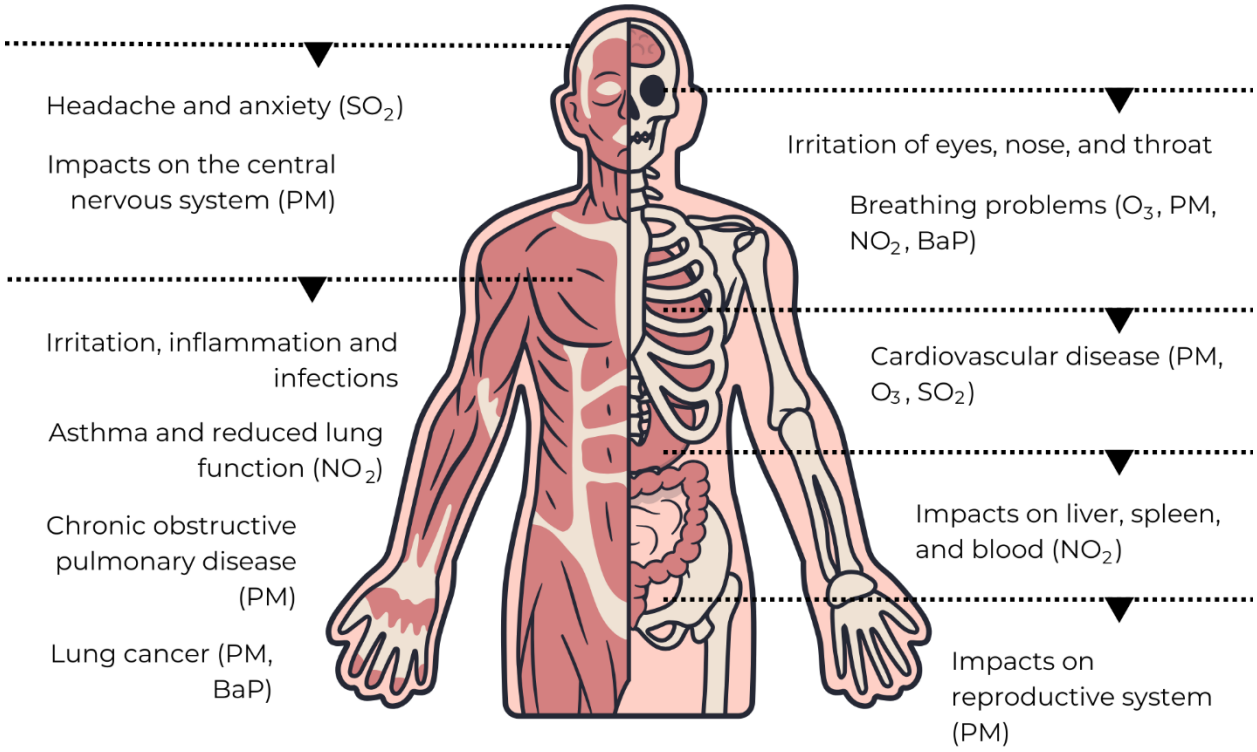

Figure 1. Health impacts of air pollution, highlighting key air pollutants associated with specific health outcomes. Particulate matter (PM) with a diameter of 2.5 µm or less ($PM_{2.5}$), particulate matter with a diameter of 10 µm or less (PM_{10}), ozone (O_3), nitrogen dioxide (NO_2), benzo[a]pyrene (BaP) and sulphur dioxide (SO_2). Adapted from EEA (2024).

Moreover, prolonged exposure to airborne pollutants can reduce life expectancy by an average of 2.9 years (2.3–3.5 years), which is approximately twice as high as earlier estimates and even exceeds the impact of tobacco smoking (Lelieveld et al., 2020). Air pollution impairs immune function primarily through oxidative stress and inflammation, as exposure to pollutants such as $PM_{2.5}$ and O_3 generates reactive oxygen species (ROS) that trigger inflammatory pathways, weaken host defenses, and increase susceptibility to infections and allergic diseases (Glencross et al., 2020; Lodovici and Bigagli, 2011; Serafini et al., 2022; Tuazon et al., 2022). Ural et al. (2022) have revealed that inhaled PM tends to accumulate in lung-draining lymph nodes, especially after the age of 40. There, the particles become sequestered in specific macrophage subsets located within T cell zones, leading to impaired T cell activation, reduced production of pro-inflammatory cytokines, and diminished phagocytic activity. This accumulation disrupts the normal structure and organization of the lymphoid tissue, essential for effective immune surveillance in the respiratory tract, underscoring the importance of maintaining optimal air quality to safeguard immune health

against both current and emerging pathogens. Furthermore, recent research suggests that long-term exposure to air pollution increases the risk of developing various types of cancer, including lung, throat, and bladder cancer (Chen et al., 2022; Turner et al., 2020; Wang et al., 2023b). Turner et al. (2020) reviewed multiple meta-analyses, which indicate that for every 10 μg/m³ increase in $PM_{2.5}$, lung cancer incidence or mortality rises by approximately 9% to 14%. Based on global exposure estimates, where the average population-weighted $PM_{2.5}$ concentration worldwide is around 46 $\mu g/m^3$ (compared to the WHO guideline of 10 $\mu g/m^3$), which corresponds to an estimated 60% increased risk of all-cause mortality. A similar analysis for PM_{10} reported an 8% increase in mortality risk per 10 $\mu g/m^3$ increment (Turner et al., 2020). Furthermore, data from the UK Biobank demonstrate that long-term exposure to ambient air pollutants (including NO, NO_2, $PM_{2.5}$, and PM_{10}) is associated with an elevated risk of laryngeal cancer. This association is particularly pronounced in individuals with pre-existing risk factors such as female sex, smoking, elevated systolic blood pressure (≥120 mmHg), diabetes, or higher genetic susceptibility (Wang et al., 2023b). Beyond its health effects, air pollution significantly impacts the economy by increasing healthcare costs, reducing life expectancy, and causing lost workdays across various sectors (EEA, 2023). Between 2014 and 2021, the annual economic burden of air pollution in the EU was estimated at €770 billion, equivalent to 6% of the EU's gross domestic product (GDP), aligning with previous estimates by the World Bank and the European Commission, which placed annual costs between €330 billion and €940 billion (European Commission, 2022; Mejino-López & Oliu-Barton, 2024). Taken together, the staggering health risks and economic burdens imposed by air pollution underscore the need for rigorous measures to reduce emissions and improve air quality, thereby safeguarding public health, supporting economic stability, and ensuring a sustainable future for all.

2.1.1. Particulate matter

Particulate matter (PM) consists of a heterogeneous mixture of solid and liquid particles suspended in the air, varying in chemical composition, morphology, and size. According to the U.S. Environmental Protection Agency (EPA), these particles can be grouped into two main categories. Coarse particles (PM_{10}) are those with diameters generally larger than 2.5 μm but smaller than or equal to 10 μm (with particles larger than 10 μm typically classified separately as large coarse particles). Fine particles ($PM_{2.5}$) are defined as particles with diameters of 2.5 μm or

less; this category also encompasses ultrafine particles and nanoparticles ($PM_{0.1}$), which are generally classified as having diameters less than 0.1 µm (US EPA) (Figure 2).

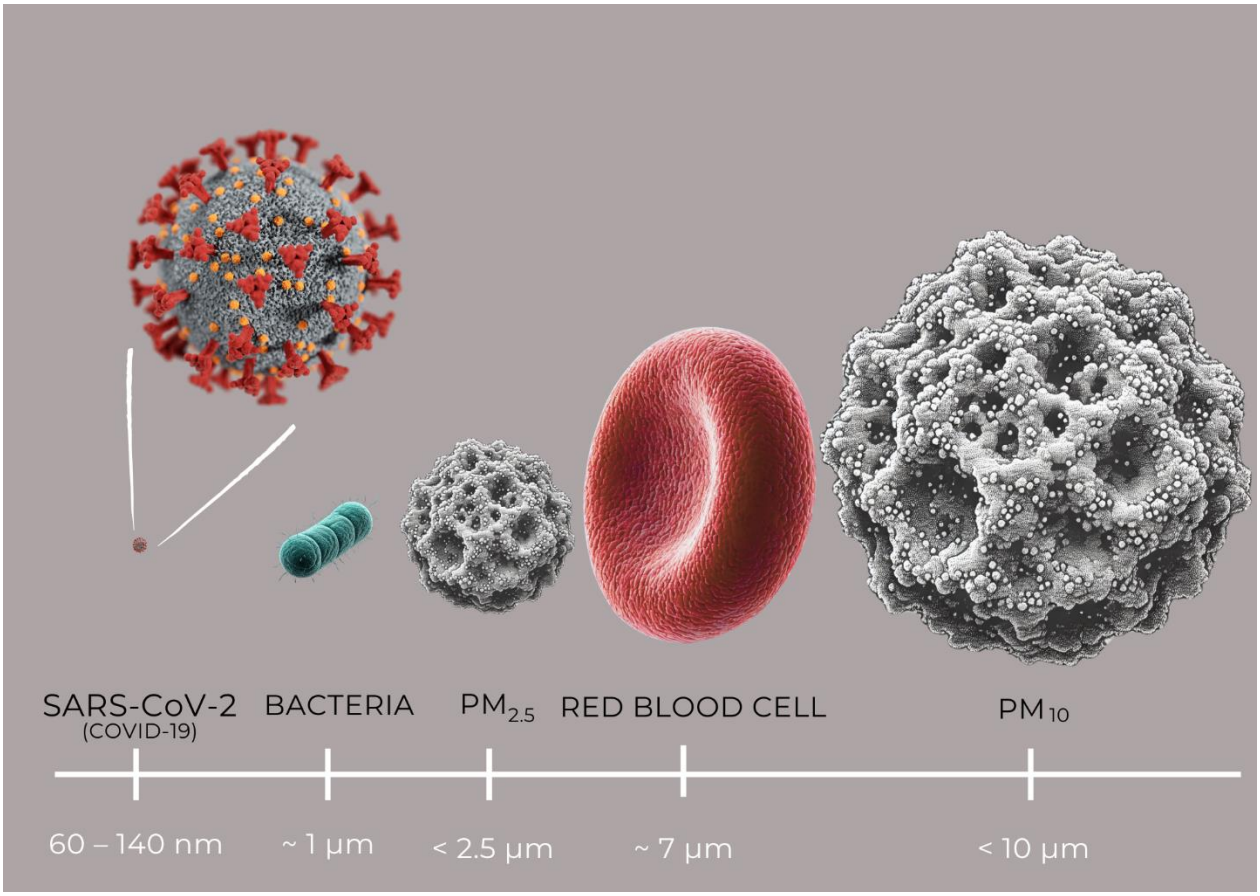

Figure 2. Size comparison for coarse particles (PM_{10}) and fine particles ($PM_{2.5}$) alongside representative sizes of eukaryotic cells, prokaryotic cells, and virus particles. Adapted from See the Air (2022).

PM originate from a range of sources, including industrial processes, traffic, household activities (such as heating and cooking), agriculture, as well as natural phenomena like soil erosion and volcanic eruptions. Their ability to penetrate biological tissues depends largely on their size. For instance, PM_{10} tend to deposit in the upper airways and are largely cleared via mucociliary mechanisms, though their soluble components can still interact with epithelial cells and elicit local biological responses (Misiukiewicz-Stepien and Paplinska-Goryca, 2021). In contrast, $PM_{2.5}$ and especially $PM_{0.1}$ are of particular concern because their small size enables them to evade the respiratory system's natural defense mechanisms. These particles can penetrate deep into the alveolar regions of the lungs and, in some cases, cross the alveolar-capillary barrier to enter the

bloodstream (Figure 3) (Agudelo-Castañeda et al., 2017; Jaafari et al., 2020; Thangavel et al., 2022). Acute exposure to elevated PM levels has been associated with acute respiratory and cardiovascular events—including asthma exacerbations, bronchitis, arrhythmias, and myocardial infarction—linked to immediate cellular stress responses (Thangavel et al., 2022). Chronic exposure to elevated levels of PM is especially concerning. For instance, long-term exposure to $PM_{2.5}$ concentrations exceeding WHO guideline thresholds, typically in the range of 5–10 μg/m³ annually, has been consistently linked to increased risks of respiratory, cardiovascular, and neoplastic diseases (Guo et al., 2023). These adverse outcomes are mediated by multiple mechanisms, including the generation of ROS, DNA damage, mitochondrial disruption, and impaired cellular repair processes (Shan et al., 2022; Wang et al., 2021b). Additionally, the metallic components of $PM_{2.5}$ have been associated with cellular deformation, inhibited proliferation, and further DNA damage, ultimately leading to cell cycle arrest or apoptosis (Dong et al., 2019). High concentrations of $PM_{2.5}$ have also been shown to affect genetic pathways in bronchial cells and peripheral blood samples, particularly those related to inflammation and immune responses (Corsini et al., 2009; Feng et al., 2016; Michael et al., 2013; Mostafavi et al., 2018). Nevertheless, emerging research indicates that even very low concentrations of PM can adversely affect human health, particularly with chronic exposure. Acute exposure at low concentrations may not result in overt clinical symptoms in healthy individuals; however, sensitive populations (e.g., children, the elderly, and those with preexisting respiratory or cardiovascular conditions) may still experience subtle respiratory irritation and transient declines in lung function (Aithal et al., 2023; Simoni et al., 2015; Wang et al., 2023d). Persistent low-level exposure—even at concentrations below former "acceptable" thresholds—can lead to subclinical inflammation, cumulative DNA damage, and gradual impairment of cardiovascular and pulmonary function. For instance, the revised WHO air quality guidelines now recommend an annual $PM_{2.5}$ mean of around 5 $\mu g/m^3$, reflecting mounting evidence that adverse health effects occur at lower exposures than previously recognized (Hoffmann et al., 2021). In fact, epidemiological studies have long demonstrated that even modest increases in PM concentrations are associated with measurable increases in mortality and morbidity. Study by Pope et al. (2002) and subsequent work by Brook et al. (2010) have linked long-term exposure to fine particles with heightened risks of cardiopulmonary diseases and lung cancer, even when exposure levels are relatively low. These findings underscore that there is essentially no "safe" threshold for PM exposure, as both acute high-level and chronic low-level

exposures contribute substantially to the global health burden. Notably, the International Agency for Research on Cancer (IARC) classifies outdoor air pollution, with PM as a major component, as carcinogenic to humans (Group 1). A comprehensive understanding of the health impacts and biological mechanisms of PM is crucial for establishing the theoretical foundation necessary for early prevention strategies and the identification of biomarkers for air pollution-related diseases. Furthermore, PM can act as a carrier for a variety of harmful substances and pollutants, including PAHs, toxic metals, organic compounds, sulfates, nitrates, as well as bacteria and allergens.

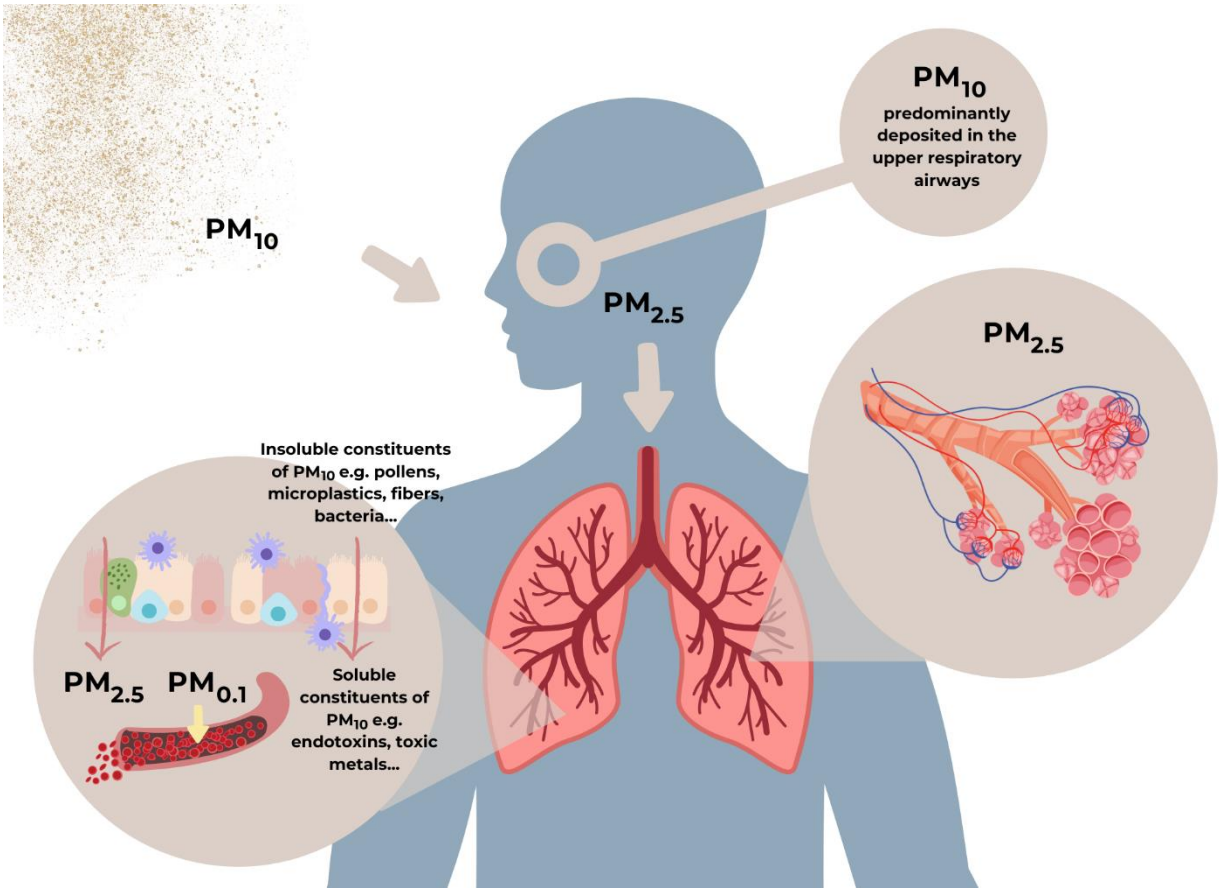

Figure 3. Schematic illustration of particulate matter (PM) translocation through the lung–blood barrier. The diagram classifies PM by aerodynamic diameter into three groups: $PM_{0.1}$ (particles ≤0.1 μm), $PM_{2.5}$ (particles <2.5 μm), and PM_{10} (particles <10 μm). It shows that while larger PM_{10} particles are predominantly deposited in the upper airways and cleared by mucociliary mechanisms, finer particles ($PM_{2.5}$ and $PM_{0.1}$) can reach the alveolar spaces. Once in the alveoli, these small particles may cross the alveolar epithelial layer and capillary endothelium, thereby entering systemic circulation. Adapted from Misiukiewicz-Stepien and Paplinska-Goryca (2021).

2.1.2. Polycyclic Aromatic Hydrocarbons

Polycyclic aromatic hydrocarbons (PAHs) are a complex mixture comprising more than 100 different organic compounds, each consisting of two or more aromatic rings (Figure 4). These compounds are ubiquitous environmental pollutants that originate from both natural and anthropogenic sources, predominantly from the incomplete combustion of organic materials such as coal, oil, and fuel (e.g., vehicle exhaust) as well as from biomass burning (wood, animal dung, etc.) (Patel et al., 2020; Peng et al., 2011). Exposure to PAHs can occur through ingestion, inhalation (mostly particle-bound PAHs), and dermal absorption, with the severity of toxic effects depending on both the duration of exposure and the received dose (Choi H et al., 2010; Tong et al., 2018). Regarding respiratory pathophysiology, inhalation of PAHs is associated with reduced lung function, exacerbation of asthma, and a higher incidence of COPD and cardiovascular conditions (Zhang et al., 2021a). Several studies have demonstrated a correlation between PAH exposure and the development of asthma, as well as an increase in asthmatic symptoms in children. For instance, PAHs such as benzo[a]pyrene (BaP) are metabolized by cytochrome P450 enzymes into reactive intermediates that can bind to DNA and form adducts, leading to measurable increases in biomarkers of DNA damage, such as 8-hydroxy-2′-deoxyguanosine (8-OHdG). This genotoxic stress not only triggers pro-inflammatory pathways but also contributes to airway remodeling and hyperresponsiveness, thereby heightening the risk and severity of asthma in children (Hu et al., 2021; Låg et al., 2020). WHO has underscored the need for additional epidemiological and experimental studies to fully clarify the potential impact of ambient PAH exposure on conditions such as asthma and other non-malignant respiratory diseases (WHO, 2021). Moreover, epidemiological studies, reviewed by Kelly et al. (2021) and recognized by WHO (2021), have consistently demonstrated that chronic PAH exposure is associated with higher incidences of lung, skin, and bladder cancers, thereby establishing the causal link between PAHs and increased cancer risk. The IARC and the IARC Monographs program (IARC, 2010) have evaluated experimental data on a total of 60 individual PAHs. Many of these compounds have been classified either as carcinogenic or as potential carcinogens and mutagens. Specifically, benzo[a]pyrene is classified as carcinogenic to humans (Group 1), while other PAHs—such as benzo[a]anthracene (BaA), dibenzo[a,h]anthracene (DahA), benzo[b]fluoranthene (BbF), benzo[j]fluoranthene (BjF), benzo[k]fluoranthene (BkF), and indeno[1,2,3-cd]pyrene (IP)—are classified as probably carcinogenic to humans (Group 2A) or possibly carcinogenic to humans (Group 2B). Other PAHs,

such as benzo[ghi]perylene (BghiP), cannot be classified (Group 3) due to insufficient evidence. The carcinogenic and mutagenic potential of PAHs and their metabolites primarily arises from their ability to bind to DNA and form adducts, which can lead to genotoxic and cytotoxic effects (Ewa and Danuta, 2017). Upon entering the human body, PAHs undergo metabolic activation primarily via cytochrome P450 enzymes (especially CYP1A1 and CYP1B1), forming hydroxylated metabolites (OH-PAHs). These are then conjugated with glucuronic acid or sulfate by phase II enzymes and excreted through urine. A variety of urinary PAH metabolites can be detected, including monohydroxy derivatives of phenanthrene, fluoranthene, pyrene, chrysene, and naphthalene. However, three metabolites—1-naphthol, 2-naphthol, and 1-hydroxypyrene (1-OHP)—are most frequently measured in human biomonitoring studies due to their relatively high excretion rates, analytical stability, and linkage to prevalent PAH sources. Specifically, 1- and 2-naphthol reflect exposure to naphthalene, while 1-OHP is a commonly used surrogate for overall PAH exposure, as pyrene is present in most PAH mixtures and strongly correlates with other carcinogenic PAHs (IARC, 2013; Meeker et al., 2007; Zhu et al., 2021).

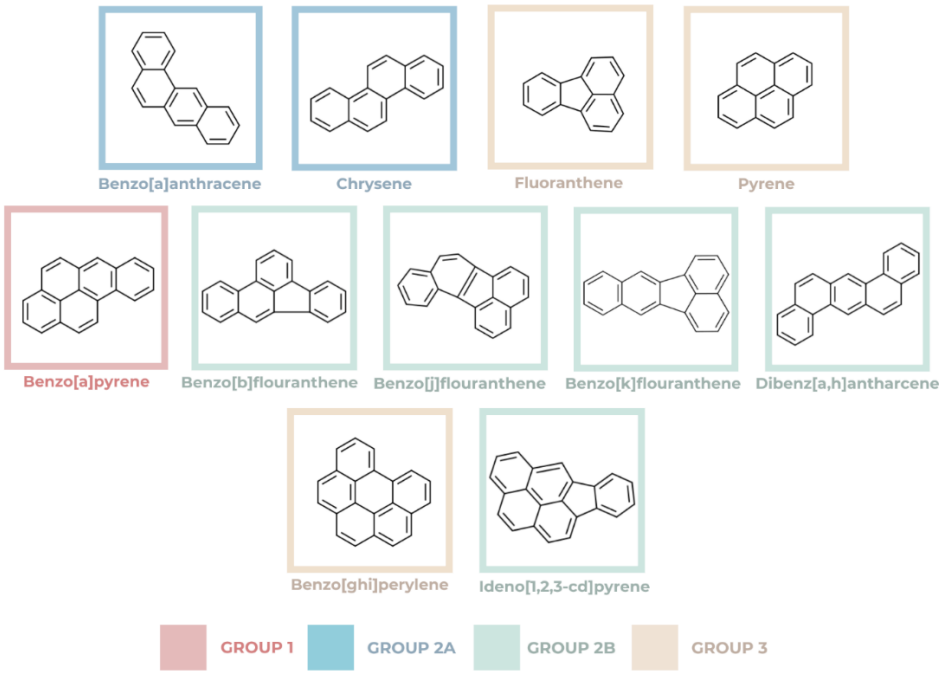

Figure 4. Structural formulas of selected polycyclic aromatic hydrocarbons (PAHs). This figure displays the structural formulas of 11 PAHs, present in the ambient air of Zagreb, chosen for their diverse number (4, 5 or 6) of aromatic rings. According to carcinogenic classifications by IARC, this selection includes Group 1 compounds (e.g., benzo[a]pyrene), as well as PAHs classified as Group 2A and 2B, and Group 3.

2.1.3. Toxic Metals

Exposure to toxic metals occurs primarily through the ingestion of contaminated food and water; however, inhalation of PM-bound metals also substantially contributes to the overall body burden, especially in urban environments (Guo et al., 2021). Toxic metals present in the air, such as Pb, Cd, As, Ni, Mn, Cu, and Fe, originate from diverse sources including industrial emissions, traffic-related pollution, waste incineration, and natural processes like soil dust resuspension and volcanic activity and have serious adverse effects on human health (Joshirvani et al., 2021; Pandey et al., 2013). Lead is commonly released from industrial processes, deteriorating lead-based paints, and the historical use of leaded gasoline. It can cause neurological disorders, kidney damage, and reproductive pathologies, posing a particular threat to children who are especially vulnerable to its effects (Gatzke-Kopp et al., 2021; Rasnick et al., 2021). Cadmium is primarily emitted from industrial operations, waste incineration, and contaminated soils. It accumulates in the kidneys and has been linked to renal diseases, osteoporosis, and various cancers (Genchi et al., 2020b; Qu and Zheng, 2024). Arsenic, which may be released from smelting operations as well as occurring naturally in groundwater and soils, is well known for its carcinogenic properties. It is associated with an increased risk of skin, lung, bladder, and liver cancers and is classified by the IARC as a Group 1 carcinogen (IARC, 2012; Speer et al., 2023). Nickel is emitted from industrial processes and fossil fuel combustion. It can trigger allergic reactions, exacerbate asthma, and elevate the risk of lung cancer. Certain nickel compounds are also classified as Group 1 carcinogens by IARC (Genchi et al., 2020a; IARC, 2012). Manganese is released mainly from mining activities and the combustion of fossil fuels. Although it is an essential trace element, higher exposures can cause neurotoxicity and damage the nervous system (Ávila et al., 2021; Cheng et al., 2023). Copper is an essential element that plays a critical role in antioxidant defense by serving as a cofactor for enzymes such as superoxide dismutase (SOD). However, at elevated concentrations—often originating from mining, smelting, brake wear, and corrosion of copper-containing infrastructure—copper can induce gastrointestinal distress and liver damage (Taylor et al., 2020). In fact, Pujol et al. (2016) reported that airborne copper exposure in school environments is associated with poorer motor skills and alterations in the basal ganglia in children. Iron, although vital for numerous physiological processes, can also be harmful when present in excess. Iron is abundant in urban dust and is released from industrial and construction activities; excess iron can lead to oxidative stress and has been linked to cardiovascular diseases (Li and Zhang, 2021; Morgan et al., 2020; Yan et

al., 2022). These metals are often bound to PM. Upon inhalation, they can enter the bloodstream, where they may induce oxidative stress, inflammation, and a cascade of adverse health effects—including respiratory and cardiovascular diseases as well as an increased risk of cancer (Lequy et al., 2023). Although the toxic potential of airborne metals is well documented, their combined exposure, whether through additive or synergistic effects, may further amplify their adverse health impacts, making them a significant public health concern, particularly in densely populated urban areas where industrial and traffic-related emissions contribute to higher ambient concentrations.

2.1.4. Volatile Organic Compounds

Volatile organic compounds (VOCs) include all organic chemicals that have a high vapor pressure and become gaseous under elevated temperatures and pressures (Atkinson, 2000). Although VOCs are emitted from both natural and anthropogenic sources, human activities, such as fossil fuel combustion, industrial processes, and solvent use, are the dominant contributors to ambient VOC levels, particularly in urban and industrialized areas. However, certain VOCs, such as isoprene, limonene, and pinene, are predominantly emitted from biogenic sources, particularly vegetation (Zhang et al., 2019). Among the various VOCs, benzene, toluene, ethylbenzene, and the xylene isomers (*o*-, *m*-, and *p*-xylene)—collectively known as BTEX—account for nearly 80% of total VOC emissions. These compounds mainly originate from vehicle exhaust, tobacco smoke, gasoline, paints, adhesives, and solvents (Dimitriou and Kassomenos, 2020; Padhi and Gokhale, 2017). Because many VOCs do not reach detectable levels in ambient air, BTEX compounds serve as reliable indicators of overall VOC emissions (Bulog et al., 2011). Moreover, since BTEX compounds are not produced endogenously, their measurement in biological samples is considered a specific marker of exposure. Benzene is the most extensively studied compound in this group, primarily because of its well-documented carcinogenicity—especially in the context of occupational exposure as demonstrated in numerous epidemiological studies in occupational medicine (Chiavarini et al., 2024; Scholten et al., 2020; Wan et al., 2024; Zhou et al., 2020). In urban outdoor environments, the primary sources of benzene are crude oil, gasoline, and industrial emissions, whereas tobacco smoke is the predominant indoor source. In non-smokers, benzene exposure is mainly related to ambient environmental levels, but in smokers, approximately 90% of the benzene in the body is derived from tobacco smoke (Brajenović et al., 2015; Brčić, 2004). In Central European urban areas, annual average ambient benzene concentrations are reported to be

around 2–5 μg/m^3 (Sekar et al., 2019). The IARC classifies benzene as a Group 1 and ethylbenzene as a Group 2B carcinogen (IARC, 2000, 2018). At low concentrations, benzene exposure can cause headaches and nausea, while long-term and high-level exposure has been associated with the development of leukemia. In the human body, benzene is metabolically oxidized in the liver into phenol, catechol, and hydroquinone. These metabolites accumulate in the bone marrow and are directly linked to leukemogenesis (Sekar et al., 2019). Ethylbenzene may lead to respiratory issues and irritation of the eyes and throat; chronic exposure can result in hearing loss and liver damage (ATSDR, 2010). Although toluene and xylenes are not classified as carcinogens by IARC, their ingestion or inhalation can still cause systemic toxicity. Reported adverse effects include nausea, skin inflammation, nervous system impairment, and damage to the kidneys and liver, among other health issues (Dehghani et al., 2022).

2.1.5. Other Chemical and Biological Air Pollutants

Beyond the previously discussed air pollutants, including PMs, VOCs, and toxic metals, air pollution also encompasses a variety of gaseous pollutants that play a crucial role in shaping overall air quality. For example, O_3, carbon compounds—primarily carbon monoxide (CO) and carbon dioxide (CO_2)—and nitrogen oxides (NOx, including nitric oxide (NO) and NO_2) are ubiquitous in both urban and rural atmospheres (Safieddine et al., 2013). Anthropogenic emissions, primarily from the combustion of fossil fuels, are responsible for the majority of NOx, CO, and previously covered VOCs present in the atmosphere. The interactions between these pollutants in the atmosphere, including the photochemical formation of ground-level O_3 from VOCs and NOx, further complicate air quality management and contribute to the broader environmental and health challenges associated with air pollution (Figure 5) (Zhang et al., 2019).

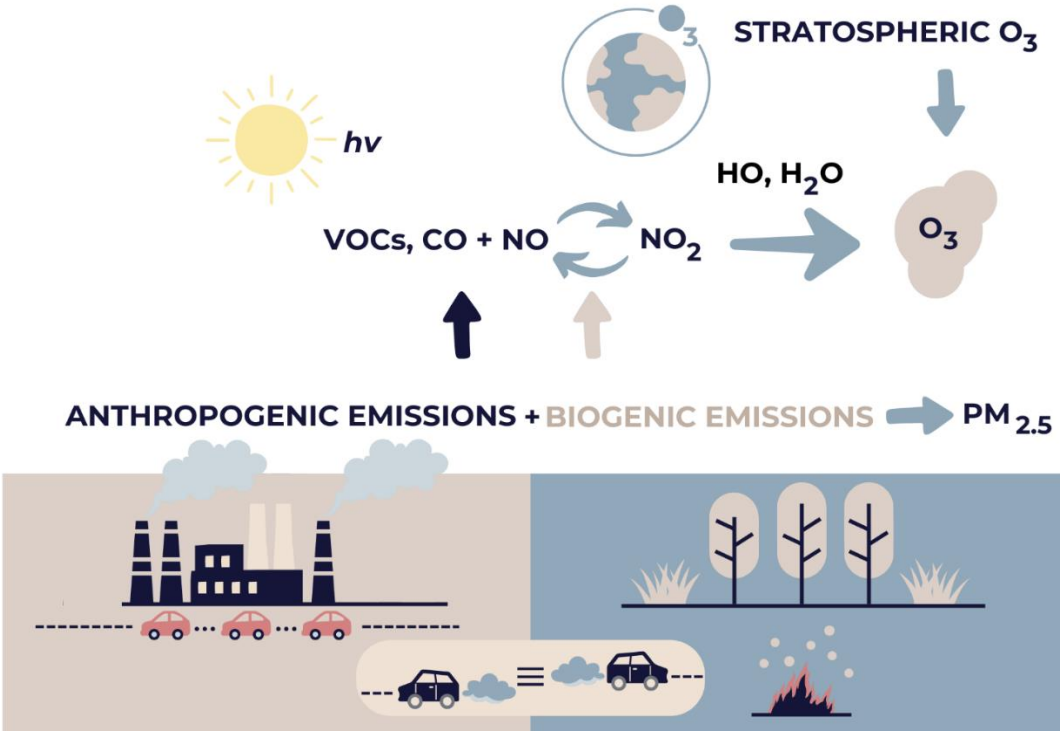

Figure 5. Formation of ground-level O_3 through photochemical reactions involving VOCs and nitrogen oxides, emitted from both anthropogenic (e.g., vehicle exhaust, industrial activities) and biogenic sources (e.g., vegetation). When exposed to sunlight, these precursors react to produce O_3 in the troposphere. Additionally, O_3 can descend from the stratosphere through stratosphere-troposphere exchange, contributing to its ground levels. VOC – volatile organic compound, CO – carbon monoxide, NO – nitric oxide, NO_2 – nitrogen dioxide, HO – hydroxyl, H_2O – water, O_3 – ozone, $PM_{2.5}$ – particulate matter < 2.5 μm

High concentrations of O_3 can cause irritation of the airways, coughing, reduced lung function, and the exacerbation of asthma. Moreover, even relatively low doses of O_3, when experienced over a prolonged period, can negatively affect lung function in children and older adults (Holm and Balmes, 2022). Chronic exposure to elevated O_3 levels has been associated with the development of chronic lung diseases and an increased risk of mortality from both respiratory and cardiovascular causes (Kazemiparkouhi et al., 2019; Turner et al., 2016). NO_2, which primarily originates from vehicle emissions and power plants, can cause airway irritation and worsen asthma symptoms, effects that are especially pronounced in children and the elderly (Kowalska et al., 2020). He et al. (2020) investigated the association between short-term NO_2 exposure and mortality. They observed a significant cumulative effect on non-accidental mortality over a period of up to seven days, with an increase of over 3% in respiratory-related deaths for every 10 $\mu g/m^3$ increment in NO_2. When

examining cumulative exposure over 30 days, a similar trend was observed, though the increase did not reach statistical significance. Furthermore, Huangfu and Atkinson (2020), using a meta-analytical approach, found a positive association between long-term NO_2 exposure and mortality, while the evidence for O_3 was more limited. The high heterogeneity in these results underlines the need for multipollutant models to better understand the combined effects of these pollutants and more accurately assess their relationships with health outcomes.

In addition to these chemical pollutants, biological agents such as pollen also play a critical role in air quality. Pollen consists of fine dust (microscopic grains produced by plants for reproduction) that is dispersed by air currents and can trigger allergic reactions in sensitive individuals (Kitinoja et al., 2020). When airborne pollen interacts with urban pollutants such as PM, O_3, and NO_2, it undergoes physical and chemical modifications. These interactions can damage the pollen's outer surface, making it more fragile and promoting the release of smaller sub-pollen particles that can penetrate deeper into the respiratory tract (Capone et al., 2023). In parallel, air pollutants can alter the biochemical profile of pollen, increasing the expression of allergenic proteins and enhancing its immunogenicity (Venkatesan et al., 2024). These combined effects are believed to amplify the severity and prevalence of allergic diseases, including asthma and rhinitis. In line with these mechanisms, the global burden of allergic respiratory conditions has risen dramatically in recent decades, especially in industrialized regions, with an estimated 400 million people affected by allergic rhinitis and over 260 million living with asthma (Abbafati et al., 2020; Nur Husna et al., 2022). While global asthma incidence declined between 1990 and 2021, projections indicate that the age-standardized incidence rate will stabilize at relatively high levels from 2022 to 2050, particularly among adults (20–80 years), highlighting asthma as an ongoing public health concern despite previous reductions (Yuan et al., 2025). Although this issue is most pronounced in industrialized regions, developing countries also face serious health challenges due to the interaction between polluted air and pollen, which exacerbates allergic diseases. Climate change, rising CO_2 levels, and extreme weather conditions further influence pollen production and distribution, leading to increased sensitivity and a higher incidence of asthma (Zhang and Steiner, 2022). In Croatia, the annual asthma incidence rate is approximately 3,000 per 100,000 inhabitants, with about 12,000 new cases each year (HZJZ, 2022). This figure is close to the global asthma prevalence reported by Yuan et al. (2025), estimated at 3,340 cases per 100,000. However, Croatia’s adult asthma prevalence is estimated at 5% (5,000 per 100,000), placing it within the

broader European range of 5.1% to 8.2% (Eurostat, 2021; Wecker et al., 2023). This contrast highlights that Croatia, and Europe more broadly, faces a disproportionately higher asthma burden than the global average. These national differences in prevalence are shaped not only by environmental exposures such as air pollution and aeroallergens but also by underlying genetic susceptibilities, diagnostic practices, and access to healthcare, all of which influence how asthma is detected, managed, and reported across regions. Monitoring pollen trends throughout the year is particularly relevant for asthma management; a pollen calendar helps individuals with asthma identify periods of high pollen concentrations (expressed as the number of grains per m^3), thereby enabling them to take preventive measures and adjust their daily activities to reduce exposure and better manage their symptoms (Figure 6).

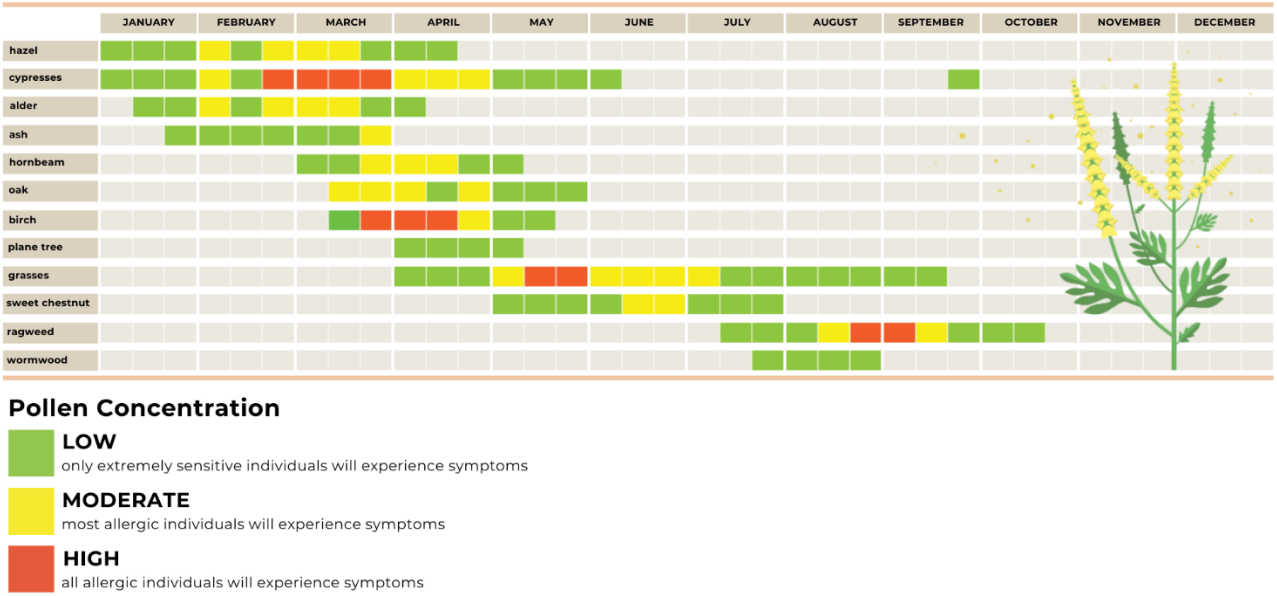

Criteria for assessing pollen levels in the air

Pollen levels	Pollen concentration in the air (number of grains/m³ of air)		
	Trees	Grasses	Weeds
low	1 – 15	1 – 5	1 – 10
moderate	16 – 90	6 – 20	11 – 50
high	91 – 1500	21 – 200	51 – 500
very high	more than 1500	more than 200	more than 500

Figure 6. Pollen Calendar of the City of Zagreb. Based on the original 10-year results from the Teaching Institute for Public Health "Dr. Andrija Štampar" (NZJZ, 2020). It outlines the seasonal occurrence and peak periods of allergenic tree, grass, and weed pollens, with defined concentration thresholds.

2.1.6. The Impact of Meteorological Conditions and Seasonal Variations

Meteorological conditions can significantly influence air pollution in various ways. For instance, high temperatures can increase air pollution, especially in urban areas where urban heat island effects are common (Piracha and Chaudhary, 2022; Wang et al., 2021a). Urban heat islands occur when densely built-up areas retain heat, which can elevate the concentration of pollutants in the air, such as O_3 and secondary aerosols (Deilami et al., 2018). Conversely, low temperatures during winter are often accompanied by temperature inversions, wherein a layer of warm air traps cooler air near the ground, preventing pollutant dispersion and leading to higher concentrations of $PM_{2.5}$ and PM_{10} particles (Nejad et al., 2023). These inversions also promote the transformation of primary emissions, such as NO_x and SO_2, into secondary pollutants like nitrates and sulfates, further increasing PM concentrations (Wang et al., 2023a). Strong winds can dilute pollutants by dispersing them, thereby reducing their local concentrations (Liu et al., 2020). However, wind can also transport pollutants from one area to another, potentially increasing pollution levels in regions far from the original source (Xie et al., 2022). Rain and snow help remove pollutants from the air by washing out particles and gases and depositing them on the ground (Tian et al., 2021; Wang et al., 2023b). On the other hand, precipitation can create favorable conditions for the formation of certain types of pollution, such as acid rain (Payus et al., 2020). Moreover, high humidity can contribute to the formation of some pollutants, including sulfates and various aerosols (Fang et al., 2019; Flueckiger and Petrucci, 2024).

Seasonal variations also have a significant impact on air pollution levels due to changes in weather conditions and human activities throughout the year. During winter, the frequent occurrence of temperature inversions exacerbates air pollution by trapping pollutants near the surface. The use of heating systems, particularly those that burn fossil fuels or biomass, increases emissions of PM, SO_2, NO_x, VOCs, PAHs, and other pollutants (Mahmoud et al., 2021). In Croatia, studies have demonstrated that wintertime pollution levels are largely influenced by residential heating, particularly the combustion of wood and solid fuels, which significantly contributes to ambient PM and PAH concentrations (Godec et al., 2016; Pehnec et al., 2020). Additionally, traffic emissions play a substantial role in urban areas, as colder temperatures and adverse weather conditions lead to increased vehicle use and prolonged engine idling, further elevating pollution levels (Jakovljević et al., 2018; Pehnec and Jakovljević, 2018). However, shorter days and lower

levels of sunlight reduce the rate of photochemical reactions, resulting in lower levels of secondary pollutants, such as O_3 (Al-Qassimi and Al-Salem, 2020). In spring, an increase in pollen levels occurs; although pollen is not a classical pollutant, it affects air quality and the health of allergy sufferers (Figure 6). Springtime conditions, with moderate temperatures and increased humidity, can enhance the formation of secondary organic aerosols (SOAs) from VOC oxidation. These reactions contribute to $PM_{2.5}$ concentrations, particularly in areas with high biogenic VOC emissions from vegetation (Madronich et al., 2023; Mahilang et al., 2021). During summer, higher temperatures and increased solar radiation accelerate photochemical reactions, leading to elevated ground-level O_3 and smog, especially in urban areas with heavy traffic (Al-Qassimi and Al-Salem, 2020). The photochemical formation of O_3 occurs when NO_x and VOCs react under sunlight, a process intensified during heatwaves and stagnant air conditions (Wang et al., 2023a). Additionally, air conditioning systems, particularly older or less efficient models, boost energy demand, which in turn results in greater fossil fuel consumption by power plants and increased emissions of NOx and VOCs. In autumn, agricultural fires frequently occur, releasing large quantities of $PM_{2.5}$ and other pollutants into the atmosphere (Pinakana et al., 2024; Sopčić et al., 2025). By understanding these seasonal variations, policymakers and environmental agencies can better design and implement strategies to reduce air pollution and protect public health throughout the year.

2.1.7. Air Quality Monitoring

Air pollution in Europe and around the world is monitored through a network of various measurement stations and surveillance systems. In Europe, the European Environment Agency (EEA) coordinates the collection, analysis, and publication of air quality data through the European Air Quality Monitoring Network. This network comprises thousands of monitoring stations spread across Europe, which track various air pollution parameters, including PM, NO_x, O_3, and other harmful substances (data available at: https://airindex.eea.europa.eu/AQI/index.html). In addition, national monitoring systems exist in each European Union (EU) member state to complement the EU-level data. Worldwide, similar monitoring networks are present in most developed countries, and data are frequently shared via international programs and organizations such as the WHO and the United Nations Environment Programme (UNEP), facilitating a global understanding and management of air pollution. These monitoring systems enable informed decision-making to

protect public health and the environment by identifying pollution sources, tracking trends, and assessing the effectiveness of emission reduction measures. In Croatia, air quality monitoring is carried out through a national network of measurement stations coordinated by the Environmental Protection Agency (EPA). In Zagreb, local monitoring is conducted by a network of stations managed by the Teaching Institute of Public Health "Dr. Andrija Štampar". The Croatian Meteorological and Hydrological Service (Croat. DHMZ) operates a network of six monitoring stations to track air quality in Zagreb. The data collected are integrated into the national air quality monitoring system and made available to the public via the DHMZ website (https://meteo.hr/index_kz.php?tab=kz). In addition to air quality monitoring, DHMZ conducts other meteorological and hydrological measurements and provides relevant information and forecasts to the public and pertinent institutions. The Institute for Medical Research and Occupational Health (IMROH) plays a significant role in researching the impact of air pollution on human health and in providing expert analyses and recommendations to improve air quality in Zagreb and beyond. This station contributes to comprehensive urban air quality surveillance and is part of the AirQ project (https://www.airq.hr/o-projektu/)—an international initiative conducted in collaboration with the EU aimed at improving air quality and reducing air pollution in cities across Europe. It is important to note that in 2021, according to WHO guidelines (Table 1)**,** 76% of the urban population in the EU was exposed to PM_{10} concentrations exceeding recommended levels, while this percentage was 97% for $PM_{2.5}$ and 64% for BaP (EEA, 2023).

Table 1. Threshold and proposed limit values for outdoor air pollutants.

Pollutant	Averaging period	Threshold limit value	Threshold limit value	Guideline
		Current EU Directive	**Proposed EU Directive**	**WHO 2021**
Benzene	Annual average	5 μg/m^3	Alignment with WHO guidelines by 2030	No safe level: recommended as low as possible
Toluene	NA	No specific limit in ambient air	No new specific proposals	260 μg/m^3 (1-week)
Ethylbenzene	NA	No specific limit in ambient air	No new specific proposals	Not specified
Xylene	NA	No specific limit in ambient air	No new specific proposals	100 μg/m^3 (24 h)
O_3	8 h	120 μg/m^3 (*more than 25 times a year)	120 μg/m^3 (*more than 18 times a year)	100 μg/m^3 (*more than 3-4 times a year)
PM_{10}	24 h	50 μg/m^3 (*more than 35 times a year)	45 μg/m^3 (*more than 18 times a year)	45 μg/m^3 (*more than 3-4 times a year)
	Annual average	40 μg/m^3	20 μg/m^3	15 μg/m^3
$PM_{2.5}$	24 h		25 μg/m^3 (*more than 18 times a year)	15 μg/m^3 (*more than 3-4 times a year)
	Annual average	25 μg/m^3	10 μg/m^3	5 μg/m^3
NO_2	1 h	200 μg/m^3 (*more than 18 times a year)	200 μg/m^3 (*more than 18 times a year)	200 μg/m^3
	24 h		50 μg/m^3 (*more than 18 times a year)	25 μg/m^3 (*more than 3-4 times a year)
	Annual average	40 μg/m^3	20 μg/m^3	10 μg/m^3

* should not be exceeded more than

However, under EU directives, the proportion of the urban population exceeding regulatory limits was significantly lower—10% for PM_{10}, less than 1% for $PM_{2.5}$, and 14% for BaP. According to EEA (2023) report on air quality in Europe, air pollution levels in Croatia, as in many other European countries, have occasionally exceeded regulatory thresholds, particularly during winter months. While annual average PM_{10} concentrations generally remained below the EU limit value of 40 μg/m^3, daily PM_{10} levels sometimes surpassed the EU 24-hour limit value of 50 μg/m^3, which

is permitted to be exceeded on no more than 35 days per year. Similarly, instances of $PM_{2.5}$ levels exceeding the EU annual limit value of 25 $\mu g/m^3$ were reported, though compliance with this standard was more frequent compared to the stricter WHO guideline of 5 $\mu g/m^3$. Additionally, monitoring stations in Zagreb recorded annual BaP concentrations exceeding the EU target value of 1 ng/m^3 in 2021 (EEA, 2023). While air pollution levels in Croatia have occasionally exceeded regulatory thresholds, particularly during winter months, long-term monitoring data indicate a general downward trend in PM concentrations in Zagreb. Lovrić et al. (2022) conducted a comprehensive analysis of PM concentrations over a 12-year period (2009–2020), demonstrating that annual averages of PM_{10} and $PM_{2.5}$ remained below the Croatian and EU regulatory limits. Since 2017, the daily EU 24-hour limit value for PM_{10} has not been exceeded at the monitored location. This progress reflects broader historical improvements: ambient PM and Pb concentrations in Zagreb have been decreasing steadily since the late 1970s, driven by industrial restructuring, fuel quality improvements, and the phase-out of leaded gasoline (Šega and Hršak, 1995; Vadjić et al., 2009). However, not all pollutants follow this downward trend. For example, O_3 and NO_2 have exhibited either stable or increasing concentrations in some areas, particularly near traffic corridors and during summer months, due to secondary pollutant formation and continued vehicular emissions (Matasović et al., 2021; Pehnec et al., 2011). These divergent trends highlight the need for pollutant-specific strategies in air quality management, particularly as urban areas continue to grow and climate-related factors influence emission dynamics and atmospheric chemistry.

2.2. Human Biomonitoring and Biomarkers of Toxicity

Human biomonitoring (HBM) is crucial for assessing exposure to biological, chemical, and physical agents present in the environment. This interdisciplinary approach combines chemical (and physical) analyses to determine the concentrations of chemical compounds with biological analyses that measure the organism's responses to pollution, thereby reflecting the biologically available fraction of pollutants (Angerer et al., 2007). In addition to quantifying exposure, HBM can also assess, where applicable, some of the biological effects triggered by these exposures, contributing to a more comprehensive understanding of their potential health implications. The primary goal of HBM is to evaluate the levels of various pollutants within the human body, providing valuable data on exposure to harmful substances (Ladeira and Viegas, 2016; Zare Jeddi

et al., 2021b). HBM research is becoming increasingly important due to growing concerns about environmental and occupational exposures. By monitoring the presence of various substances in the human body, researchers can establish reference values and identify populations that are at a greater risk. For example, the Human Biomonitoring for Europe (HBM4EU) initiative has prioritized several substances of concern—including toxic metals, PAHs, bisphenols, and phthalates—highlighting the necessity of systematic biomonitoring for public health protection (HBM4EU, 2024). This information is vital for public health, as it aids in the assessment of potential health risks and the formulation of regulatory policies to reduce exposure to hazardous substances (Zare Jeddi et al., 2022). One significant advantage of HBM is its ability to provide direct evidence of exposure, often with greater accuracy than indirect methods such as environmental monitoring or questionnaires. However, interpreting HBM data can be complex (Zare Jeddi et al., 2021b). It involves comparing biomonitoring results with health-based reference values and considering factors such as individual variability and mixed exposures to multiple chemicals. HBM also faces ethical challenges, particularly concerning informed consent, data privacy, and the communication of results to participants. Adhering to proper ethical guidelines ensures that participants' rights are respected and that the collected data are used responsibly. Taken together, the HBM approach is extremely important in environmental health research, as it provides insights into exposure levels and supports public health protection through informed decision-making and regulatory actions (WHO, 2015).

Biomarkers are substances, structures, or processes that can be quantified within an organism or its by-products. A biomarker indicates a change in the biological response, which may include molecular, cellular, physiological, and behavioral alterations associated with exposure to and the toxic effects of specific agents (Strimbu and Tavel, 2010). Biomarkers can be measured at various biological levels, from molecules and cells to populations and ecosystems. According to the WHO, biomarkers encompass all measurable functional and physiological, biochemical, and molecular interactions between a biological system and a potentially harmful agent of chemical, biological, or physical nature. Ideally, biomarkers are easily accessible, non-invasive, simple, and inexpensive to test. The development and validation of biomarkers is a lengthy process that involves basic research and pilot studies in humans, ultimately culminating in comprehensive epidemiological evaluations (WHO and IPCS, 2001). At the molecular and cellular levels, biomarkers are especially valuable for measuring acute, short-term effects because of their high

sensitivity and specificity. They also provide a foundation for understanding long-term effects, although the sensitivity and specificity in such contexts are generally lower (Van Gestel and Van Brummelen, 1996). Biomarkers are classified according to their application into diagnostic, monitoring, pharmacodynamic, predictive, prognostic, as well as risk and safety biomarkers. In the field of genetic toxicology, biomarkers are usually divided into those that measure exposure, susceptibility, and effect (Figure 7) (de Oliveira et al., 2022; Ladeira and Viegas, 2016; WHO and IPCS, 2001).

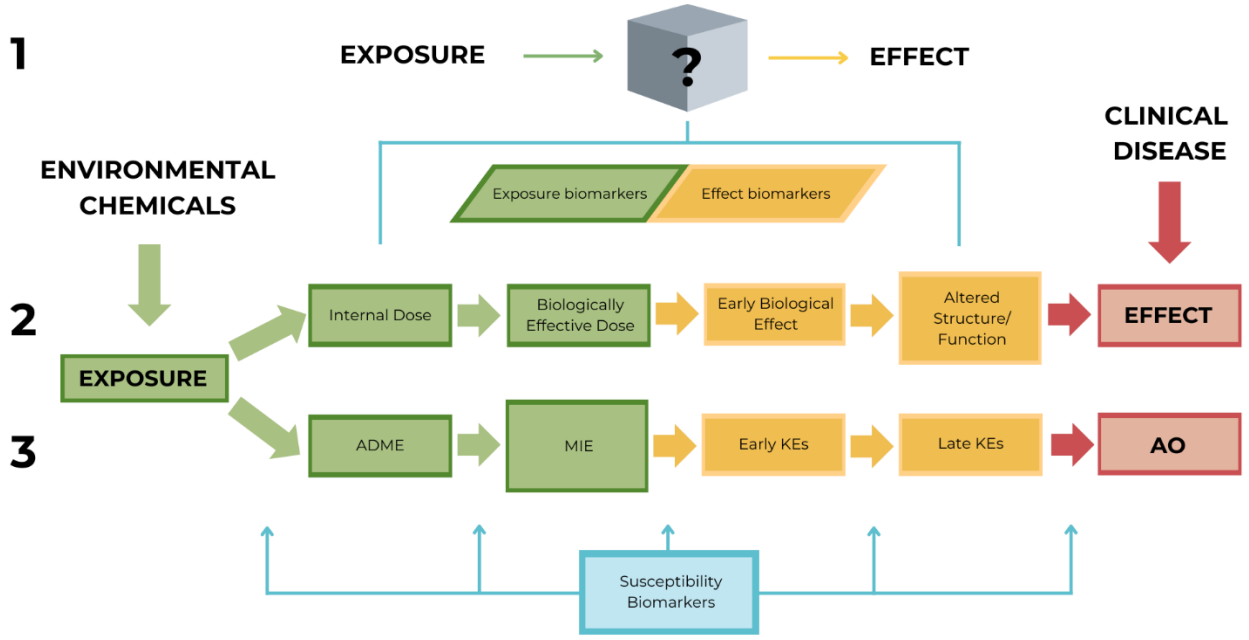

Figure 7. Epidemiological 'Black Box' Model Integrating Exposure, Biomarkers, and Adverse Outcome Pathways (AOP). This figure illustrates three conceptual models: (1) the classical model linking external exposure to the effect. (2) the National Research Council's (NRC) biomarker paradigm, and (3) the Adverse Outcome Pathway framework. Schemes (2) and (3) demonstrate the equivalence between the biomarker paradigm and its parallel structure within the AOP framework, mapping the continuum from exposure through internal processing to adverse outcomes (AO). The model incorporates ADME processes—absorption, distribution, metabolism, and excretion—which determine the internal dose, followed by a molecular initiating event (MIE) that triggers a cascade of key events (KE) leading to the final adverse outcome. This integrated approach underscores the critical role of biomarkers in bridging exposure data with biological responses, thereby enhancing risk assessment and disease prevention strategies. Adapted from Rodríguez-Carrillo et al. (2023).

2.2.1. Biomarkers of Exposure

In the context of the intricate interplay between environmental pollutants and human health, outlined in the previous sections, exposure biomarkers serve as a critical bridge between external environmental monitoring and internal biological response. By quantifying the absorbed dose of harmful agents, these biomarkers provide direct evidence of exposure, enhancing our understanding of the toxicological impact of various chemicals. Biomarkers of exposure are measurable indicators that provide information on an individual's contact with specific agents (e.g., chemicals, toxins, drugs, or environmental agents) or quantify their absorption into the biological system. This is crucial for monitoring environmental conditions, occupational diseases, and clinical research (Madden and Gallagher, 1999). Chemical biomarkers assess exposure to particular chemicals, while metabolites indicate exposure through degradation products. Some of these chemicals are lipophilic, necessitating further metabolic transformation via Phase I and Phase II metabolism (Wang and Zang, 2023). In terms of detecting airborne pollutants**,** biomarkers of exposure are classified into internal dose markers and effective dose markers: the former indicates the occurrence and extent of an organism’s exposure, while the latter reflects the exposure at the level of a targeted molecule, structure, or cell. For example, the presence of benzene can be tracked by measuring its concentration in blood, whereas its metabolite, trans,trans-muconic acid (t,t-MA), can be detected in urine (Madden and Gallagher, 1999). Glutathione conjugates and urinary biomarkers—such as 1-OHP, 1-hydroxynaphthalene, and 2-hydroxynaphthalene—are examples of internal dose biomarkers for exposure to PAHs, while BTEX in blood serve as indicators of exposure to aromatic hydrocarbons. Effective dose biomarkers, such as DNA and protein adducts, assess the biologically active fraction of xenobiotics (Decaprio, 1997). These biomarkers aid in risk assessment, regulatory decision-making, epidemiological studies, and the development of strategies to reduce health risks associated with exposure.

2.2.2. Biomarkers of Susceptibility

Biomarkers of susceptibility provide information about inherent or acquired characteristics that may predispose an individual to a higher risk of developing disease upon exposure to environmental hazards. These biomarkers are broadly categorized into genetic and environmental types (Pedrete and Moreira, 2018). Genetic biomarkers include variations in the genotype, such as single nucleotide polymorphisms (SNPs) and genetic mutations that increase the risk for diseases.

These variations are often identified through approaches like Genome-Wide Association Studies (GWAS) and are linked to heightened susceptibility to conditions such as cancer, cardiovascular diseases, and neurodegenerative disorders (Uffelmann et al., 2021). Environmental susceptibility biomarkers reflect how external factors (e.g., exposure to toxins, pollutants, or radiation) and lifestyle behaviors (such as diet, physical activity, and smoking) modulate an individual's risk of developing disease. For instance, baseline inflammatory markers (e.g., levels of certain cytokines) may indicate a predisposed physiological state that enhances sensitivity to environmental exposures, even though these markers are less specific than genetic or epigenetic indicators (Pedrete and Moreira, 2018).

2.2.3. Biomarkers of Effect

Building on the insights provided by exposure and susceptibility biomarkers, biomarkers of effect serve as the crucial bridge in toxicological assessments by capturing the early biological responses to toxic insults. Biomarkers of effect, or biological response biomarkers, have been increasingly utilized over the past several decades. They are employed in biomonitoring to systematically measure changes at the cellular and molecular levels within biological systems. The development of molecular epidemiology has introduced the concept of effect biomarkers to provide evidence for the causal relationship between exposure to harmful agents and adverse outcomes—especially in the early stages before the onset of overt disease, which is crucial for preventive interventions (Rodríguez-Carrillo et al., 2023). As previously described, oxidative stress might be one of the drivers of air pollution-related toxicity. Exposure to pollutants like $PM_{2.5}$ and O_3 generates ROS, causing oxidative stress and triggering inflammatory responses. Accordingly, oxidative stress biomarkers are among the most widely used indicators of early cellular damage in environmental health studies. Common markers such as malondialdehyde (MDA) and 8-OHdG reflect lipid peroxidation and DNA damage, respectively (Checa and Aran, 2020; Valavanidis et al., 2009). Changes in the activity of key antioxidant enzymes like SOD, glutathione peroxidase (GPx), and catalase (CAT) further support the evaluation of oxidative stress (Demirci-Çekiç et al., 2022). At the molecular level, pollutants can directly modify DNA, leading to genotoxic effects. DNA adducts represent chemical modifications of DNA molecules caused by interactions with specific substances, serving as crucial indicators of exposure-induced genetic damage (Luo et al., 2019). DNA methylation alterations, on the other hand, reflect epigenetic modifications that

influence gene expression, further linking environmental exposures to disease development (Brucker et al., 2020). In the field of genotoxicology, effect biomarkers are essential for assessing the biological impact of exposure to genotoxic agents. Damage to genetic material—such as single- and double- strand DNA breaks, chromosomal aberrations, micronuclei (MNi) formation, and the modulation of enzyme activity—can signal early biological responses preceding clinical disease (Annangi et al., 2016; Bonassi et al., 2007, 2008, 2016, 2021; Fenech, 2020; Zare Jeddi et al., 2021a). Similarly, in cytotoxicology, biomarkers of effect are used to measure changes in cellular functions. These may include alterations in the activity of specific organelles, such as mitochondria, or changes in cellular processes like inflammatory responses and programmed cell death. Such biomarkers provide valuable insights into the early biological effects of exposure before the manifestation of overt toxicity. Before these biomarkers of effect can be implemented in HBM programs, rigorous validation is required. Selected biomarkers must be reliable, easily identifiable, and capable of quantifying specific biological changes using precise and dependable testing methods (Rodríguez-Carrillo et al., 2023; Zare Jeddi et al., 2021a). Moreover, advances in genomics, epigenomics, transcriptomics, lipidomics, proteomics, and metabolomics continue to expand the repertoire of effect biomarkers, thereby opening new research avenues in the field of biomonitoring.

2.2.3.1. Epigenetic Biomarkers

Epigenetics involves modifications in gene function without altering the underlying DNA sequence. Such changes, which can affect cellular and physiological characteristics, may occur as part of normal developmental processes or be induced by environmental factors. Epigenetic variations can thus reveal the systemic effects of environmental exposures, such as air pollution, providing valuable insight into individual susceptibility (Mukherjee et al., 2021). DNA methylation, the covalent addition of a methyl group to cytosine, is the most extensively studied epigenetic modification, particularly within cytosine-guanine dinucleotides (CpG) (Wu et al., 2021). Early studies have indicated that air pollution can influence global methylation levels in peripheral blood, often assessed using repetitive elements such as long interspersed nuclear elements (LINE-1) (Alfano et al., 2018; Baccarelli et al., 2012; Lee et al., 2017; Wang et al., 2020). Sequence-specific analyses have further revealed differential methylation in gene regions—such as those associated with inducible NO synthase (iNOS), intercellular adhesion molecule-1, Toll-

like receptor 2, interferon-γ, and interleukin-6 (Bind et al., 2014; Coull et al., 2015; Rider and Carlsten, 2019). Mostafavi et al. (2018) demonstrated that individual exposure to $PM_{2.5}$ is associated with methylation changes at specific CpG sites and differentially methylated regions (DMRs). Moreover, recent research has linked air pollution, particularly exposure to CO and O_3, with alterations in the expression or function of the FOXP3 gene, which plays a key role in regulating immune responses and maintaining self-tolerance (Kohli et al., 2012; Prunicki et al., 2021; Rider and Carlsten, 2019). Pollutants such as PM, VOCs, and toxic metals can disrupt immune balance and promote inflammatory responses. Monitoring the expression levels of FOXP3 or the activity of regulatory T cells (Treg) could serve as a biomarker for assessing the impact of air pollution on immune function and the development of diseases such as asthma (Rider and Carlsten, 2019; Tuazon et al., 2022). Changes in DNA methylation can affect gene expression and have been linked to the development of diseases such as cancer and various other disorders, including neurodegenerative conditions (Lu et al., 2020; Martínez-Iglesias et al., 2020; Robertson, 2005). Methylation profiles can offer insights into an individual's susceptibility to diseases and their response to environmental factors. The interaction between genetic predisposition, epigenetic changes, and environmental factors is complex, and the presence of susceptibility biomarkers does not necessarily imply the eventual development of disease.

2.2.3.2. Biomarkers of Oxidative Stress

Biomarkers of oxidative stress are crucial for assessing the balance between ROS and the body's antioxidant mechanisms. ROS include both free radicals and non-radical oxygen intermediates (peroxides), such as superoxide radicals ($O_2\bullet^-$), hydrogen peroxide (H_2O_2), hydroxyl radicals (OH•), and singlet oxygen ($^1O_2$). They are generated as by-products of normal metabolism or in response to external factors such as air pollution, cigarette smoke, or ultraviolet (UV) radiation (Checa and Aran, 2020). Although ROS play an important role in cell signaling and immune defense, high concentrations can induce oxidative stress, leading to damage of biomolecules such as proteins, lipids, and DNA (Demirci-Çekiç et al., 2022; Jomova et al., 2023; Marín et al., 2023). To mitigate oxidative damage, the body employs a complex defense system composed of both enzymatic and non-enzymatic components. Among the enzymatic antioxidants, SOD catalyzes the dismutation of $O_2\bullet^-$ into H_2O_2, which is then neutralized by CAT and GPx, the latter using glutathione (GSH) as a reducing cofactor (Demirci-Çekiç et al., 2022; Jomova et al., 2023). GSH

itself is a major non-enzymatic antioxidant, acting both as a direct ROS scavenger and as a substrate for enzymatic detoxification. The ratio of reduced (GSH) to oxidized (GSSG) glutathione is widely used as an indicator of intracellular redox status (Aquilano et al., 2014). Other important non-enzymatic antioxidants include uric acid, which neutralizes $^1O_2$ and peroxynitrite ($ONOO^-$), and vitamin C and E, which contribute to plasma antioxidant capacity (Santos et al., 1999). In parallel with these defense systems, biomarkers that reflect oxidative damage to biomolecules offer critical insight into the severity and biological impact of oxidative stress. Lipid peroxidation is a major consequence of ROS attack on polyunsaturated fatty acids in cell membranes, leading to the formation of reactive aldehydes such as MDA and 4-hydroxynonenal (4-HNE). MDA, in particular, is commonly measured in blood and urine and serves as a reliable indicator of membrane damage and oxidative burden (Jomova et al., 2023). Proteins are also vulnerable to oxidative damage, with modifications such as carbonylation, disulfide bond formation, and nitration impairing function and promoting degradation. Protein carbonyl content is thus a widely used biomarker of protein oxidation, associated with both aging and various pathological conditions (Song et al., 2020). Oxidative stress also affects nucleic acids, particularly DNA. Guanine bases are especially susceptible to oxidation, resulting in the formation of 8-OHdG, a widely validated biomarker of oxidative DNA damage. Elevated 8-OHdG levels have been linked to mutagenesis, carcinogenesis, and disease progression (Guo et al., 2016; Shukla et al., 2020; Valavanidis et al., 2009). While not a classical ROS, NO plays a dual role in oxidative biology. Under normal physiological conditions, NO regulates vascular tone, immune responses, and neurotransmission. However, in oxidative environments, NO can react with $O_2^{\bullet -}$ to form $ONOO^-$, a highly reactive nitrogen species capable of inducing protein nitration and further oxidative damage (Pa´ et al., 2007). Thus, NO-related biomarkers such as nitrate/nitrite levels or 3-nitrotyrosine may provide additional insight into redox-related cellular dysfunction.

Understanding the mechanisms of oxidative stress and monitoring these biomarkers in biological samples is essential for assessing the risk of diseases linked to oxidative stress, such as cancer, neurodegenerative disorders, and cardiovascular diseases (Barnham et al., 2004; Hayes et al., 2020; Mahmoud and Junejo, 2024). This information is vital for diagnosis, therapy monitoring, and the development of preventive strategies against oxidative damage.

2.2.3.3. Micronucleus Assay

The micronucleus (MN) assay is a well-established method for assessing genomic instability and DNA damage, making it a valuable tool in biomonitoring individuals exposed to genotoxic agents. The presence of MNi serves as an indicator of chromosomal aberrations, reflecting both structural chromosome damage and whole chromosome loss due to mitotic errors. An increased frequency of MNi in healthy individuals is indicative of genomic instability, which heightens the risk of cancer development, making this test a predictive factor in carcinogenesis (Bonassi et al., 2007; Fenech et al., 2020; Gajski et al., 2024). This assay is widely applied in occupational, environmental, and clinical studies to evaluate baseline DNA damage and the effects of exposure to chemical and physical agents (Bolognesi et al., 2015; Bolognesi and Fenech, 2019; Fenech, 2020; Gajski et al., 2018, 2022, 2024; Nersesyan et al., 2016).

2.2.3.3.1. MN Assay in Peripheral Blood Lymphocytes

The MN assay in peripheral blood lymphocytes is one of the most frequently used approaches for genotoxicity and biomonitoring studies. It enables the detection of both structural chromosomal damage (MNi formation) and numerical chromosome alterations. The most commonly used method is the cytokinesis-block micronucleus (CBMN) assay, in which cytochalasin B is added to prevent cell division after one nuclear replication cycle (Fenech, 2007).

MNi are small extranuclear chromatin bodies that arise when acentric chromosomal fragments or whole chromosomes fail to be incorporated into daughter nuclei during mitosis. Their frequency serves as a key biomarker of DNA damage, chromosomal instability, and defective mitotic segregation (Fenech, 2020; Fenech et al., 2011). In addition to MNi, the assay also detects nucleoplasmic bridges (NPBs) and nuclear buds (NBUDs) (Figure 8). NPBs connect two nuclei within a binucleated cell, reflecting dicentric chromosome formation due to telomere fusion or improper chromatid separation. Their presence indicates misrepaired DNA breaks or defective recombination mechanisms. NBUDs appear as DNA-containing structures protruding from the main nucleus. They are associated with gene amplification, elimination of damaged DNA, or repair complexes (Fenech, 2020; Fenech et al., 2011). In addition to genotoxic endpoints, the CBMN assay provides insight into both cytotoxicity (apoptosis and necrosis) and cytostasis by calculating the mitotic index expressed either as Cytokinesis-Block Proliferation Index (CBPI) or Nuclear Division Index (NDI), which reflects the average number of cell divisions that a cell population

has undergone. Proliferation index is calculated based on the distribution of mono-, bi-, and multinucleated cells and serves as a measure of cell proliferation kinetics under experimental conditions. A lower proliferation index may indicate cytostatic effects caused by toxic exposures, helping to differentiate DNA damage from general cytotoxicity (Kirsch-Volders et al., 2003; OECD, 2023).

Scoring of MNi, NPBs, and NBUDs is traditionally performed using light microscopy. However, manual scoring is time-consuming and requires extensive training. To increase throughput and reduce observer bias, automated scoring systems like the Metafer system have been developed. These systems use fluorescent dyes e.g. DAPI imaging to detect MNi more efficiently, improving reproducibility and standardization (Rossnerova et al., 2011).

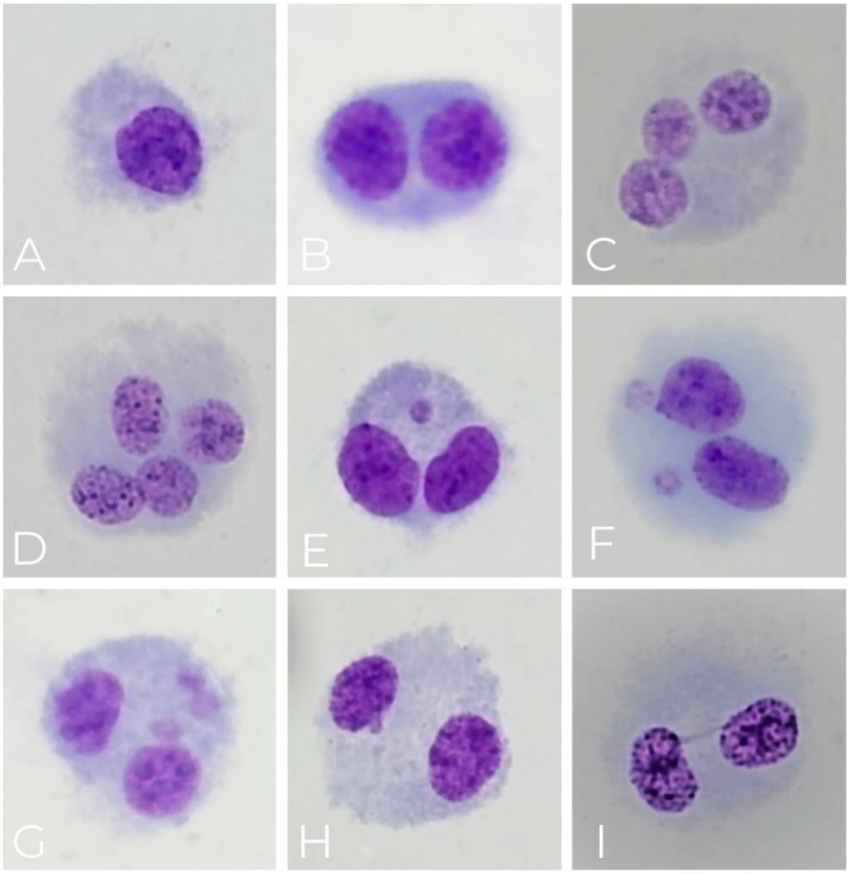

Figure 8. Microphotographs of cells analyzed in the CBMN assay, illustrating a mononucleated cell (A), a binucleated cell (B), multinucleated cells (C, D), a binucleated cell containing a single micronucleus (E), two micronuclei (F), three micronuclei (G), a nuclear bud (H), and a nucleoplasmic bridge (I). The microphotographs of cells, stained with 5% Giemsa solution, were captured using light microscopy under 400× magnification.

2.2.3.3.2. MN Assay in Buccal Epithelial Cells

Beyond peripheral blood lymphocytes, the MN assay is also widely applied to buccal epithelial cells, offering a minimally invasive and easily accessible method for monitoring genotoxic effects of environmental pollutants (Bolognesi and Fenech, 2019; Sommer et al., 2020; Thomas et al., 2009). Compared to lymphocytes, buccal cells are directly exposed to inhaled pollutants and other environmental contaminants, making them a suitable surrogate tissue for assessing airborne genotoxicants (Milić et al., 2020). The buccal MN assay is commonly used to evaluate exposure to air pollution, toxic metals, and occupational carcinogens (Bolognesi et al., 2015; Hopf et al., 2019; Panico et al., 2020).

The buccal MN assay allows for the assessment of various nuclear abnormalities, which provide insights into both genotoxicity and cytotoxicity (Figure 9). Among these, condensed chromatin cells are characterized by intensely stained, shrunken nuclei, indicative of early apoptosis. Karyorrhectic cells display nuclear fragmentation, marking late apoptosis, while pyknotic cells show small, highly condensed nuclei, representing early necrotic events. Karyolitic cells exhibit faint or absent nuclear staining, a hallmark of late necrosis due to complete DNA degradation. Another key feature observed in the buccal MN assay is broken egg nuclei, identified by DNA extrusion through a narrow constriction, which suggests chromatin instability and potential genotoxic damage. The frequencies of these abnormalities serve as indicators of different forms of cell damage and may complement MN frequencies in assessing the overall impact of genotoxic agents on epithelial tissues. However, the biological significance of anomalies in buccal epithelial cells is not yet fully understood, necessitating further standardization, validation, and automation of the test (Fenech et al., 2024).

While both lymphocyte and buccal MN assays provide valuable insights into genomic instability, key differences exist between the two methods. The lymphocyte MN assay requires cell culture, cytokinesis-blocking, and specialized conditions, making it a more labor-intensive technique, but it allows for systemic genotoxicity assessment. In contrast, the buccal MN assay is minimally invasive, requires no cell culture, and reflects direct exposure to inhaled or ingested pollutants at the primary site of contact. Some studies suggest a correlation between MN frequencies in lymphocytes and buccal cells, despite differences in toxicokinetic and proliferation patterns (Ceppi et al., 2010; Haveric et al., 2010; Nersesyan et al., 2025).

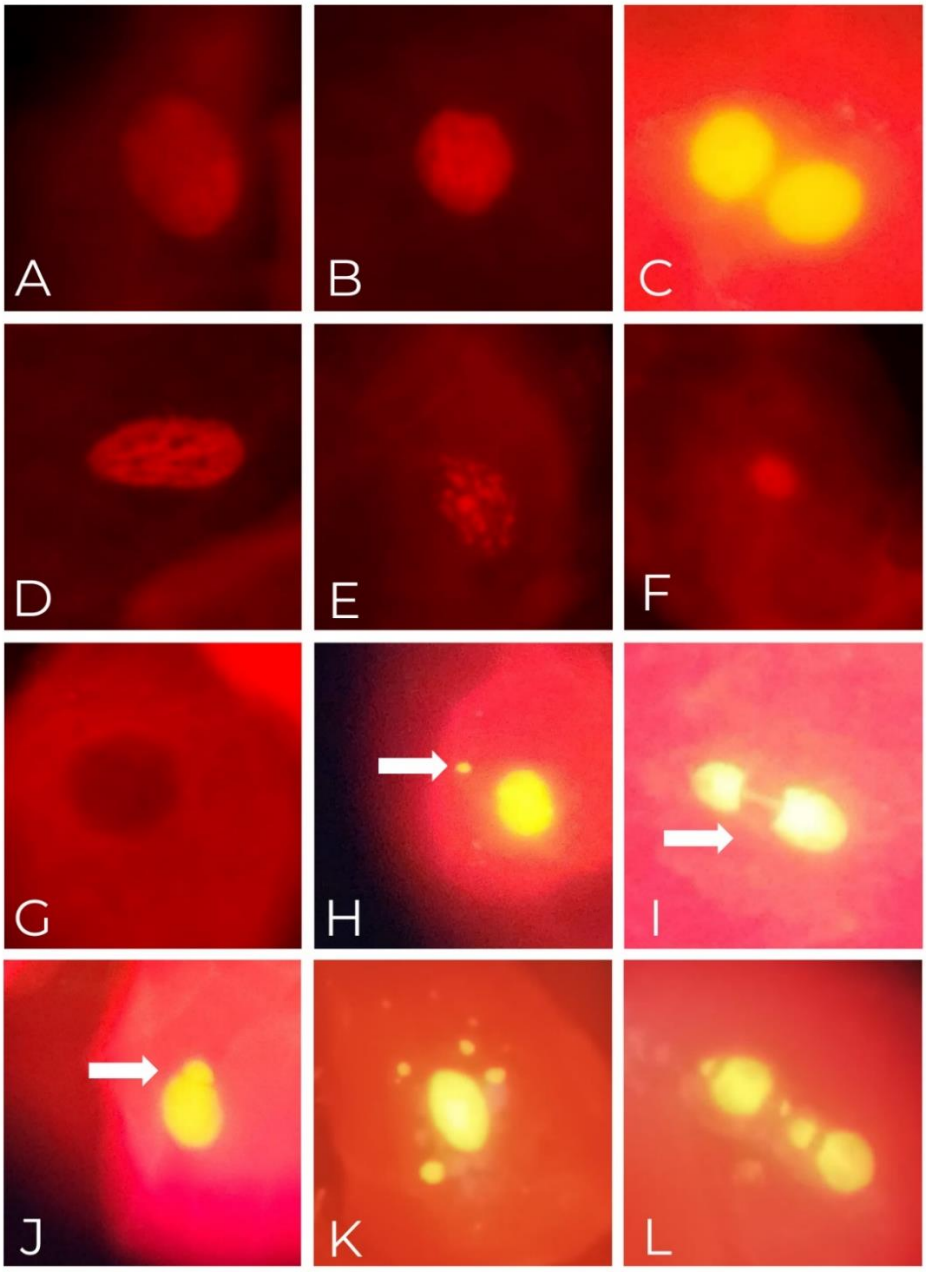

Figure 9. Microphotographs of cells analyzed in the BMN assay, depicting a normal basal cell (A), a normal differentiated cell (B), a binucleated cell (C), a cell with condensed chromatin indicating early apoptosis (D), a cell with karyorrhectic chromatin characteristic of late apoptosis (E), a pyknotic cell representing early necrosis (F), a karyolytic cell indicative of late necrosis (G), a cell containing micronuclei (H), a broken egg formation (I), a cell with a nuclear bud (J), a differentiated cell with multiple micronuclei (K), and a highly damaged cell (L). The microphotographs of cells, stained with Fast Green were captured using fluorescence microscopy at 1000× magnification under green fluorescence.

2.2.3.4. Comet Assay

The comet assay, also known as single-cell gel electrophoresis (SCGE), is a highly sensitive method for assessing DNA damage in individual cells and has become a key tool in genotoxicology and DNA damage research (Azqueta et al., 2020; Collins et al., 2014, 2023; Milić et al., 2021). The method is based on the ability of damaged DNA loops to migrate from the nucleoid toward the anode under an electric field. After electrophoresis, the nucleoid appears as a "comet" under a fluorescent microscope, with the intensity and length of the comet tail being proportional to the extent and size of the DNA damage (Figure 10). The comet assay is widely used in genotoxicological studies to assess the effects of chemicals, radiation, and other genotoxic agents, as well as in clinical and environmental studies (Azqueta et al., 2020; Ladeira et al., 2024; Møller et al., 2020). It is capable of detecting single- and double-strand DNA breaks, alkali-labile sites, and incomplete excision repair sites, making it highly informative in the context of environmental and occupational exposures (Azqueta et al., 2019; Azqueta and Collins, 2013; Collins and Azqueta, 2012). In human biomonitoring studies, the assay is commonly performed on peripheral blood cells, though it can also be applied to a wide range of other cell types, including cultured epithelial cells, animal or plan tissues, and exfoliated cells from buccal or nasal mucosa (Fenech et al., 2024; Gajski et al., 2019a, 2019b, 2021; Møller, 2018; Tyutereva et al., 2024). The primary descriptors measured include tail intensity (TI), tail length (TL), and tail moment (TM), which quantitatively assess DNA damage. Persistent DNA damage compromises genomic stability and increases the likelihood of mutations and chromosomal aberrations, which are key mechanisms underlying the development of chronic diseases such as cancer, neurodegenerative, and cardiovascular disorders (Azqueta et al., 2020; Collins et al., 2014; Ladeira et al., 2024). These conditions often manifest years after the initial exposure, contributing to long-term public health burdens, especially in aging populations, and placing substantial pressure on healthcare systems (Viegas et al., 2017). Given its sensitivity to early DNA damage, the comet assay has been increasingly recognized as a valuable tool in preventive strategies aimed at detecting early effects of environmental and occupational exposures, particularly in the context of non-communicable diseases (Bonassi et al., 2021). Despite its usefulness in evaluating DNA damage at the single-cell level, several factors can introduce variability, including protocol differences and data analysis methods, as recognized by the Minimum Information for Reporting Comet Assay (MIRCA) guidelines (Møller et al., 2020). Additionally, the use of different analysis software can be problematic due to variability in

measurement algorithms, leading to inconsistencies and complicating comparisons across studies. Therefore, it is important to develop and implement semi/fully automated scoring systems, such as the Metafer software, to enhance consistency and reduce subjectivity (Rossnerova et al., 2011).

A key challenge in comet assay research is the need to analyze large sample sets, particularly in biomonitoring and field studies, where sample collection occurs under variable conditions. To address this, the assay can be performed on both fresh and frozen blood samples, allowing for better sample management, extended storage, and flexibility in experimental design (Gajski et al., 2020a; Matković et al., 2024; Møller et al., 2021). This adaptability makes the comet assay an invaluable tool for studying genotoxic effects of environmental exposures and cellular responses to DNA damage.

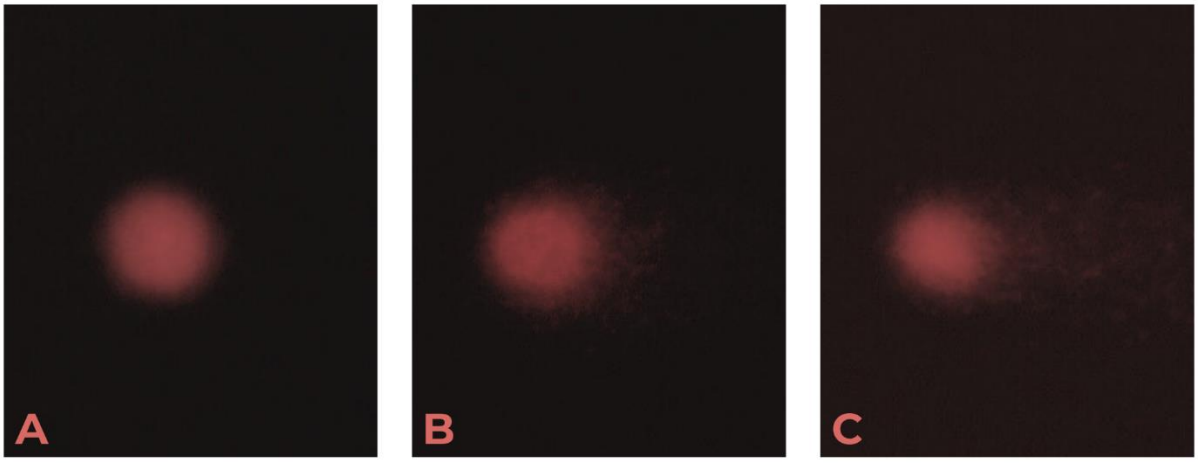

Figure 10. Comet assay image. This photograph, captured using the Comet Assay IV Software system and stained with ethidium bromide (EtBr), displays a comparison between nucleoids exhibiting different levels of DNA migration: (A) an intact nucleoid, (B) a nucleoid exhibiting slight DNA migration, and (C) a nucleoid exhibiting extensive DNA migration. The presence and extent of the comet tail visually represent DNA strand breaks, serving as an indicator of genotoxicity.

2.3. Data Analysis

An omics-based approach, including genomics, proteomics, metabolomics, and related fields, provides a comprehensive method for understanding the complex interactions between environmental factors, such as air pollution, and human health (Gruszecka-Kosowska et al., 2022; Kumari et al., 2024). By analyzing large datasets of genes, proteins, and metabolites, scientists can identify biomarkers that indicate exposure to pollutants and assess their impact on human health

(Wen et al., 2024). Advanced statistical methods and machine learning are becoming crucial for processing these complex datasets, enabling the integration of data from diverse sources, including environmental monitoring, biological samples, and medical records. Techniques such as regression analysis, hierarchical modeling, and Bayesian approaches are employed to identify associations and causal relationships between air pollutants and health outcomes (Houssein et al., 2023). Complementing these statistical techniques, machine learning algorithms—such as random forests, support vector machines, and neural networks—help uncover hidden patterns and make predictions from multidimensional data (Peng et al., 2024; Qian et al., 2023). These advanced analytical tools not only enhance our understanding of the intricate relationships between environmental exposures and biological responses but also support targeted interventions and inform policy decisions aimed at reducing the health risks associated with air pollution.

3. MATERIALS AND METHODS

3.1. Air Pollution Measurements

3.1.1. Study Area and Sampling Network

The study area encompasses the wide urban region of Zagreb, where air pollution data were systematically collected through a multi-tiered network of monitoring stations. The network includes six local stations, funded by the City of Zagreb, and four national stations supported by the State budget and the Environmental Protection and Energy Efficiency Fund. For this study, data were utilized only from eight stations that provided the most complete and relevant measurements for our analysis (Figure 11). These stations were strategically selected to represent a range of urban environments (urban background, traffic-dense, suburban, and industrial areas) in compliance with EU air quality directives. Detailed information regarding station distribution, sampling strategies, and monitoring schedules is available on the "Air Quality in Croatia" web portal (https://iszz.azo.hr/iskzl/). To ensure the integrity of the data, all monitoring procedures were subject to stringent Quality Control and Quality Assurance (QC/QA) protocols. The Division of Environmental Hygiene at the Institute for Medical Research and Occupational Health—accredited under EN ISO/IEC 17025:2017—serves as the national reference laboratory for PM measurements and chemical characterization. This laboratory implements standard operating procedures, regular instrument calibrations, and the use of certified reference materials to maintain data accuracy. Measurements of gaseous pollutants are performed by the Croatian Meteorological and Hydrological Service (https://meteo.hr/index_en.php), which adheres to similarly rigorous QC/QA guidelines. In addition to air pollution data, the Croatian Meteorological and Hydrological Service provided meteorological parameters, including temperature, relative humidity, wind speed, wind direction, atmospheric pressure, global solar radiation, and ultraviolet B (UVB) radiation, ensuring a comprehensive assessment of environmental conditions. Together, these integrated measures ensure that the collected air quality and meteorological data are both reliable and comparable over time, providing a solid foundation for subsequent environmental health assessments.

Figure 11. Locations of eight chosen measuring stations for air quality monitoring in the city of Zagreb, covering different residential areas, to provide a comprehensive overview of air pollution levels across the urban environment.

3.1.2. Pollutants and Analytical Methods

This study comprehensively assessed a range of air pollutants to evaluate their potential impact on environmental and public health. The measured parameters include: PM_{10} and $PM_{2.5}$, NO_2, O_3, BTEX, PAHs (a subset of 11 PAHs within the PM_{10} fraction), metals (selected metal isotopes), and pollen. The PAHs analyzed included fluoranthene (Flu), pyrene (Pyr), benzo[a]anthracene (BaA), chrysene (Chry), benzo[j]fluoranthene (BjF), benzo[k]fluoranthene (BkF), benzo[a]pyrene (BaP), dibenzo[ah]anthracene (DahA), benzo[ghi]perylene (BghiP), benzo[b]fluoranthene (BbF), and indeno[1,2,3-cd]pyrene (IP). The selected PAHs were chosen based on their regulatory and environmental relevance and established toxicological profiles. The panel included high- and mid-molecular-weight PAHs from the U.S. EPA's list of priority compounds, mandated for monitoring according to Directive (EU) 2024/2881 (EUR-Lex, 2024). In contrast, low-molecular-weight PAHs (e.g., naphthalene, acenaphthylene, acenaphthene,

fluorene, phenanthrene) were not included, as they predominantly partition to the gas phase under ambient conditions and are less stable in the particulate-bound fraction typically analyzed in PM_{10} (Račić et al., 2025).

3.1.2.1. Particulate Matter (PM)

Twenty-four-hour integrated samples of PM_{10} and $PM_{2.5}$ were collected on quartz filters (47 mm diameter, Whatman, UK) using low-volume samplers (LVS 3, Sven Leckel Ingenieurbüro GmbH, Germany) with an airflow of approximately 55 m^3/day. Each sampler was equipped with an impactor to segregate the desired particle fraction. Gravimetric analysis of the filters was conducted using an MX-5 microbalance (Mettler Toledo, USA) in accordance with the EN 12341:2014 standard for determining PM mass concentration.

3.1.2.2. Polycyclic Aromatic Hydrocarbons (PAHs)

Mass concentrations of 11 PAHs in the PM_{10} fraction were quantified by high-performance liquid chromatography coupled with a fluorescence detector (HPLC/FLD; Agilent Technologies, USA). The chromatographic separation was performed using a mobile phase composed of acetonitrile and water (60:40, v/v) at a flow rate of 1 mL/min. PAHs were first extracted from quartz filters using a solvent mixture (cyclohexene:toluene, 3:7, v/v) in an ultrasonic bath. After centrifugation, the extract was evaporated under a gentle nitrogen stream and re-dissolved in acetonitrile for analysis. Data quality was ensured through the analysis of a certified standard solution (EPA 610 PAH mix, Supelco, USA) and a certified reference material (SRM NIST 1649b, Urban Dust, Merck, Germany) (Jakovljević et al., 2015; Pehnec and Jakovljević, 2018; Šišović et al., 2012).

3.1.2.3. Toxic Metals

For the analysis of metals, PM filter samples were digested with 25% nitric acid (v/v) using a high-pressure microwave digestion system (Ultraclave IV, Milestone, Italy). The digested samples were then diluted with deionized water before analysis. Metal concentrations were determined by inductively coupled plasma mass spectrometry (ICP-MS; model 7500cx, Agilent Technologies). The following isotopes were selected for analysis: ^{55}Mn, ^{56}Fe, ^{60}Ni, ^{65}Cu, ^{66}Zn, ^{75}As, ^{111}Cd, and ^{206}Pb. Integration times were set at 0.5 sec for As and Cd and 0.1 sec for the other metals, with three acquisition points per peak. Internal standards—Sc, Ge, Rh, and Bi—were added

to correct for matrix effects. The ICP-MS was tuned to achieve an oxide ratio and a doubly charged ratio below 1.5% and operated in He mode. Instrument parameters were optimized to minimize interferences while maximizing sensitivity. Calibration curves were prepared from single-element stock solutions (1000 μg/mL, SCP SCIENCE) diluted in 5% HNO_3 (v/v) at eight concentration levels, with calibration performed immediately before sample analysis. The accuracy of the method was verified by analyzing PM_{10}-like reference materials (NIST 1648a and ERM CZ120, Merck) processed in the same manner as the samples, achieving recoveries ranging from 87% to 108% for the analyzed metals (Beslic et al., 2020; Vađić et al., 2013).

3.1.2.4. Benzene, Toluene, Ethylbenzene, and Xylenes (BTEX)

Airborne concentrations of BTEX compounds were measured using an automatic gas chromatograph (airmoVOC C2C12, Chromatotec, France), following the European standard EN 14662-3:2015. This instrument utilizes an absorbent trap for sample collection, followed by regulated thermal desorption and *in situ* gas chromatography with a flame ionization detector (FID). With two parallel channels operating alternately—each sampling for 15 min and then analyzing—the system provides continuous hourly average BTEX concentrations. The detection limit is 10 ppt (v/v), corresponding to approximately 0.032 $\mu g/m^3$ for benzene, 0.038 $\mu g/m^3$ for toluene, and 0.043 $\mu g/m^3$ for xylenes and ethylbenzene.

3.1.2.5. Nitrogen Dioxide (NO_2) and Ozone (O_3)

NO_2 and O_3 concentrations were continuously monitored using type-approved chemiluminescence and UV photometry instruments, respectively. The monitors operate according to the European standards EN 14211:2012 (for NO_2) and EN 14625:2012 (for O_3). These devices sample air automatically every second, and hourly average concentrations are calculated from the one-second data. The detection limits are 0.5 ppb (v/v), corresponding to approximately 0.94 $\mu g/m^3$ for NO_2 and 0.98 $\mu g/m^3$ for O_3 at standard temperature and pressure (25 °C and 101.3 kPa).

3.1.2.6. Pollen data

Pollen data were obtained from the official pollen monitoring program managed by the Teaching Institute of Public Health "Dr. Andrija Štampar, with funding provided by the Zagreb City Office for Social Protection, Health, War Veterans and People with Disabilities. Airborne pollen samples were collected using standardized volumetric spore traps (Hirst-type) located at

representative urban sites in Zagreb. These traps continuously capture pollen grains over specified sampling intervals according to established protocols recommended by the European Aeroallergen Network (EAN). Collected samples were processed and analyzed microscopically by trained palynologists. Pollen grains were identified to the major taxonomic groups (trees, grasses, and weeds) and quantified to generate daily concentration values. These data were then aggregated to produce a monthly pollen calendar that details the seasonal dynamics and peak periods of different allergenic pollens in Zagreb. The pollen calendar serves not only as a tool for monitoring airborne pollen but also aids in assessing potential correlations between pollen levels and respiratory health outcomes.

3.2. Study Participants and Sample Collection

3.2.1. Participant Recruitment and Eligibility

Participants were recruited from the general Croatian population residing in Zagreb wide urban region for at least one year. Recruitment was mainly conducted via flyers distributed throughout the community, which provided detailed information about the study and participation instructions. However, we also utilized mailing lists and an established database of volunteers from previous projects who had given consent to be contacted for participation in similar biomonitoring campaigns. Eligible participants were adults aged 18–55 years, with a body mass index (BMI) between 18.5 and 30 kg/m^2, and in generally good health at the time of blood sampling, with no signs of acute illness. Exclusion criteria included the use of antibiotics, corticosteroids, or cytostatic medications within one month prior to sampling, as well as exposure to diagnostic ionizing radiation in the same period, to minimize confounding effects on biomarker levels. Occasional or over-the-counter medications (e.g., analgesics or anxiolytics) were not considered exclusionary. All participants provided written informed consent and completed a comprehensive questionnaire capturing socio-demographic details, lifestyle factors (e.g., smoking, alcohol consumption, physical activity, time spent outdoors), and occupational and non-occupational exposures to potential chemical or physical hazards (including BTEX, pesticides, and radiation). The study was conducted in two distinct sampling periods: during the colder months (November–December 2021) and the warmer months (May–July 2022) to assess seasonal variations. Note that some participants dropped out between the two periods, and these losses were accounted for in the analysis.

3.2.2. Ethical Considerations

This study was approved by the Ethics Committee of the Institute for Medical Research and Occupational Health (approval code: 100-21/20-1; approval date: 14 January 2020) and the Ethics Committee of the Medical Faculty, University of Zagreb (approval code: 380-59-10106-23-111/70; approval date: 20 April 2023). All procedures adhered to ethical standards, ensuring the confidentiality and anonymity of participants and compliance with research ethics guidelines. The study was conducted following the principles outlined in the Declaration of Helsinki and applicable institutional and national regulations.

3.2.3. Biological Sample Collection and Processing

Biological samples (blood, urine, and buccal epithelial cells) were collected to enable a comprehensive evaluation of exposure and effect biomarkers (Figure 12). Venous blood was drawn in the morning by certified medical technicians using both heparin-coated and EDTA-coated tubes (Becton Dickinson, UK). Blood collected in heparin-coated tubes (Becton Dickinson) was used immediately for the comet assay, MN assay, and for BTEX analysis. The excess blood from the heparin-coated tubes was stored at -20 °C and later used for DNA extraction and methylation analysis of the FOXP3 gene. From EDTA-coated tubes, 100 μL aliquots were snap-frozen at -80 °C for subsequent elemental analysis and frozen comet assay. The remaining blood was centrifuged (Rotofix 32, Hettich, Germany) at 3000 rpm for 10 min to separate plasma. Plasma aliquots were stored at -80 °C for later oxidative stress analysis and additional element measurements. Additionally, the first void of the first morning urine was collected in sterile polypropylene containers (Deltalab, Spain) and stored at -20 °C until analysis. These samples were used to assess urinary PAH metabolites relevant to the study. Besides, buccal epithelial cells were collected using minimally-invasive swabs. These cells were immediately processed for the buccal MN assay to evaluate cytogenotoxic effects in the oral epithelium.

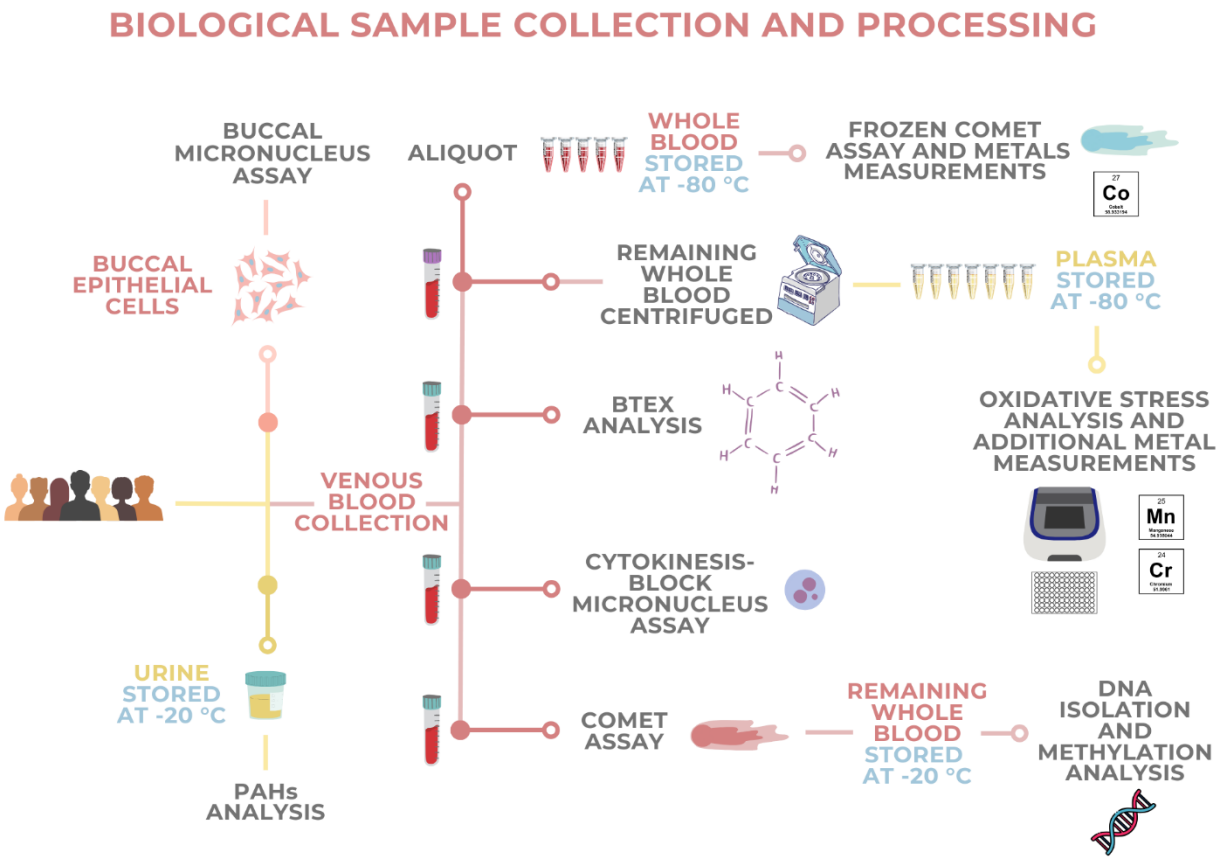

Figure 12. Overview of biological sample collection and processing. Venous blood was collected in heparin- and EDTA-coated tubes for various analyses. Heparinized blood was immediately used for the comet assay, micronucleus assay, and BTEX analysis, with samples stored at -20 °C for DNA extraction and methylation analysis. EDTA blood was aliquoted and snap-frozen at -80 °C for elemental analysis and frozen comet assay, while the remaining blood was centrifuged to obtain plasma, which was stored at -80 °C for oxidative stress and elemental measurements. First-morning urine was collected and stored at -20 °C for PAH metabolite analysis. Buccal epithelial cells were collected via non-invasive swabs and immediately processed for the buccal micronucleus assay.

3.3. BTEX Determination in Blood Samples

Blood concentrations of BTEX compounds were quantified using a modified headspace solid-phase microextraction (HS-SPME) method coupled with gas chromatography-mass spectrometry (GC-MS), based on the approach described by Karačonji and Skender (2007) (Figure 13). In brief, 1 mL aliquots of blood were transferred into 6 mL clear glass headspace vials, which were then sealed with butyl septa (Supelco) and holed aluminum caps (Macherey-Nagel, Germany). The vials were incubated at 50 °C for 1 h, after which a 10 mm silica fiber coated with

a 75 μm thick carboxen/polydimethylsiloxane (CAR/PDMS) film (Supelco) was exposed to the headspace for 15 min at the same temperature. Following extraction, the fiber was immediately inserted into a septum-equipped programmable injector (SPI), where analytes were thermally desorbed at 280 °C for 8 min. Chromatographic separation was achieved using a Varian 3400 CX gas chromatograph with a Saturn 4D ion trap mass spectrometer (Varian, USA) operating in electron impact (EI) mode. An HP-5MS Ultra Inert capillary column (30 m × 0.25 mm i.d., 0.25 μm film thickness; Agilent Technologies) was employed, with the oven temperature held at 40 °C for 1 min and then ramped to 150 °C at 8 °C/min. Helium served as the carrier gas at a constant flow rate of 1 mL/min. Ion monitoring was performed at *m/z* 78 for benzene and *m/z* 91 for toluene, ethylbenzene, and xylenes. Calibration curves were established by analyzing pooled blood samples (purged with dry nitrogen at 40 °C for 30 min) spiked with BTEX standards (Merck) over a concentration range of 50–1000 ng/L. Since *m*-xylene and *p*-xylene co-eluted under the selected conditions, they were quantified as a single parameter (*m/p*-xylene). The method demonstrated recovery rates between 90% and 96%, with precision expressed as relative standard deviations (RSD) ranging from 4% to 11%. The limits of detection (LOD), determined at a signal-to-noise ratio of 3, were 16 ng/L for benzene, 8 ng/L for ethylbenzene, 21 ng/L for toluene, 19 ng/L for *m*/*p*-xylene, and 14 ng/L for *o*-xylene.

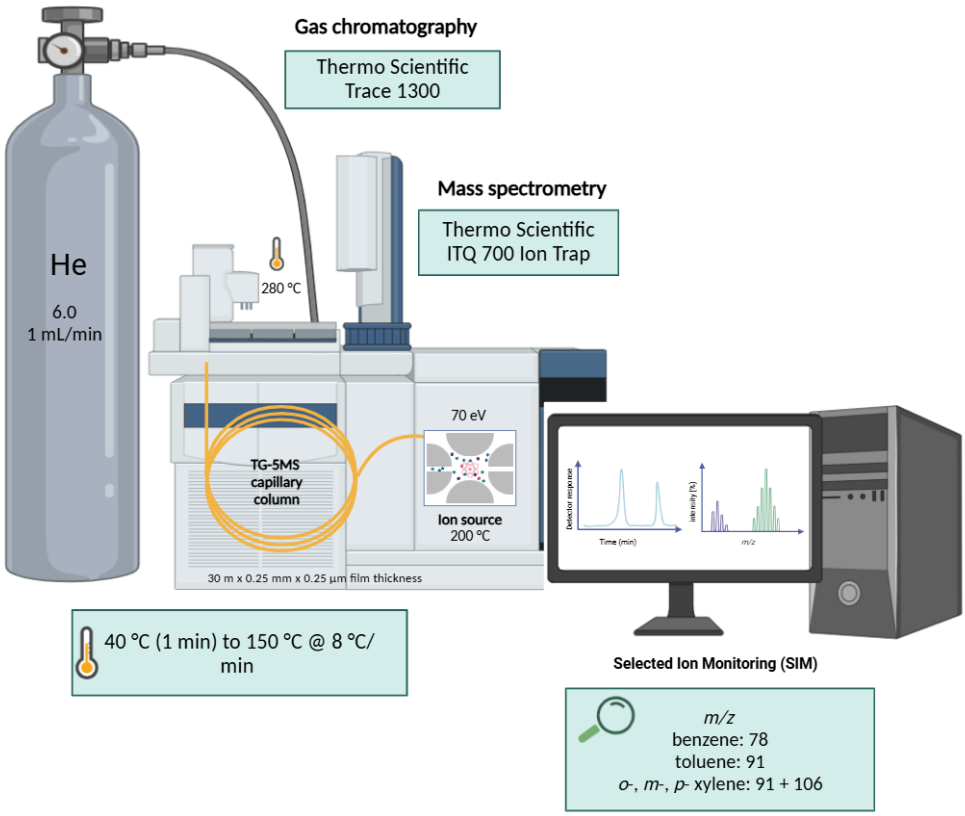

Figure 13. Schematic representation of the analytical setup for benzene, toluene, ethylbenzene, and xylenes (BTEX) determination in blood using headspace solid-phase microextraction (HS-SPME) followed by gas chromatography-mass spectrometry (GC-MS). Analysis was performed with a Trace 1300 GC coupled to an ITQ 700 Ion Trap MS (Thermo Fisher Scientific, USA). Separation was achieved on a TG-5MS capillary column using helium as the carrier gas. Selected Ion Monitoring (SIM) was applied for quantification, with *m/z* values of 78 for benzene, 91 for toluene, and 91 + 106 for xylene isomers.

3.4. Determination of PAHs in Urine Samples

Urinary concentrations of 1-hydroxypyrene (1-OHP) and 1- and 2-naphthol were quantified using high-performance liquid chromatography coupled with tandem mass spectrometry (HPLC-MS/MS). First, samples underwent enzymatic deconjugation with β-glucuronidase (from Helix pomatia, ≥100,000 units/mL) (Merck) to release conjugated metabolites according to the method of Jongeneelen et al. (1987). The deconjugated samples were then purified by solid-phase extraction (SPE) using C18 cartridges (Evolute Express, 60 mg/3 mL, Biotage, Sweden). Chromatographic separation was performed on a reverse-phase C18 column (Zorbax Eclipse Plus, 50 × 3.0 mm, 1.8 µm, Agilent Technologies) under a gradient elution. The mobile phase, consisting

of water and acetonitrile (ACN), was delivered at a flow rate of 0.5 mL/min with the following gradient: starting at 20% ACN, increasing to 70% over 3.9 min, then ramping to 100% at 4 min and held for 1.5 min, before returning to 20% ACN at 5.6 min, for a total run time of 9.6 min. Detection was carried out using a high-resolution mass spectrometer (Exploris 120, Thermo Fisher Scientific, USA) in multiple reaction monitoring (MRM) mode to enhance sensitivity and specificity. The monitored transitions were *m*/*z* 217.0659 for 1-OHP and m/z 143.0502 for both 1- and 2-naphthol. Calibration curves were constructed using standard solutions of 1-hydroxypyrene (100 mg, Merck) and 1 and 2-naphthol (1 mg/mL, Chiron, Norway) over the concentration ranges of 0.08–4.0 ng/mL for 1-OHP, 2.0–100 ng/mL for 1-naphthol, and 1.0–40 ng/mL for 2-naphthol. Quantification was achieved by comparing the peak areas from the samples to those from the calibration standards. The limits of quantification (LOQ) were determined to be 0.08 ng/mL for 1-OHP, 2 ng/mL for 1-naphthol, and 1 ng/mL for 2-naphthol.

3.5. Element Analysis in Blood and Plasma

The concentrations of toxic and essential elements in blood and plasma samples were determined using ICP-MS on an Agilent 8800 instrument (Agilent Technologies). Prior to analysis, blood and plasma samples were diluted at ratios of 1:70 and 1:20, respectively, using a diluent containing 3 µg/L of internal standards, 0.01 mM EDTA, 0.7 mM NH_3, and 0.07% (v/v) Triton X-100 (Merck) (Sekovanić et al., 2018). Instrument parameters were optimized with a tuning solution containing 1 µg/L of ^{7}Li, ^{59}Co, ^{89}Y, ^{140}Ce, and ^{205}Tl. Sample preparation and analysis were performed in a laboratory equipped with a Heating, Ventilation, and Air Conditioning (HVAC) system combined with High-Efficiency Particulate Air (HEPA) filters to minimize contamination. Calibration was carried out using working standards prepared from single-element stock solutions at multiple concentration levels, and the method's accuracy, which ranged from 93% to 115%, was verified by analyzing certified reference materials and through regular participation in the UK National External Quality Assessment Scheme (NEQAS) Interlaboratory Comparison Program for Trace Elements in blood and serum. In whole blood, trace elements measured included Mn, Co, As, Cd, Hg, Tl, and Pb, with concentrations expressed in µg/L. In plasma, the analysis focused on essential and trace elements, with Mg and Ca reported in mg/L, and Fe in mg/L as well, while Mn, Cu, Zn, Se, Mo, I, V, and Cr were quantified in µg/L. These elements were selected based on their critical roles in physiological processes and their potential implications for human health.

3.6. DNA Extraction and Methylation

To investigate the potential epigenetic effects of environmental exposures, we focused on the methylation status of the FOXP3 gene, a key transcription factor involved in the regulation and function of regulatory T cells (Tregs). DNA was extracted from whole blood samples and subsequently analyzed for methylation levels at specific CpG sites within the FOXP3 gene. Given the critical role of FOXP3 in immune homeostasis, alterations in its methylation profile may provide insights into immune dysregulation linked to environmental factors. The following sections describe the protocols used for DNA extraction and methylation analysis.

3.6.1. DNA Extraction from Whole Blood

Genomic DNA was extracted from whole blood samples using the DNeasy Blood & Tissue Kit (Qiagen, Merck) following the "Purification of Total DNA from Animal Blood or Cells (Spin-Column Protocol)" with minor modifications. The protocol is optimized for the efficient recovery of high-quality DNA by utilizing silica-membrane technology within spin columns. All steps were performed at room temperature (15–25 °C), and centrifugation steps were carried out using a Pico™ 21 Microcentrifuge (Thermo Fisher Scientific). For each extraction, 100 µL of anticoagulated whole blood was mixed with 20 µL of Proteinase K in a 1.5 mL microcentrifuge tube. To ensure a uniform processing volume, phosphate-buffered saline (PBS: 137 mM NaCl, 10 mM Na_2HPO_4, 2.7 mM KCl, and 1.8 mM KH_2PO_4, pH 7; Kemika, Croatia) was added to reach a final volume of 220 µL. Lysis was achieved by adding 200 µL of Buffer AL, which contains chaotropic salts to disrupt cell membranes and promote protein denaturation, followed by thorough mixing via vortexing. The mixture was then incubated at 56 °C for 10 min to enhance the efficiency of cell lysis. After incubation, 200 µL of 96–100% ethanol was added to facilitate DNA precipitation and subsequent binding to the silica membrane of the DNeasy Mini spin column. The lysate-ethanol mixture was transferred onto the spin column, which was placed in a 2 mL collection tube. Centrifugation at ≥6,000 × g (8,000 rpm) for 1 min allowed selective DNA adsorption while removing cellular debris and contaminants. The bound DNA underwent two sequential wash steps: first, 500 µL of Buffer AW1, a mild chaotropic buffer that removes proteins and polysaccharides, was added and centrifuged for 1 min; second, 500 µL of Buffer AW2, an ethanol-based wash buffer designed to eliminate residual salts, was applied, followed by centrifugation at 20,000 × g (14,000 rpm) for 3 min to ensure thorough membrane drying. For DNA elution, the spin column was placed

in a clean 1.5 mL microcentrifuge tube, and 200 µL of Buffer AE (10 mM Tris·Cl, 0.5 mM EDTA, pH 9) was applied directly onto the silica membrane. After a brief incubation at room temperature (1 min), DNA was eluted by centrifugation at ≥6,000 × g (8,000 rpm) for 1 min. The resulting DNA samples were quantified spectrophotometrically, yielding A260/A280 ratios of 1.7–1.9, indicating high purity suitable for downstream analyses such as DNA methylation.

3.6.2. DNA Methylation Analysis

3.6.2.1 Bisulfite Conversion of Total Genomic DNA

Genomic DNA isolated from blood was bisulfite converted using the EZ DNA Methylation-Gold Kit (Zymo Research Europe, Germany) according to the manufacturer's instructions. Briefly, 20 µL of DNA was treated with 130 µL of CT conversion reagent. The reaction was incubated in a thermal cycler according to the following protocol: 98 °C for 10 min, followed by 2 h and 30 min at 64 °C. The reaction mix was loaded onto a Zymo-Spin™ IC Column containing 600 µL M-Binding Buffer and centrifuged at 10,000 × g for 30 s. The column was washed with 100 µL of M-Wash Buffer. Next, 200 µL of M-Desulphonation Buffer was added to the column and incubated at room temperature for 20 min. After the incubation, the column was centrifuged at 10,000 × g for 30 s and washed two times by the addition of 200 µL of M-Wash Buffer. The column was placed into a 1.5 mL microcentrifuge tube, and the bisulfite-converted DNA was eluted in 10 µL of M-Elution Buffer.

3.6.2.2. PCR Amplification and Pyrosequencing

The converted DNA was used as a template for PCR amplification. A 197 bp fragment of the promotor region of FOXP3 was amplified using primers FOXP3 Fwd (5' GGTGAAGTGGATTGATAGAAAAGGATTAGT 3') and a biotinylated FOXP3 Rev_B primer (5' TATAAAAACCCCTCCCCACCC 3') with the PyroMark PCR Kit (Qiagen) according to the manufacturer's instructions. The PCR reaction mix contained 12.5 µL PyroMark PCR Master Mix, 2.5 µl CoralLoad (10×), 0.5 µL FOXP3 Fwd primer (10 µM) and 0.5 µL FOXP3 Rev_B primer (10 µM), 8 µl H_2O and 1 µL DNA template, and was carried out with the following settings: initial denaturation for 15 min at 95 °C; 50 cycles of 30 s at 95 °C, 30 s at 57 °C and 30 s at 72 °C; final extension for 10 min at 72 °C. The PCR products were analyzed by gel electrophoresis in a 1% agarose gel containing GelRed (Biotium, USA) for visualization of DNA.

The amplified fragments were pyrosequenced on the PyroMark Q24 Advanced instrument according to the manufacturer's protocol. First, biotinylated PCR products were immobilized on streptavidin coated Sepharose beads (Streptavidin Sepharose High Performance, GE Healthcare, USA). The immobilization mixture consisted of 1 µL Streptavidin Sepharose High Performance beads, 39 µL PyroMark Bindinig Buffer, 30 µL H_2O and 10 µL of the PCR product. The mixture was incubated for 10 min at room temperature with agitation and then processed on the PyroMark Q24 Vacuum Workstation. The sequencing primer was diluted to 0.3 µM in Annealing Buffer, and 25 µL of the diluted primer solution was added to each well of a PyroMark Q24 Plate. The sepharose beads containing the processed PCR product were released into the primer solution by gentle shaking. The sequencing primer was annealed by incubating the PyroMark Q24 Plate on the PyroMark Q24 Plate Holder at 80 °C for 2 min. After cooling, the samples were run on the PyroMark Q24 Instrument. The results of the pyrosequencing reactions were analyzed with the PyroMark Q24 Advanced Software, and the level of methylation of each CpG is shown as a percentage.

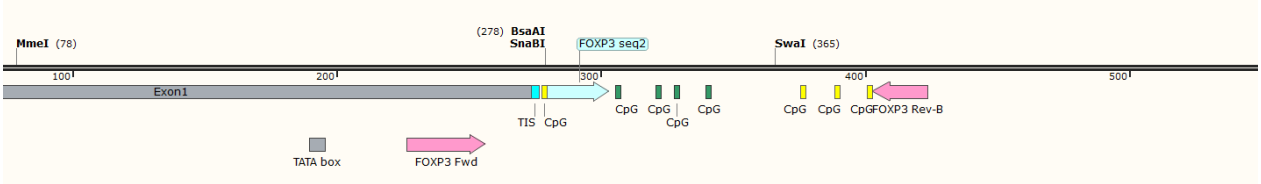

Figure 14. Position of PCR and sequencing primers in relation to exon 1 of the FOXP3 gene. Analyzed CpG dinucleotides are shown in green. TIS – transcription initiation site. Image was created using the SnapGene® software (from Dotmatics; available at snapgene.com).

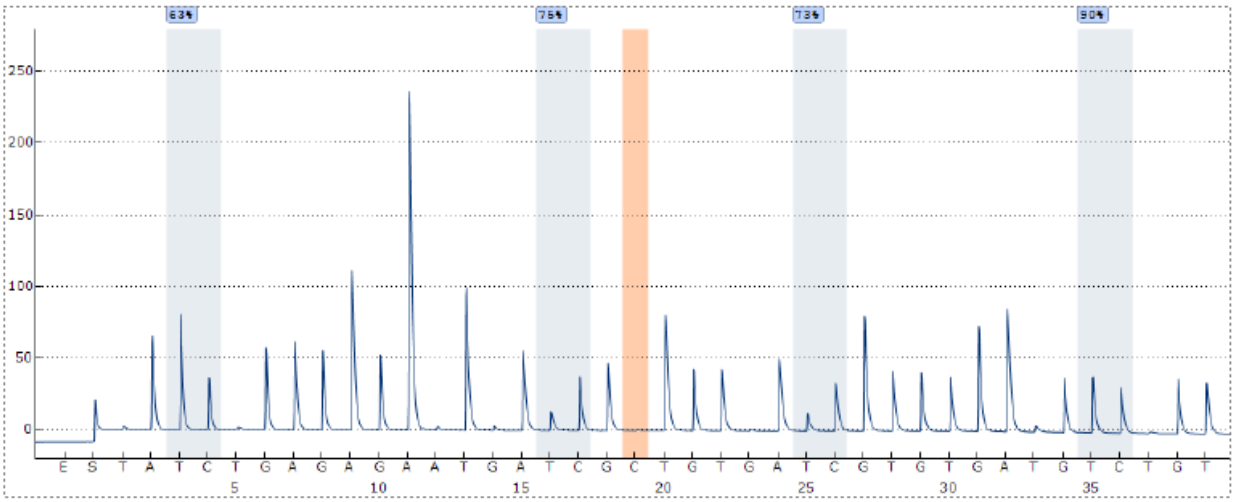

Figure 15. Pyrogram of the FOXP3 PCR product using the FOXP3 seq2 sequencing primer. Methylation of CpG dinucleotides is expressed as a percentage, and the blue squares indicate the highest quality assessment. Bisulfite conversion treatment control (C) is shown in orange highlight. The pyrogram is created using the PyroMark Q24 Analysis Software (QIAGEN).

3.7. Biomarkers of Oxidative Stress

To assess the biochemical impact of environmental exposures, a range of oxidative stress biomarkers in plasma were quantified. These biomarkers reflect both the direct damage caused by ROS and the capacity of the body's antioxidant defenses. In this chapter, the methodologies used to measure key parameters such as superoxide radicals, GSH, MDA, and the activities of antioxidant enzymes, including SOD, CAT and GPx, in addition to NO, are described.

3.7.1. Reactive Oxygen Species Determination in Plasma

The measurement of superoxide radicals was conducted using a dihydroethidium (DHE)-based fluorescent assay, following the protocol by Vujčić Bok et al. (2023) with minor modifications. A stock solution of DHE (Merck) was first prepared in dimethyl sulfoxide (DMSO) (Kemika) and then diluted to a final working concentration of 20 µM. Due to its sensitivity to oxidation and light exposure, the DHE solution was protected from light by wrapping the container in aluminum foil. Prior to the assay, plasma samples were gently thawed at room temperature and centrifuged at 10,000 rpm for 7 min to remove any cellular debris and ensure a clear matrix. For the assay, 50 µL of each plasma sample was dispensed in duplicate into black-bottom 96-well

plates, and an equal volume (50 µL) of the DHE working solution was added to each well. Blanks were prepared by combining 50 µL of water with 50 µL of DHE to correct for background fluorescence. The plates were then incubated at room temperature in the dark, and fluorescence was measured using a SpectraMax iD3 microplate reader (Molecular Devices, USA) with an excitation wavelength range of 480–520 nm and an emission wavelength range of 570–600 nm. Each plate was read twice to obtain technical replicates, and the final relative fluorescence unit (rFU) values were determined by averaging the replicates and subtracting the mean blank value for each plate.

3.7.2. Reduced Glutathione Determination in Plasma

The concentration of GSH in plasma was determined using a spectrophotometric assay, following the protocol by Duka et al. (2020) with minor modifications. This method is based on the reaction of GSH with 5,5'-dithiobis(2-nitrobenzoic acid) (DTNB, Merck), also known as Ellman's reagent. In slightly alkaline conditions (pH 7–8), DTNB reacts with the thiol (-SH) groups of GSH to form a yellow-colored 2-nitro-5-thiobenzoate (TNB) anion (Figure 16). The intensity of this yellow color, measured at 412 nm using a SpectraMax iD3 microplate reader, is directly proportional to the GSH concentration in the sample, as calculated via Lambert–Beer's law:

$$c = \frac{A}{\varepsilon}$$

Where c is GSH concentration, A is absorbance measured in the sample, and ε is the extinction coefficient for DTNB at 25 °C (14,150 M^{-1} cm^{-1}) (Eyer et al., 2003).

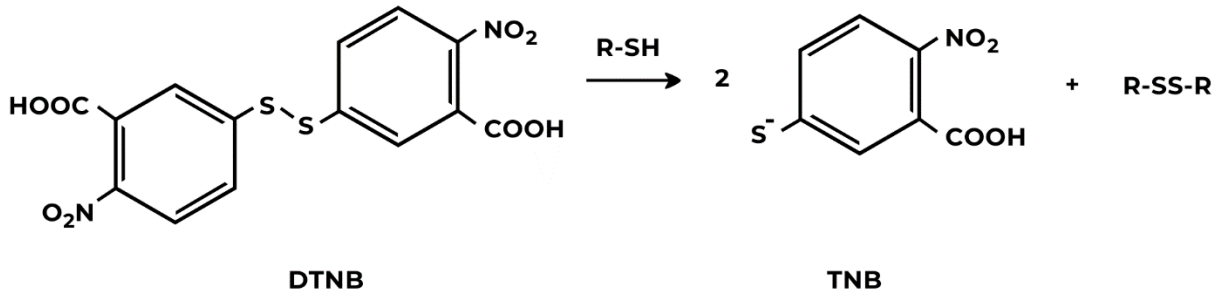

Figure 16. Ellman's Reagent Reaction. Under slightly alkaline conditions, 5,5′-dithiobis(2-nitrobenzoic acid) (DTNB) reacts with the free thiol group (R–SH) of reduced glutathione to yield the yellow-colored 5-thio-2-nitrobenzoate (TNB) and the corresponding disulfide (R–SS–R).

For the assay, plasma samples were gently thawed at room temperature and then analyzed in transparent-bottom 96-well plates (Greiner, Austria). In each well, 25 µL of plasma was mixed with 100 µL of PBS containing 0.1 mM EDTA (Merck), used to chelate metal ions and prevent GSH autoxidation, and 40 µL of a freshly prepared 1 mM DTNB solution (diluted in 1 M K-phosphate buffer). The reaction was allowed to proceed at room temperature, and absorbance was measured in duplicate. Blank wells (containing buffer and DTNB without plasma) were used to correct for background absorbance. The final GSH concentration was determined from the mean corrected absorbance value.

3.7.3. Malondialdehyde Determination in Plasma

The concentration of MDA in plasma was determined using a spectrophotometric assay, following the protocol by Domijan et al. (2015) with minor modifications. This method is based on the reaction of MDA with 2-thiobarbituric acid (TBA, Merck) under acidic conditions (Figure 17). In these conditions, TBA reacts with MDA to form a red-colored MDA-TBA_2 adduct, whose absorbance is measured at 532 nm. A 0.6% TBA solution was prepared by dissolving 0.6 g of TBA in 100 mL of distilled water with gentle heating to ensure complete dissolution. For the assay, 50 µL of plasma was mixed with 100 µL of the freshly prepared TBA reagent. From this mixture, 70 µL aliquots were pipetted into wells of a transparent 96-well plate (Greiner), and each sample was run in duplicate. Blank wells containing 50 µL of distilled water mixed with 100 µL of TBA reagent were included for background correction. The plate was incubated in a heating block (CB500 Hotplate, Stuart, UK) at 90 °C for 30 min to facilitate the formation of the MDA-TBA_2 adduct. Following incubation, the plate was rapidly cooled on ice to halt the reaction, and the absorbance was recorded at 532 nm using a SpectraMax iD3 microplate reader. MDA concentrations were calculated using Lambert–Beer's law with an extinction coefficient of 156 mM^{-1} cm^{-1} (Janero, 1990).

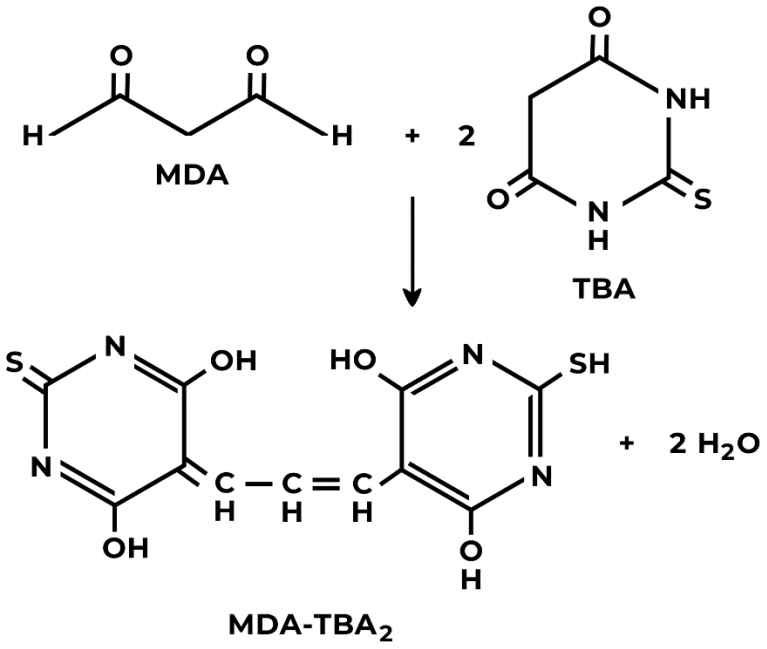

Figure 17. Reaction between malondialdehyde (MDA) and 2-thiobarbituric acid (TBA). Under acidic conditions and elevated temperature, MDA condenses with two equivalents of TBA to form the red-colored MDA–TBA_2 adduct, which can be measured spectrophotometrically.

3.7.4. Superoxide Dismutase Determination in Plasma

Plasma SOD activity was measured using the Superoxide Dismutase Assay Kit (Cayman Chemical, USA) according to the manufacturer's protocol, with minor modifications for our plasma samples. Prior to the assay, plasma samples were diluted fivefold in the assay buffer provided by the kit. To prepare the working reagent, all components were first equilibrated to room temperature. The tetrazolium salt solution and reaction buffer were combined as specified in the kit instructions, and the xanthine oxidase working solution was added immediately before use. Since the generation of superoxide radicals, and hence the reduction of the tetrazolium salt, is highly time-sensitive, the working reagent was prepared fresh and kept protected from light by wrapping in aluminum foil. For the assay, 20 µL of each diluted plasma sample (or SOD standard) was pipetted in duplicate into the wells of a transparent 96-well plate (Greiner). To each well, 200 µL of the freshly prepared working reagent was added, bringing the final volume to 220 µL per well. The reaction mixture was then incubated at room temperature in the dark for 30 min. During this time, superoxide radicals generated by the xanthine oxidase reduce the tetrazolium salt

to form a formazan dye, and the presence of SOD in the sample inhibits this reaction (Figure 18). The absorbance was measured at 450 nm using a SpectraMax iD3 microplate reader.

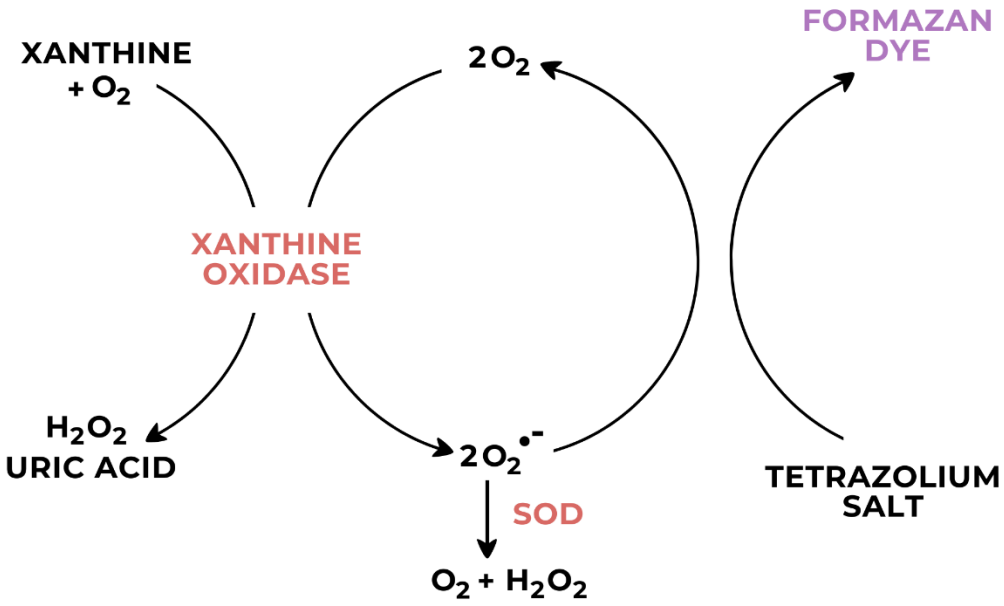

Figure 18. Scheme of the Superoxide Dismutase (SOD) Assay. Xanthine oxidase generates superoxide radicals (O_2^-) from xanthine and molecular oxygen, which then reduce a tetrazolium salt to form a colored formazan dye. The presence of SOD scavenges these superoxide radicals by catalyzing their dismutation into hydrogen peroxide (H_2O_2) and oxygen (O_2), thereby decreasing formazan formation and enabling the quantification of SOD activity.

The degree of inhibition of the formazan dye formation is inversely proportional to the SOD activity in the sample. SOD activity was calculated using the following formula:

$$\% \text{ Inhibition} = \left(\frac{A_{blank} - A_{sample}}{A_{blank}}\right) \times 100$$

where A_{blank} is the absorbance of the reaction without sample, and A_{sample} is the absorbance with plasma. A standard curve was constructed using serial dilutions of the SOD standard provided in the kit, and one unit of SOD activity was defined as the amount of enzyme required to inhibit the rate of formazan formation by 50%. SOD activity in the plasma samples (expressed in U/mL) was then determined by interpolating the percent inhibition from the standard curve and correcting for the fivefold dilution.

3.7.5. Glutathione Peroxidase Determination in Plasma

Plasma GPx activity was determined using the Glutathione Peroxidase Assay Kit (Cayman Chemical). Prior to the assay, plasma samples were diluted 1:2 in the provided assay buffer. All reagents and samples were equilibrated to room temperature before use. To prepare the working reagent, the assay buffer, a freshly prepared reduced GSH solution, glutathione reductase, and NADPH were combined according to the manufacturer's instructions. The hydroperoxide substrate was then added last to initiate the reaction; because the substrate is light-sensitive, all reagent preparation was performed under yellow dim light. For each reaction, 20 µL of the diluted plasma sample was added in duplicate into the wells of a transparent 96-well plate (Greiner), followed by 200 µL of the freshly prepared working reagent, resulting in a total volume of 220 µL per well. The plate was incubated at room temperature in the dark for 30 min, during which the GPx present in the sample catalyzed the reduction of the hydroperoxide by oxidizing GSH to glutathione disulfide (GSSG). In the presence of glutathione reductase and NADPH, GSSG was immediately recycled back to GSH with concomitant oxidation of NADPH to $NADP^+$. The decrease in NADPH absorbance was continuously monitored at 340 nm using a SpectraMax iD3 microplate reader (Molecular Devices) to obtain six time points. GPx activity was calculated using the following equation:

$$\text{GPX activity } \left(\frac{\text{U}}{\text{mL}}\right) = \frac{\Delta\text{A340/ min} \times V_{total}}{\varepsilon \times l \times V_{sample} \times \text{DF}}$$

where $\Delta A_{340/min}$ represents the change in absorbance per min, V_{total} is the final reaction volume (0.19 mL), ε is the molar extinction coefficient of NADPH (3.73 mM^{-1} cm^{-1}), l is the optical path length (assumed to be 1 cm), V_{sample} is the volume of plasma added (0.02 mL), and DF is the dilution factor (in this case three). The change in absorbance per min was obtained by plotting the absorbance values as a function of time to obtain the slope (rate) of the linear proportion of the curve.

3.7.6. Catalase Activity Determination in Plasma

CAT activity in plasma was determined using a spectrophotometric method that measures the decomposition of H_2O_2 (Kemika) by CAT, as described by Shangari and O'Brien (2006). In this assay, the enzymatic breakdown of H_2O_2 leads to a reduction in its concentration, which is

monitored as a decrease in absorbance at 240 nm over time using a kinetic program. Prior to analysis, plasma samples were first diluted 100-fold with 50 mM phosphate buffer (pH 7). The phosphate buffer was prepared by dissolving appropriate amounts of potassium dihydrogen phosphate (KH_2PO_4, Kemika) and dipotassium hydrogen phosphate (K_2HPO_4, Kemika) in Milli-Q water, adjusting the pH to 7, and diluting to a final volume. A 30 mM H_2O_2 solution was freshly prepared by diluting 0.34 mL of commercially available 30% H_2O_2 with the 50 mM phosphate buffer to a final volume of 100 mL. For the assay, 4 µL of plasma was mixed with 400 µL of the 50 mM phosphate buffer in an Eppendorf tube and then vortexed (Vortex-Heidolph REAX top, Heidolph Instruments, Germany) thoroughly. From this diluted plasma, 100 µL aliquots were transferred in triplicate into the wells of a UV-transparent 96-well plate (Greiner). To each well, 50 µL of the 30 mM H_2O_2 solution was added, and the plate was immediately placed in a plate reader (SpectraMax iD3) set to monitor absorbance at 240 nm every 30 s over a period of 1 min at 24 °C. The decrease in absorbance ($\Delta A_{(240)}$/min) reflects the rate of H_2O_2 decomposition and is directly proportional to catalase activity. CAT activity (expressed in U/mL, where one unit is defined as the amount of enzyme that decomposes 1 µmol of H_2O_2 per min) was calculated using the formula:

$$\text{Catalase Activity } \left(\frac{\text{U}}{\text{mL}}\right) = \frac{\Delta A_{blank} - \Delta A_{sample}}{\varepsilon \times l} \times \frac{d \times v}{V}$$

Where ΔA_{blank} and ΔA_{sample} are the changes in absorbance per min for the blank and the plasma sample, respectively, ε is the molar extinction coefficient of H_2O_2 at 240 nm (0.0436 $Lcm^{-1}mM^{-1}$), l is the optical path length (assumed to be 1 cm), d is the dilution factor (100), v is the total reaction volume (150 µL), and V is the volume of plasma used in the reaction (4 µL). Blank wells containing only 50 µL of 30 mM H_2O_2 and 100 µL of buffer (without plasma) were included for background correction. This method yields a sensitive and reproducible measure of catalase activity in plasma, serving as an important indicator of the antioxidant defense capacity against oxidative stress.

3.7.7. Nitric Oxide Determination in Plasma

Plasma NO levels were determined using a fluorescent assay based on the reaction of NO with a NO-sensitive fluorescent reagent DAF-FM (Chemodex, Switzerland), following a modified protocol from Abd El-Hay and Colyer (2017). Plasma samples were first centrifuged to ensure clarity, then diluted 1:1 in PBS. For each well of a black-bottom 96-well plate, 50 µL of the diluted

plasma sample was combined with 50 µL of a freshly prepared 5 µM solution of the fluorescent reagent in PBS. The plate was incubated at room temperature in the dark for 30 min to allow the formation of the fluorescent product, which is directly proportional to the NO concentration. Fluorescence was measured using a SpectraMax iD3 microplate reader with an excitation wavelength of 485 nm and an emission wavelength of 525 nm. Blank wells containing 50 µL of PBS and 50 µL of the reagent were included for background correction, and the final NO concentration was calculated by subtracting the blank signal from the sample readings.

3.8. Fractional Exhaled Nitric Oxide (FeNO) Measurement

FeNO was measured using the NIOX VERO® device (NIOX Group plc., UK) as a non-invasive biomarker of airway inflammation using a standardized chemiluminescence-based analyzer following the American Thoracic Society (ATS) and European Respiratory Society (ERS) guidelines (Dweik et al., 2011). The measurement procedure involved a controlled exhalation maneuver at a fixed flow rate of 50 mL/s, ensuring stable NO production from the airway epithelium while minimizing contamination from nasal NO sources. Participants were instructed to inhale fully to total lung capacity through a filtered mouthpiece and then exhale at a steady flow for at least 10 s. Interpretation of FeNO levels was based on ATS-defined cut-off values expressed in parts per billion (ppb): low (< 25 ppb), intermediate (25–50 ppb), and high (> 50 ppb).

3.9. The Cytokinesis-Block Micronucleus Assay in Peripheral Blood Lymphocytes

The CBMN assay was performed according to the protocol established by Fenech (2007), with minor modifications (Gajski et al., 2024). This method is widely used to assess chromosomal damage and genome instability by detecting MNi, NPBs, and NBUDs in binucleated cells.

Within 6 h of blood collection, 500 µL of whole blood was directly added to Chromosome Kit P tubes (Euroclone S.p.A., Italy), which contains all necessary supplements, including fetal bovine serum (FBS), phytohemagglutinin (PHA) for lymphocyte stimulation, and antibiotics (penicillin and streptomycin). Tubes were then gently inverted 3–4 times and incubated at 37 °C in a humidified 5% CO_2 atmosphere for a total of 69 h in a Heracell™ Vios 250i incubator (Thermo Fisher Scientific). At 44 h of incubation, Cytochalasin-B (Merck) was added at a final concentration of 6 µg/mL to prevent cytokinesis, allowing the formation of binucleated cells, which are required for the CBMN assay. After 69 h of incubation, lymphocytes were harvested

through a series of washing and fixation steps to ensure the preservation of cytoplasmic and nuclear structures. The entire culture content from each Chromosome Kit P tube was transferred into 15 mL conical centrifuge tubes using a Pasteur pipette and centrifuged (Rotofix 32) at 800 rpm (100 × g) for 8 min at room temperature. The supernatant was carefully removed, leaving behind the cell pellet, which was then resuspended in 5 mL of cold (4 °C) 0.9% NaCl saline solution. The suspension was gently mixed using a Pasteur pipette to prevent cell clumping and was left to stand at room temperature for 15 min to allow osmotic stabilization. This step was followed by another centrifugation at 800 rpm (100 × g) for 8 min, after which the supernatant was discarded. Fixation was initiated by adding 5 mL of cold methanol–acetic acid (3:1) fixative (Kemika) to the pellet. To enhance cytoplasmic preservation, 40 µL of formaldehyde was added. The suspension was gently mixed to ensure thorough fixation before being centrifuged again at 800 rpm (100 × g) for 8 min. The supernatant was discarded, and the fixation step was repeated three additional times, each time replacing the fixative with 5 mL of fresh cold fixative and gently resuspending the cells. This process was continued until the pellets appeared white, indicating complete removal of hemoglobin and other unwanted cellular components. After the final centrifugation, the supernatant was discarded, and the cell pellet was resuspended in a small volume (~0.5 mL) of cold fixative to obtain a dense suspension suitable for slide preparation. Fixed cell suspensions were carefully smeared onto microscope slides (VitroGnost Standard Grade, BioGnost, Croatia) and allowed to air dry overnight. Slides were then stained in 5% Giemsa solution (Merck) for 10 min at room temperature. After rinsing in tap water and air drying, slides were stored in a dust-free environment until analysis. Slide analysis was performed under light microscopy (Reichert Diastar 420, Germany) at 400× magnification. A 1,000 binucleated cells per participant were analyzed for MNi, NPBs, and NBUDs, following established cytogenetic criteria (Fenech, 2007; Fenech et al., 2003):

- MNi: Small, round or oval structures not linked to the main nuclei, with the same staining intensity as the main nuclei, but with a diameter of 1/16 to 1/3 of the main nucleus;
- NPBs: Continuous, DNA-containing structures linking two nuclei, whose width is not more than 1/4 of the diameter of the main nuclei, with the same staining intensity as the main nuclei;
- NBUDs: Small MN-like protrusions connected to the main nucleus.

To assess proliferation kinetics, 500 cells per participant were counted to determine the Cytokinesis-Block Proliferation Index (CBPI) using the formula

$$CBPI = \frac{1 \times M1 + 2 \times M2 + 3 \times (M3 + M4)}{N},$$

where *M1*, *M2*, *M3*, and *M4* are a number of cells with 1, 2, 3, or 4 nuclei, respectively, and *N* is a number of counted cells (500 in this case) (Kirsch-Volders et al., 2003).

Slide scoring was also done on unstained duplicate slides using the Metafer system (MetaSystems, Germany) (Figure 19). The Metafer system is an advanced automated image analysis platform designed for high-throughput cytogenetic assessments. It enables precise and reproducible scoring of various nuclear anomalies, including MNi. The system integrates a motorized microscope (Zeiss Axio Imager, Germany), high-resolution digital camera, and sophisticated image analysis software (Metafer 4.0) to detect and classify cellular structures based on predefined morphological criteria. The system's motorized stage allows precise slide scanning, while its autofocus and scanning algorithms ensure consistent image acquisition across the entire slide. A high-resolution digital camera captures images of binucleated cells under fluorescence conditions. The Metafer 4.0 image analysis software applies pattern recognition algorithms and machine-learning classifiers to identify and classify nuclear anomalies based on size, shape, fluorescence intensity, and spatial distribution. Although the system performs automated scoring, manual review by an expert cytogeneticist ensures accuracy and validation.

Figure 19. Metafer automated scanning system used for high-throughput slide analysis. The system consists of a high-resolution Zeiss Axio Imager microscope equipped with a motorized stage, a high-sensitivity camera, and dedicated Metafer software (MetaSystems, Germany) for automated detection and scoring of micronuclei and comet assay parameters (Rossnerova et al., 2011).

Slides were stained with DAPI (VECTASHIELD® Antifade Mounting Medium with DAPI (H-1200-10), Vector Laboratories, USA) to facilitate automated detection of MNi within binucleated cells. A minimum of 1,000 binucleated cells per slide were analyzed to allow comparison with conventional light microscopy scoring.

3.10. Buccal Micronucleus Assay

The BMN Assay was performed according to the protocol outlined by Thomas et al. (2009). Buccal cell samples were collected from participants using a clean, unused hard toothbrush following a standardized procedure to ensure consistency. Prior to sampling, participants were instructed to thoroughly rinse their mouths three times with tap or still bottled water to remove residual debris. Buccal cells were collected by scraping the inner cheek using ten circular motions per side. The collected material was immediately immersed in 15–20 mL of buccal cell buffer, ensuring that the entire toothbrush head was submerged in the solution. The buffer was prepared by dissolving 1.6 g Tris-HCl, 38 g EDTA (both from Merck), and 1.2 g sodium chloride (Kemika) in 600 mL of Milli-Q water (IMROH, Croatia), adjusting the volume to 1 L, and autoclaving at 121 °C for 10 min. Samples were stored in 50 mL conical tubes (TPP or Eppendorf, Germany) and processed within 2 h to ensure optimal cell recovery. Each sample was thoroughly mixed using a dedicated 10 mL syringe (BD, UK) and a 16G needle (BD, UK), followed by centrifugation at 600 × g for 10 min (if the supernatant still contained cells after centrifugation, centrifugation at increased g-force was repeat until clear) using a Megafuge ST Plus Series centrifuge (Thermo Fisher Scientific). The supernatant was discarded, and the pellet was resuspended in 10 mL of fresh buccal cell buffer. The sample was then filtered through a 100 µm nylon membrane filter (Millipore, UK) held inside a closed Swinnex filter holder (Millipore, UK) and sealed with a rubber gasket (Swinnex-gasket, Merck). The filtration process, facilitated by syringe pressure, removed debris and improved sample purity, and the filtrate was collected in a 15 mL conical tube (TPP, Germany). A second centrifugation at 600 × g for 10 min was performed (with increased force if necessary), and after discarding the supernatant, the pellet was resuspended in 1 mL of fresh buccal cell buffer and vortexed. The total cell count was determined using a Bürker-Türk counting chamber (Fein Optik, Germany), and the final concentration was adjusted to 8×10^4 cells/mL.

To prepare slides, cytocentrifugation was performed using the Cytospin 4 system (Epredia, Shandon Diagnostics Ltd., UK). Each slide (Vitrognost Ultragrade, Biognost) was mounted within

a cytocentrifuge assembly, including a filter card with holes for the funnel (Filter Cards, white, sample size 0.5 mL, Epredia), a sample funnel chamber (Thermo Fisher Scientific), and a metallic cytoclip holder (Epredia). Initially, 60 µL of buccal cell buffer was added to the funnel and centrifuged at 600 rpm for 6 min, followed by the addition of 120 µL of the prepared cell suspension and another round of cytocentrifugation under the same conditions. Given that the cytocentrifuge applies minimal force, centrifugation was measured in rpm instead of *g*-force. The slides were carefully removed from the cytoclip assembly to avoid disturbing the adhered cells and were air-dried for at least 30 min, followed by fixation in ethanol–glacial acetic acid (3:1) for 10 min (Kemika). After fixation and drying, Feulgen staining, a DNA-specific staining method, was applied to enhance nuclear structures for micronucleus (MN) identification. The staining process involved sequential immersion in 50% ethanol (1 min), 20% ethanol (1 min) (Kemika), and Milli-Q water (2 min), followed by hydrolysis in 5 M HCl (Kemika) at room temperature for 30 min. After hydrolysis, slides were rinsed under running tap water for 5 min and air-dried. Schiff's reagent (Merck) was applied for 30–60 min in the dark. After an additional drying step, slides were briefly immersed in Fast Green stain (5 mg/mL, Merck) for 5 s, washed twice with tap water and once with Milli-Q water, and left to dry overnight. Fluorescence microscopy (Olympus BX-51, Japan) was used to inspect the slides, after which 30 µL of Depex mounting medium (Merck) was applied to each sample spot, covered with 24 × 24 mm coverslips (Biognost), and left to air dry. Slides were stored in a dry box until analysis.

The analysis was performed by fluorescence microscopy (Olympus BX-51) at 1000× magnification under green fluorescence. A 1000 cells per sample were assessed for the frequency of basal cells, binucleated cells (proliferation parameters), and various cytotoxicity markers (cell death parameters), including condensed chromatin (early apoptosis), karyorrhectic cells (late apoptosis), pyknotic cells (early necrosis), and karyolytic cells (late necrosis). Additionally, 2000 differentiated buccal cells were examined for the presence of MNi, NBUDs, and broken egg structures (genotoxicity parameters), with their frequencies expressed per 1000 binucleated cells to ensure consistency in comparisons, following established criteria by Thomas et al. (2009):

- Basal cells**:** These cells have a smaller, more oval shape with a larger nucleus-to-cytoplasm ratio and a uniformly stained nucleus. The cytoplasm typically stains darker compared to differentiated cells.
- Differentiated cells: Larger with a smaller nucleus-to-cytoplasm ratio, uniformly stained and oval or round, indicating they are terminally differentiated. These cells do not exhibit mitosis.
- MNi: Cells containing one or more small, round or oval-shaped micronuclei, with a diameter ranging between 1/3 and 1/16 of the main nucleus. MNi have the same staining intensity and texture as the main nucleus. Only differentiated cells with uniformly stained nuclei are scored for MNi.
- NBUDs: Cells with a sharp constriction at one end of the nucleus, suggestive of nuclear material elimination. The nuclear bud is attached to the main nucleus and typically has a smaller diameter. A structure called a broken egg is a form of NBUD, characterized by a longer constriction that resembles a bridge, connecting the nuclear bud to the main nucleus. This bridge-like appearance distinguishes it from typical nuclear buds, which usually have a more compact connection.
- Binucleated cells: Cells with two main nuclei, often indicative of failed cytokinesis.
- Condensed chromatin: Cells that show aggregated chromatin, often in early apoptosis. The nucleus appears striated with extensive chromatin aggregation.
- Karyorrhectic cells: Cells with dense speckled chromatin, indicative of nuclear fragmentation.
- Pyknotic cells: Cells with a shrunken, intensely stained nucleus, indicating a stage of cell death.
- Karyolytic cells: Cells with a completely degraded nucleus, showing no Feulgen staining and appearing ghost-like, representing a very late stage of cell death.

3.11. Alkaline Comet Assay from Whole Blood

The alkaline comet assay was performed following the standardized protocol described by Collins et al. (2023) and Gajski et al. (2020b), adhering to the MIRCA guidelines (Møller et al., 2020). This technique was employed to assess DNA strand breaks in peripheral blood cells, with both fresh and frozen blood samples analyzed to evaluate potential genotoxic damage. No more

than two hours elapsed between sample collection and either performing the comet assay or freezing the samples for the frozen comet assay, with blood kept at 4 °C during this period.

For fresh blood samples, fully frosted glass slides (Surgipath, Leica Biosystems, Germany) were first coated with 1% normal melting point (NMP) agarose (Merck) and then carefully removed to create a clean, pre-coated surface. A second layer of 300 µL of 0.6% NMP agarose (Merck) was then applied and allowed to solidify. Following this, 5 µL of whole blood was mixed with 100 µL of 0.5% low melting point (LMP) agarose (Merck) and layered onto the prepared slide, followed by an additional 100 µL of LMP agarose to form a protective top layer. For frozen blood samples, 6 µL of whole blood was used following a rapid thawing step in a 37 °C water bath for 2-3 min, with all subsequent steps performed identically to those for fresh samples. After agarose solidification, the coverslips were removed, and slides were immersed overnight in a cold lysis solution (4 °C) to break down cellular and nuclear membranes, enabling access to DNA. The lysis solution was composed of 10 mM Tris-HCl, 100 mM Na_2EDTA, 1% sodium sarcosinate, and 1% Triton X-100 (all from Merck), along with 2.5 M NaCl and 10% DMSO (both from Kemika). Following lysis, slides were transferred into freshly prepared alkaline electrophoresis buffer consisting of 1 mM Na_2EDTA and 300 mM NaOH (both from Kemika), adjusted to pH 13 and maintained at 4 °C. The slides were incubated in this buffer for 20 min to allow DNA unwinding and expression of alkali-labile sites. Electrophoresis was then conducted using gel electrophoresis apparatus (Horizon 11.14, Life Technologies, Gibco, USA) at 1 V/cm across the platform for 20 min under the same alkaline conditions (4 °C). This step facilitated migration of DNA loops, forming the characteristic comet-like structures under fluorescence microscopy. After electrophoresis, slides were neutralized by three successive washes (5 min each) in 0.4 M Tris buffer (pH 7.5) to restore the DNA to its native conformation. The slides were then stained with 10 µg/mL ethidium bromide (Merck) and left for 10 min in the dark before washing with Tris buffer and analysis. Comet images were captured using an epifluorescence microscope (Leitz, Germany) at 400× magnification equipped with a fluorescence filter for ethidium bromide (λ_{ex} = 518 nm, λ_{em} = 605 nm). A 100 nuclei per individual were analyzed, and DNA damage was quantified using Comet Assay II software (Instem, USA). The following comet descriptors were evaluated:

- Tail Length (TL, µm) – The distance of DNA migration measured from the center of the comet head to the end of the tail.

- Tail DNA % (TI, %) – The percentage of total DNA in the tail, indicating the degree of DNA damage.
- Tail Moment (TM, arbitrary units) – A combined measure of tail length and tail intensity, reflecting overall DNA damage.

3.12. Statistical Analysis

All analyses were performed using R version 4.4.3. The primary packages employed for data manipulation and statistical modeling included dplyr, tidyverse, ggplot2, broom, leaps, lme4, and mediation. All descriptive statistics were computed for the colder and warmer seasons, and pooled measures were used in further analysis when it was decided to examine inter-seasonal correlations. Descriptive analyses, including histograms, density plots, and Q–Q plots, were generated for key variables.

3.12.1. Air Pollution Exposure Assessment and Composite Score Generation

To characterize exposure patterns and reduce dimensionality in the environmental dataset, hierarchical clustering was first performed on pollutant variables, not on individual-level data. The aim was to group pollutants with similar temporal behavior into coherent clusters that reflect shared sources or environmental dynamics. For each exposure window (one day, three days, and seven days), relevant ambient pollutant variables were selected, while meteorological parameters and pollen data were excluded from clustering. Variables with zero variance were removed, and a logarithmic transformation was applied to normalize the remaining pollutant values. The transformed data were then centered, and a correlation matrix was calculated. This matrix was converted to a dissimilarity matrix using the transformation $1 - |correlation|$, which captures similarity in pollutant behavior over time. Hierarchical clustering was conducted using the Ward.D2 method. To determine the optimal number of clusters, silhouette widths were computed for solutions ranging from two to five clusters, and the number of clusters yielding the highest average silhouette width was selected. Composite exposure scores were then generated by averaging the centered, log-transformed values of the pollutants within each identified cluster. A similar approach was applied to oxidative stress biomarkers to derive composite oxidative stress scores based on their intercorrelations. Pollen exposure was assessed separately, with counts (in particles per m^3) recorded for three categories—trees, grasses, and weeds—and summed for each

sampling event to obtain total pollen exposure. Finally, to evaluate the influence of meteorological variables on the derived composite scores, linear regression models were fitted using composite scores as dependent variables and temperature, atmospheric pressure, humidity, wind speed, and UVB radiation as predictors. Model diagnostics and residual analyses were performed to confirm validity, and statistical significance was assessed using p-values.

3.12.2. Exposure Biomarkers Assessment

Internal exposure biomarkers were quantified from biological specimens. In cases where a large proportion of observations were below detection limits (LOD), substitution methods were applied for exploratory analyses only, and those variables were excluded from further modeling.

3.12.3. Effect Biomarkers Assessment

Effect biomarkers were evaluated through multiple analytical approaches. For the comet assay, TI was selected as the key descriptor of DNA damage. For each participant, a mean TI value was calculated from individual cell measurements, and these subject-level means were used to compute group-level averages. Given the right-skewed distribution of TI values, log transformation was applied following inspection of density plots. Distributions of CBMN parameters and buccal MN were also examined using histogram plots. As expected, MN frequency followed an approximately Poisson distribution, reflecting the discrete and count-based nature of this endpoint. Immune function was characterized by measuring FOXP3 methylation and FeNO as indices of airway inflammation. Oxidative stress was assessed by hierarchical clustering of seven biomarkers that reflected pro-oxidant and antioxidant capacities. Multivariate regression and mediation analyses were used to explore the relationships between ambient exposures and biological effect biomarkers. Depending on the model, independent variables included composite exposure clusters, meteorological parameters, pollen levels, and socio-demographic factors, while dependent variables included FOXP3 methylation, TI, and MN frequencies. FeNO and oxidative stress composite scores were tested as potential mediators to assess indirect effects within these exposure–response pathways.

3.12.4. Statistical Modeling

Best subset regression analyses were performed using the *regsubsets()* function from the leaps package to identify influential predictors, selected based on adjusted R^2. Separate models

were built for different exposure timeframes. For endpoints measured repeatedly in the same subjects, random intercepts for subjects were incorporated to account for within-subject correlation. For count outcomes (e.g. MN), quasi-Poisson regression was used to accommodate overdispersion. In cases where repeated measures were present, generalized linear mixed models were fitted with observation-level random effects as needed. A mediation framework was specified to evaluate the hypothesized biological pathways (Bellavia et al., 2019). One approach assumed that pollen exposure affects FeNO indirectly through its effect on FOXP3 methylation, with FOXP3 serving as the mediator. The mediator model was specified as

$$FOXP3_{ij} = \alpha_0 + \alpha_1 \, log\big(Pollen_{ij}\big) + \alpha_2 CC + \alpha_3 covariates + \varepsilon_{ij}$$

and the outcome model was specified as

$$FENO_{ij} = \gamma_0 + \gamma_1 \, FOXP3_{ij} + \gamma_2 log\big(Pollen_{ij}\big) + \gamma_3 CC + \gamma_4 covariates + \mathrm{n}_{ij}.$$

In these equations, the subscript *i* indexes individual subjects, and *j* indexes the repeated measures or time points. The coefficients α represent the fixed-effect estimates in the mediator model, and the coefficients γ correspond to those in the outcome model. The indirect effect (average causal mediation effect, ACME) is computed as the product $\alpha_1 \times \gamma_1$, while the average direct effect (ADE) is given by γ_2; the total effect is then the sum of these components. Bootstrapping (with 1,000 simulations) was used to obtain robust confidence intervals for the mediation effects. Similar mediation pathways were explored for DNA and cytogenetic damage endpoints.

To assess model generalizability and minimize overfitting, five-fold cross-validation was applied to all predictive models using the caret package. The dataset was randomly partitioned into five equally sized subsets ("folds"). For each fold, the model was trained on the remaining four and evaluated on the held-out fold. This process was repeated five times so each fold served once as the test set. For generalized linear models (GLMs), such as those using a quasi-Poisson distribution for count outcomes, model performance was evaluated using a deviance-based pseudo R^2, which approximates the proportion of variance explained. Unlike traditional adjusted R^2 used in linear models, pseudo R^2 is adapted for non-Gaussian error structures and is computed from the deviance of the fitted model relative to a null model. To ensure model stability and interpretability, variance inflation factors (VIFs) were also calculated for all final models to assess multicollinearity among predictors.

4. RESULTS

Data from the study were first characterized with respect to the study population from questionnaires collected during the colder and warmer seasons. Demographic and lifestyle characteristics were compared across seasons, revealing modest differences in variables such as sex, age, BMI, residency duration, physical activity, and smoking status. Ambient air pollutant exposures were estimated for several time frames by linking participants' residential locations to nearby monitoring stations. Exposure data were averaged over one, three, and seven days preceding the sampling. However, the three-day data yielded a five-cluster solution that was less consistent with the one-day and seven-day profiles and introduced unnecessary complexity. Consequently, only the one-day and seven-day composite exposure scores were retained for further analysis. Internal exposure biomarkers, including BTEX in peripheral blood, urinary PAH metabolites, and elements in blood/plasma, were evaluated. In addition, correlations between the derived exposure composite scores and these biomarkers were assessed to characterize the relationships between external exposures and internal dose. The evaluation of effect biomarkers encompassed measurements of immune function (FOXP3 methylation and FeNO), oxidative stress, along with DNA and cytogenetic damage. DNA and cytogenetic damage were quantified using multiple assays, including the comet assay in blood cells and MN assay in both blood and buccal cells. Multivariate modeling and mediation analyses were performed to explore the direct and indirect pathways linking ambient exposures to these biological outcomes. For instance, direct associations and potential mediatory roles of oxidative stress in relation to DNA damage endpoints were examined. Together, these analyses provide a comprehensive assessment of the impact of ambient air pollution on internal exposure and effect biomarkers.

4.1. Study Population and Survey Data

The study was conducted over two distinct periods: the colder season (November–December 2021) and the warmer season (May–July 2022). Initially, 66 participants were recruited during the colder season. However, based on our exclusion criteria (as described in *3.2.1. Participant Recruitment and Eligibility*), a subset of these participants was excluded from the colder season analyses. Consequently, the effective sample size for the colder season was reduced (N=60). In contrast, during the warmer season, participants who were previously excluded due to these transient conditions were allowed to participate once they met the criteria, although some

participants were lost to follow-up (N=61). This resulted in a final sample of 57 pairs of participants who appeared in both sampling periods. The differences in sample composition between the two periods are reflected in demographic variables and responses obtained by the questionnaires. For example, some participants exhibited changes in BMI and lifestyle factors between the colder and warmer seasons. The descriptive statistics for key variables are presented separately for the colder and warmer periods, as well as in a combined dataset (Table 2).

Table 2. The population characteristics and lifestyle factors of the study population are shown as mean values ± standard deviation or N (%).

Season	**Cold**	**Warm**
	N=60	N=61
Sex		
female	34 (57%)	33 (54%)
male	26 (43%)	28 (46%)
Age (years)	36 ± 7	36 ± 7
BMI (kg/m^3)	23.6 ± 2.8	23.7 ± 2.7
Residency in Zagreb (years)	11 ± 11	25 ± 13
Physical activity level[1]		
high	33 (55%)	34 (56%)
intermediate	15 (25%)	10 (16%)
low	12 (20%)	17 (28%)
Daily time spent outdoors (h)	1.6 ± 1.0	2.5 ± 1.7
Family history of cancer	32 (53%)	37 (61%)
Active smokers[2]	8 (13%)	9 (15%)
Passive smokers	8 (13%)	8 (13%)

[1]The Godin-Shephard leisure-time physical activity questionnaire (Godin, 2011).

[2]Active smokers self-reported as smoking less than 15 cigarettes per day, thus categorised as light smokers

4.2. Air Pollution Exposure Assessment

For each study participant, exposure to air pollutants over three different time frames—one, three, and seven days—preceding the blood sampling was evaluated. This multi-time-frame approach was chosen because different health outcome biomarkers appear to respond over different exposure periods. For instance, comet assay descriptors (like TI) are more sensitive to short-term exposures (one- and three-day averages), whereas MN assay results reflect a longer exposure window (seven-day average). To estimate individual exposures, each participant's residential address was linked to the nearest air quality monitoring station. For each participant, the mean and standard deviation of pollutant concentrations were computed by averaging the individual exposure data points corresponding to the relevant time frame. Notably, exposure levels varied considerably among participants, reflecting the spatial heterogeneity of air pollutant levels across different monitoring stations and thereby providing a more accurate representation of actual environmental conditions. After filtering out missing values and performing a logarithmic transformation to stabilize variance, the data were used for subsequent multivariate analyses. Although raw exposure data are not presented here, the processed dataset served as the basis for advanced analyses, including variable clustering, factor analysis, and the investigation of meteorological influences on exposure patterns. These methods allowed us to derive composite scores that capture the underlying structure of the air pollutant mixture, which were subsequently linked to both meteorological conditions and health outcomes.

4.2.1. Exposure Composite Scores

In order to create meaningful exposure profiles, hierarchical clustering on the pollutant data for each of the previously mentioned time frames was performed. This approach grouped pollutants based on their similarity in concentration patterns, which were subsequently used to form composite scores. These composite scores capture the underlying structure of the pollutants and allow for a simplified representation of exposure. The one-day exposure clusters revealed Cluster 1, consisting of VOCs—including xylenes, benzene, and toluene—along with PAHs, PMs, Zn, and O_3. Cluster 2 was dominated by NO_2, Cu, Fe, Mn bound to PM_{10}, and ethylbenzene, while Cluster 3 grouped toxic metals including As, Cd, and Pb. For the three-day exposure, the clustering largely mirrored the one-day exposure, with Cluster 1 still dominated by PAHs, PMs and VOCs, but did not include PM_{10} bounded Zn. Cluster 2 remained focused on NO_2, while Cluster 3 still comprised

toxic metals in PM_{10} (As, Cd, Pb). Notably, Cluster 4 emerged with metals like Cu, Fe, Zn, and Mn. The fifth cluster centered on ethylbenzene, a pollutant appearing consistently across time frames, particularly in Cluster 2. For the seven-day exposure period, the clustering pattern further emphasized Cluster 1, which maintained the grouping of PAHs alongside xylene, benzene, PMs, and O_3. Cluster 2, in this case, focused on NO_2 and ethylbenzene, while Cluster 3 retained the grouping of toxic metals in PM_{10} (As, Cd, Pb). These findings highlight the evolving nature of air pollution exposure across different time periods, with PAHs consistently clustering together in Cluster 1 across all time frames and differences emerging in the toxic metals and traffic-related pollutants across the time periods. The dendrograms for the one-, three-, and seven-day exposures provide a clear visual representation of these variations (Figures 20-22). To evaluate the clustering quality, average silhouette widths were also calculated for each exposure window, with average silhouette values supporting the selected number of clusters (Supplementary Figures 1–3). Given the inconsistency and added complexity of the five-cluster solution obtained for the three-day exposure frame, it was opted not to include it in further analyses. Instead, the focus was on the one- and seven-day time frames, which provided more stable, interpretable, and comparable composite scores.

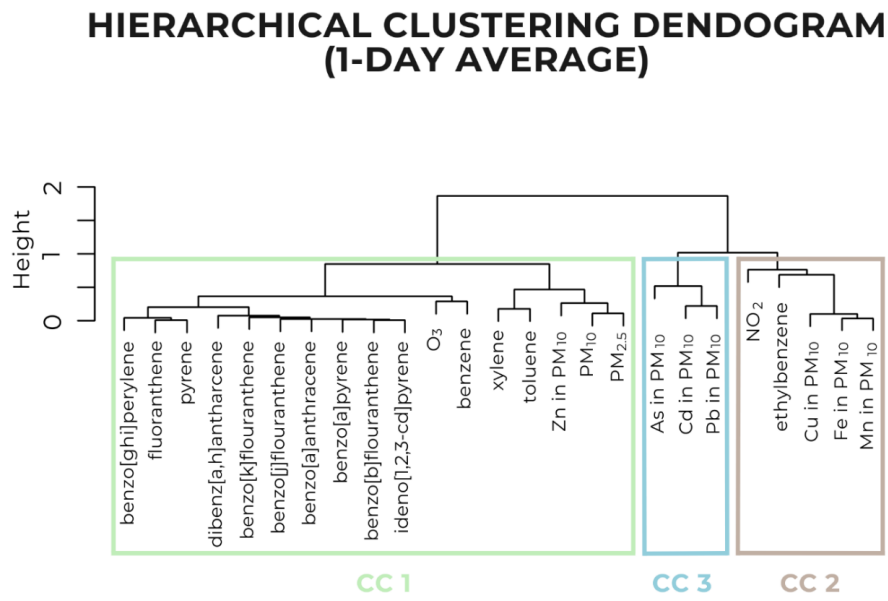

Figure 20. Dendrogram showing air pollutant clustering for a one-day exposure time frame. Hierarchical clustering was performed on one-day exposure data for air pollutants. The dendrogram is color-coded to highlight the distinct clusters. The labels in the dendrograms represent the specific air pollutants later included in creating each composite cluster (CC).

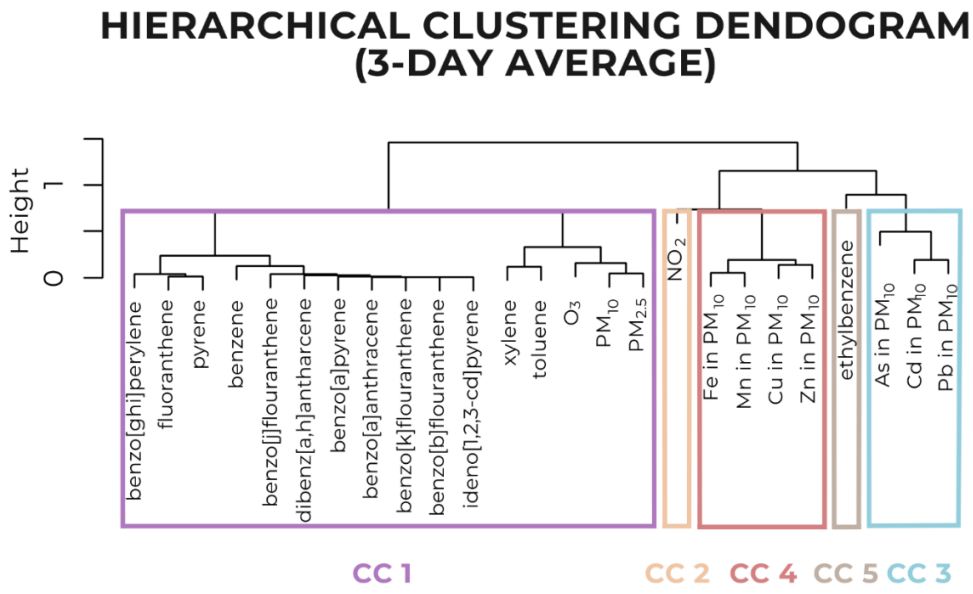

Figure 21. Dendrogram showing air pollutant clustering for a three-day exposure time frame. Hierarchical clustering was performed on three-day exposure data for air pollutants. The dendrogram is color-coded to highlight the distinct clusters. The labels in the dendrograms represent the specific air pollutants later included in creating each composite cluster (CC).

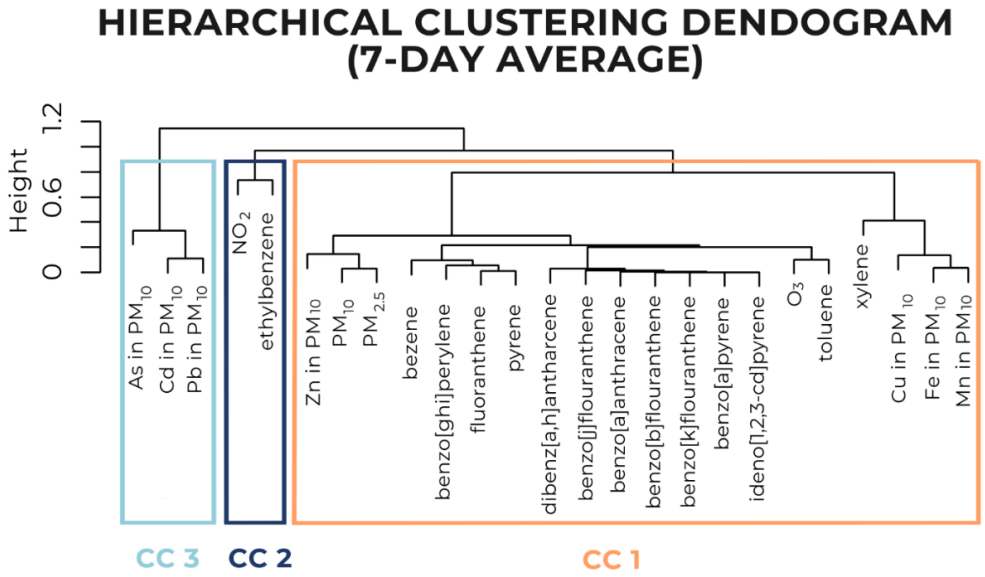

Figure 22. Dendrogram showing air pollutant clustering for a seven-day exposure time frame. Hierarchical clustering was performed on seven-day exposure data for air pollutants. The dendrogram is color-coded to highlight the distinct clusters. The labels in the dendrograms represent the specific air pollutants later included in creating each composite cluster (CC).

4.2.2. Meteorological Influence on the Exposure Composite Clusters

To explore the meteorological influences on the exposure clusters, multivariate linear regression modeling was used to examine the relationships between the derived composite scores and several meteorological variables. Predictor variables included one- or seven-day average values for temperature, atmospheric pressure, relative humidity, wind speed, and UVB radiation. All predictor variables were retained across the models, as the primary aim was to evaluate their individual associations with each cluster rather than optimize predictive performance. For the one-day exposure clusters, the results show that Composite Cluster 1 (CC1) is significantly influenced by atmospheric pressure and UVB radiation (Figure 23). Composite Cluster 2 (CC2) is mainly influenced by atmospheric pressure, humidity, and UVB radiation, while Composite Cluster 3 (CC3) showed a stronger influence of atmospheric pressure and marginal effects from UVB, which suggests a slightly different meteorological relationship from CC1 and CC2. The results for the seven-day exposure clusters revealed a more consistent relationship with meteorological variables across CC1 and CC2 (Figure 24). CC1 was strongly influenced by temperature, pressure, humidity, wind speed, and UVB radiation. CC2 was similarly influenced by temperature, atmospheric pressure, and UVB radiation. CC3, on the other hand, showed atmospheric pressure and humidity as the only significant meteorological predictors. Cross-validated R^2 estimates showed excellent and consistent predictive performance for CC1 across both one-day (mean $R^2 = 0.93$, SD = 0.04) and seven-day (mean $R^2 = 0.96$, SD = 0.01) models. CC2 and CC3 demonstrated more modest performance, particularly at the seven-day time frame, where mean R^2 dropped to 0.33 and 0.30, respectively, with higher variability between folds. These results indicate that CC1 is more strongly and reliably associated with meteorological conditions, while CC2 and CC3 may reflect more complex or non-meteorological influences. A visual summary of the explained variance for each model is provided in Supplementary Figure 4, which displays the proportion of variance in each CC accounted for by the included meteorological variables. CC1 shows consistently high predictive accuracy in both time frames, particularly in the seven-day model ($R^2 = 0.95$), supporting its close linkage with ambient meteorological dynamics.

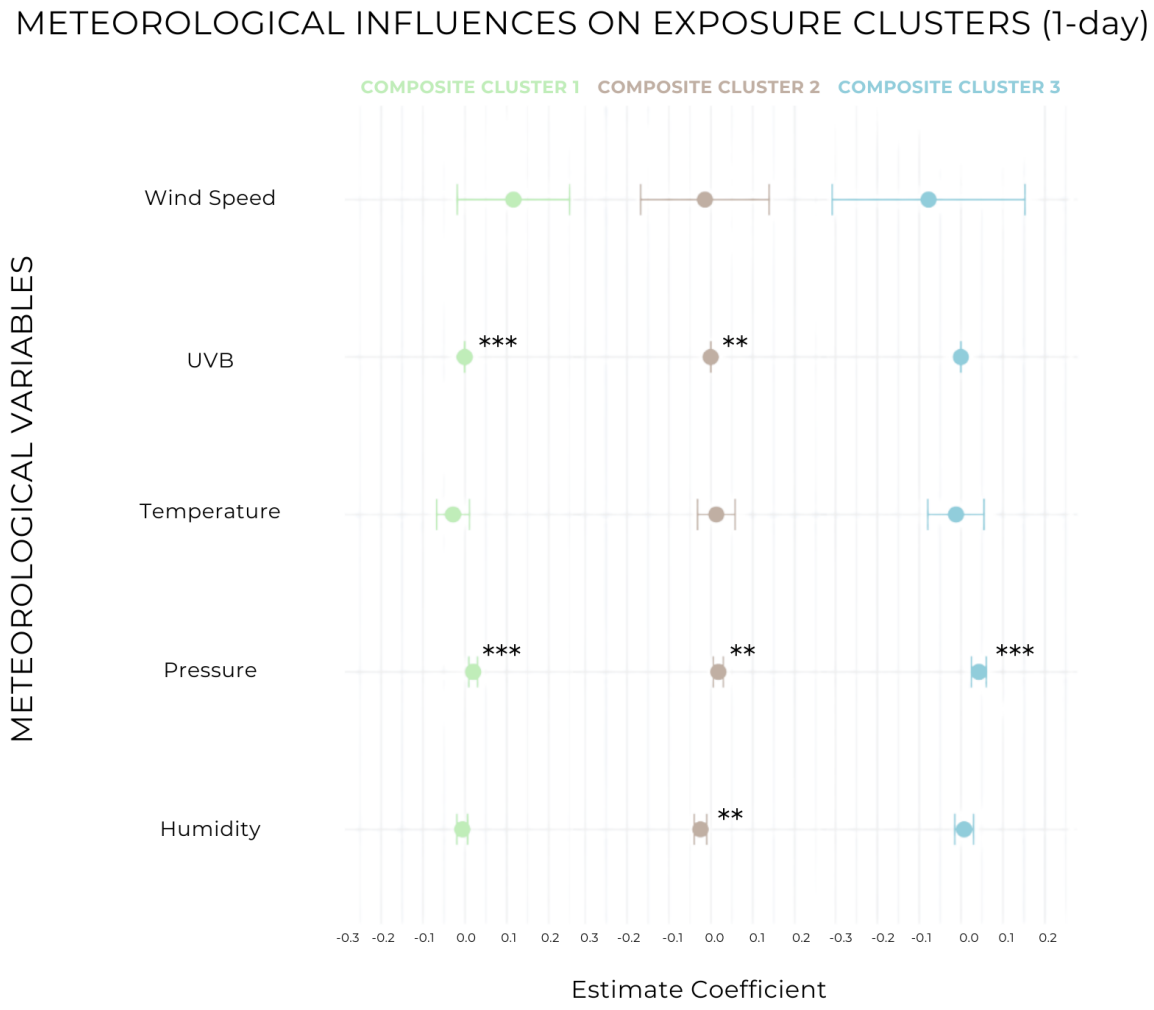

Figure 23. Meteorological Influences on Exposure Clusters (1-Day). This plot shows the results of the multivariate linear regression modeling the influence of meteorological variables on the one-day frame composite exposure clusters. The estimates for each meteorological variable across different clusters are plotted with their corresponding confidence intervals. Significant predictors are marked with * ($p < 0.05$), ** ($p < 0.01$), *** ($p < 0.001$).

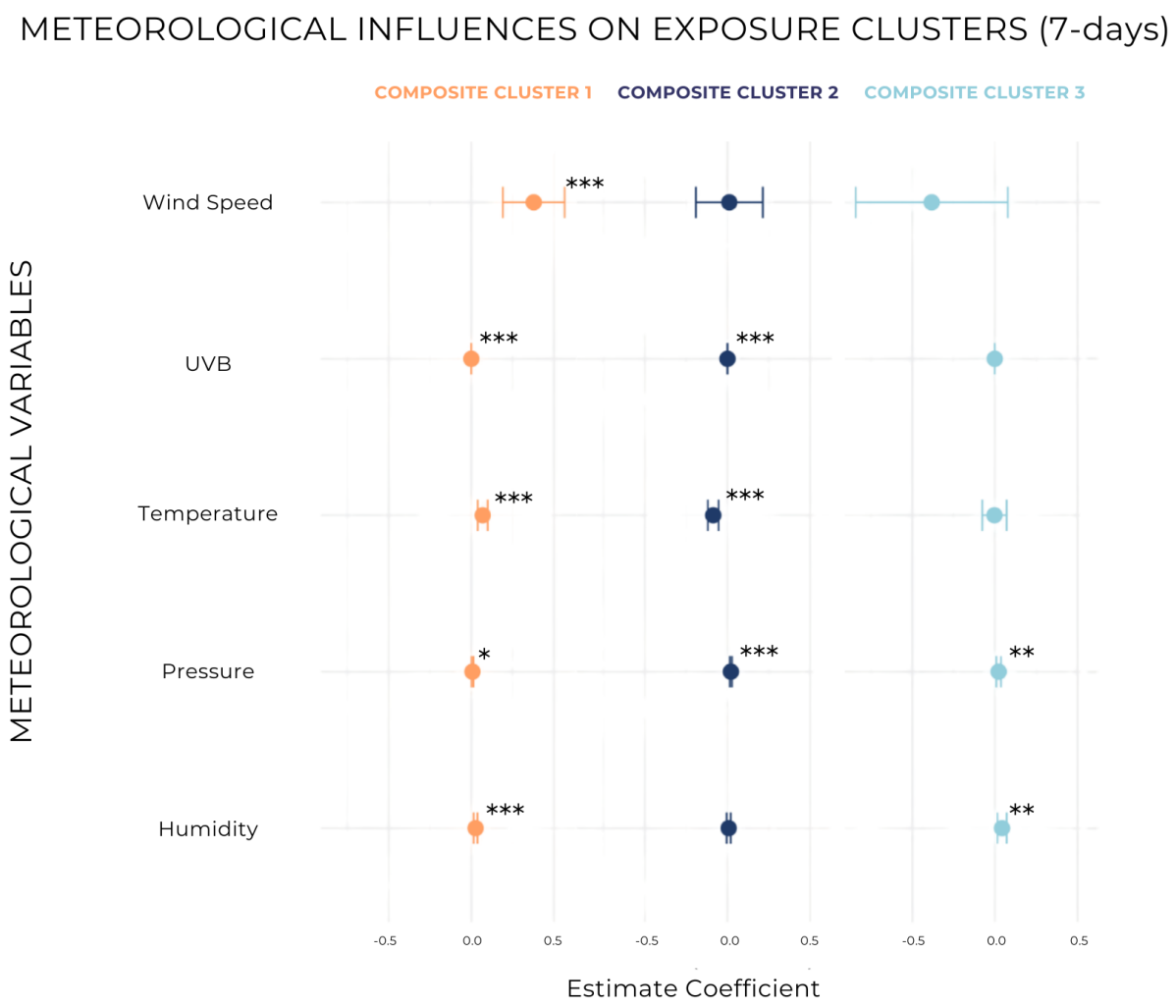

Figure 24. Meteorological Influences on Exposure Clusters (7-Day). This plot shows the results of the multivariate linear regression modeling the influence of meteorological variables on the seven-day frame composite exposure clusters. The estimates for each meteorological variable across different clusters are plotted with their corresponding confidence intervals. Significant predictors are marked with * ($p < 0.05$), ** ($p < 0.01$), *** ($p < 0.001$).

4.3. Exposure Biomarkers Assessment

In addition to estimating ambient exposures, internal exposure biomarkers were measured to assess the individual dose of air pollutants. BTEX compounds in peripheral blood were quantified and reported as medians and ranges stratified by season; however, because a large proportion of BTEX values fell below the detection limit—particularly during the warm season—the substitution method (assigning half the LOD) was used only for exploratory correlation analyses, and these variables were not incorporated into subsequent modeling. Urinary PAH

metabolites were also measured, but only 2-naphthol was carried forward for further analysis, as 1-naphthol and OH-pyrene were frequently below detection limits. Metal concentrations in blood and plasma were found to be similar between seasons; therefore, an overall pooled mean was used to enhance statistical power and simplify interpretation. Spearman's rank correlations were computed between the exposure composite clusters and these internal biomarkers to explore their interrelationships.

4.3.1. BTEX in peripheral blood samples

Median values and ranges for measured BTEX in peripheral blood samples of the participants, stratified by season, are presented in Table 3. In each case, the lowest values in the range fell below the LOD. During the colder season, the percentages of participants with BTEX levels below the LOD were 8.3% for benzene, 10% for toluene, 38.3% for ethylbenzene, 38.3% for *m-/p*-xylene, and 60% for *o*-xylene. In contrast, during the warm season, the BTEX levels were substantially lower, with values below the LOD for 98.4% of participants for benzene, 29.5% for toluene, 100% for ethylbenzene, 75.4% for *m*-/*p*-xylene, and 100% for *o*-xylene. These BTEX measurements were only incorporated into the correlation plots after assigning half the LOD to values that were below the detection limit; however, they were not further used in additional statistical modeling or hypothesis testing. This decision was made because the high proportion of <LOD values, particularly in the warm season, compromises the reliability and validity of the data for robust quantitative analysis. When such a large fraction of observations falls below the detection threshold, the substitution approach (e.g. assigning half the LOD) can introduce significant bias and reduce the statistical power of further analyses. Therefore, while the correlation plots provide an exploratory overview, these BTEX variables were excluded from subsequent modeling to ensure the integrity and interpretability of the statistical findings.

Table 3. Median values and range for measured benzene, toluene, ethylbenzene, *m-/p*-xylene and *o*-xylene (BTEX) in peripheral blood of the participants across two seasons.

Season	**Colder** N = 60	**Warmer** N = 61
Benzene (ng/L)		
Median (range)	47 (< LOD – 117)	[1](< LOD – 124)
Toluene (ng/L)		
Median (range)	65 (< LOD – 911)	86 (< LOD – 254)
Ethylbenzene (ng/L)		
Median (range)	30 (< LOD – 554)	all values < LOD
***m-/p*-Xylene (ng/L)**		
Median (range)	193 (< LOD – 673)	[1](< LOD – 431)
***o*-Xylene (ng/L)**		
Median (range)	[1](< LOD – 278)	all values < LOD

Limit of detection (LOD) values: 16 ng/L for benzene, 8 ng/L for ethylbenzene, to 21 ng/L for toluene, 19 ng/L for m/p-xylene, 14.2 ng/L for o-xylene

[1]more than half of the values are < LOD

4.3.2. Urinary PAH Metabolites

Descriptive statistics for 1-naphthol, 2-naphthol, and OH-pyrene measured in urine during colder and warmer seasons is summarized in Table 4. For samples below the LOD, the measured concentrations were replaced by the LOD value (1 ng/mL for 1-naphthol, 0.5 ng/mL for 2-naphthol, and 0.04 ng/mL for OH-pyrene). During the colder season, 71.7% of the measured 1-naphthol values were below the LOD, yielding a median equal to the LOD. In contrast, 2-naphthol had no observations below its LOD of 0.50 ng/mL, and its concentrations spanned a wider range, up to 43.9 ng/mL. For OH-pyrene, only a small fraction of samples (5%) were below the LOD, with measured concentrations generally remaining below 1 ng/mL. In the warmer season, the overall pattern remained consistent: 1-naphthol showed 73.3% of samples below the LOD, with the highest value (8.4 ng/mL) being lower than the maximum measured in the colder season. No 2-naphthol measurements fell below 0.5 ng/mL, suggesting consistently higher levels for this metabolite across participants. OH-pyrene was once again rarely below the LOD (6.6%), with a maximum

value reaching 1.1 ng/mL. Collectively, these data illustrate that, although 1-naphthol frequently appears at or below its LOD, the other metabolites typically reside above detection limits but can range substantially in concentration. Given the high frequency of values below the LOD for 1-naphthol, it was considered an unreliable variable for further modeling and hypothesis testing—any substitution (i.e. using half the LOD or the LOD value) would likely introduce bias and reduce statistical power. Although OH-pyrene concentrations were above the LOD in the majority of samples, measured levels were consistently low and exhibited minimal variability, with most values clustered tightly between 0.04 and 0.4 ng/mL. This narrow dynamic range limits the metabolite's ability to reflect inter-individual differences in PAH exposure and undermines its statistical utility in regression and mediation models. Therefore, despite their inclusion in exploratory correlation plots, only 2-naphthol, which was robustly detected across all samples, was carried forward for further statistical comparisons. To determine whether 2-naphthol concentrations significantly differed between the cold and warm seasons, we conducted a Mann–Whitney U test. This nonparametric test was chosen because the data did not meet the assumptions of normality. The results indicated no statistically significant difference in the distribution of 2-naphthol levels between the seasons.

Table 4. Urinary PAH metabolites median values and range across two seasons.

Season	**Cold** N = 60	**Warm** N = 61
1-Naphthol (ng/mL)		
Median (range)	[1](< LOD – 16.9)	[1](< LOD – 8.4)
2-Naphthol (ng/mL)		
Median (range)	8.3 (0.9 – 43.9)	7.8 (< 1.2 – 42.9)
OH-Pyrene (ng/mL)		
Median (range)	0.2 (< LOD – 1.3)	0.1 (< LOD – 1.1)

Limit of detection (LOD) values: 1 ng/mL for 1-naphthol, 0.5 ng/mL for 2-naphthol, and 0.04 ng/mL for OH-pyrene

[1]more than half of the values are < LOD

4.3.3. Metals in peripheral blood and plasma samples

The mean and SD values of metal concentrations measured in peripheral blood and plasma samples from study participants during the colder and warmer seasons are presented in Table 5.

Table 5. Metals in peripheral blood and plasma samples shown as mean values ± standard deviation for cold and warm seasons.

		Colder (N = 60**)**	**Warmer** (N = 61)
Blood	**As (µg/L)**	2.94 ± 3.50	3.12 ± 3.74
	Cd (µg/L)	0.44 ± 0.58	0.40 ± 0.42
	Co (µg/L)	0.30 ± 0.19	0.32 ± 0.22
	Hg (µg/L)	3.42 ± 4.32	3.21 ± 3.51
	Mn (µg/L)	7.08 ± 2.68	7.39 ± 2.65
	Pb (µg/L)	13.57 ± 9.26	13.11 ± 8.79
	Tl (µg/L)	0.03 ± 0.02	0.02 ± 0.01
Plasma	**Ca (mg/L)**	104.43 ± 4.78	104.59 ± 4.30
	Cr (µg/L)	0.20 ± 0.15	0.23 ± 0.09
	Cu (µg/L)	552.69 ± 122.68	560.77 ± 99.78
	Fe (mg/L)	1.27 ± 0.44	1.20 ± 0.48
	I (µg/L)	59.57 ± 11.09	60.4 ± 10.77
	Mg (mg/L)	21.98 ± 1.72	22.05 ± 1.84
	Mn (µg/L)	0.70 ± 0.28	0.86 ± 0.33
	Mo (µg/L)	0.90 ± 0.40	0.94 ± 0.43
	Se (µg/L)	92.73 ± 10.19	94.34 ± 10.44
	V (µg/L)	0.04 ± 0.01	0.05 ± 0.01
	Zn (µg/L)	1066.33 ± 184.56	1157.47 ± 102.01

The concentrations of all metals were quite similar between the two seasons. For example, As was 2.94 ± 3.50 in the colder season versus 3.12 ± 3.74 in the warmer season; likewise, Cu was 552.69 ± 122.68 compared to 560.77 ± 99.78, and Pb in blood was 13.57 ± 9.26 versus 13.11 ± 8.79. Given these minimal differences, an overall pooled mean will be used in subsequent analyses to improve statistical power and simplify interpretation.

4.3.4. Correlation of Air Pollution Clusters with Exposure Biomarkers

To explore the relationships between ambient air pollutant exposures and internal biomarkers, we computed Spearman's rank correlations across two different timeframes. We specifically examined the correlations between clustered air pollutants and biomarkers measured in blood (BTEX and metals) and urine (naphthols and OH-pyrene), considering correlations with p-values less than 0.05 as statistically significant.

In the one-day exposure analysis (Figure 25A), very strong positive associations were observed between BTEX compounds and all exposure composite clusters (CCs). For instance, benzene and toluene were significantly correlated with every CC, while ethylbenzene and *m/p*-xylene were strongly associated with CC1 and CC3, and *o*-xylene was significantly correlated with CC1. Additionally, plasma Fe showed a significant positive correlation with CC2—which is primarily composed of PM_{10}-bound Fe among a few other airborne metals, ethylbenzene, and NO_2. In contrast, the urinary biomarkers 1-naphthol, 2-naphthol, and OH-pyrene generally yielded higher p-values and did not show significant associations with the CCs. For the seven-day exposure window (Figure 25B), the overall correlation patterns were quite similar, with CC1 and CC3 remaining strongly positively correlated with all BTEX components. However, CC2 exhibited a mild positive association with 2-naphthol and a negative correlation with *m/p*-xylene, highlighting some subtle shifts in pollutant behavior over a wider exposure time frame.

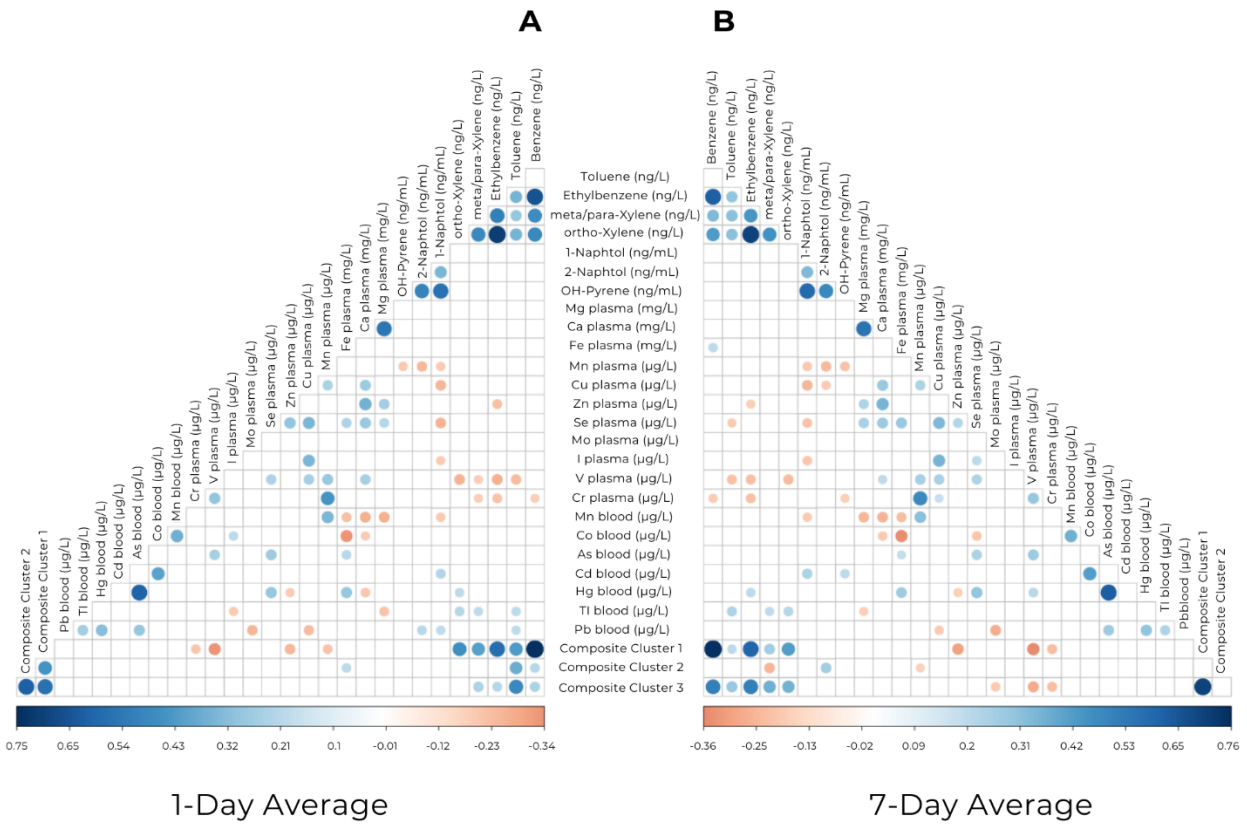

Figure 25. Correlation Plots of Air Pollution Biomarkers and Composite Exposure Scores. Subfigure (A) shows the correlation matrix for the one-day average exposure, and (B) for the seven-day average. In each panel, Spearman's rank correlation coefficients among ambient pollutant composite exposure scores derived from hierarchical clustering and internal biomarkers (including blood BTEX, urinary 1-naphthol, 2-naphthol, OH-pyrene and various blood/plasma metals) are visualized using color-coded circles. The plots display only the lower triangle of the matrix with the circle size and color reflecting the magnitude and direction of the correlations; non-significant correlations ($p > 0.05$) are left blank.

4.4. Effect Biomarkers Assessment

The impact of ambient air pollution on internal biological responses was evaluated by examining effect biomarkers that reflect immune function, oxidative stress, and DNA damage. Immune function and inflammatory markers, FOXP3 methylation and FeNO were modeled and subjected to mediation analyses. Oxidative stress was characterized by clustering seven biomarkers into two groups, of which the first cluster was found to be relevant in subsequent analyses. DNA

and cytogenetic damage were assessed using three complementary assays. The comet assay, a sensitive indicator of recent exposure, was analyzed using models fitted on one-day exposure data. For blood and buccal MN, representing more cumulative damage, quasi-Poisson regression models were used on seven-day exposure data. Overall, while mediation analyses were performed for several endpoints, the direct associations between exposure composite scores and the DNA damage biomarkers were predominant.

4.4.1. Variable Selection and Mediation Pathways of Immune Function Biomarkers

Best subset regression analyses (using adjusted R^2) were first performed to determine the most influential predictors of FOXP3 methylation and FeNO results. The initial predictor pool included demographic factors (sex, age, BMI), smoking status (active and passive), log-transformed pollen exposure, ambient meteorological variables (temperature, pressure, humidity, wind speed, UVB), and composite pollutant clusters (CC1–CC3) corresponding to the relevant time frame. For the one-day exposure frame, the best subset regression model for FOXP3 identified log-transformed pollen, sex, pressure, wind speed, and smoking as key predictors. In this model, sex, pollen, and pressure reached statistical significance. The best model for FeNO included CC3, sex, age, and pressure, with sex showing a statistically significant association. For the seven-day exposure frame, the best subset model for FOXP3 retained CC2, temperature, sex, and passive smoking, with CC2 and sex being statistically significant. The best model for FeNO included CC2, log-transformed pollen, sex, age, and smoking; in this case, CC2, pollen, sex, and smoking were statistically significant. All final models were evaluated using five-fold cross-validation. The FOXP3 models demonstrated strong predictive performance, with a cross-validated R^2 of 0.58 (SD = 0.19) for the one-day and 0.58 (SD = 0.15) for the seven-day exposure windows. In contrast, the FeNO models exhibited modest predictive ability, with $R^2 = 0.11$ (SD = 0.07) for the one-day and 0.19 (SD = 0.15) for the seven-day model. VIF diagnostics showed no major multicollinearity issues across models. The full regression results are presented as forest plots in Supplementary Figures 5 and 6, illustrating the effect sizes and confidence intervals for all included predictors.

Given the biological hypothesis that pollen exposure induces airway inflammation and that FOXP3 methylation responds to such inflammatory signals, a mediation model was primarily adopted in which FOXP3 was assumed to function as the mediator and FeNO as the outcome. Linear mixed-effects models with random intercepts were used to account for within-subject

correlation due to repeated measures. To maintain biological interpretability, FeNO was log-transformed in linear regression models due to its right-skewed distribution, which violated normality assumptions required for linear modeling, but untransformed FeNO values were used in the mediation framework. For the one-day analysis, the mediator model indicated that a one-unit increase in the log-transformed pollen count was associated with an increase in FOXP3 methylation ($\beta \approx 0.454$, $p < 0.05$), and that male subjects exhibited markedly lower FOXP3 methylation levels. In the outcome model, higher FOXP3 methylation was associated with lower FeNO ($\beta \approx -0.801$, $p < 0.05$), with ADE of pollen on FeNO estimated at 0.985. The resulting ACME—calculated as the product of the effect of pollen on FOXP3 methylation and the effect of FOXP3 on FeNO—was –0.231, yielding a total effect of approximately 0.199 (Figure 26). For the seven-day window, although the magnitude of the effects was somewhat reduced, a similar pattern was observed: the mediator model revealed that pollen had a positive association with FOXP3 methylation ($\beta \approx 0.352$, $p < 0.05$), and the outcome model showed that increased FOXP3 was related to decreased FeNO ($\beta \approx -0.660$). In this model, ACME was –0.232 and ADE of pollen on FeNO was 0.523, resulting in a total effect of roughly 0.291 (Figure 26).

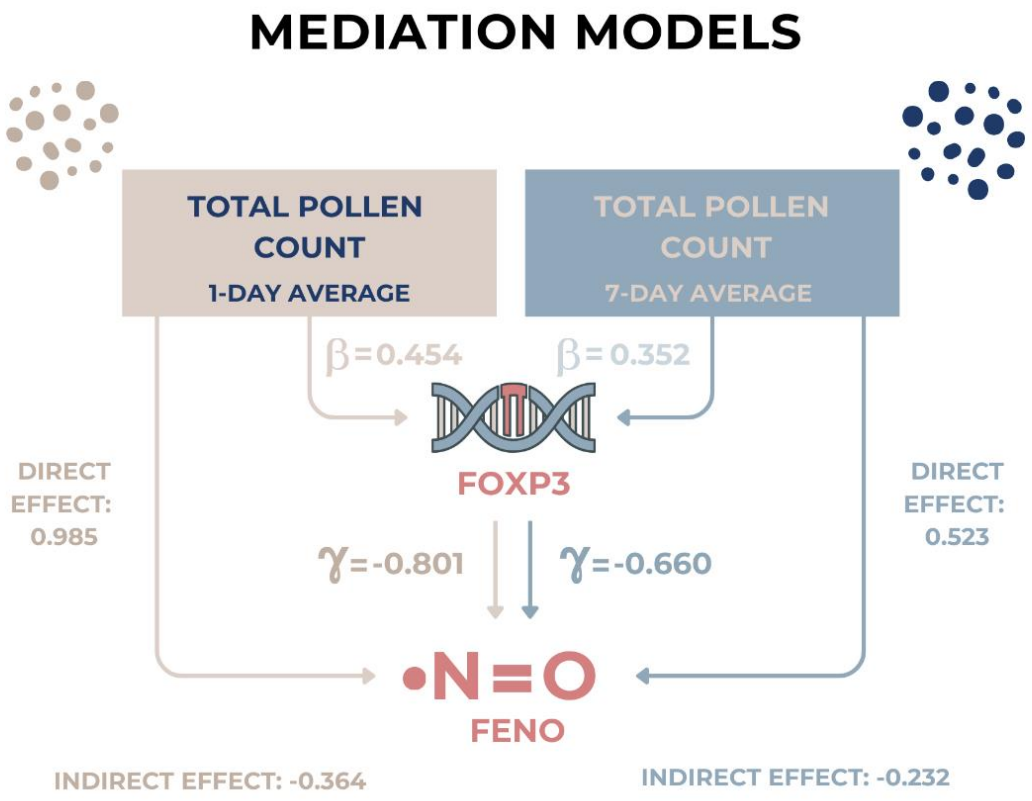

Figure 26. Schematic representation of the mediation models linking total pollen count (1-day and 7-day averages) to FeNO through FOXP3. Each arrow corresponds to the estimated path coefficient from the mediator or outcome model, with the ADE of pollen on FeNO and the ACME passing through FOXP3. Although the magnitude of effects is slightly reduced in the 7-day model, both time frames demonstrate that higher pollen levels are associated with increased methylation of the FOXP3 gene, which in turn correlates with lower FeNO.

In contrast, a reversed mediation analysis (with FeNO as the mediator and FOXP3 as the outcome) produced negligible indirect effects. Based on both statistical results and biological considerations—specifically, that pollen exposure directly modifies FOXP3 methylation, which then modulates inflammation as indexed by FeNO—we conclude that the model with FOXP3 as the mediator is the more valid representation. Notably, although the best subset regression for FeNO did not consistently emphasize pollen exposure, the mediation analysis demonstrates that pollen exposure exerts a direct pro-inflammatory effect (increasing FeNO) that is partially offset by its influence on FOXP3 methylation.

4.4.2. Oxidative Stress Assessment and Relationship with Exposure Clusters

4.4.2.1. Oxidative Stress Clustering

To examine the oxidative stress profile of the study participants, hierarchical clustering analysis on seven oxidative stress biomarkers was performed: SOD, NO, ROS, MDA, CAT, GSH, and GPx. The dendrogram (Figure 27) illustrates the clustering of these biomarkers, revealing two main groups. The first group includes SOD, NO, ROS, and MDA, while the second group is composed of CAT, GSH, and GPx. These two groups are connected at a height of approximately 0.9, indicating a moderate level of similarity between the biomarkers within each cluster. The dendrogram provides valuable insight into the association between oxidative stress biomarkers and demonstrates the underlying structure of these biomarkers within the study population. The biomarkers in the first group are representing primarily pro-oxidant processes, even though SOD is included, whereas the second group includes enzymatic and non-enzymatic antioxidative stress defense biomarkers.

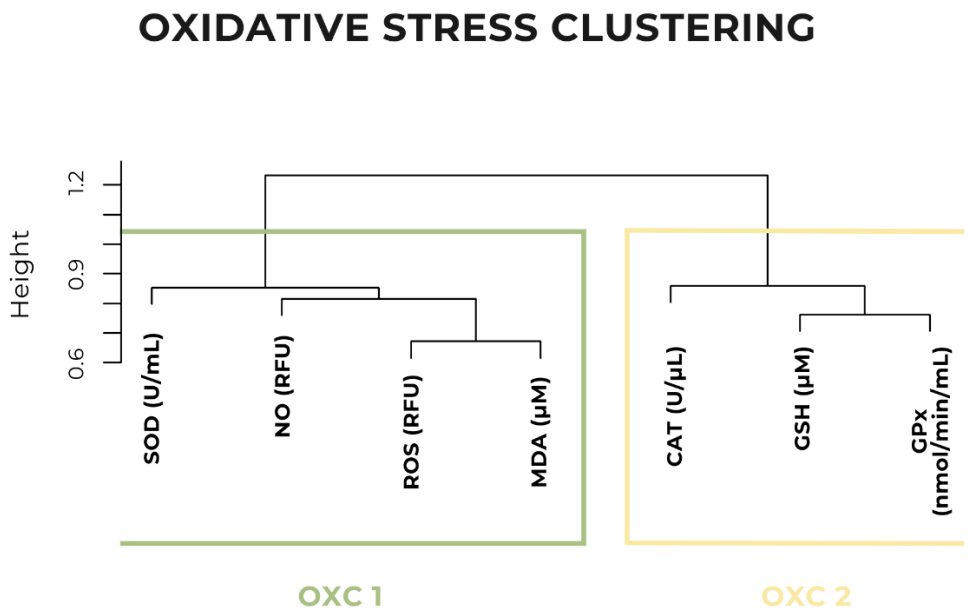

Figure 27. Dendrogram illustrating hierarchical clustering of oxidative stress biomarkers. Two primary clusters are observed: one primarily representing oxidative damage markers (NO, ROS, MDA, and additionally SOD) and the other representing antioxidative stress defense biomarkers (CAT, GSH, GPx).

4.4.2.2. Predictors of Oxidative Stress Clusters

Next, the associations between various predictors—including demographic factors, lifestyle factors, and exposure composite cluster variables—and oxidative stress clusters were explored. Regression models were run for each oxidative stress cluster using exposure and demographic variables as predictors, and the models were conducted for two different time frames (one-day and seven-day exposure) to examine how the influence of these predictors may vary over time. The modeling approach considered sex, age, BMI, physical activity, smoking status (active and passive), 2-naphthol, and composite exposure clusters (CC1–CC3) as predictors. Multicollinearity diagnostics indicated no concern, with all VIFs being below two.

In the one-day exposure model, CC1 was positively associated with OXC1 levels, whereas CC3 and higher physical activity showed negative associations (Figure 28A). Cross-validation of this model yielded an R^2 of 0.16 ± 0.18, closely matching the adjusted R^2 of 0.22, suggesting the model generalizes reasonably well. These findings suggest that oxidative stress in this cluster is contributed to by environmental exposures in combination with lifestyle behaviors such as physical activity. In the seven-day exposure analysis (Figure 28B), CC1 and sex were found to be significant predictors of OXC1. Males seem to have significantly higher oxidative stress, while high physical activity continued to exhibit a significant negative effect on oxidative stress, further confirming the role of lifestyle factors. The seven-day model performed slightly better than one-day model, with adjusted R^2 of 0.28 and cross-validated R^2 of 0.23 ± 0.15. In contrast, regression models predicting second oxidative stress cluster (OXC2) performed poorly across both exposure frames, with adjusted R^2 values below zero and cross-validated R^2 near zero ($\sim 0.02 \pm 0.02$), indicating limited predictive utility, and did not reveal any statistically significant associations with predictors across time frames (Figure 29). Therefore, OXC2 was not used in further analyses.

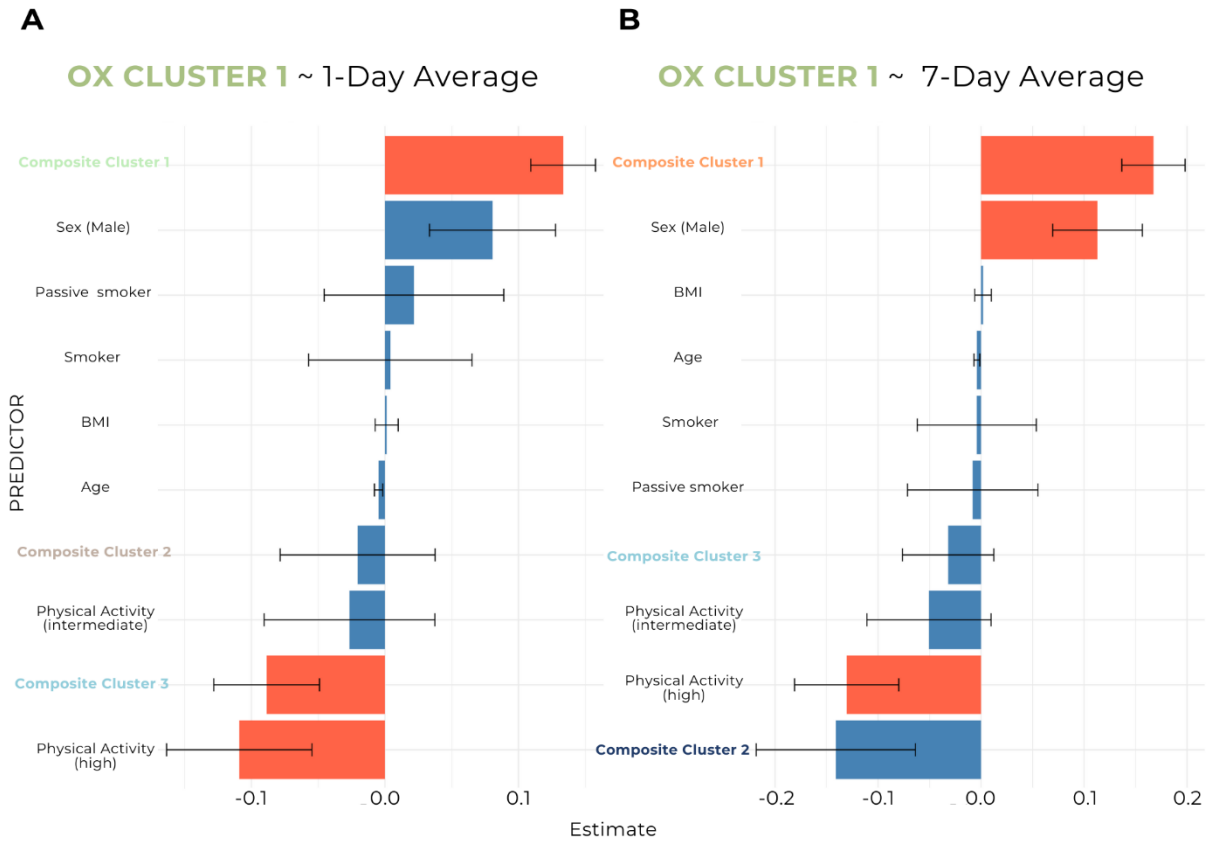

Figure 28. Forest Plot of Predictors for the First Oxidative Stress Cluster (OXC1). The figure displays the regression coefficients (with 95% confidence intervals) from the models predicting the OXC1 for both one-day (A) and seven-day (B) exposure windows. Statistically significant ($p<0.05$) predictors are color-coded red, and non-significant ones are blue. In the one-day analysis, composite exposure Cluster 1 (CC1) was significantly and positively associated with OXC1, whereas CC3 and a high level of physical activity were significantly negatively associated with OXC1. In the seven-day model, similar associations were observed; CC1 and sex remained significant predictors, and high physical activity continued to exhibit a negative effect on oxidative stress. These results collectively suggest that both ambient pollutant exposures (as captured by CC1 and CC3) and lifestyle factors are important determinants of oxidative stress.

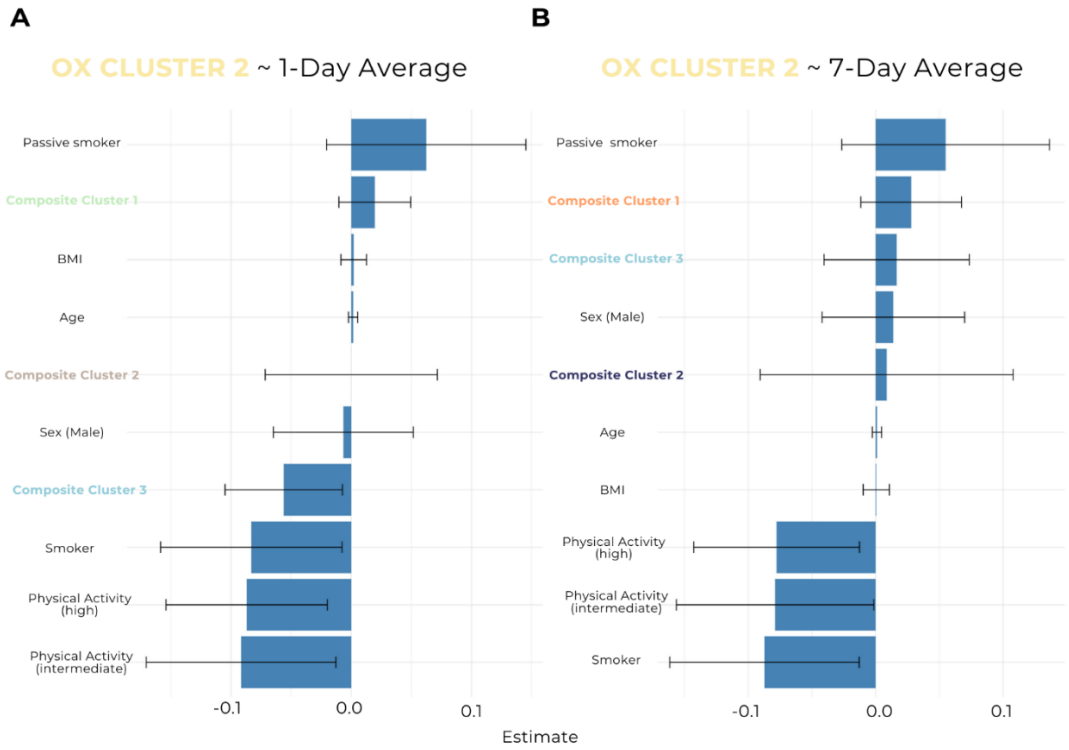

Figure 29. Forest Plot of Predictors for the Second Oxidative Stress Cluster (OXC2). This figure illustrates the regression coefficients (with 95% confidence intervals) from the models examining predictors of the second oxidative stress cluster for both one-day (A) and seven-day (B) exposures. No predictors reached statistical significance in relation to OXC2, as indicated by the wide confidence intervals and nonsignificant estimates.

4.4.3. DNA and Cytogenetic Damage Assessment and Model Building

4.4.3.1. DNA and Cytogenetic Damage Biomarkers Assessment

To assess cytogenetic damage, multiple endpoints were obtained from the MN assays, encompassing MNi, NBUDs, and NPBs in peripheral blood samples, as well as a corresponding set of MN assay parameters in buccal cells. The extent of primary DNA damage was evaluated using the comet assay. Although additional descriptors, such as TL and TM, were examined, only TI was used in subsequent analyses because it proved to be the most robust descriptor according to Moller et al (2014). Descriptive statistics of relevant results obtained by mentioned assays, for both seasons, is reported in Table 6 as population mean ± SD and range. In order to evaluate the stability of these biomarkers over time, the correlations between colder and warmer season results were calculated. Low correlations were observed, thereby justifying the pooling of data from both seasons for subsequent analyses.

Table 6. Descriptive statistics for DNA and cytogenetic damage biomarkers across study periods. Values are expressed as mean ± standard deviation (range) for each parameter, calculated separately for colder and warmer seasons.

		Colder (N = 60)	**Warmer** (N = 61)
Blood samples	**TI (%)**	1.22 ± 0.5	1.7 ± 1.37
		(0.49 - 2.91)	(0.17 - 7.94)
	MNi	4.42 ± 3.7	4.77 ± 4.16
		(0 - 12)	(0 - 18)
	NBUDs	4.45 ± 4.06	4.48 ± 2.96
		(0 - 20)	(0 - 12)
	NPBs	0.32 ± 0.5	0.07 ± 0.31
		(0 - 2)	(0 - 2)
	CBPI	2.11 ± 0.13	2.17 ± 0.06
		(1.8 - 2.46)	(1.89 - 2.29)
Buccal samples	**MNi**	2.19 ± 1.48	4.16 ± 2.47
		(0 - 6.5)	(0 - 11.5)
	NBUDs	0.58 ± 0.6	0.55 ± 0.61
		(0 - 2.5)	(0 - 2)
	Broken egg	1.43 ± 1.5	1.58 ± 1.68
		(0 - 7)	(0 - 7)
	Basal cells	0.52 ± 1.05	0.16 ± 0.73
		(0 - 5)	(0 - 5)
	Binucleated cells	19 ± 9.49	16.19 ± 10.09
		(2 - 49)	(4 - 42)
	Condensed chromatin	106.23 ± 47	73.88 ± 31.29
		(33 - 258)	(19 - 169)
	Karyorrhectic cells	43.5 ± 28.46	48.11 ± 32.12
		(6 - 135)	(4 - 154)
	Pyknotic cells	3.48 ± 8.87	1.91 ± 1.92
		(0 - 66)	(0 - 8)
	Karyolytic cells	91.2 ± 94.07	86.46 ± 50.71
		(6 - 617)	(18 - 303)

Based on the density plot and overlaid Poisson curve, the blood MN data generally show the typical shape of count data, with most counts concentrated at the lower end and a decreasing frequency for higher counts, which is consistent with a Poisson distribution (Figure 30). However, closer inspection reveals that the observed variability (especially in the higher count tail) exceeds what would be expected under a strict Poisson model. This overdispersion, where the variance is substantially greater than the mean, motivated the use of quasi-Poisson regression methods in our subsequent analyses. In other words, although the MN distribution approximately follows a Poisson pattern, the additional variability (overdispersion) necessitated a quasi-Poisson approach to obtain robust standard errors and valid inferential conclusions.

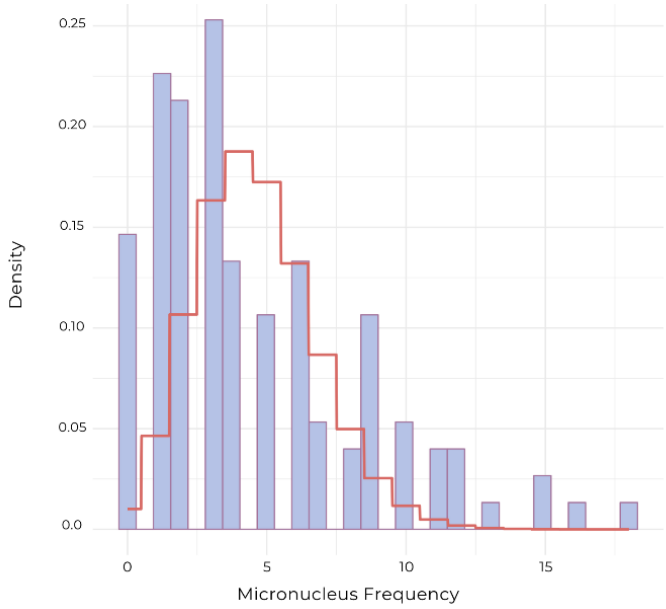

Figure 30. Histogram of micronucleus (MN) frequency overlaid with a theoretical Poisson density curve. The histogram shows the observed frequency distribution of MN counts, while the red line represents the Poisson probability density calculated using the sample mean (λ) after rounding the x values to the nearest integer. This overlay serves to illustrate the degree of conformity of the observed MN data to a Poisson distribution. Additionally, NBUD and NPB distributions are plotted using histograms but were not used in further modelling.

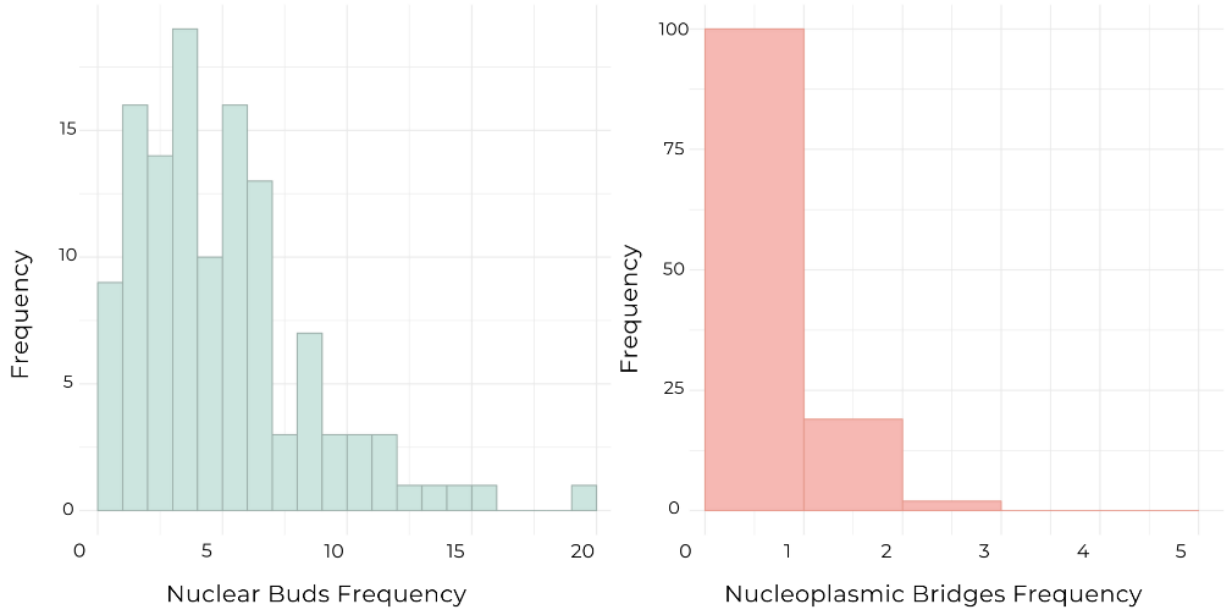

Figure 31. Histograms of nuclear buds and nucleoplasmic bridges. Both histograms are plotted with x-axis breaks at integer values to emphasize the discrete nature of these DNA damage endpoints, which are predominantly observed at lower count values.

Similarly, based on the density plot and overlaid Poisson curve, the buccal MN counts exhibit a typical count distribution, with most observations occurring at the lower end and fewer counts as values increase (Figure 32). Although the overall shape is consistent with a Poisson model, the right-hand tail shows more variability than would be expected under a strict Poisson assumption. This overdispersion, evident from the higher variability in the extreme values, justified the use of quasi-Poisson regression methods in subsequent analyses to obtain robust estimates and valid statistical inference.

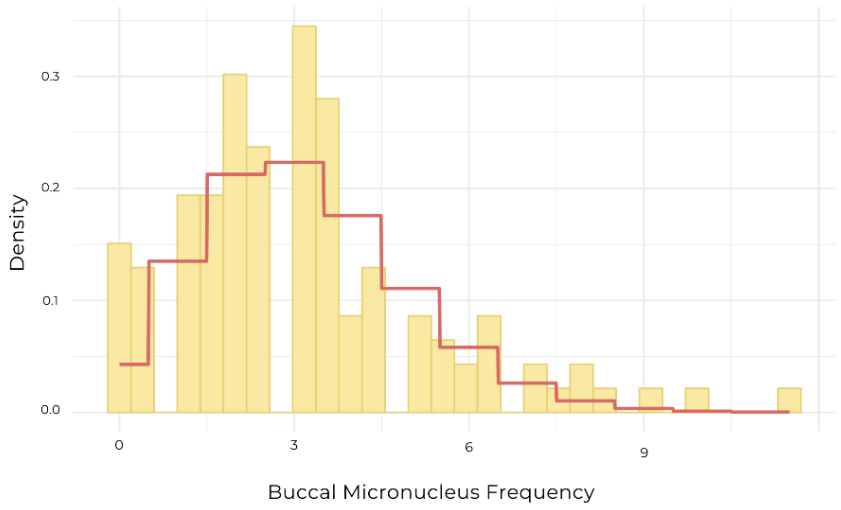

Figure 32. Histogram of buccal micronucleus (MN) counts overlaid with a theoretical Poisson density curve. The bars represent the observed frequency distribution of buccal MN counts, while the red line shows the Poisson probability density calculated using the sample mean (λ) after rounding the x values to the nearest integer. Although the distribution generally follows a Poisson-like pattern, the deviation in the upper tail indicates moderate overdispersion.

The original TI values were highly right-skewed, prompting the application of a logarithmic transformation to stabilize variance and achieve a more normal distribution. Figure 33 illustrates the distribution of TI values before and after transformation, highlighting the marked reduction in skewness following log conversion.

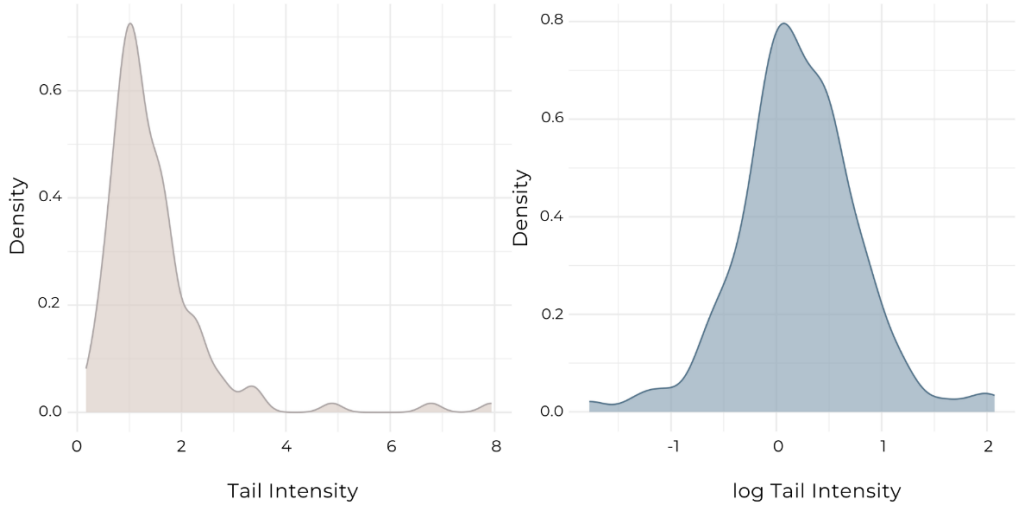

Figure 33. Density plots for comet assay descriptor tail intensity (TI). The left panel shows the original TI distribution, which is markedly right-skewed, while the right panel displays the log-transformed TI distribution, which is considerably more symmetric and approximately normal.

In addition to the comet assay from fresh blood samples, further assessments were conducted using frozen blood samples to test the usefulness of using frozen blood in large biomonitoring studies. Comet assay descriptors obtained from frozen samples were compared with those from fresh samples to evaluate whether storage conditions and sample processing might influence the observed distribution of DNA damage indices. In our findings, elevated DNA migration was found in frozen samples relative to fresh ones; however, the observed effects remained similar to those in fresh samples. Supplementary to the primary analyses based on manually scored MN slides obtained via light microscopy, further assessments were conducted using Metafer, which provides semi-automated quantification of MN frequency. A Spearman's rank correlation analysis between MN (manual scoring) and automated Metafer scoring showed a statistically significant but moderate positive association. In order to assess whether specific subjects showed consistently large discrepancies between the two methods, which might negatively impact overall agreement, differences were calculated for each subject. The exclusion of extreme outliers enhanced the consistency between manual and automated MN scoring, thereby strengthening the validity of this measurement approach.

In the subsequent analyses, TI from fresh blood samples and the manually scored MN data were retained for modeling, given their established reproducibility in our laboratory; however, these supplementary evaluations provide important validation and insight into methodological considerations.

4.4.3.2. Peripheral Blood Micronuclei as an Outcome Variable

To examine the impact of ambient exposures on chromosomal damage, MN counts were modeled using the seven-day exposure dataset. Socio-demographic data were merged with the composite exposure scores, and best subset regression was performed to identify the most influential predictors for MN. The candidate predictors included sex, age, BMI, physical activity, smoking status (active/passive), daily time spent outdoors, family history of cancer, and 2-naphthol levels, along with composite exposure clusters (CC1–CC3). The best subset selection resulted in the retention of the following predictors in the final model: sex, age, physical activity, smoking, and CC1. VIF values for all selected predictors were low (< 1.2), suggesting no concerning multicollinearity. A quasi-Poisson regression model was then fitted to account for the count nature and overdispersion observed in the MN data (Figure 34). The model explained approximately 35%

of the variance in MN counts (pseudo $R^2 = 0.35$) and demonstrated reasonably consistent predictive performance, with a cross-validated R^2 of 0.35 (SD = 0.20). The model indicated that significantly lower predicted MN counts were observed for male subjects. The predicted MN count for females was approximately six, whereas that for males was about three, demonstrating a statistically significant difference based on the regression results (Figure 35). A statistically significant positive association between age and MN counts was observed, such that each additional year of age was associated with an approximately 5% increase in MN levels on average (Figure 36). Although CC1 (intended to reflect ambient pollutant exposures) was included in the model, it did not reach statistical significance. Likewise, the effects of physical activity and smoking were not statistically significant. The dispersion parameter (estimated at 2.17) indicated that the model adequately handled the overdispersion inherent in the count data.

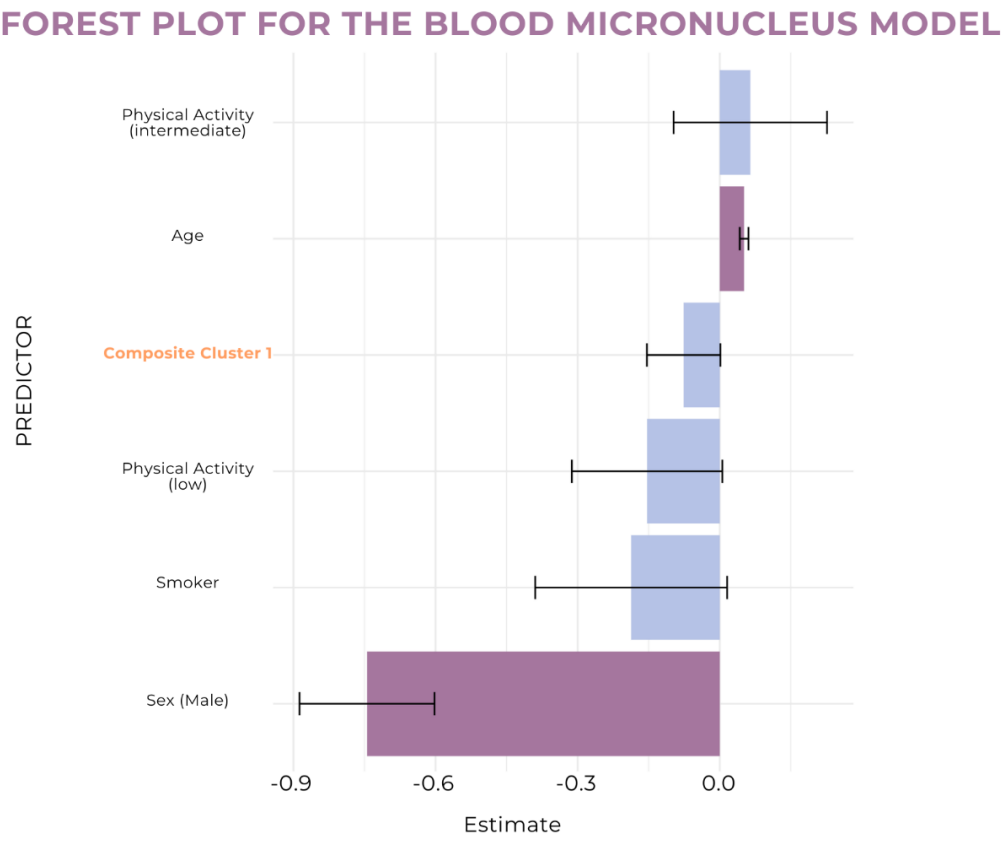

Figure 34. Forest Plot of the Final Blood Micronuclei Model. The plot displays the estimated effects (with 95% confidence intervals) for predictors included in the quasi-Poisson regression model for blood MN. Notably, age showed a significant positive association with MN, while male sex was associated with lower MN counts. Statistically significant ($p<0.05$) predictors are color coded dark purple, and non-significant light purple.

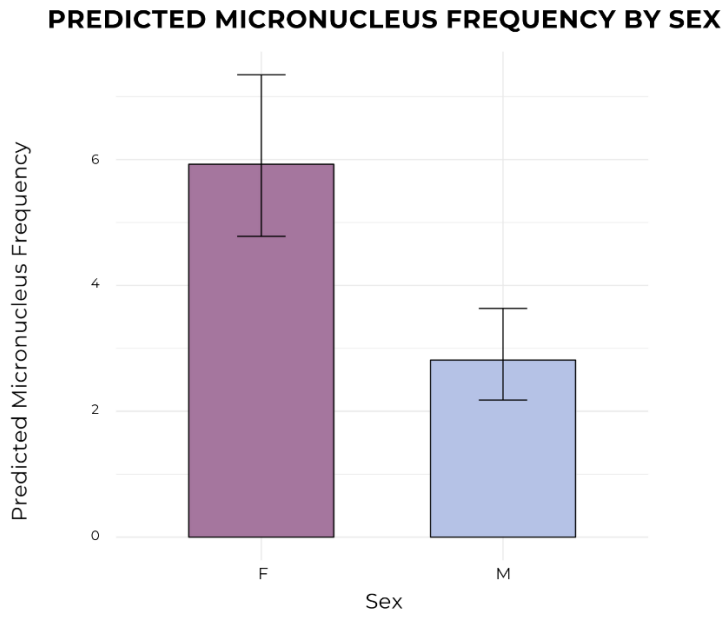

Figure 35. Predicted Micronuclei (MNi) Frequency by Sex. Predictions were derived from the final quasi-Poisson regression model in which MNi counts were modeled as a function of sex, age, physical activity, smoking, and exposure to Composite Cluster 1. Female subjects exhibited higher predicted MNi counts compared to male subjects, with error bars representing the 95% confidence intervals.

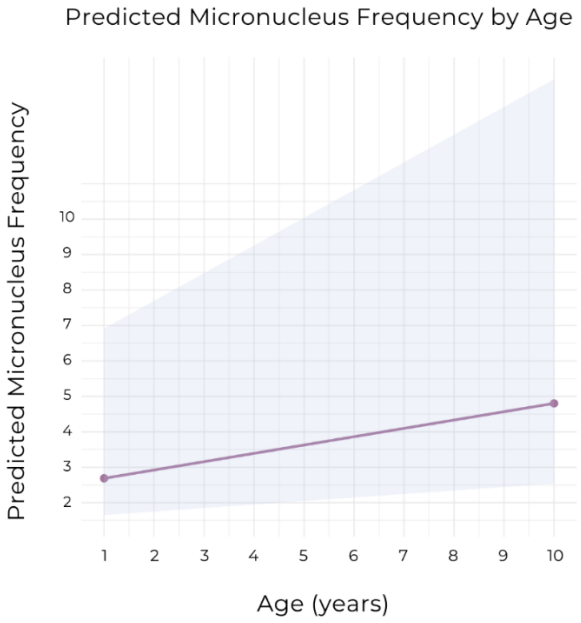

Figure 36. Predicted Micronuclei (MNi) Frequency by Age. Predictions were derived from the final quasi-Poisson regression model in which MN counts were modeled as a function of sex, age, physical activity, smoking, and exposure to Composite Cluster 1.

Testing whether oxidative stress mediated the effect of ambient exposures on MN formation was considered by using OXC1 as the mediator. However, given that CC1 was not found to be statistically significant in the direct MN model and that best subset regression highlighted sex as the primary predictor, it was determined that the mediation pathway through oxidative stress is likely minimal. Therefore, although mediation analyses were explored in other contexts, for MN, the direct model was deemed more informative.

4.4.3.3. Buccal Micronuclei as an Outcome Variable

For the buccal MN analysis using the seven-day exposure data, a set of candidate predictors was first assembled, including sex, age, BMI, physical activity, smoking status (active/passive), family history of tumors, and composite exposure clusters (CC1–CC3). Best subset regression was then applied to identify the most influential predictors for final model inclusion. This selection process retained sex, age, physical activity, CC1, CC3, and smoking status as the optimal subset of predictors. The final quasi-Poisson model indicated that male subjects had significantly lower buccal MN counts, CC1 was strongly and negatively associated with MN, and CC3 showed a significant positive association (Figure 37). The model explained a large proportion of variance, with a pseudo R^2 of 0.74. Cross-validation confirmed acceptable predictive performance, with a cross-validated R^2 of 0.18 (SD = 0.12). Multicollinearity was minimal, as all VIF values were below 1.35, supporting the stability of coefficient estimates.

To test whether oxidative stress (OXC1) mediated the effect of ambient exposures on buccal MN, a mediation model was estimated in which OXC1 was regressed on CC3 (with CC1 and sex included as covariates), and an outcome model was estimated in which buccal MN was regressed on CC3, OXC1, CC1, and sex. The mediation analysis yielded an ACME of 0.053, which was not statistically significant, while the ADE was 1.242 ($p = 0.006$), and the total effect was 1.295 ($p = 0.004$). Thus, only about 4% of the total effect of CC3 on buccal MN was mediated via oxidative stress, with the dominant effect remaining direct.

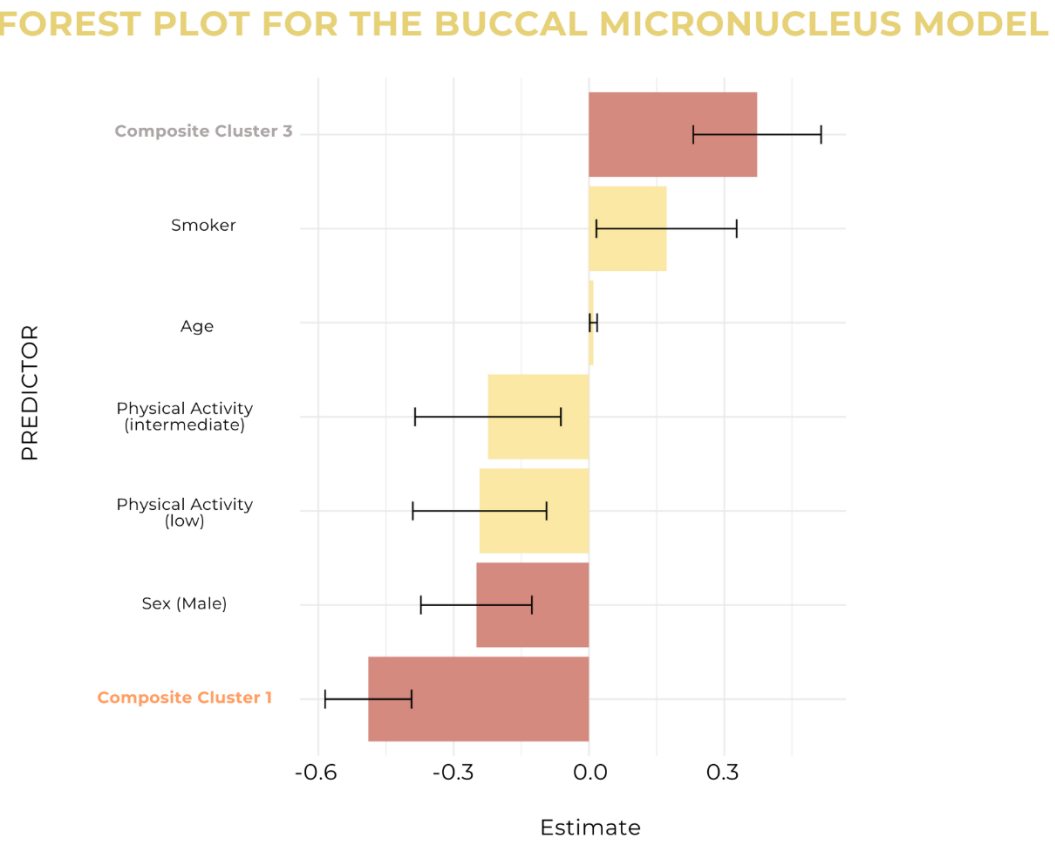

Figure 37. Forest Plot of the Final Buccal Micronuclei Model. The plot displays the estimated effects (with 95% confidence intervals) for predictors included in the quasi-Poisson regression model for buccal MN. Notably, Composite Cluster 1 showed a strong negative association and Composite Cluster 3 a significant positive association with MN, while male sex was associated with lower MN counts. Statistically significant ($p<0.05$) predictors are color coded red, and non-significant yellow.

4.4.3.4. Tail Intensity as Outcome Variable

The best subset regression on the one-day exposure dataset, with socio-demographic variables (sex, age, BMI, residence in years, physical activity, daily time spent outdoors, family history of tumors, smoking and passive smoking status) and composite exposure scores included, revealed that the most important predictors of TI were CC3 and smoking status. Specifically, individuals classified as smokers exhibited significantly higher TI ($\beta \approx 0.36$, $p = 0.021$), while CC3 was significantly inversely associated with TI ($\beta \approx -0.23$, $p = 0.0046$). Although passive smoking was retained in the model, its effect did not reach statistical significance. Variance inflation factor checks confirmed that collinearity was not an issue. The final model explained approximately 9.2% of the variance (adjusted $R^2 = 0.092$). Cross-validated performance was modest but stable, with

mean $R^2 = 0.14$ (SD = 0.09). Predicted TI was estimated from our final regression model and shown in Figure 38. The predicted log values were exponentiated to convert them back to the original scale, yielding estimates of 1.18 % (95% CI: 1.04–1.33) for non-smokers and 1.68 % (95% CI: 1.26–2.24) for smokers. These results indicate that smokers exhibit higher levels of DNA damage, as measured by TI, compared to non-smokers.

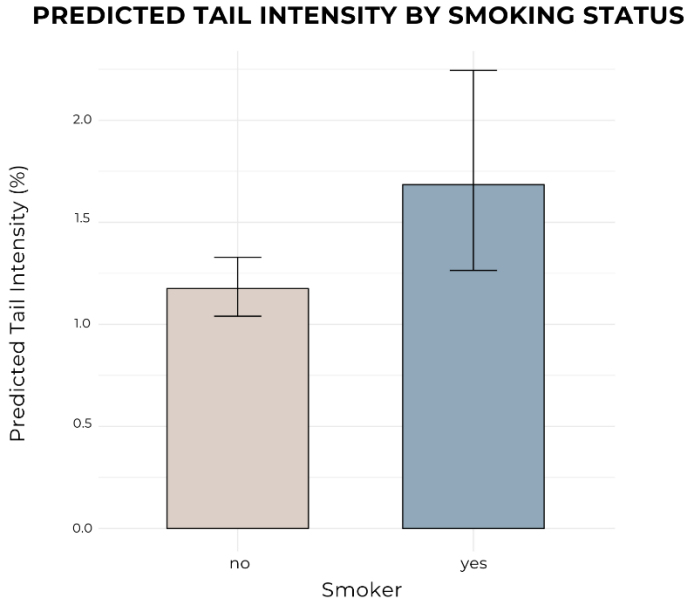

Figure 38. Predicted Tail Intensity by Smoking Status. The figure displays the model-derived predicted tail intensity (TI) (in %) for non-smokers and smokers. The final regression model was initially fitted on log-transformed TI data, and the predicted values were then exponentiated to obtain estimates on the original scale. For non-smokers, the predicted value was 1.18% (95% CI: 1.04–1.33), whereas for smokers it was 1.68% (95% CI: 1.26–2.24).

To assess whether the effect of ambient exposures on TI was mediated by oxidative stress, we conducted a mediation analysis using OXC1 as the mediator. In the mediator model, OXC1 was regressed on CC3 and smoking status; however, none of the predictors significantly influenced oxidative stress. In the outcome model, TI was regressed on CC3, OXC1, and smoking variables, with CC3 remaining a significant predictor, while OXC1 showed a non-significant effect. Consequently, the mediation analysis yielded an insignificant ACME alongside a significant ADE, resulting in a total effect of approximately –0.231 ($p = 0.010$). These findings indicate that the relationship between ambient exposures (as captured by CC3) and TI is primarily direct, with little evidence that oxidative stress, as measured here, serves as a mediator.

5. DISCUSSION

Air pollution has been recognized as one of the foremost environmental threats to public health, having been linked to an array of respiratory, cardiovascular, and other chronic diseases (de Bont et al., 2022; EEA, 2024; Låg et al., 2020). The complexity inherent in urban pollutant mixtures, which include VOCs, PMs, PAHs, O_3, NO_x, and toxic metals, creates a substantial challenge in outlining their combined effects on human health. Omics-based approaches have been increasingly employed to integrate large and complex datasets, yet the relationships between exposure biomarkers and effect biomarkers remain multifaceted and, in many cases, elusive in terms of direct causality, especially in real-life urban settings (Gruszecka-Kosowska et al., 2022; Kumari et al., 2024).

This study aimed to address this complexity by integrating environmental exposure data with biomarker-based health assessments in an urban cohort sampled during two distinct seasons. Specifically, the study pursued three core objectives: (1) to characterize external exposure to ambient air pollution by applying hierarchical clustering to derive composite exposure profiles (Composite Clusters, CCs), enabling dimensionality reduction while preserving relevant pollutant groupings; (2) to assess internal exposure biomarkers, including measurements of BTEX, PAH metabolites, and metals; (3) to associate external exposure to effect biomarkers, focusing on immune function (FOXP3 methylation and FeNO) alongside oxidative stress biomarkers, and cytogeneticoutcomes (TI, MN in blood and/or buccal cells).

Using a structured statistical approach—including best subset regression, mediation analysis, and multivariate modeling—the study identified key associations between clustered pollutant profiles and effect biomarkers. Composite Clusters 1 and 3 emerged as consistent predictors of oxidative and immune responses. Importantly, pollen exposure and CC3 were significantly linked to FOXP3 methylation and FeNO, with mediation models suggesting that FOXP3 may act as a regulatory buffer against inflammation. Also, CC1 was significantly and positively associated with the first oxidative stress cluster (OXC1), primarily composed of oxidative damage biomarkers (SOD, NO, ROS, MDA). In terms of genotoxicity, demographic factors such as age, sex, and smoking showed stronger associations with DNA damage than pollutant exposures *per se*, though certain pollutant clusters (notably CC3) were implicated in buccal MN formation. Mediation analyses showed minimal and insignificant oxidative stress

mediation for both TI and MN, suggesting more direct genotoxic effects of the assessed air pollutants.

The choice of statistical methods in this study was guided by the need to address the complex, multidimensional nature of air pollution exposure and its biological effects, aligning with recommendations from recent literature on environmental health and exposure assessment (Houssein et al., 2023; Peng et al., 2024; Qian et al., 2023; Sauvain et al., 2025; Zhu et al., 2024). Hierarchical clustering of air pollution-related variables was employed to derive composite exposure scores, reducing the dimensionality of pollutant data while preserving meaningful patterns. This approach is consistent with Bodor et al. (2022), who advocate for clustering techniques to handle the multicollinearity and heterogeneity inherent in air pollution data. By grouping pollutants into clusters, this study effectively captured the underlying structure of exposure, facilitating subsequent analyses without overfitting or loss of interpretability and demonstrated the value of advanced modeling techniques in uncovering meaningful biological associations.

5.1 Air Pollution Exposure Assessment

To capture the temporal variability in pollutant exposure and its biological effects, a multi-time-frame exposure model (one-, three-, and seven-day averages) was employed. This approach aligns with previous findings indicating that different biomarkers respond to varying exposure durations: the comet assay is particularly sensitive to short-term exposures, while the CBMN assay reflects cumulative damage over longer periods (Gajski et al., 2018; Gerić et al., 2018). As Rousseeuw (1987) cautions, a high overall silhouette width can be driven by trivial splits—e.g. isolating an "outlier" cluster—rather than true, substantive groupings; in our three-day exposure solution two of the five clusters contained only a single variable yet exhibited high silhouette score, indicating the algorithm was merely singling out extreme pollutants rather than revealing coherent exposure patterns, so we excluded that time frame in favor of the more parsimonious three-cluster solutions. The one- and seven-day composite exposure scores effectively captured the multidimensional nature of air pollution, in line with recent studies that recommend approaches like factor analysis and regression on factor scores (Gajski et al., 2022; Gerić et al., 2024; Sauvain et al., 2025). Hence, three pollutant groups were identified: Cluster 1 (PAHs, BTEX, PMs, O_3), Cluster 2 (NO_2, ethylbenzene, PM_{10}-bound metals: Cu, Fe, Mn), and Cluster 3 (PM_{10}-bound

metals: As, Cd, Pb). These findings are in line with recent European source apportionment studies. For example, Coelho et al. (2022) analyzed urban air quality in six European cities and reported that NO_2 was predominantly influenced by local traffic sources, particularly exhaust emissions and brake wear metals, whereas PM components had significant contributions from regional and transboundary transport. This helps explain why NO_2 clustered with metals rather than with PM and BTEX, the latter being associated more with mixed combustion sources, including residential heating and industrial activities. These results are also consistent with recent findings from Croatia by Jakovljević et al. (2025), who analyzed air pollution data from three Croatian cities (Zagreb, Slavonski Brod, and Vinkovci) and demonstrated that NO_2 and certain transition metals shared common urban traffic sources. In contrast, $PM_{2.5}$ and PAHs were more heavily influenced by seasonal heating and long-range transport. This interpretation is further supported by Godec et al. (2016), which identified relevant traffic and combustion signatures for both urban (Zagreb) and rural (north-eastern outskirt of Delnice) air pollution profiles in relation to PAHs, elemental and organic carbon, and PM_{10}, with slight seasonal variations in PAH ratios attributed to biomass burning in rural areas. Jakovljević et al. (2025) reported mean wintertime $PM_{2.5}$ concentrations ranging from 21.6 to 27.4 $\mu g/m^3$ across the aforementioned three cities, values that align closely with our 27.2 $\mu g/m^3$ average for one-day exposures. These concentrations exceed the WHO's 24-hour guideline of 15 $\mu g/m^3$ and are substantially higher than values typically observed in Western European capitals, which generally report average $PM_{2.5}$ levels below 15 $\mu g/m^3$, largely due to implementation of stricter environmental regulations, widespread adoption of low-emission transport such as electric vehicles and cycling, and a strong cultural emphasis on sustainable urban living (EEA, 2023; Hoffmann et al., 2022). However, the values observed in Zagreb are mostly within the proposed EU Directive for daily $PM_{2.5}$ concentrations (25 $\mu g/m^3$, not to be exceeded more than 18 times per year), indicating partial compliance with future regulatory expectations. Moreover, Croatian urban areas are still far better than many cities in the Western Balkans and Eastern Europe, where daily mean values often exceed 40–50 $\mu g/m^3$ during winter months (Belis et al., 2019; EEA, 2023). A significant portion of Zagreb's air pollution originates beyond the city itself. These findings are further supported by a recent high-resolution modeling study by Garatachea et al. (2024), which applied a source-receptor model to estimate exposure and cross-border contributions across Europe. Their results show that up to 50% of annual O_3 exposure in parts of Croatia can be attributed to emissions originating outside the country, particularly from

northern Italy's Po Valley, Central Europe, and other neighboring states. Sector-specific analysis identified residential combustion, industrial activity, and agriculture as the dominant contributors to this long-range transport, with residential heating especially impactful during winter months. The study highlights how air masses can carry pollutants over several hundred kilometers, making even relatively distant sources highly relevant for local exposure levels in Zagreb. According to Belis et al. (2019), transboundary pollution accounts for approximately 44% of $PM_{2.5}$ concentrations in the region. Croatia's geographical proximity to non-EU countries such as Serbia and Bosnia and Herzegovina, where there is lower environmental protection awareness and higher levels of air pollution, further contributes to elevated particulate levels in Zagreb. In Bosnia and Herzegovina, widespread reliance on coal and wood for household heating, along with outdated thermal power plants, results in some of the highest $PM_{2.5}$ air quality in Europe (Cetkovic et al., 2023; EEA, 2023.; Hasanovic et al., 2023). The annual average $PM_{2.5}$ in the capital city Sarajevo, in 2023 was reported at 27.6 $\mu g/m^3$, exceeding both the EU annual limit value of 25 $\mu g/m^3$ and the WHO guideline of 5 $\mu g/m^3$. Similarly, Belgrade recorded an annual average $PM_{2.5}$ concentration of 20.1 $\mu g/m^3$ in 2023, which is four times higher than the WHO's recommended limit (EEA, 2025). These elevated levels are primarily attributed to widespread use of solid fuels for household heating, industrial emissions, and vehicular traffic.

The influence of meteorological conditions on pollutant concentrations was found to be substantial, as these factors regulate the dispersion, chemical transformation, and atmospheric accumulation of airborne contaminants (Liu et al., 2020; Lovrić et al., 2022; Nejad et al., 2023; Wang et al., 2023a; Xie et al., 2022). In this study, both atmospheric pressure and UVB radiation were identified as influencing one- and seven-day composite exposure scores. In addition, temperature, relative humidity, and wind speed were observed to significantly modulate seven-day pollutant loads, particularly for Cluster 1 pollutants. These associations reflect well-known meteorological mechanisms. For instance, high-pressure systems are often associated with stable air masses and low wind speeds, promoting pollutant stagnation near the ground. Likewise, low UVB radiation and reduced vertical mixing in winter months favor the buildup of particulate and gaseous pollutants, while higher humidity can influence chemical reactions among NO_2 and VOCs (Al-Qassimi and Al-Salem, 2020; Fang et al., 2019; Flueckiger and Petrucci, 2024; Nejad et al., 2023). These findings must be interpreted in light of Zagreb's geographical and climatic setting. The city is positioned between the Sava River floodplain and the Medvednica Mountain, and

although not located within a classic valley, a basin-like configuration has been created by this terrain. Under winter conditions, this configuration has been shown to promote the occurrence of temperature inversions, during which a warm air layer traps colder air and pollutants near the surface. These events are frequently accompanied by low wind speeds, fog, and cold-air pooling, conditions that reduce atmospheric mixing and enhance pollutant accumulation near ground level, leading to smog formation (Lovrić et al., 2022; Račić et al., 2025). Comparable meteorological effects have been documented in other European cities with similar topographic constraints. For example, in Kraków, Poland, elevated $PM_{2.5}$ concentrations have been attributed to cold air pooling, frequent temperature inversions, light winds, and fog. These conditions trap pollutants near the ground, often resulting in smog and air quality levels that exceed legal limits (Ziernicka-Wojtaszek et al., 2024). Likewise, Sarajevo, located in a deep valley surrounded by mountains, experiences frequent and intense inversion episodes. In January 2020, $PM_{2.5}$ levels there peaked at 167.3 $\mu g/m^3$ due to the combined effects of thermal inversion, traffic, and solid-fuel heating, illustrating how topography and meteorology can dramatically exacerbate pollution exposure (Cetkovic et al., 2023; Mašić et al., 2016).

5.2 Exposure Biomarkers

Exposure biomarkers (BTEX in blood, urinary PAH metabolites, and elements in blood/plasma) provided insights into the absorbed dose of pollutants. The high proportion of BTEX values below LOD, especially in the warmer season (e.g. 98.4% for benzene), limited their usefulness for modeling, reflecting both lower ambient concentrations and rapid metabolic clearance of VOCs. For example, the German Research Foundation (Ger. *Deutsche Forschungsgemeinschaft*, DFG) has established occupational exposure equivalent values for carcinogenic substances (EKA values). For benzene, the EKA in blood corresponds to airborne concentrations ranging from 0.3 to 4 mg/m^3, which are associated with blood levels between 0.9 and 38 µg/L when measured at the end of a work shift (DFG, 2013). In comparison, the median blood benzene concentrations measured in this study were markedly lower: 47 ng/L in the colder season and below LOD in most samples during the warmer season. This substantial difference emphasizes that the measured benzene levels in our cohort reflect low environmental exposures rather than occupational settings and fall far below thresholds of concern for occupational risk. Unmetabolized benzene in blood is considered a direct and reliable biomarker, particularly relevant

at low exposure levels, but is often challenging to detect in environmental settings due to its short half-life and rapid clearance (Boogaard, 2022). Biomonitoring Equivalents (BEs) offer additional context for interpreting such levels: Hays et al. (2012) propose a BE of 150 ng/L for blood benzene as consistent with the U.S. EPA's inhalation reference concentration (RfC). Our findings, with a median of 47 ng/L and most values below the LOD in the warmer season, are also well below this BE threshold, further supporting the interpretation of low exposure and minimal health concern. This seasonal pattern aligns with studies showing reduced VOC emissions in warmer months due to decreased heating-related combustion and enhanced photochemical degradation (Mahmoud et al., 2021; Zhang et al., 2019). The decision to exclude BTEX measured in blood from further analyses due to detection limit issues was prudent, as simple substitution methods (e.g. half the LOD) can bias results, especially when more than half the data is censored (Helsel, 2011). Furthermore, VOCs such as benzene and toluene exhibit multi-phase elimination kinetics in the human body, with initial half-lives ranging from minutes to a few hours and terminal half-lives extending up to 90 h, particularly in adipose tissue. This biphasic clearance supports the interpretation that blood VOCs primarily reflect recent exposures, while bioaccumulation may occur with frequent or sustained contact (Ashley et al., 1996).

Urinary PAH metabolites (1-naphthol, 2-naphthol, and OH-pyrene) also offer valuable insight into PAH exposure, though their interpretation is highly context-dependent. Among these, 2-naphthol was consistently detected across all samples, with median concentrations of 8.3 ng/mL in the cold season and 7.8 ng/mL in the warm season. Its high detection rate and wide concentration range affirm its status as a sensitive biomarker for naphthalene exposure, particularly *via* inhalation. Hoseini et al. (2018) reported a geometric mean 2-naphthol concentration of 3.52 ng/mL in an urban population of Tehran, which suggests slightly lower concentrations than our findings, potentially reflecting differences in local emission sources or population characteristics. They observed that urinary 2-naphthol was associated with traffic-related air pollution exposure, even after adjusting for smoking, highlighting its relevance in ambient air studies. Similarly, in Guangzhou, southern China, median reported 2-naphthol levels were 3.16 ng/mL (Yang et al., 2021). In our study, seasonal differences in 2-naphthol levels were not significant, suggesting relatively stable background exposure, potentially influenced by indoor or mixed sources such as ambient traffic-related emissions and lack of seasonal indoor combustion. Notably, Burkhardt et al. (2023) observed a significant temporal increase in urinary 2-naphthol levels over the years in

Germany, unlike other PAH metabolites such as 1-naphthol and OH-pyrene, which remained stable or declined. This rise was attributed to increasing exposure to naphthalene from ambient sources, particularly traffic-related emissions and VOCs in urban environments. Naphthalene, a low-molecular-weight PAH, is prevalent in vehicle exhaust, industrial emissions, and consumer products such as mothballs and air fresheners, which may contribute to elevated 2-naphthol levels (Jia and Batterman, 2010). Burkhardt et al. (2023) suggest that changes in urban air quality, including shifts in fuel composition and increased use of naphthalene-containing products, could drive this trend. In our study, the high detection rate and wide concentration range of 2-naphthol support its sensitivity to these sources, with the slightly higher median in the colder season potentially reflecting increased indoor heating or reduced atmospheric dispersion of pollutants. Meeker et al. (2007) observed sex and gender adjusted median 2-naphthol levels of 9.84 ng/mL among smokers and 0.96 ng/mL for non-smokers in a U.S. cohort. Interestingly, we did not observe a statistically significant difference between smokers and non-smokers in our study; however, we did observe a significant elevation of 2-naphthol levels in passive smokers. Furthermore, Bartolomé et al. (2015) found that, in the Spanish adult population, 1-naphthol levels were significantly higher in both active and passive smokers, further highlighting the potential confounding effects of passive smoking in PAH related biomonitoring studies. In our study, 1-naphthol exhibited high censoring (>70% below LOD), with median concentrations at LOD in both seasons (colder: <LOD–16.9 ng/mL; warmer: <LOD–8.4 ng/mL), limiting its value for quantitative analysis. This is consistent with findings from Thai et al. (2020), who noted that elevated 1-naphthol levels can reflect exposure to specific pesticides like carbaryl, rather than airborne PAHs, suggesting it may be a less reliable biomarker of general air pollution exposure in urban settings. For OH-pyrene, detection rates were high, but concentrations remained low (<1 ng/mL), indicating limited recent exposure to pyrene. Importantly, several studies have suggested that OH-pyrene is more indicative of dietary PAH intake (e.g. grilled or smoked foods) or occupational exposures rather than ambient air pollution (Bartolomé et al., 2015; Hoseini et al., 2018). This is consistent with Yang et al. (2021), who reported median OH-pyrene levels of 0.14 ng/mL in the general population of Guangzhou. In our cohort, questionnaire data revealed a relatively low fried food consumption averaging only 1.5 days per week. These findings reinforce the interpretation that OH-pyrene is less responsive to short-term ambient air pollution and may instead reflect dietary or occupational exposure routes. Overall, the contrasting detectability and

variability of these metabolites underline the importance of selecting appropriate biomarkers. In this urban population, 2-naphthol proved to be the most suitable urinary PAH biomarker, offering reliable exposure assessment across seasons, whereas 1-naphthol and OH-pyrene were less informative due to frequent censoring and dietary or occupational confounding.

Minimal seasonal variation was observed in blood and plasma metal concentrations, indicating stable exposure patterns throughout the year. For example, mean levels of toxic metals in blood were As: 2.94 ± 3.50 µg/L (colder) *vs.* 3.12 ± 3.74 µg/L (warmer); Cd: 0.44 ± 0.58 µg/L *vs.* 0.40 ± 0.42 µg/L; and Pb: 13.57 ± 9.26 µg/L *vs.* 13.11 ± 8.79 µg/L. Essential trace elements in plasma, such as copper (Cu: 552.69 ± 122.68 µg/L colder *vs.* 560.77 ± 99.78 µg/L warmer) and zinc (Zn: 1066.33 ± 184.56 µg/L *vs.* 1157.47 ± 102.01 µg/L), also demonstrated limited seasonal fluctuation. This stability justified the pooling of seasonal data in statistical analyses, enhancing analytical power and reducing random variation. This consistency likely reflects chronic low-level environmental and dietary exposures, rather than acute or seasonal sources. Our findings are aligned with those reported by Mengelers et al. (2024), who observed comparable blood levels of Pb (17.16 ± 12.14 µg/L) and Cd (0.40 ± 0.30 µg/L) in the Dutch adult population. Similarly, Hoet et al. (2021) found stable plasma Cu (540–580 µg/L) and Zn (1000–1200 µg/L) concentrations in Belgian adults, supporting the idea of tight physiological homeostasis for essential metals, which is consistent with our data. Compared to more industrialized regions, such as Acerra in southern Italy, metal concentrations in our cohort were substantially lower. Lotrecchiano et al. (2022) reported blood As levels of 8–15 µg/L, Cd levels of 2.6–4.5 µg/L, and Pb values between 59.7–79.6 µg/L in residents exposed to industrial emissions. The comparatively lower concentrations in Zagreb residents support the interpretation of a less industrialized exposure profile (two to three-fold lower PM_{10}-bound As and Cd concentrations), dominated by diffuse urban sources such as traffic emissions and legacy lead in infrastructure. Notably, plasma Fe showed a significant correlation with CC2 (NO_2, ethylbenzene, and PM_{10}-bound metals), suggesting source-specific exposure patterns likely attributable to resuspended traffic-related dust (Wiseman et al., 2021). This association reinforces the value of composite exposure clusters in capturing complex environmental mixtures and linking them to internal biomarkers. However, other metals did not show significant positive associations with specific exposure clusters, indicating that their presence in blood may be more influenced by dietary intake or other sources, rather than by ambient air pollution. Finally, strong associations between exposure clusters (especially CC1 and CC3) and

blood-based BTEX/metals—but weaker links with urinary PAH metabolites—highlight the complementary role of different biomonitoring matrices. Blood-based biomarkers appear to better capture recent inhalation exposures to VOCs and metals, whereas urinary PAH metabolites may reflect intermittent or cumulative exposure from diverse sources, including diet and indoor environments. These findings underscore the importance of selecting appropriate biological matrices based on the pollutant class and exposure timeframe in biomonitoring studies (Sauvain et al., 2025).

5.3 Effect Biomarkers

5.3.1 Immune Function and Inflammation

FeNO is primarily produced by the bronchial epithelium through the activity of inducible iNOS, an enzyme upregulated in response to type II inflammatory cytokines such as IL-4 and IL-13. The elevated FeNO levels reflect eosinophilic airway inflammation, commonly observed in allergic responses but also related to air pollution exposure (Anand et al., 2024; Chen et al., 2020; Delfino et al., 2006; Guo et al., 2022). To investigate the potential mechanisms linking environmental exposures to airway inflammation, a mediation analysis was conducted to evaluate whether the epigenetic regulation of immune function—specifically, methylation of the FOXP3 gene—could mediate the relationship between pollen exposure and FeNO levels. The gene FOXP3, which encodes a transcription factor critical for the development and suppressive activity of T_{reg}, was selected as a mediator due to its established role in maintaining immune tolerance and modulating T_{h2}-driven allergic responses (Lal et al., 2009; Tuazon et al., 2022; Zhang et al., 2022). Mediation model found that increased pollen levels were significantly associated with elevated FOXP3 methylation, and this epigenetic modification was further linked to variation in FeNO levels. Notably, the one-day pollen exposure model exhibited a stronger direct effect on FeNO (ADE = 0.985) than the seven-day one (ADE = 0.523), indicating a more pronounced acute inflammatory response (Galli et al., 2008). The indirect pathway through FOXP3 methylation was also supported in both models, with an ACME of approximately –0.231 in the one-day model and –0.232 in the seven-day model. The slightly reduced effect observed in the seven-day model may be explained by meteorological factors such as temperature, wind speed, and pollen dispersion (González-Alonso et al., 2024). These findings align with previous research indicating that FOXP3 expression is reduced in patients with asthma and allergies, implicating its role in immune

homeostasis and the suppression of T_{h2} responses following allergen exposure (Marques et al., 2015). Furthermore, this pattern aligns with findings from an Italian large population-based study by Olivieri et al. (2022), in which FeNO levels were shown to increase in a dose-dependent manner with both the number of pollen species present in the environment and the degree of individual sensitization. Furthermore, Nassikas et al. (2024) found that short-term pollen exposure was linked to increased airway inflammation, as measured by FeNO, in adolescents regardless of asthma or allergy status. Their findings suggest that pollen can provoke inflammatory responses even in individuals without pre-existing allergic conditions, consistent with evidence that pollen exposure triggers acute inflammatory markers and symptoms in healthy people. Although the direct effects of total pollen count on elevated FeNO were expected, the observed indirect effects—indicating a modest decrease in FeNO *via* FOXP3 methylation—are consistent with the characteristics of the general adult population studied and the non-case-control design of the research. Nonetheless, the mediation models yielded meaningful insights, highlighting the importance of both short-term and long-term environmental exposures in shaping immune and respiratory biomarkers. These findings support the utility of such models in future epidemiological studies that include both healthy individuals and those with respiratory conditions. To fully evaluate the directionality of the proposed pathway and assess the robustness of the mediation framework, an alternative model was also tested in which FeNO was considered as a potential mediator between pollen exposure and FOXP3 methylation. The reversed mediation model, in which FeNO was positioned as the mediator of the relationship between pollen exposure and FOXP3 methylation, was found to be both statistically unsupported and biologically implausible. This reinforces the interpretation of FOXP3 methylation as an upstream immunological regulator, rather than a downstream target. In contrast, FeNO is widely accepted as a non-invasive marker of ongoing eosinophilic airway inflammation, reflecting downstream effects of immune dysregulation rather than initiating them (Dweik et al., 2011).

Although CCs were not significant independent predictors of FOXP3 methylation in our cohort, previous studies have linked pollutants such as PAHs and black carbon to altered FOXP3 methylation. For example, Hew et al. (2015) found that long-term PAH exposure over one to twelve months was associated with increased FOXP3 methylation in adolescents, while Lovinsky-Desir et al. (2017) observed black carbon-related FOXP3 methylation changes over a six-day period in children, modulated by physical activity. However, these studies often included children or

asthmatic individuals, and used cell-specific or personal exposure data. In contrast, our cohort consisted of healthy adults, and FOXP3 methylation was measured in whole blood, which may explain the absence of strong air pollution associations. Furthermore, the influence of air pollution on FeNO has been well-documented in both controlled exposure studies and epidemiological research (Cottini et al., 2025; Delfino et al., 2006; Zhang et al., 2021b). Various pollutants—including PMs, NO_2, O_3, and traffic-related air pollution—have been associated with increased FeNO levels, indicating pollutant-induced eosinophilic airway inflammation (Anand et al., 2024; Chen et al., 2020). Additionally, in this study, toxic metals in CC3 (As, Cd, Pb) independently predicted FeNO, highlighting their role in airway inflammation through mechanisms distinct from pollen exposure. This interpretation is supported by epidemiological findings demonstrating that exposure to Pb, Cd, and As alters both innate and adaptive immune cell populations, disrupts cytokine regulation, and is associated with an increased risk of immune-mediated conditions such as asthma and allergic disease in children (Zheng et al., 2023). For example, Pb exposure has been associated with elevated levels of eosinophils, neutrophils, and pro-inflammatory cytokines such as IL-1β and TNF-α, while Cd exposure has been linked to altered T cell subsets and increased risk of respiratory allergic conditions (Ganguly et al., 2018). Similarly, As exposure has been associated with enhanced T_{h2}-type immune responses and increased levels of IgE and IL-4, which are characteristic of allergic airway inflammation, as reviewed by Zheng et al. (2023). These findings indicate the interplay between environmental allergens and pollutants in shaping immune responses, with potential relevance for allergic disease management in urban settings.

5.3.2 Oxidative Stress Assessment

Hierarchical clustering of oxidative stress biomarkers into two groups, mostly pro-oxidant products (SOD, NO, ROS, MDA) and antioxidant defense (CAT, GSH, GPx), provided a nuanced view of redox balance. SOD clustered with the first set of biomarkers, likely due to its catalytic role in converting superoxide radicals into H_2O_2, which itself can contribute to oxidative stress if not efficiently cleared by downstream antioxidants such as CAT or GPx (Demirci-Çekiç et al., 2022; Jomova et al., 2023). Superoxide is one of the primary ROS generated in response to environmental stressors, and its detection in this study—*via* DHE fluorescence—supports the hypothesis that this radical is a major contributor to the observed oxidative burden. The significant association of OXC1 with CC1 (PMs, PAHs, BTEX, etc.) and demographic factors (sex, physical

activity) in both one-day and seven-day analyses emphasizes the influence of ambient exposures and lifestyle choices on oxidative damage. The significant positive association observed between OXC1 and CC1 likely reflects established mechanisms by which components of urban air pollution (especially PAHs, VOCs, O_3, and PMs) induce oxidative stress (Gangwar et al., 2020; Lodovici and Bigagli, 2011; Ryu and Hong, 2024). PAHs and VOCs are known to undergo metabolic activation *via* cytochrome P450 enzymes (CYP1A1, CYP1A2, CYP1B1), forming reactive intermediates that not only bind DNA but also engage in redox cycling, generating superoxide and subsequently H_2O_2 (Bukowska and Duchnowicz, 2022; Ewa and Danuta, 2017; Xue and Warshawsky, 2005). Transition metals like Fe and Cu, often bound to airborne PM, catalyze further redox reactions, such as the Fenton reaction, producing OH• capable of inducing lipid peroxidation and damaging DNA and cellular structures (Husain and Mahmood, 2019; Mesnage, 2025; Yan et al., 2022). A study by Cipryan et al. (2024) conducted in the Czechia examined the interplay between long-term air pollution exposure, cardiorespiratory fitness, and oxidative stress markers. Participants residing in high air pollution regions exhibited significantly elevated levels of GPx, indicating a compensatory response to oxidative stress induced by prolonged pollutant exposure. Furthermore, Ryu and Hong (2024) evaluated the relationship between PAH exposure and oxidative stress from the perspective of mixed PAHs in Korean adults and found a significant association. While physical activity emerged as a significant modulator of oxidative stress in this study, it is important to recognize that exercise-induced ROS generation is a well-characterized physiological response. As reviewed by Powers et al. (2020), skeletal muscles are a major source of ROS during exercise, primarily *via* NADPH oxidase activity. This adaptive response to exercise-induced oxidative stress exemplifies the concept of hormesis, where low-level stressors stimulate protective mechanisms. However, it is noteworthy that excessive or intense physical activity may transiently increase oxidative stress, highlighting the importance of exercise intensity and duration in redox balance (Lu et al., 2021). Sex differences in oxidative stress responses were also observed, with men exhibiting higher levels of oxidative stress markers compared to women. Similarly, Ide et al. (2002) showed that biomarkers of oxidative stress were higher in young men than in women of the same age. This finding aligns with previous research indicating that hormonal variations, particularly estrogen levels, influence redox status (Martínez de Toda et al., 2023; Torrens-Mas et al., 2020). Furthermore, the absence of significant predictors for OXC2, encompassing antioxidant biomarkers, suggests that antioxidant responses may be governed by more stable, homeostatic

mechanisms less susceptible to short-term environmental fluctuations. This stability could reflect the body's intrinsic capacity to maintain redox equilibrium through tightly regulated antioxidant systems (Sies and Jones, 2020). While many past studies relied on limited cross-sectional or occupational cohorts, there is little data on general human populations to conclude whether different air pollutants have different magnitudes of association with oxidative stress outcomes (Delfino et al., 2011). Our approach, using within-subject temporal comparisons, enhances statistical power and controls for interindividual variability—allowing clearer attribution of biomarker changes to pollutant exposure events.

5.3.3 Cytogenetic and DNA Damage

The assessment of DNA damage in blood cells *via* the comet assay and further cytogenetic damage *via* MN assays in both the blood and buccal cells revealed distinct patterns. Although some biomonitoring studies—particularly in heavily polluted regions such as northern Italy and parts of the Southeast Europe—have reported significant increase in MN frequency due to air pollution exposure (Ceretti et al., 2020; Cetkovic et al., 2023; Santovito and Gendusa, 2020; Zani et al., 2021), we did not observe a significant association between blood MN frequency and seven-day ambient exposure to CC1. This mirrors Gajski et al. (2022), who, despite a detailed analysis of three-, seven-, and 30-day pollutant exposure windows, found no consistent positive associations, attributing this to low overall pollutant levels, inter-individual variability, and potential indoor shielding during high-exposure periods. On the other hand, buccal MN model revealed CC3 and CC1 to be significant predictors of MN frequency along with sex (females having higher MN frequency). Furthermore, these models revealed a significant positive association with CC3 and a negative association with CC1, indicating differential cellular responses to distinct pollutant groups. Meta-analysis by Annangi et al. (2016) demonstrated that most of the occupational and environmental biomonitoring studies found an increase in blood and buccal MN among As exposed individuals, although it is important to note that As environmental source was mainly contaminated drinking water. In contrast to our environmentally exposed but non-occupationally burdened population, Alabi et al. (2020) reported dramatically elevated buccal MN frequencies among electronic waste scavengers in Lagos, Nigeria, with a mean of 168.04 ± 0.02 in the exposed group compared to 3.23 ± 0.18 in controls. These levels were accompanied by significantly higher blood Pb (38.34 ± 24.04 μg/dL) and Cd (2.85 ± 0.66 μg/L) concentrations, emphasizing the genotoxic

potential of intense, unprotected occupational exposures. In our study, MN frequencies ranged from 2.19 ± 1.48 in the colder period to 4.16 ± 2.47 in the warmer period, with much lower Pb (13.57 ± 9.26 μg/dL) and Cd (0.44 ± 0.58 μg/L) levels, further underscoring the distinction in exposure intensity. Similarly, Aksu et al. (2019) found increased DNA damage and MN frequencies among male welders, linking occupational fume exposure to elevated Cd and Pb levels. Khan et al. (2010) observed elevated buccal MN frequencies in lead-exposed painters, supporting toxic metals as potent genotoxicants in workplace settings. Nagaraju et al. (2022) reinforced this through a systematic review showing consistent increases in MN frequency, sister chromatid exchanges (SCEs), chromosomal aberrations, and oxidative DNA damage in Pb-exposed workers, regardless of job type or exposure duration. Importantly, their review highlighted that telomere shortening also occurs with chronic Pb exposure, and CDC guidelines (Alarcon et al., 2019) that define blood Pb levels ≥10 μg/dL in the adult population as elevated and warranting investigation. Compared to these occupational cohorts, our study provides insight into the subtler genomic effects in the general population. Notably, despite lower exposures, we still observed a seasonal increase in MN frequency, suggesting that environmental factors such as temperature and pollution dynamics could influence genomic integrity. This was also reflected in Panxhaj et al. (2024), who observed higher buccal MN frequencies during winter in Prishtina (Kosovo), coinciding with higher pollution levels. Together, these findings highlight the utility of buccal MN assays as sensitive indicators of metal-induced genotoxicity, while also cautioning against overinterpretation of results from low-level, short-term exposures to complex airborne mixtures.

Additionally, for blood MN, age and sex were significant predictors, with older age increasing MN counts and males showing lower counts. As reviewed by Dhillon et al. (2021), the frequency MN in human lymphocytes tends to increase with age, and females generally exhibit higher frequencies compared to males. This trend starts from a low baseline of 0–2 MN per 1,000 cells at birth. However, exposure to genotoxic agents—such as chemicals, radiation, or environmental pollutants—can further elevate MN frequency. As individuals age, there is a documented decline in the efficiency of DNA repair mechanisms, particularly in pathways like non-homologous end joining (NHEJ) and homologous recombination (HR) (Li et al., 2016). This decline leads to the accumulation of DNA double-strand breaks and genomic instability, which are precursors to MN formation (Fenech, 2020; Fenech et al., 2011). Telomere shortening is another critical factor associated with aging (Škrobot Vidaček et al. 2018). Telomeres, the protective caps

at the ends of chromosomes, progressively shorten with each cell division (Harley et al., 1990). When they become critically short, they can no longer protect chromosomes effectively, leading to end-to-end fusions, chromosomal breakage, and the formation of MNi. Furthermore, Mesnage (2025) emphasizes that environmental pollutants—ranging from airborne PM and toxic metals to endocrine disruptors and microplastics—accelerate biological aging by inflicting damage on DNA, proteins, and lipids, leading to telomere shortening and epigenetic age acceleration. The observed sex difference may be partly explained by the mechanisms described by Fenech et al. (2011), who reported that MN can result from chromosomal missegregation, particularly involving the X chromosome. Females, having two X chromosomes, may be more susceptible to the formation of MN due to increased chances of sex chromosome loss or misrepair events during cell division. Additionally, factors such as hypomethylation of pericentromeric DNA and spindle assembly defects—more prevalent in cells under genotoxic stress—can further contribute to higher MN formation in females. This is consistent with the large-scale study by Gajski et al. (2024), who reported a clear age-related increase in MN frequency and higher values in females across the Croatian general population. Our seasonal MN values (4.42 ± 3.7 in colder *vs* 4.77 ± 4.16 in warmer period) fall within their established baseline (5.3 ± 4.3), and are well below their 95^{th} percentile cut-off of 14 MNi, supporting the idea that our study population was largely within expected genomic stability ranges. Similar patterns were seen for NBUDs (4.45 ± 4.06 colder *vs* 4.48 ± 2.96 warmer), which were slightly elevated compared to the so far Croatian mean (3.45 ± 2.10), and for NPBs, where we observed a higher mean in colder months (0.32 ± 0.5) compared to warmer (0.07 ± 0.31), both values falling below their reported mean (1.22 ± 1.51). The proliferation rate measured by the mitotic index (CBPI) in our cohort (2.11–2.17) was consistent with the Croatian mean (2.00 ± 0.12), reflecting expected cell proliferation activity. Our findings suggest that while internal factors like age and sex are reliable predictors of genomic instability markers, the subtle effects of ambient air pollution may be masked without higher exposure contrasts or longer-term cumulative assessments.

The inverse association observed between CC3 (As, Cd, Pb) and TI was unexpected, as these metals are well-known for their genotoxicity (Dikilitas et al., 2016; Qu and Zheng, 2024; Speer et al., 2023). As primarily induces genotoxicity indirectly by inhibiting DNA repair enzymes, particularly those involved in base excision repair, and by promoting oxidative stress through mitochondrial dysfunction and redox cycling (Speer et al., 2023; Zhou et al., 2021). Cd generates

ROS, disrupts redox homeostasis, and interferes with key DNA repair mechanisms such as nucleotide excision and mismatch repair, while also affecting genes involved in cell cycle control and apoptosis (Qu and Zheng, 2024). Pb contributes to genomic instability by increasing oxidative stress, inhibiting DNA polymerases, and promoting replication errors and chromosomal damage (Dikilitas et al., 2016). Collectively, these mechanisms disrupt DNA integrity through both direct and indirect pathways. However, the lack of a positive association in our data may reflect low exposure levels or the possibility of confounding factors that were not measured in this study, such as variations in metabolic processing or the presence of protective genetic factors that may mitigate the typical DNA-damaging effects of these metals. For example, genetic polymorphisms in DNA repair genes (e.g. XRCC1, GSTT1) have been shown to influence individual susceptibility to DNA damage from both cigarette smoke and environmental pollutants (Pinto et al., 2025). This could explain the unexpected result, highlighting the importance of considering genetic susceptibility when evaluating environmental exposures. Furthermore, this study hypothesized that oxidative stress mediates the relationship between ambient exposures and DNA damage. However, our mediation analysis showed that OXC1 (SOD, NO, ROS, MDA) did not significantly mediate this relationship. While CC3 remained a significant predictor of TI, OXC1 had no significant effect on TI, and ACME was insignificant. This suggests that, in this study cohort, the effect of ambient exposures on DNA damage operates primarily through a direct pathway. This finding contrasts with previous studies that have linked oxidative stress to DNA strand breaks and increased levels of 8-OHdG in high-exposure populations (Cavallo et al., 2021). However, in our study, the overall mean TI levels were relatively low (1.22% for the colder period *vs* 1.7% for the warmer period). These values suggest minimal DNA strand breakage, likely insufficient to robustly reflect oxidative stress pathways as a key mediator mechanism. A comparable study by Gerić et al. (2018), which examined seasonal variations in comet assay descriptors among Zagreb residents, found higher average TI values, notably 1.43% in winter *vs* 1.98% in summer. Notably, they reported strong correlations between TI values and meteorological parameters such as temperature, solar radiation, and insolation, with the summer season producing the highest DNA damage across comet assay parameters. Hence, the slightly higher TI values observed during the warmer period may be more attributable to meteorological factors, such as UV radiation, rather than air pollution. A more recent study by Gerić et al. (2024) found no significant associations between air pollution exposure factors

(including PM, metals, and other pollutants) and comet assay descriptors, including TI, among 123 Zagreb residents enrolled between 2011 and 2015.

In our study, smoking status emerged as a significant individual predictor of TI, with smokers exhibiting higher TI estimates (1.68 % for smokers compared to 1.18 % for non-smokers). Previous studies have shown that both active and passive exposure to tobacco smoke can induce cytogenetic damage. In a recent systematic review by Pinto et al. (2025), 15 out of 18 included studies reported genotoxicity due to cigarette smoking, and all reported some association between a genetic polymorphism and the aforementioned genotoxicity. For example, Chandirasekar et al. (2014) found a significant increase in DNA damage in smokers and smokeless tobacco users compared to controls, supporting the genotoxic effects of tobacco use. In our previous work on a broader Croatian cohort, lifestyle factors—including smoking and alcohol consumption—were associated with increased DNA migration, emphasizing their relevance as contributors to background DNA damage levels (Matković et al., 2024).

5.4. Limitations and Future Perspectives

This study incorporates several methodological strengths that enhance the validity of its findings. The application of a multi-time-frame exposure model (one-, three-, and seven-day pollutant averages), hierarchical clustering to derive composite exposure groups, and advanced statistical tools—including multivariate regression, best subset selection, and mediation analysis—enabled a nuanced investigation of exposure–effect relationships. The simultaneous use of exposure biomarkers (e.g. BTEX, PAH metabolites, essential elements and toxic metals), oxidative stress markers, and effect biomarkers (including both systemic and tissue-specific endpoints such as blood and buccal MNi, FOXP3 methylation, and FeNO) provided a comprehensive picture of biological response. The inclusion of both manual, semi-automated and automated scoring methods further bolstered the reliability of molecular-biological and cytogenetic endpoints. Nonetheless, several limitations must be acknowledged. The use of fixed-site monitoring station data to estimate ambient pollutant concentrations likely introduced spatial exposure misclassification, particularly for more mobile participants, which may have diluted observed associations. Several studies have shown that the use of personal sampling systems can provide more accurate individual exposure data, encompassing both indoor and outdoor air (Anand et al., 2024; Delfino et al., 2006; Matthaios et al., 2024; Mostafavi et al., 2018; Panchal et al., 2022). However, deploying numerous low-cost

sensors, which are still not entirely reliable, may not be feasible (Hayward et al., 2024; Kang et al., 2022; Lu, 2021). While within-subject comparisons helped control for seasonal variability, the relatively modest sample size (N=57 paired participants, N=121 overall) may have limited statistical power for detecting subtle effects—particularly in mediation models where indirect effects are often small. To support statistical robustness despite these limitations, a small proportion of active smokers (14%) were included in the final cohort, all of whom reported light smoking habits and were instructed to abstain for at least 16 h before sampling. Our preliminary validation showed no significant elevation of BTEX in their blood under these conditions (Matković et al., 2025), and comparisons in the current study confirmed no meaningful differences between smokers and non-smokers across most biomarkers except TI, where smokers showed modestly higher values. Importantly, these differences were minor in biological terms (1.02% vs. 0.81%) and align with Bonassi et al. (2003) who showed that light smokers without concurrent occupational exposure do not experience an overall increase in genotoxic damage, as measured by the MN assay. Passive smoking was also recorded and controlled for in statistical models. These decisions reflect both analytical requirements of multivariate methods and the reality of light smoking prevalence in urban populations.

To address the challenge of scaling future biomonitoring studies, we tested several methodological adaptations that could support higher-throughput analyses. First, in addition to fresh samples, we applied the comet assay to frozen blood samples. Based on those results and available literature, conducting the comet assay on frozen blood samples emerges as a practical and efficient approach for biomonitoring and epidemiological research as long as one does not directly compare fresh with frozen samples due to apparent differences with frozen samples displaying to some extent higher values of DNA damage (Gajski et al., 2020a; Matković et al., 2024; Møller et al., 2021). Second, to optimize the analysis of cytogenetic damage, we utilized Metafer, a semi-automated imaging system for MN scoring. While manual and automated scores showed only moderate correlation, the exclusion of outlier cases with large discrepancies substantially improved agreement, suggesting that Metafer-based assessments, once carefully validated, could offer a reliable and more time-efficient solution for expanding sample capacity in our future research. Additionally, the high proportion of non-detectable values for BTEX and certain PAH metabolites constrained their use in exposure modeling, highlighting a need for more sensitive analytical methods in low-exposure urban cohorts. Importantly, the incorporation of

FOXP3 methylation reflects growing interest in epigenetic biomarkers as sensitive indicators of environmentally induced immune modulation. This aligns with exposome-based frameworks, which emphasize the cumulative and dynamic nature of environmental exposures and their molecular imprints across the life course (Rider and Carlsten, 2019; Saenen et al., 2019; Wild, 2025). Although our overall findings suggest that air pollution levels in Zagreb may not exert a strong genotoxic effect, this does not imply that ambient air in the city is benign from a broader public health perspective. Non-genotoxic respiratory outcomes such as asthma, allergic rhinitis, and COPD remain prevalent in urban populations and are frequently aggravated by even moderate levels of traffic-related air pollution and pollen exposure. The study by Kranjčić et al. (2022) supports this concern by modeling the potential for air quality improvement through targeted urban greening strategies in Zagreb. Their analysis, using satellite imagery and machine learning techniques, identified over 400,000 m^2 of potential green buffer zones along heavily trafficked roads—areas particularly relevant for reducing pollutant exposure and mitigating respiratory symptoms. These nature-based interventions may not directly affect DNA damage endpoints but could significantly alleviate inflammatory and allergic airway conditions, especially in sensitive subpopulations such as children, the elderly, and individuals with preexisting respiratory disease. It is also important to note that air quality in Zagreb is generally good, with concentrations of most pollutants, especially PM levels, decreasing over the past decade (Lovrić et al., 2022). This progress reflects broader historical improvements, driven by industrial restructuring, fuel quality enhancements, and the phase-out of leaded gasoline (Šega and Hršak, 1995; Vadjić et al., 2009). According to the Air Quality Life Index, Croatia's potential gain in life expectancy from $PM_{2.5}$ reduction to WHO guideline levels (5 $\mu g/m^3$) has improved significantly—from 1.54 years in 1998 to 0.9 years in 2022, reflecting notable progress in ambient air quality (AQLI, 2025). Further improvement could be achieved by integrating innovative technologies and green infrastructure. Reducing urban air pollution requires a multifaceted approach, and several strategies show promise for realistic and impactful implementation. As reviewed by Gulia et al. (2020), stricter vehicular emission standards, combined with the promotion of low-emission zones and accelerated fleet renewal programs, present viable options for targeting a major source of pollutants. Urban planning interventions—such as enhanced public transit systems, infrastructure for active mobility, and intelligent traffic management—may further reduce emissions by shifting travel behavior and alleviating congestion. Environmental design solutions, including the creation of ventilation

corridors, strategic urban greening, and measures to control road dust (e.g. paving and street cleaning), offer additional potential for localized improvements in air quality. For example, vertical green walls, pollution-filtering towers that support greenhouse agriculture, and comprehensive sensor networks for real-time air quality monitoring have been proposed as part of a more integrated urban response to air pollution. The expansion of low-cost sensor networks could enable more granular monitoring and adaptive policy responses. While the effectiveness of these measures may vary by context, their integration—particularly when guided by environmental justice considerations—represents a promising pathway toward healthier urban environments.

Implementing Low Emission Zones (LEZs) and Zero Emission Zones (ZEZs) could further enhance air quality in Zagreb. LEZs restrict access to certain areas for vehicles that do not meet specific emission standards, thereby reducing traffic-related air pollution. ZEZs take this a step further by allowing only zero-emission vehicles, pedestrians, and cyclists unrestricted access, effectively eliminating tailpipe emissions within these zones. European cities like London, Berlin, and Brussels have successfully implemented LEZs, leading to significant reductions in pollutants (Cui et al., 2021; Gu et al., 2022). Implementing LEZs and ZEZs in Zagreb could complement potential greening initiatives by targeting vehicular emissions directly. Such zones could be strategically placed in areas with high traffic density and pollution levels. However, it's essential to consider potential challenges, such as ensuring equitable access and mitigating impacts on low-income populations who may rely on older vehicles. Lessons from other cities highlight the importance of accompanying these zones with supportive measures, like vehicle upgrade incentives and improved public transportation options. Furthermore, considering that people in Croatia predominantly spend time indoors (more than 21 h on average), the reliance on outdoor monitoring stations may not accurately reflect individual exposures. This raises questions about indoor air quality, which warrants further investigation (Kazensky et al., 2024; Lovrić et al., 2025). Taken together, these limitations suggest caution in drawing causal inferences and underscore the value of future longitudinal studies with personal exposure monitoring and larger cohorts. Such studies would better capture individual-level variability, facilitate time-resolved analyses, and support cumulative risk assessments. Future studies could build on this design by integrating high-resolution exposomic data with multi-omics approaches, including epigenetic profiling, to better characterize the mechanistic pathways linking complex exposures to health outcomes (Pandics et al., 2023; Wild, 2025).

6. CONCLUSION

This study demonstrates that ambient air pollution in an urban European setting exerts measurable biological effects through multiple mechanistic pathways—including oxidative stress, immune modulation, and genomic damage—shaped by both environmental and individual-level factors. By integrating external exposure assessments with exposure biomarkers and effect endpoints across two seasons, this research provides one of the most comprehensive evaluations to date of pollution-related health risks in the general population of Zagreb, Croatia. Key findings include the identification of specific pollutant composite clusters—notably CC1 (PMs, PAHs, BTEX, O_3, PM_{10}- bound metals) and CC3 (PM_{10}-bound As, Pb, Cd)—that significantly influence oxidative and immunological biomarkers, the detection of a mediating role for FOXP3 methylation in pollen-related airway inflammation, and the observation that cytogenetic outcomes are modulated by both demographic factors (e.g. age, sex, smoking) and metal-rich exposure sources. Importantly, while some biomarkers—such as oxidative stress indices—showed sensitivity to short-term exposures and modifiable lifestyle factors like physical activity, others reflected more stable background exposure or regulatory responses. These results underscore the complexity of real-life exposure scenarios and highlight the need for integrated, matrix-appropriate biomonitoring approaches. While air quality in Zagreb has improved over recent decades—largely due to industrial restructuring, cleaner fuels, and policy changes—certain pollutant sources, particularly traffic-related emissions and PM-bound metals, still pose localized health risks. This study confirms that even in a city with generally declining ambient pollution levels, biologically relevant effects are detectable and shaped by seasonal variation, pollutant composition, and personal characteristics, along with lifestyle habits. Beyond their scientific relevance, the findings carry clear implications for public health and urban policy: reducing metal-rich emissions, improving regional air quality coordination, and promoting protective behaviors could collectively mitigate the health burden of air pollution. As urban populations continue to grow, precision environmental health approaches, linking mechanistic biomarkers with exposure profiling, will be essential for informed decision-making and targeted interventions.

7. REFERENCES

Abbafati, C., Abbas, K. M., Abbasi, M., Abbasifard, M., Abbasi-Kangevari, M., Abbastabar, H., Abd-Allah, F., Abdelalim, A., Abdollahi, M., Abdollahpour, I., Abedi, A., Abedi, P., Abegaz, K. H., Abolhassani, H., Abosetugn, A. E., Aboyans, V., Abrams, E. M., Abreu, L. G., Abrigo, M. R. M., … Murray, C. J. L. (2020). Global burden of 369 diseases and injuries in 204 countries and territories, 1990–2019: a systematic analysis for the Global Burden of Disease Study 2019. *The Lancet*, *396*(10258), 1204–1222. https://doi.org/10.1016/S0140-6736(20)30925-9

Abd El-Hay, S. S., and Colyer, C. L. (2017). Development of High-Throughput Method for Measurement of Vascular Nitric Oxide Generation in Microplate Reader. *Molecules 2017, Vol. 22, Page 127*, *22*(1), 127. https://doi.org/10.3390/MOLECULES22010127

Agudelo-Castañeda, D., Teixeira, E., Schneider, I., Lara, S. R., and Silva, L. F. O. (2017). Exposure to polycyclic aromatic hydrocarbons in atmospheric PM1.0 of urban environments: Carcinogenic and mutagenic respiratory health risk by age groups. *Environmental Pollution*, *224*, 158–170. https://doi.org/10.1016/J.ENVPOL.2017.01.075

Aithal, S. S., Sachdeva, I., and Kurmi, O. P. (2023). Air quality and respiratory health in children. *Breathe*, *19*(2), 230040. https://doi.org/10.1183/20734735.0040-2023

Aksu, İ., Anlar, H. G., Taner, G., Bacanlı, M., İritaş, S., Tutkun, E., and Basaran, N. (2019). Assessment of DNA damage in welders using comet and micronucleus assays. *Mutation Research/Genetic Toxicology and Environmental Mutagenesis*, *843*, 40–45. https://doi.org/10.1016/J.MRGENTOX.2018.11.006

Alabi, O. A., Adeoluwa, Y. M., and Bakare, A. A. (2020). Elevated Serum Pb, Ni, Cd, and Cr Levels and DNA Damage in Exfoliated Buccal Cells of Teenage Scavengers at a Major Electronic Waste Dumpsite in Lagos, Nigeria. *Biological Trace Element Research*, *194*(1), 24–33. https://doi.org/10.1007/S12011-019-01745-Z/FIGURES/2

Alarcon, W. A., Davidson, S., Dufour, B., Roach, M., Tsang, K., Payne, S. F., DeLoreto, A. M., St. Louis, T., Rajagopalan, S., Watkins, S., Chalmers, J., Shen, T., Turner, J. M., Leinenkugel, K., Asamoah, M., Lewis, J., Keyvan, E., Roseman, K., Kica, J., … Melia, S. (2019). Elevated Blood Lead Levels Among Employed Adults — United States, 1994–2013. *MMWR. Morbidity and Mortality Weekly Report*, *63*(55), 59–65. https://doi.org/10.15585/MMWR.MM6355A5

Alfano, R., Herceg, Z., Nawrot, T. S., Chadeau-Hyam, M., Ghantous, A., and Plusquin, M. (2018). The Impact of Air Pollution on Our Epigenome: How Far Is the Evidence? (A Systematic Review). In *Current environmental health reports* (Vol. 5, Issue 4, pp. 544–578). Springer. https://doi.org/10.1007/s40572-018-0218-8

Al-Qassimi, M., and Al-Salem, S. M. (2020). Ozone (O3) ambient levels as a secondary airborne precursor in Fahaheel urban area, the State of Kuwait. *Atmospheric Science Letters*, *21*(9), e983. https://doi.org/10.1002/ASL.983

Ambient air pollution. (n.d.). Retrieved June 27, 2024, from https://www.who.int/data/gho/data/themes/topics/indicator-groups/indicator-group-details/GHO/ambient-air-pollution

Anand, A., Castiglia, E., and Zamora, M. L. (2024). The Association Between Personal Air Pollution Exposures and Fractional Exhaled Nitric Oxide (FeNO): A Systematic Review. *Current Environmental Health Reports*, *11*(2), 210–224. https://doi.org/10.1007/S40572-024-00430-1/FIGURES/2

Angerer, J., Ewers, U., and Wilhelm, M. (2007). Human biomonitoring: State of the art. *International Journal of Hygiene and Environmental Health*, *210*(3–4), 201–228. https://doi.org/10.1016/J.IJHEH.2007.01.024

Annangi, B., Bonassi, S., Marcos, R., and Hernández, A. (2016). Biomonitoring of humans exposed to arsenic, chromium, nickel, vanadium, and complex mixtures of metals by using the micronucleus test in lymphocytes. *Mutation Research/Reviews in Mutation Research*, *770*, 140–161. https://doi.org/10.1016/J.MRREV.2016.03.003

Aquilano, K., Baldelli, S., and Ciriolo, M. R. (2014). Glutathione: new roles in redox signaling for an old antioxidant. *Frontiers in Pharmacology*, *5*, 196. https://doi.org/10.3389/FPHAR.2014.00196

Ashley, D. L., Bonin, M. A., Cardinali, F. L., Mccraw, J. M., and Wooten, J. V. (1996). Measurement of Volatile Organic Compounds in Human Blood. In *Environ Health Perspect* (Vol. 104, Issue 5).

Atkinson, R. (2000). Atmospheric chemistry of VOCs and NOx. *Atmospheric Environment*, *34*(12–14), 2063–2101. https://doi.org/10.1016/S1352-2310(99)00460-4

Atsdr. (2010). *TOXICOLOGICAL PROFILE FOR ETHYLBENZENE*.

Ávila, D. S., Rocha, J. B. T., Tizabi, Y., dos Santos, A. P. M., Santamaría, A., Bowman, A. B., and Aschner, M. (2021). Manganese Neurotoxicity. *Handbook of Neurotoxicity*, 1–26. https://doi.org/10.1007/978-3-030-71519-9_3-1

Azqueta, A., and Collins, A. R. (2013). The essential comet assay: A comprehensive guide to measuring DNA damage and repair. *Archives of Toxicology*, *87*(6), 949–968. https://doi.org/10.1007/S00204-013-1070-0

Azqueta, A., Ladeira, C., Giovannelli, L., Boutet-Robinet, E., Bonassi, S., Neri, M., Gajski, G., Duthie, S., Del Bo', C., Riso, P., Koppen, G., Basaran, N., Collins, A., and Møller, P. (2020). Application of the comet assay in human biomonitoring: An hCOMET perspective. *Mutation Research/Reviews in Mutation Research*, *783*, 108288. https://doi.org/10.1016/J.MRREV.2019.108288

Azqueta, A., Langie, S. A. S., Boutet-Robinet, E., Duthie, S., Ladeira, C., Møller, P., Collins, A. R., and Godschalk, R. W. L. (2019). DNA repair as a human biomonitoring tool: Comet

assay approaches. *Mutation Research/Reviews in Mutation Research*, *781*, 71–87. https://doi.org/10.1016/J.MRREV.2019.03.002

Baccarelli, A., Wright, R. O., Bollati, V., Tarantini, L., Litonjua, A. A., Suh, H. H., Zanobetti, A., Sparrow, D., Vokonas, P. S., and Schwartz, J. (2012). Rapid DNA Methylation Changes after Exposure to Traffic Particles. *Https://Doi.Org/10.1164/Rccm.200807-1097OC*, *179*(7), 572–578. https://doi.org/10.1164/RCCM.200807-1097OC

Barnham, K. J., Masters, C. L., and Bush, A. I. (2004). Neurodegenerative diseases and oxidative stress. *Nature Reviews Drug Discovery 2004 3:3*, *3*(3), 205–214. https://doi.org/10.1038/nrd1330

Bartolomé, M., Ramos, J. J., Cutanda, F., Huetos, O., Esteban, M., Ruiz-Moraga, M., Calvo, E., Pérez-Gómez, B., González, O., Castaño, A., Aleixandre, J. L., Aragonés, N., Cañas, A. I., Cervantes-Amat, M., Cortés, M. V., Jimenez, J. A., López-Abente, G., López-Herranz, A., Mayor, J., … Román, J. (2015). Urinary polycyclic aromatic hydrocarbon metabolites levels in a representative sample of the Spanish adult population: The BIOAMBIENT.ES project. *Chemosphere*, *135*, 436–446. https://doi.org/10.1016/J.CHEMOSPHERE.2014.12.008

Belis, C. A., Pisoni, E., Degraeuwe, B., Peduzzi, E., Thunis, P., Monforti-Ferrario, F., and Guizzardi, D. (2019). Urban pollution in the Danube and Western Balkans regions: The impact of major PM2.5 sources. *Environment International*, *133*. https://doi.org/10.1016/j.envint.2019.105158

Bellavia, A., James-Todd, T., and Williams, P. L. (2019). Approaches for incorporating environmental mixtures as mediators in mediation analysis. *Environment International*, *123*, 368–374. https://doi.org/10.1016/J.ENVINT.2018.12.024

Beslic, I., Burger, J., Cadoni, F., Centioli, D., Kranjc, I., Van den Bril, B., Rinkovec, J., Sega, K., Zang, T., Zuzul, S., and Gladtke, D. (2020). Determination of As, Cd, Ni and Pb in PM10 – comparison of different sample work-up and analysis methods/Bestimmung von As, Cd, Ni und Pb in PM10 – Vergleich verschiedener Probenaufbereitungs- und Analysenverfahren. *Gefahrstoffe*, *80*(06), 227–233. https://doi.org/10.37544/0949-8036-2020-06-17

Bind, M.-A., Lepeule, J., Zanobetti, A., Gasparrini, A., Baccarelli, A. A., Coull, B. A., Tarantini, L., Vokonas, P. S., Koutrakis, P., and Schwartz, J. (2014). Air pollution and gene-specific methylation in the Normative Aging Study Association, effect modification, and mediation analysis View supplementary material. *Epigenetics*, *9*, 448–458. https://doi.org/10.4161/epi.27584

Bodor, K., Szép, R., and Bodor, Z. (2022). Time series analysis of the air pollution around Ploiesti oil refining complex, one of the most polluted regions in Romania. *Scientific Reports 2022 12:1*, *12*(1), 1–11. https://doi.org/10.1038/s41598-022-16015-7

Bolognesi, C., Bonassi, S., Knasmueller, S., Fenech, M., Bruzzone, M., Lando, C., and Ceppi, M. (2015). Clinical application of micronucleus test in exfoliated buccal cells: A systematic

review and metanalysis. *Mutation Research. Reviews in Mutation Research*, *766*, 20–31. https://doi.org/10.1016/J.MRREV.2015.07.002

Bolognesi, C., and Fenech, M. (2019). Micronucleus Cytome Assays in Human Lymphocytes and Buccal Cells. *Methods in Molecular Biology (Clifton, N.J.)*, *2031*, 147–163. https://doi.org/10.1007/978-1-4939-9646-9_8

Bonassi, S., Ceppi, M., Møller, P., Azqueta, A., Milić, M., Monica, N., Brunborg, G., Godschalk, R., Koppen, G., Langie, S. A. S., Teixeira, J. P., Bruzzone, M., Da Silva, J., Benedetti, D., Cavallo, D., Ursini, C. L., Giovannelli, L., Moretti, S., Riso, P., … Stopper, H. (2021). DNA damage in circulating leukocytes measured with the comet assay may predict the risk of death. *Scientific Reports*, *11*(1). https://doi.org/10.1038/s41598-021-95976-7

Bonassi, S., Milić, M., and Neri, M. (2016). Frequency of micronuclei and other biomarkers of DNA damage in populations exposed to dusts, asbestos and other fibers. A systematic review. In *Mutation Research - Reviews in Mutation Research* (Vol. 770, pp. 106–118). Elsevier B.V. https://doi.org/10.1016/j.mrrev.2016.05.004

Bonassi, S., Neri, M., Lando, C., Ceppi, M., Lin, Y. P., Chang, W. P., Holland, N., Kirsch-Volders, M., Zeiger, E., Fenech, M., Ban, S., Barale, R., Bigatti, M. P., Bolognesi, C., Jia, C., Di Giorgio, M., Ferguson, L. R., Fucic, A., Hrelia, P., … Zijno, A. (2003). Effect of smoking habit on the frequency of micronuclei in human lymphocytes: Results from the Human MicroNucleus project. *Mutation Research - Reviews in Mutation Research*, *543*(2), 155–166. https://doi.org/10.1016/S1383-5742(03)00013-9

Bonassi, S., Norppa, H., Ceppi, M., Strömberg, U., Vermeulen, R., Znaor, A., Cebulska-Wasilewska, A., Fabianova, E., Fucic, A., Gundy, S., Hansteen, I. L., Knudsen, L. E., Lazutka, J., Rossner, P., Sram, R. J., and Boffetta, P. (2008). Chromosomal aberration frequency in lymphocytes predicts the risk of cancer: results from a pooled cohort study of 22 358 subjects in 11 countries. *Carcinogenesis*, *29*(6), 1178–1183. https://doi.org/10.1093/CARCIN/BGN075

Bonassi, S., Znaor, A., Ceppi, M., Lando, C., Chang, W. P., Holland, N., Kirsch-Volders, M., Zeiger, E., Ban, S., Barale, R., Bigatti, M. P., Bolognesi, C., Cebulska-Wasilewska, A., Fabianova, E., Fucic, A., Hagmar, L., Joksic, G., Martelli, A., Migliore, L., … Fenech, M. (2007). An increased micronucleus frequency in peripheral blood lymphocytes predicts the risk of cancer in humans. *Carcinogenesis*, *28*(3), 625–631. https://doi.org/10.1093/CARCIN/BGL177

Boogaard, P. J. (2022). Human biomonitoring of low-level benzene exposures. *Critical Reviews in Toxicology*, *52*(10), 799–810. https://doi.org/10.1080/10408444.2023.2175642

Brajenović, N., Karačonji, I. B., and Bulog, A. (2015). Evaluation of Urinary Btex, Nicotine, and Cotinine as Biomarkers of Airborne Pollutants in Nonsmokers and Smokers. *Journal of Toxicology and Environmental Health, Part A*, *78*(17), 1133–1136. https://doi.org/10.1080/15287394.2015.1066286

Brčić, I. (2004). Izloženost opće populacije hlapljivim aromatskim ugljikovodicima. *Arh Hig Rada Toksiko*, *55*, 291–300.

Brook, R. D., Rajagopalan, S., Pope, C. A., Brook, J. R., Bhatnagar, A., Diez-Roux, A. V., Holguin, F., Hong, Y., Luepker, R. V., Mittleman, M. A., Peters, A., Siscovick, D., Smith, S. C., Whitsel, L., and Kaufman, J. D. (2010). Particulate matter air pollution and cardiovascular disease: An update to the scientific statement from the american heart association. *Circulation*, *121*(21), 2331–2378. https://doi.org/10.1161/CIR.0B013E3181DBECE1/ASSET/5060294E-E298-4A64-B3F3-683ED116BEF0/ASSETS/GRAPHIC/14FF3.JPEG

Brucker, N., do Nascimento, S. N., Bernardini, L., Charão, M. F., and Garcia, S. C. (2020). Biomarkers of exposure, effect, and susceptibility in occupational exposure to traffic-related air pollution: A review. *Journal of Applied Toxicology*, *40*(6), 722–736. https://doi.org/10.1002/JAT.3940

Bukowska, B., and Duchnowicz, P. (2022). Molecular Mechanisms of Action of Selected Substances Involved in the Reduction of Benzo[a]pyrene-Induced Oxidative Stress. *Molecules 2022, Vol. 27, Page 1379*, *27*(4), 1379. https://doi.org/10.3390/MOLECULES27041379

Bulog, A., Kara~onji, I. B., Uti}, I. [, and Mi}ovi}, V. (2011). Immunomodulation of Cell-Mediated Cytotoxicity after Chronic Exposure to Vapors. In *Coll. Antropol* (Vol. 35).

Burkhardt, T., Scherer, M., Scherer, G., Pluym, N., Weber, T., and Kolossa-Gehring, M. (2023). Time trend of exposure to secondhand tobacco smoke and polycyclic aromatic hydrocarbons between 1995 and 2019 in Germany – Showcases for successful European legislation. *Environmental Research*, *216*, 114638. https://doi.org/10.1016/J.ENVRES.2022.114638

Capone, P., Lancia, A., and D'Ovidio, M. C. (2023). Interaction between Air Pollutants and Pollen Grains: Effects on Public and Occupational Health. *Atmosphere 2023, Vol. 14, Page 1544*, *14*(10), 1544. https://doi.org/10.3390/ATMOS14101544

Cavallo, D., Ursini, C. L., Fresegna, A. M., Ciervo, A., Maiello, R., Buresti, G., Paci, E., Pigini, D., Gherardi, M., Carbonari, D., Sisto, R., Tranfo, G., and Iavicoli, S. (2021). Occupational Exposure in Industrial Painters: Sensitive and Noninvasive Biomarkers to Evaluate Early Cytotoxicity, Genotoxicity and Oxidative Stress. *International Journal of Environmental Research and Public Health 2021, Vol. 18, Page 4645*, *18*(9), 4645. https://doi.org/10.3390/IJERPH18094645

Ceppi, M., Biasotti, B., Fenech, M., and Bonassi, S. (2010). Human population studies with the exfoliated buccal micronucleus assay: Statistical and epidemiological issues. *Mutation Research/Reviews in Mutation Research*, *705*(1), 11–19. https://doi.org/10.1016/J.MRREV.2009.11.001

Ceretti, E., Donato, F., Zani, C., Villarini, M., Verani, M., De Donno, A., Bonetta, S., Feretti, D., Carducci, A., Idolo, A., Carraro, E., Covolo, L., Moretti, M., Palomba, G., Grassi, T.,

Bonetti, A., Bonizzoni, S., Biggeri, A., Gelatti, U., … Casini, B. (2020). Results from the European Union MAPEC_LIFE cohort study on air pollution and chromosomal damage in children: are public health policies sufficiently protective? *Environmental Sciences Europe*, *32*(1), 1–11. https://doi.org/10.1186/S12302-020-00352-3/FIGURES/3

Cetkovic, T., Haveric, A., Behmen, S., Hadzic Omanovic, M., Caluk Klacar, L., Dzaferspahic, A., Durmisevic, I., Mehanovic, M., and Haveric, S. (2023). A pilot biomonitoring study of air pollution in the urban area of Sarajevo, Bosnia and Herzegovina: genotoxicity assessment in buccal cells. *Mutagenesis*, *38*(1), 33–42. https://doi.org/10.1093/MUTAGE/GEAC016

Chandirasekar, R., Kumar, B. L., Sasikala, K., Jayakumar, R., Suresh, K., Venkatesan, R., Jacob, R., Krishnapriya, E. K., Kavitha, H., and Ganesh, G. K. (2014). Assessment of genotoxic and molecular mechanisms of cancer risk in smoking and smokeless tobacco users. *Mutation Research/Genetic Toxicology and Environmental Mutagenesis*, *767*, 21–27. https://doi.org/10.1016/J.MRGENTOX.2014.04.007

Checa, J., and Aran, J. M. (2020). Reactive Oxygen Species: Drivers of Physiological and Pathological Processes. *Journal of Inflammation Research*, *13*, 1057. https://doi.org/10.2147/JIR.S275595

Cheng, H., Villahoz, B. F., Ponzio, R. D., Aschner, M., and Chen, P. (2023). Signaling Pathways Involved in Manganese-Induced Neurotoxicity. *Cells 2023, Vol. 12, Page 2842*, *12*(24), 2842. https://doi.org/10.3390/CELLS12242842

Chen, J., Rodopoulou, S., Strak, M., de Hoogh, K., Taj, T., Poulsen, A. H., Andersen, Z. J., Bellander, T., Brandt, J., Zitt, E., Fecht, D., Forastiere, F., Gulliver, J., Hertel, O., Hoffmann, B., Hvidtfeldt, U. A., Verschuren, W. M. M., Jørgensen, J. T., Katsouyanni, K., … Hoek, G. (2022). Long-term exposure to ambient air pollution and bladder cancer incidence in a pooled European cohort: the ELAPSE project. *British Journal of Cancer*, *126*(10), 1499–1507. https://doi.org/10.1038/S41416-022-01735-4

Chen, X., Liu, F., Niu, Z., Mao, S., Tang, H., Li, N., Chen, G., Liu, S., Lu, Y., and Xiang, H. (2020). The association between short-term exposure to ambient air pollution and fractional exhaled nitric oxide level: A systematic review and meta-analysis of panel studies. *Environmental Pollution*, *265*, 114833. https://doi.org/10.1016/J.ENVPOL.2020.114833

Chiavarini, M., Rosignoli, P., Sorbara, B., Giacchetta, I., and Fabiani, R. (2024). Benzene Exposure and Lung Cancer Risk: A Systematic Review and Meta-Analysis of Human Studies. *International Journal of Environmental Research and Public Health*, *21*(2), 205. https://doi.org/10.3390/IJERPH21020205/S1

Choi H, Harrison R, Komulainen H, and Delgado Saborit JM. (2010). *Polycyclic aromatic hydrocarbons - WHO Guidelines for Indoor Air Quality: Selected Pollutants - NCBI Bookshelf*. WHO. https://www.ncbi.nlm.nih.gov/books/NBK138709/

Cipryan, L., Litschmannova, M., Barot, T., Dostal, T., Sindler, D., Kutac, P., Jandacka, D., and Hofmann, P. (2024). Air pollution, cardiorespiratory fitness and biomarkers of oxidative status and inflammation in the 4HAIE study. *Scientific Reports*, *14*(1), 1–10. https://doi.org/10.1038/S41598-024-60388-W;SUBJMETA=499,692,699;KWRD=DISEASES,RISK+FACTORS

Coelho, S., Ferreira, J., Rodrigues, V., and Lopes, M. (2022). Source apportionment of air pollution in European urban areas: Lessons from the ClairCity project. *Journal of Environmental Management*, *320*, 115899. https://doi.org/10.1016/J.JENVMAN.2022.115899

Collins, A., and Azqueta, A. (2012). DNA repair as a biomarker in human biomonitoring studies; further applications of the comet assay. *Mutation Research/Fundamental and Molecular Mechanisms of Mutagenesis*, *736*(1–2), 122–129. https://doi.org/10.1016/J.MRFMMM.2011.03.005

Collins, A., Koppen, G., Valdiglesias, V., Dusinska, M., Kruszewski, M., Møller, P., Rojas, E., Dhawan, A., Benzie, I., Coskun, E., Moretti, M., Speit, G., and Bonassi, S. (2014). The comet assay as a tool for human biomonitoring studies: The ComNet Project. *Mutation Research/Reviews in Mutation Research*, *759*(1), 27–39. https://doi.org/10.1016/J.MRREV.2013.10.001

Collins, A., Møller, P., Gajski, G., Vodenková, S., Abdulwahed, A., Anderson, D., Bankoglu, E. E., Bonassi, S., Boutet-Robinet, E., Brunborg, G., Chao, C., Cooke, M. S., Costa, C., Costa, S., Dhawan, A., de Lapuente, J., Bo', C. Del, Dubus, J., Dusinska, M., … Azqueta, A. (2023). Measuring DNA modifications with the comet assay: a compendium of protocols. *Nature Protocols 2023 18:3*, *18*(3), 929–989. https://doi.org/10.1038/s41596-022-00754-y

Copenhagen: WHO Regional Office for Europe. (2015). *Human biomonitoring: facts and figures*. http://www.euro.who.int/pubrequest

Corsini, E., Budello, S., Marabini, L., Galbiati, V., Piazzalunga, A., Barbieri, P., Cozzutto, S., Marinovich, M., Pitea, D., and Galli, C. L. (2009). Comparison of wood smoke PM2.5 obtained from the combustion of FIR and beech pellets on inflammation and DNA damage in A549 and THP-1 human cell lines. *Archives of Toxicology*, *87*(12), 2187–2199. https://doi.org/10.1007/S00204-013-1071-Z

Cottini, M., Ventura, L., Lombardi, C., Landi, M., Imeri, G., Di Marco, F., Comberiati, P., and Berti, A. (2025). Small airway dysfunction mediates the relationship between Fractional Exhaled Nitric Oxide and asthma control. *Annals of Allergy, Asthma & Immunology*, *134*(5), 548-555.e4. https://doi.org/10.1016/J.ANAI.2025.01.003

Coull, B. A., Peters, A., Baccarelli, A. A., Tarantini, L., Cantone, L., Vokonas, P. S., Koutrakis, P., and Schwartz, J. D. (2015). Beyond the Mean: Quantile Regression to Explore the Association of Air Pollution with Gene-Specific Methylation in the Normative Aging Study. *Environmental Health Perspectives •*, *123*(8), 759–765. https://doi.org/10.1289/ehp.1307824

Cui, H., Gode, P., and Wappelhorst, S. (2021). *A global overview of zero-emission zones in cities and their development progress*. https://www.greengrowthknowledge.org/guidance/how-guide-

de Bont, J., Jaganathan, S., Dahlquist, M., Persson, Å., Stafoggia, M., and Ljungman, P. (2022). Ambient air pollution and cardiovascular diseases: An umbrella review of systematic reviews and meta-analyses. *Journal of Internal Medicine*, *291*(6), 779. https://doi.org/10.1111/JOIM.13467

Decaprio, A. P. (1997). Biomarkers: Coming of Age for Environmental Health and Risk Assessment. *Environmental Science and Technology*, *31*(7), 1837–1848. https://doi.org/10.1021/ES960920A

Dehghani, M., Mohammadpour, A., Abbasi, A., Rostami, I., Gharehchahi, E., Derakhshan, Z., Ferrante, M., and Conti, G. O. (2022). Health risks of inhalation exposure to BTEX in a municipal wastewater treatment plant in Middle East city: Shiraz, Iran. *Environmental Research*, *204*, 112155. https://doi.org/10.1016/J.ENVRES.2021.112155

Deilami, K., Kamruzzaman, M., and Liu, Y. (2018). Urban heat island effect: A systematic review of spatio-temporal factors, data, methods, and mitigation measures. *International Journal of Applied Earth Observation and Geoinformation*, *67*, 30–42. https://doi.org/10.1016/J.JAG.2017.12.009

Delfino, R. J., Staimer, N., Gillen, D., Tjoa, T., Sioutas, C., Fung, K., George, S. C., and Kleinman, M. T. (2006). Personal and ambient air pollution is associated with increased exhaled nitric oxide in children with asthma. *Environmental Health Perspectives*, *114*(11), 1736–1743. https://doi.org/10.1289/EHP.9141,

Delfino, R. J., Staimer, N., and Vaziri, N. D. (2011). Air pollution and circulating biomarkers of oxidative stress. *Air Quality, Atmosphere and Health*, *4*(1), 37–52. https://doi.org/10.1007/s11869-010-0095-2

Demirci-Çekiç, S., Özkan, G., Avan, A. N., Uzunboy, S., Çapanoğlu, E., and Apak, R. (2022). Biomarkers of Oxidative Stress and Antioxidant Defense. *Journal of Pharmaceutical and Biomedical Analysis*, *209*, 114477. https://doi.org/10.1016/J.JPBA.2021.114477

de Oliveira, M. M. M., Barreira Morais, S., and Rodrigues, F. P. L. M. (2022). An essential guide to occupational exposure. *An Essential Guide to Occupational Exposure*, 1–193. https://doi.org/10.52305/VGMC6738

Deutsche Forschungsgemeinschaft (DFG). (2013). MAK- und BAT-Werte-Liste 2013. *MAK-Und BAT-Werte-Liste 2013*. https://doi.org/10.1002/9783527675135

Dhillon, V. S., Deo, P., Bonassi, S., and Fenech, M. (2021). Lymphocyte micronuclei frequencies in skin, haematological, prostate, colorectal and esophageal cancer cases: A systematic review and meta-analysis. *Mutation Research/Reviews in Mutation Research*, *787*, 108372. https://doi.org/10.1016/J.MRREV.2021.108372

Dikilitas, M., Karakas, S., and Ahmad, P. (2016). Effect of Lead on Plant and Human DNA Damages and Its Impact on the Environment. *Plant Metal Interaction: Emerging Remediation Techniques*, 41–67. https://doi.org/10.1016/B978-0-12-803158-2.00003-5

Dimitriou, K., and Kassomenos, P. (2020). Background concentrations of benzene, potential long range transport influences and corresponding cancer risk in four cities of central Europe, in relation to air mass origination. *Journal of Environmental Management*, *262*, 110374. https://doi.org/10.1016/J.JENVMAN.2020.110374

Directive - EU - 2024/2881 - EN - EUR-Lex. (n.d.). Retrieved May 13, 2025, from https://eur-lex.europa.eu/eli/dir/2024/2881/oj/eng

Domijan, A. M., Ralić, J., Radić Brkanac, S., Rumora, L., and Žanić-Grubišić, T. (2015). Quantification of malondialdehyde by HPLC-FL - application to various biological samples. *Biomedical Chromatography : BMC*, *29*(1), 41–46. https://doi.org/10.1002/BMC.3361

Dong, H., Zheng, L., Duan, X., Zhao, W., Chen, J., Liu, S., and Sui, G. (2019). Cytotoxicity analysis of ambient fine particle in BEAS-2B cells on an air-liquid interface (ALI) microfluidics system. *Science of The Total Environment*, *677*, 108–119. https://doi.org/10.1016/J.SCITOTENV.2019.04.203

Duka, I., Gerić, M., Gajski, G., Friščić, M., Maleš, Ž., Domijan, A. M., and Turčić, P. (2020). Optimization of a fast screening method for the assessment of low molecular weight thiols in human blood and plasma suitable for biomonitoring studies. *Journal of Environmental Science and Health. Part A, Toxic/Hazardous Substances & Environmental Engineering*, *55*(3), 275–280. https://doi.org/10.1080/10934529.2019.1687236

Dweik, R. A., Boggs, P. B., Erzurum, S. C., Irvin, C. G., Leigh, M. W., Lundberg, J. O., Olin, A. C., Plummer, A. L., and Taylor, D. R. (2011). An Official ATS Clinical Practice Guideline: Interpretation of Exhaled Nitric Oxide Levels (FeNO) for Clinical Applications. *American Journal of Respiratory and Critical Care Medicine*, *184*(5), 602. https://doi.org/10.1164/RCCM.9120-11ST

EEA. (2021). *Air quality in Europe 2021*. https://doi.org/10.2800/549289

Europe's air quality status 2023 — European Environment Agency. (n.d.). Retrieved June 18, 2024, from https://www.eea.europa.eu/publications/europes-air-quality-status-2023

Ewa, B., and Danuta, M. Š. (2017). Polycyclic aromatic hydrocarbons and PAH-related DNA adducts. *Journal of Applied Genetics*, *58*(3), 321–330. https://doi.org/10.1007/S13353-016-0380-3/TABLES/1

Eyer, P., Worek, F., Kiderlen, D., Sinko, G., Stuglin, A., Simeon-Rudolf, V., and Reiner, E. (2003). Molar absorption coefficients for the reduced ellman reagent: Reassessment. *Analytical Biochemistry*, *312*(2), 224–227. https://doi.org/10.1016/S0003-2697(02)00506-7

Fang, Y., Ye, C., Wang, J., Wu, Y., Hu, M., Lin, W., Xu, F., and Zhu, T. (2019). Relative humidity and O3 concentration as two prerequisites for sulfate formation. *Atmospheric Chemistry and Physics*, *19*(19), 12295–12307. https://doi.org/10.5194/ACP-19-12295-2019

Fenech, M. (2007). Cytokinesis-block micronucleus cytome assay. *Nature Protocols 2007 2:5*, *2*(5), 1084–1104. https://doi.org/10.1038/nprot.2007.77

Fenech, M. (2020). Cytokinesis-Block Micronucleus Cytome Assay Evolution into a More Comprehensive Method to Measure Chromosomal Instability. *Genes 2020, Vol. 11, Page 1203*, *11*(10), 1203. https://doi.org/10.3390/GENES11101203

Fenech, M., Chang, W. P., Kirsch-Volders, M., Holland, N., Bonassi, S., and Zeiger, E. (2003). HUMN project: detailed description of the scoring criteria for the cytokinesis-block micronucleus assay using isolated human lymphocyte cultures. *Mutation Research/Genetic Toxicology and Environmental Mutagenesis*, *534*(1–2), 65–75. https://doi.org/10.1016/S1383-5718(02)00249-8

Fenech, M., Kirsch-Volders, M., Natarajan, A. T., Surralles, J., Crott, J. W., Parry, J., Norppa, H., Eastmond, D. A., Tucker, J. D., and Thomas, P. (2011). Molecular mechanisms of micronucleus, nucleoplasmic bridge and nuclear bud formation in mammalian and human cells. *Mutagenesis*, *26*(1), 125–132. https://doi.org/10.1093/MUTAGE/GEQ052

Fenech, M., Knasmueller, S., Bolognesi, C., Holland, N., Bonassi, S., and Kirsch-Volders, M. (2020). Micronuclei as biomarkers of DNA damage, aneuploidy, inducers of chromosomal hypermutation and as sources of pro-inflammatory DNA in humans. *Mutation Research. Reviews in Mutation Research*, *786*. https://doi.org/10.1016/J.MRREV.2020.108342

Fenech, M., Knasmueller, S., Nersesyan, A., Bolognesi, C., Wultsch, G., Schunck, C., Volpi, E., and Bonassi, S. (2024). The buccal micronucleus cytome assay: New horizons for its implementation in human studies. *Mutation Research/Genetic Toxicology and Environmental Mutagenesis*, *894*, 503724. https://doi.org/10.1016/J.MRGENTOX.2023.503724

Feng, S., Gao, D., Liao, F., Zhou, F., and Wang, X. (2016). The health effects of ambient PM2.5 and potential mechanisms. *Ecotoxicology and Environmental Safety*, *128*, 67–74. https://doi.org/10.1016/J.ECOENV.2016.01.030

Finland: EU country with highest share of asthmatics - Products Eurostat News - Eurostat. (n.d.). Retrieved May 12, 2025, from https://ec.europa.eu/eurostat/web/products-eurostat-news/-/edn-20210924-1

Flueckiger, A. C., and Petrucci, G. A. (2024). Effect of Relative Humidity on the Rate of New Particle Formation for Different VOCs. *Atmosphere 2024, Vol. 15, Page 480*, *15*(4), 480. https://doi.org/10.3390/ATMOS15040480

Gajski, G., Gerić, M., Oreščanin, V., and Garaj-Vrhovac, V. (2018). Cytokinesis-block micronucleus cytome assay parameters in peripheral blood lymphocytes of the general

population: Contribution of age, sex, seasonal variations and lifestyle factors. *Ecotoxicology and Environmental Safety*, *148*, 561–570. https://doi.org/10.1016/J.ECOENV.2017.11.003

Gajski, G., Gerić, M., Pehnec, G., Matković, K., Rinkovec, J., Jakovljević, I., Godec, R., Žužul, S., Bešlić, I., Cvitković, A., Wild, P., Guseva Canu, I., and Hopf, N. B. (2022). Associating Air Pollution with Cytokinesis-Block Micronucleus Assay Parameters in Lymphocytes of the General Population in Zagreb (Croatia). *International Journal of Molecular Sciences*, *23*(17), 10083. https://doi.org/10.3390/IJMS231710083/S1

Gajski, G., Gerić, M., Živković Semren, T., Tariba Lovaković, B., Oreščanin, V., and Pizent, A. (2020a). Application of the comet assay for the evaluation of DNA damage from frozen human whole blood samples: Implications for human biomonitoring. *Toxicology Letters*, *319*, 58–65. https://doi.org/10.1016/J.TOXLET.2019.11.010

Gajski, G., Kašuba, V., Milić, M., Gerić, M., Matković, K., Delić, L., Nikolić, M., Pavičić, M., Rozgaj, R., Garaj-Vrhovac, V., and Kopjar, N. (2024). Exploring cytokinesis block micronucleus assay in Croatia: A journey through the past, present, and future in biomonitoring of the general population. *Mutation Research. Genetic Toxicology and Environmental Mutagenesis*, *895*. https://doi.org/10.1016/J.MRGENTOX.2024.503749

Gajski, G., Langie, S., and Zhanataev, A. (2020b). Recent applications of the Comet Assay: A report from the International Comet Assay Workshop 2019. *Toxicology Letters*, *333*, 1–3. https://doi.org/10.1016/J.TOXLET.2020.07.022

Gajski, G., Ravlić, S., Godschalk, R., Collins, A., Dusinska, M., and Brunborg, G. (2021). Application of the comet assay for the evaluation of DNA damage in mature sperm. *Mutation Research/Reviews in Mutation Research*, *788*, 108398. https://doi.org/10.1016/J.MRREV.2021.108398

Gajski, G., Žegura, B., Ladeira, C., Novak, M., Sramkova, M., Pourrut, B., Del Bo, C., Milić, M., Gutzkow, K. B., Costa, S., Dusinska, M., Brunborg, G., and Collins, A. (2019a). The comet assay in animal models: From bugs to whales – (Part 2 Vertebrates). *Mutation Research - Reviews in Mutation Research*, *781*, 130–164. https://doi.org/10.1016/j.mrrev.2019.04.002

Gajski, G., Žegura, B., Ladeira, C., Pourrut, B., Del Bo, C., Novak, M., Sramkova, M., Milić, M., Gutzkow, K. B., Costa, S., Dusinska, M., Brunborg, G., and Collins, A. (2019b). The comet assay in animal models: From bugs to whales - (Part 1 Invertebrates). *Mutation Research. Reviews in Mutation Research*, *779*, 82–113. https://doi.org/10.1016/J.MRREV.2019.02.003

Galli, S. J., Tsai, M., and Piliponsky, A. M. (2008). The development of allergic inflammation. *Nature*, *454*(7203), 445–454. https://doi.org/10.1038/NATURE07204;KWRD=SCIENCE

Ganguly, K., Levänen, B., Palmberg, L., Åkesson, A., and Lindén, A. (2018). Cadmium in tobacco smokers: a neglected link to lung disease? *European Respiratory Review*, *27*(147). https://doi.org/10.1183/16000617.0122-2017

Gangwar, R. S., Bevan, G. H., Palanivel, R., Das, L., and Rajagopalan, S. (2020). Oxidative stress pathways of air pollution mediated toxicity: Recent insights. *Redox Biology*, *34*, 101545. https://doi.org/10.1016/J.REDOX.2020.101545

Garatachea, R., Pay, M. T., Achebak, H., Jorba, O., Bowdalo, D., Guevara, M., Petetin, H., Ballester, J., and Pérez García-Pando, C. (2024). National and transboundary contributions to surface ozone concentration across European countries. *Communications Earth and Environment*, *5*(1), 1–17. https://doi.org/10.1038/S43247-024-01716-W;SUBJMETA=169,172,4081,704,824;KWRD=ATMOSPHERIC+CHEMISTRY,ENVIRONMENTAL+IMPACT

Gatzke-Kopp, L. M., Warkentien, S., Willoughby, M., Fowler, C., Folch, D. C., and Blair, C. (2021). Proximity to Sources of Airborne Lead is Associated with Reductions in Children's Executive Function in the First Four Years of Life. *Health & Place*, *68*, 102517. https://doi.org/10.1016/J.HEALTHPLACE.2021.102517

Genchi, G., Carocci, A., Lauria, G., Sinicropi, M. S., and Catalano, A. (2020a). Nickel: Human Health and Environmental Toxicology. *International Journal of Environmental Research and Public Health*, *17*(3). https://doi.org/10.3390/IJERPH17030679

Genchi, G., Sinicropi, M. S., Lauria, G., Carocci, A., and Catalano, A. (2020b). The Effects of Cadmium Toxicity. *International Journal of Environmental Research and Public Health*, *17*(11). https://doi.org/10.3390/IJERPH17113782

Gerić, M., Gajski, G., Oreščanin, V., and Garaj-Vrhovac, V. (2018). Seasonal variations as predictive factors of the comet assay parameters: a retrospective study. *Mutagenesis*, *33*(1), 53–60. https://doi.org/10.1093/MUTAGE/GEX023

Gerić, M., Pehnec, G., Matković, K., Rinkovec, J., Jakovljević, I., Godec, R., Žužul, S., Bešlić, I., Cvitković, A., Delić, L., Wild, P., Guseva Canu, I., Hopf, N. B., and Gajski, G. (2024). Air Pollution and Primary DNA Damage among Zagreb (Croatia) Residents: A Cross-Sectional Study. *Journal of Xenobiotics*, *14*(1), 368–379. https://doi.org/10.3390/jox14010023

Glencross, D. A., Ho, T. R., Camiña, N., Hawrylowicz, C. M., and Pfeffer, P. E. (2020). Air pollution and its effects on the immune system. *Free Radical Biology and Medicine*, *151*, 56–68. https://doi.org/10.1016/J.FREERADBIOMED.2020.01.179

Godec, R., Jakovljević, I., Šega, K., Čačković, M., Bešlić, I., Davila, S., and Pehnec, G. (2016). Carbon species in PM10 particle fraction at different monitoring sites. *Environmental Pollution (Barking, Essex : 1987)*, *216*, 700–710. https://doi.org/10.1016/J.ENVPOL.2016.06.034

Godin, G. (2011). The Godin-Shephard Leisure-Time Physical Activity Questionnaire. *The Health & Fitness Journal of Canada*, *4*(1), 18–22. https://doi.org/10.14288/HFJC.V4I1.82

González-Alonso, M., Oteros, J., Widmann, M., Maya-Manzano, J. M., Skjøth, C., Grewling, L., O'Connor, D., Sofiev, M., Tummon, F., Crouzy, B., Clot, B., Buters, J., Kadantsev, E., Palamarchuk, Y., Martinez-Bracero, M., Pope, F. D., Mills, S., Šikoparija, B., Matavulj, P.,

… Ørby, P. V. (2024). Influence of meteorological variables and air pollutants on measurements from automatic pollen sampling devices. *Science of The Total Environment*, *931*, 172913. https://doi.org/10.1016/J.SCITOTENV.2024.172913

Gruszecka-Kosowska, A., Ampatzoglou, A., and Aguilera, M. (2022). Integration of Omics Approaches Enhances the Impact of Scientific Research in Environmental Applications. *International Journal of Environmental Research and Public Health*, *19*(14), 8758. https://doi.org/10.3390/IJERPH19148758

Gu, J., Deffner, V., Küchenhoff, H., Pickford, R., Breitner, S., Schneider, A., Kowalski, M., Peters, A., Lutz, M., Kerschbaumer, A., Slama, R., Morelli, X., Wichmann, H. E., and Cyrys, J. (2022). Low emission zones reduced PM10 but not NO2 concentrations in Berlin and Munich, Germany. *Journal of Environmental Management*, *302*, 114048. https://doi.org/10.1016/J.JENVMAN.2021.114048

Gulia, S., Tiwari, R., Mendiratta, S., Kaur, S., Goyal, S. K., and Kumar, R. (2020). Review of scientific technology-based solutions for vehicular pollution control. *Clean Technologies and Environmental Policy*, *22*(10), 1955–1966. https://doi.org/10.1007/S10098-020-01952-6/FIGURES/2

Guo, C., Li, X., Wang, R., Yu, J., Ye, M., Mao, L., Zhang, S., and Zheng, S. (2016). Association between Oxidative DNA Damage and Risk of Colorectal Cancer: Sensitive Determination of Urinary 8-Hydroxy-2′-deoxyguanosine by UPLC-MS/MS Analysis. *Scientific Reports 2016 6:1*, *6*(1), 1–9. https://doi.org/10.1038/srep32581

Guo, C., Lv, S., Liu, Y., and Li, Y. (2022). Biomarkers for the adverse effects on respiratory system health associated with atmospheric particulate matter exposure. *Journal of Hazardous Materials*, *421*, 126760. https://doi.org/10.1016/J.JHAZMAT.2021.126760

Guo, J., Chai, G., Song, X., Hui, X., Li, Z., Feng, X., and Yang, K. (2023). Long-term exposure to particulate matter on cardiovascular and respiratory diseases in low- and middle-income countries: A systematic review and meta-analysis. *Frontiers in Public Health*, *11*, 1134341. https://doi.org/10.3389/FPUBH.2023.1134341/FULL

Guo, L. C., Liu, T., He, G., Lin, H., Hu, J., Xiao, J., Li, X., Zeng, W., Zhou, Y., Li, M., Yu, S., Xu, Y., Zhang, H., Lv, Z., Zhang, J., and Ma, W. (2021). Short-term mortality risks of daily PM2.5-bound metals in urban region of Guangzhou, China, an indication of health risks of PM2.5 exposure. *Ecotoxicology and Environmental Safety*, *228*, 113049. https://doi.org/10.1016/J.ECOENV.2021.113049

Harley, C. B., Futcher, A. B., and Greider, C. W. (1990). Telomeres shorten during ageing of human fibroblasts. *Nature*, *345*(6274), 458–460. https://doi.org/10.1038/345458A0;KWRD=SCIENCE

Harm to human health from air pollution in Europe: burden of disease 2023 — European Environment Agency. (n.d.). Retrieved June 27, 2024, from https://www.eea.europa.eu/publications/harm-to-human-health-from-air-pollution/

Harm to human health from air pollution in Europe: burden of disease status, 2024 | European Environment Agency's home page. (n.d.). Retrieved February 12, 2025, from https://www.eea.europa.eu/en/analysis/publications/harm-to-human-health-from-air-pollution-2024

Hasanovic, M., Cetkovic, T., Pourrut, B., Caluk Klacar, L., Hadzic Omanovic, M., Durmic-Pasic, A., Haveric, S., and Haveric, A. (2023). Air pollution in Sarajevo, Bosnia and Herzegovina, assessed by plant comet assay. *Mutagenesis*, *38*(1), 43–50. https://doi.org/10.1093/MUTAGE/GEAC022

Haveric, A., Haveric, S., and Ibrulj, S. (2010). Micronuclei frequencies in peripheral blood and buccal exfoliated cells of young smokers and non-smokers. *Toxicology Mechanisms and Methods*, *20*(5), 260–266. https://doi.org/10.3109/15376516.2010.482962

Hayes, J. D., Dinkova-Kostova, A. T., and Tew, K. D. (2020). Oxidative Stress in Cancer. *Cancer Cell*, *38*(2), 167–197. https://doi.org/10.1016/J.CCELL.2020.06.001

Hays, S. M., Pyatt, D. W., Kirman, C. R., and Aylward, L. L. (2012). Biomonitoring Equivalents for benzene. *Regulatory Toxicology and Pharmacology*, *62*(1), 62–73. https://doi.org/10.1016/J.YRTPH.2011.12.001

Hayward, I., Martin, N. A., Ferracci, V., Kazemimanesh, M., and Kumar, P. (2024). Low-Cost Air Quality Sensors: Biases, Corrections and Challenges in Their Comparability. *Atmosphere 2024, Vol. 15, Page 1523*, *15*(12), 1523. https://doi.org/10.3390/ATMOS15121523

HBM4EU Priority Substances – HBM4EU – science and policy for a healthy future. (n.d.). Retrieved March 13, 2025, from https://www.hbm4eu.eu/hbm4eu-substances/hbm4eu-priority-substances/

Helsel, D. R. (2011). Statistics for Censored Environmental Data Using Minitab® and R: Second Edition. In *Statistics for Censored Environmental Data Using Minitab® and R: Second Edition*. John Wiley and Sons. https://doi.org/10.1002/9781118162729

He, M. Z., Kinney, P. L., Li, T., Chen, C., Sun, Q., Ban, J., Wang, J., Liu, S., Goldsmith, J., and Kioumourtzoglou, M. A. (2020). Short- and intermediate-term exposure to NO2 and mortality: A multi-county analysis in China. *Environmental Pollution*, *261*, 114165. https://doi.org/10.1016/J.ENVPOL.2020.114165

Hew, K. M., Walker, A. I., Kohli, A., Garcia, M., Syed, A., Mcdonald-Hyman, C., Noth, E. M., Mann, J. K., Pratt, B., Balmes, J., Hammond, S. K., Eisen, E. A., and Nadeau, K. C. (2015). Childhood exposure to ambient polycyclic aromatic hydrocarbons is linked to epigenetic modifications and impaired systemic immunity in T cells. *Clinical & Experimental Allergy*, *45*(1), 238–248. https://doi.org/10.1111/CEA.12377

Hoet, P., Jacquerye, C., Deumer, G., Lison, D., and Haufroid, V. (2021). Reference values of trace elements in blood and/or plasma in adults living in Belgium. *Clinical Chemistry and*

Laboratory Medicine, *59*(4), 729–742. https://doi.org/10.1515/CCLM-2020-1019/MACHINEREADABLECITATION/RIS

Hoffmann, B., Boogaard, H., de Nazelle, A., Andersen, Z. J., Abramson, M., Brauer, M., Brunekreef, B., Forastiere, F., Huang, W., Kan, H., Kaufman, J. D., Katsouyanni, K., Krzyzanowski, M., Kuenzli, N., Laden, F., Nieuwenhuijsen, M., Mustapha, A., Powell, P., Rice, M., … Thurston, G. (2021). WHO Air Quality Guidelines 2021–Aiming for Healthier Air for all: A Joint Statement by Medical, Public Health, Scientific Societies and Patient Representative Organisations. *International Journal of Public Health*, *66*(1), 23. https://doi.org/10.3389/IJPH.2021.1604465

Hoffmann, B., Brunekreef, B., Andersen, Z. J., Forastiere, F., and Boogaard, H. (2022). Benefits of future clean air policies in Europe: Proposed analyses of the mortality impacts of PM2.5 and NO2. *Environmental Epidemiology*, *6*(5), e221. https://doi.org/10.1097/EE9.0000000000000221

Holm, S. M., and Balmes, J. R. (2022). Systematic Review of Ozone Effects on Human Lung Function, 2013 Through 2020. *CHEST*, *161*(1), 190–201. https://doi.org/10.1016/J.CHEST.2021.07.2170

Hopf, N. B., Bolognesi, C., Danuser, B., and Wild, P. (2019). Biological monitoring of workers exposed to carcinogens using the buccal micronucleus approach: A systematic review and meta-analysis. *Mutation Research/Reviews in Mutation Research*, *781*, 11–29. https://doi.org/10.1016/J.MRREV.2019.02.006

Hoseini, M., Nabizadeh, R., Delgado-Saborit, J. M., Rafiee, A., Yaghmaeian, K., Parmy, S., Faridi, S., Hassanvand, M. S., Yunesian, M., and Naddafi, K. (2018). Environmental and lifestyle factors affecting exposure to polycyclic aromatic hydrocarbons in the general population in a Middle Eastern area. *Environmental Pollution*, *240*, 781–792. https://doi.org/10.1016/J.ENVPOL.2018.04.077

Houssein, E. H., Hosney, M. E., Emam, M. M., Younis, E. M. G., Ali, A. A., and Mohamed, W. M. (2023). Soft computing techniques for biomedical data analysis: open issues and challenges. *Artificial Intelligence Review*, *56*(2), 2599–2649. https://doi.org/10.1007/S10462-023-10585-2/TABLES/6

Huangfu, P., and Atkinson, R. (2020). Long-term exposure to NO2 and O3 and all-cause and respiratory mortality: A systematic review and meta-analysis. In *Environment International* (Vol. 144). Elsevier Ltd. https://doi.org/10.1016/j.envint.2020.105998

Hu, J., Bao, Y., Huang, H., Zhang, Z., Chen, F., Li, L., and Wu, Q. (2021). The preliminary investigation of potential response biomarkers to PAHs exposure on childhood asthma. *Journal of Exposure Science & Environmental Epidemiology 2021 32:1*, *32*(1), 82–93. https://doi.org/10.1038/s41370-021-00334-4

Human health effects of polycyclic aromatic hydrocarbons as ambient air pollutants Report of the Working Group on Polycyclic Aromatic Hydrocarbons of the Joint Task Force on the Health Aspects of Air Pollution. (2021). https://apps.who.int/bookorders/.

Husain, N., and Mahmood, R. (2019). Copper(II) generates ROS and RNS, impairs antioxidant system and damages membrane and DNA in human blood cells. *Environmental Science and Pollution Research 2019 26:20*, *26*(20), 20654–20668. https://doi.org/10.1007/S11356-019-05345-1

HZJZ. (2022). *Rezultati projekta EUROSTAT "Morbidity Statistics" Podaci za Hrvatsku*. www.hzjz.hr

IARC. (2000). Ethylbenzene. *IARC Summary & Evaluation, Volume 77*, 227. https://www.inchem.org/documents/iarc/vol77/77-05.html

IARC. (2013). Air Pollution and Cancer. In *Air pollution and cancer, IARC scientific publications NO. 161* (Issue 104, pp. 240–251). IARC Scientific Publication.

IARC. (2018). *Benzene* (Vol. 120). IARC Monogr Eval Carcinog Risks Hum.

IARC Working Group on the Evaluation of Carcinogenic Risks to Humans. (2010). Some Non-heterocyclic Polycyclic Aromatic Hydrocarbons and Some Related Exposures. *IARC Monographs on the Evaluation of Carcinogenic Risks to Humans / World Health Organization, International Agency for Research on Cancer*, *92*, 1–853. https://www.ncbi.nlm.nih.gov/books/NBK321712/

Ide, T., Tsutsui, H., Ohashi, N., Hayashidani, S., Suematsu, N., Tsuchihashi, M., Tamai, H., and Takeshita, A. (2002). Greater oxidative stress in healthy young men compared with premenopausal women. *Arteriosclerosis, Thrombosis, and Vascular Biology*, *22*(3), 438–442. https://doi.org/10.1161/HQ0302.104515/ASSET/4B30416A-8EB8-4513-BCB3-D6AC8F821C55/ASSETS/GRAPHIC/G14FF2.JPEG

International Agency for Research on Cancer (IARC). (2012). Arsenic, Metals, Fibres, and Dusts. In *IARC* (Vol. 100, Issue Arsenic, metals, fibres, and dusts). https://www.iarc.fr/

Jaafari, J., Naddafi, K., Yunesian, M., Nabizadeh, R., Hassanvand, M. S., Ghozikali, M. G., Shamsollahi, H. R., Nazmara, S., and Yaghmaeian, K. (2020). Characterization, risk assessment and potential source identification of PM10 in Tehran. *Microchemical Journal*, *154*, 104533. https://doi.org/10.1016/J.MICROC.2019.104533

Jakovljević, I., Pehnec, G., Vađić, V., Čačković, M., Tomašić, V., and Jelinić, J. D. (2018). Polycyclic aromatic hydrocarbons in PM10, PM2.5 and PM1 particle fractions in an urban area. *Air Quality, Atmosphere and Health*, *11*(7), 843–854. https://doi.org/10.1007/s11869-018-0603-3

Jakovljević, I., Pehnec, G., Vadjić, V., Šišović, A., Davila, S., and Bešlić, I. (2015). Carcinogenic activity of polycyclic aromatic hydrocarbons bounded on particle fraction. *Environmental*

Science and Pollution Research International, *22*(20), 15931–15940. https://doi.org/10.1007/S11356-015-4777-Z

Jakovljević, I., Štrukil, Z. S., Pehnec, G., Horvat, T., Sanković, M., Šumanovac, A., Davila, S., Račić, N., and Gajski, G. (2025). Ambient air pollution and carcinogenic activity at three different urban locations. *Ecotoxicology and Environmental Safety*, *289*, 117704. https://doi.org/10.1016/J.ECOENV.2025.117704

Janero, D. R. (1990). Malondialdehyde and thiobarbituric acid-reactivity as diagnostic indices of lipid peroxidation and peroxidative tissue injury. *Free Radical Biology and Medicine*, *9*(6), 515–540. https://doi.org/10.1016/0891-5849(90)90131-2

Jia, C., and Batterman, S. (2010). A Critical Review of Naphthalene Sources and Exposures Relevant to Indoor and Outdoor Air. *International Journal of Environmental Research and Public Health*, *7*(7), 2903. https://doi.org/10.3390/IJERPH7072903

Jomova, K., Raptova, R., Alomar, S. Y., Alwasel, S. H., Nepovimova, E., Kuca, K., and Valko, M. (2023). Reactive oxygen species, toxicity, oxidative stress, and antioxidants: chronic diseases and aging. *Archives of Toxicology 2023 97:10*, *97*(10), 2499–2574. https://doi.org/10.1007/S00204-023-03562-9

Jongeneelen, F. J., Anzion, R. B. M., and Henderson, P. T. (1987). Determination of hydroxylated metabolites of polycyclic aromatic hydrocarbons in urine. *Journal of Chromatography B: Biomedical Sciences and Applications*, *413*(C), 227–232. https://doi.org/10.1016/0378-4347(87)80230-X

Joshirvani, A., Samarghandi, M. R., and Leili, M. (2021). PM10 Concentration, Its Potentially Toxic Metals Content, and Human Health Risk Assessment in Hamadan, Iran. *CLEAN – Soil, Air, Water*, *49*(6), 2000174. https://doi.org/10.1002/CLEN.202000174

Kang, Y., Aye, L., Ngo, T. D., and Zhou, J. (2022). Performance evaluation of low-cost air quality sensors: A review. *Science of The Total Environment*, *818*, 151769. https://doi.org/10.1016/J.SCITOTENV.2021.151769

Karačonji, I. B., and Skender, L. (2007). Comparison between dynamic headspace and headspace solid-phase microextraction for gas chromatography of BTEX in urine. *Arhiv Za Higijenu Rada i Toksikologiju*, *58*(4), 421–427. https://doi.org/10.2478/V10004-007-0035-1

Kazemiparkouhi, F., Eum, K. Do, Wang, B., Manjourides, J., and Suh, H. H. (2019). Long-term ozone exposures and cause-specific mortality in a US Medicare cohort. *Journal of Exposure Science & Environmental Epidemiology 2019 30:4*, *30*(4), 650–658. https://doi.org/10.1038/s41370-019-0135-4

Kazensky, L., Matković, K., Gerić, M., Žegura, B., Pehnec, G., and Gajski, G. (2024). Impact of indoor air pollution on DNA damage and chromosome stability: a systematic review. *Archives of Toxicology*. https://doi.org/10.1007/s00204-024-03785-4

Kelly, J. M., Ivatt, P. D., Evans, M. J., Kroll, J. H., Hrdina, A. I. H., Kohale, I. N., White, F. M., Engelward, B. P., and Selin, N. E. (2021). Global Cancer Risk From Unregulated Polycyclic Aromatic Hydrocarbons. *GeoHealth*, *5*(9), e2021GH000401. https://doi.org/10.1029/2021GH000401

Khan, M. I., Ahmad, I., Mahdi, A. A., Akhtar, M. J., Islam, N., Ashquin, M., and Venkatesh, T. (2010). Elevated blood lead levels and cytogenetic markers in buccal epithelial cells of painters in India. *Environmental Science and Pollution Research*, *17*(7), 1347–1354. https://doi.org/10.1007/S11356-010-0319-X/FIGURES/1

Kirsch-Volders, M., Sofuni, T., Aardema, M., Albertini, S., Eastmond, D., Fenech, M., Ishidate, M., Kirchner, S., Lorge, E., Morita, T., Norppa, H., Surrallés, J., Vanhauwaert, A., and Wakata, A. (2003). Report from the in vitro micronucleus assay working group. *Mutation Research/Genetic Toxicology and Environmental Mutagenesis*, *540*(2), 153–163. https://doi.org/10.1016/J.MRGENTOX.2003.07.005

Kitinoja, M. A., Hugg, T. T., Siddika, N., Rodriguez Yanez, D., Jaakkola, M. S., and Jaakkola, J. J. K. (2020). Original research: Short-term exposure to pollen and the risk of allergic and asthmatic manifestations: a systematic review and meta-analysis. *BMJ Open*, *10*(1), 29069. https://doi.org/10.1136/BMJOPEN-2019-029069

Kohli, A., Garcia, M. A., Miller, R. L., Maher, C., Humblet, O., Hammond, S. K., and Nadeau, K. (2012). Secondhand smoke in combination with ambient air pollution exposure is associated with increasedx CpG methylation and decreased expression of IFN-γ in T effector cells and Foxp3 in T regulatory cells in children. *Clinical Epigenetics 2012 4:1*, *4*(1), 1–16. https://doi.org/10.1186/1868-7083-4-17

Kowalska, M., Skrzypek, M., Kowalski, M., and Cyrys, J. (2020). Effect of NOx and NO2 Concentration Increase in Ambient Air to Daily Bronchitis and Asthma Exacerbation, Silesian Voivodeship in Poland. *International Journal of Environmental Research and Public Health 2020, Vol. 17, Page 754*, *17*(3), 754. https://doi.org/10.3390/IJERPH17030754

Kranjčić, N., Dogančić, D., Đurin, B., and Siročić, A. P. (2022). Analyzing Air Pollutant Reduction Possibilities in the City of Zagreb. *ISPRS International Journal of Geo-Information 2022, Vol. 11, Page 259*, *11*(4), 259. https://doi.org/10.3390/IJGI11040259

Kumari, R., Kaur, P., Verma, S. K., Ratre, P., Mishra, P. K., Kumari, R., Kaur, P., Verma, S. K., Ratre, P., and Mishra, P. K. (2024). Omics-based cutting-edge technologies for identifying predictive biomarkers to measure the impact of air borne particulate matter exposure on male reproductive health. *Journal of Reproductive Healthcare and Medicine*, *5*, 2. https://doi.org/10.25259/JRHM_25_2023

Ladeira, C., Møller, P., Giovannelli, L., Gajski, G., Haveric, A., Eyluel Bankoglu, E., Azqueta, A., Geri´c, M. G., Stopper, H., Cabêda, J., Tonin, F. S., and Collins, A. (2024). The Comet Assay as a Tool in Human Biomonitoring Studies of Environmental and Occupational

Exposure to Chemicals—A Systematic Scoping Review. *Toxics 2024, Vol. 12, Page 270*, *12*(4), 270. https://doi.org/10.3390/TOXICS12040270

Ladeira, C., and Viegas, S. (2016). Human Biomonitoring – An overview on biomarkers and their application in Occupational and Environmental Health. *Biomonitoring*, *3*(1). https://doi.org/10.1515/BIMO-2016-0003

Låg, M., Øvrevik, J., Refsnes, M., and Holme, J. A. (2020). Potential role of polycyclic aromatic hydrocarbons in air pollution-induced non-malignant respiratory diseases. *Respiratory Research 2020 21:1*, *21*(1), 1–22. https://doi.org/10.1186/S12931-020-01563-1

Lal, G., Zhang, N., van der Touw, W., Ding, Y., Ju, W., Bottinger, E. P., Reid, St. P., Levy, D. E., and Bromberg, J. S. (2009). Epigenetic Regulation of Foxp3 Expression in Regulatory T Cells by DNA Methylation. *The Journal of Immunology*, *182*(1), 259–273. https://doi.org/10.4049/JIMMUNOL.182.1.259

Lee, J., Kalia, V., Perera, F., Herbstman, J., Li, T., Nie, J., Qu, L. R., Yu, J., and Tang, D. (2017). Prenatal airborne polycyclic aromatic hydrocarbon exposure, LINE1 methylation and child development in a Chinese cohort. *Environment International*, *99*, 315–320. https://doi.org/10.1016/J.ENVINT.2016.12.009

Lelieveld, J., Haines, A., Burnett, R., Tonne, C., Klingmüller, K., Münzel, T., and Pozzer, A. (2023). Air pollution deaths attributable to fossil fuels: observational and modelling study. *BMJ*, *383*. https://doi.org/10.1136/BMJ-2023-077784

Lelieveld, J., Pozzer, A., Pöschl, U., Fnais, M., Haines, A., and Münzel, T. (2020). Loss of life expectancy from air pollution compared to other risk factors: a worldwide perspective. *Cardiovascular Research*, *116*(11), 1910–1917. https://doi.org/10.1093/CVR/CVAA025

Lequy, E., Leblond, S., Siemiatycki, J., Meyer, C., Vienneau, D., de Hoogh, K., Zins, M., Goldberg, M., and Jacquemin, B. (2023). Long-term exposure to airborne metals and risk of cancer in the French cohort Gazel. *Environment International*, *177*, 107999. https://doi.org/10.1016/J.ENVINT.2023.107999

Li, S., and Zhang, X. (2021). Iron in Cardiovascular Disease: Challenges and Potentials. *Frontiers in Cardiovascular Medicine*, *8*, 707138. https://doi.org/10.3389/FCVM.2021.707138

Liu, Y., Zhou, Y., and Lu, J. (2020). Exploring the relationship between air pollution and meteorological conditions in China under environmental governance. *Scientific Reports*, *10*(1). https://doi.org/10.1038/s41598-020-71338-7

Li, Z., Zhang, W., Chen, Y., Guo, W., Zhang, J., Tang, H., Xu, Z., Zhang, H., Tao, Y., Wang, F., Jiang, Y., Sun, F. L., and Mao, Z. (2016). Impaired DNA double-strand break repair contributes to the age-associated rise of genomic instability in humans. *Cell Death and Differentiation*, *23*(11), 1765. https://doi.org/10.1038/CDD.2016.65

Lodovici, M., and Bigagli, E. (2011). Oxidative Stress and Air Pollution Exposure. *Journal of Toxicology*, *2011*(1), 487074. https://doi.org/10.1155/2011/487074

Lotrecchiano, N., Montano, L., Bonapace, I. M., Giancarlo, T., Trucillo, P., and Sofia, D. (2022). Comparison Process of Blood Heavy Metals Absorption Linked to Measured Air Quality Data in Areas with High and Low Environmental Impact. *Processes 2022, Vol. 10, Page 1409*, *10*(7), 1409. https://doi.org/10.3390/PR10071409

Lovinsky-Desir, S., Jung, K. H., Jezioro, J. R., Torrone, D. Z., de Planell-Saguer, M., Yan, B., Perera, F. P., Rundle, A. G., Perzanowski, M. S., Chillrud, S. N., and Miller, R. L. (2017). Physical activity, black carbon exposure, and DNA methylation in the FOXP3 promoter. *Clinical Epigenetics*, *9*(1), 1–12. https://doi.org/10.1186/S13148-017-0364-0/TABLES/3

Lovrić, M., Antunović, M., Šunić, I., Vuković, M., Kecorius, S., Kröll, M., Bešlić, I., Godec, R., Pehnec, G., Geiger, B. C., Grange, S. K., and Šimić, I. (2022). Machine Learning and Meteorological Normalization for Assessment of Particulate Matter Changes during the COVID-19 Lockdown in Zagreb, Croatia. *International Journal of Environmental Research and Public Health 2022, Vol. 19, Page 6937*, *19*(11), 6937. https://doi.org/10.3390/IJERPH19116937

Lovrić, M., Gajski, G., Fernández-Agüera, J., Pöhlker, M., Gursch, H., Lovrić, M., Switters, J., Borg, A., Mureddu, F., Auguštin, D. H., Šunić, I., Šarac, J., Žebec, M. S., Dodigović, L., Bošnjaković, A., Karlović, N., Gajski, G., Gerić, M., Milić, M., … Mureddu, F. (2025). Evidence-driven indoor air quality improvement: An innovative and interdisciplinary approach to improving indoor air quality. *BioFactors*, *51*(1), e2126. https://doi.org/10.1002/BIOF.2126;CTYPE:STRING:JOURNAL

Lu, A. T., Narayan, P., Grant, M. J., Langfelder, P., Wang, N., Kwak, S., Wilkinson, H., Chen, R. Z., Chen, J., Simon Bawden, C., Rudiger, S. R., Ciosi, M., Chatzi, A., Maxwell, A., Hore, T. A., Aaronson, J., Rosinski, J., Preiss, A., Vogt, T. F., … Horvath, S. (2020). DNA methylation study of Huntington's disease and motor progression in patients and in animal models. *Nature Communications 2020 11:1*, *11*(1), 1–15. https://doi.org/10.1038/s41467-020-18255-5

Luo, K., Stepanov, I., and Hecht, S. S. (2019). Chemical biomarkers of exposure and early damage from potentially carcinogenic airborne pollutants. *Annals of Cancer Epidemiology*, *3*(0), 5–5. https://doi.org/10.21037/ACE.2019.08.01

Lu, Y. (2021). Beyond air pollution at home: Assessment of personal exposure to PM2.5 using activity-based travel demand model and low-cost air sensor network data. *Environmental Research*, *201*, 111549. https://doi.org/10.1016/J.ENVRES.2021.111549

Lu, Y., Wiltshire, H. D., Baker, J. S., and Wang, Q. (2021). Effects of High Intensity Exercise on Oxidative Stress and Antioxidant Status in Untrained Humans: A Systematic Review. *Biology 2021, Vol. 10, Page 1272*, *10*(12), 1272. https://doi.org/10.3390/BIOLOGY10121272

Madden, M. C., and Gallagher, J. E. (1999). Biomarkers of Exposure. *Air Pollution and Health*, 417–430. https://doi.org/10.1016/B978-012352335-8/50094-6

Madronich, S., Sulzberger, B., Longstreth, J. D., Schikowski, T., Andersen, M. P. S., Solomon, K. R., and Wilson, S. R. (2023). Changes in tropospheric air quality related to the protection of stratospheric ozone in a changing climate. *Photochemical & Photobiological Sciences*, *22*(5), 1. https://doi.org/10.1007/S43630-023-00369-6

Mahilang, M., Deb, M. K., Pervez, S., Tiwari, S., and Jain, V. K. (2021). Biogenic secondary organic aerosol formation in an urban area of eastern central India: Seasonal variation, size distribution and source characterization. *Environmental Research*, *195*, 110802. https://doi.org/10.1016/J.ENVRES.2021.110802

Mahmoud, A., and Junejo, R. (2024). Oxidative Stress in Cardiovascular Diseases. *Biomarkers of Oxidative Stress*, 45–70. https://doi.org/10.1007/978-3-031-69962-7_3

Mahmoud, M., Ramadan, M., Naher, S., Pullen, K., and Olabi, A. G. (2021). The impacts of different heating systems on the environment: A review. *Science of The Total Environment*, *766*, 142625. https://doi.org/10.1016/J.SCITOTENV.2020.142625

Marín, R., Abad, C., Rojas, D., Chiarello, D. I., and Alejandro, T. G. (2023). Biomarkers of oxidative stress and reproductive complications. *Advances in Clinical Chemistry*, *113*, 157–233. https://doi.org/10.1016/BS.ACC.2022.11.004

Marques, C. R., Costa, R. S., Costa, G. N. de O., da Silva, T. M., Teixeira, T. O., de Andrade, E. M. M., Galvão, A. A., Carneiro, V. L., and Figueiredo, C. A. (2015). Genetic and epigenetic studies of FOXP3 in asthma and allergy. *Asthma Research and Practice*, *1*(1), 10. https://doi.org/10.1186/S40733-015-0012-4

Martínez de Toda, I., González-Sánchez, M., Díaz-Del Cerro, E., Valera, G., Carracedo, J., and Guerra-Pérez, N. (2023). Sex differences in markers of oxidation and inflammation. Implications for ageing. *Mechanisms of Ageing and Development*, *211*, 111797. https://doi.org/10.1016/J.MAD.2023.111797

Martínez-Iglesias, O., Carrera, I., Carril, J. C., Fernández-Novoa, L., Cacabelos, N., and Cacabelos, R. (2020). DNA Methylation in Neurodegenerative and Cerebrovascular Disorders. *International Journal of Molecular Sciences 2020, Vol. 21, Page 2220*, *21*(6), 2220. https://doi.org/10.3390/IJMS21062220

Mašić, A., Musemić, R., and Džaferović-Mašić, E. (2016). Temperature inversion measurements in sarajevo valley using unmanned aerial vehicles. *Annals of DAAAM and Proceedings of the International DAAAM Symposium*, *27*(1), 423–427. https://doi.org/10.2507/27th.daaam.proceedings.062

Matasović, B., Pehnec, G., Bešlić, I., Davila, S., and Babić, D. (2021). Assessment of ozone concentration data from the northern Zagreb area, Croatia, for the period from 2003 to 2016. *Environmental Science and Pollution Research*, *28*(27), 36640–36650. https://doi.org/10.1007/S11356-021-13295-W/FIGURES/9

Matković, K., Gerić, M., Kazensky, L., Milić, M., Kašuba, V., Cvitković, A., Sanković, M., Šumanovac, A., Møller, P., and Gajski, G. (2024). Comparison of DNA damage in fresh and frozen blood samples: implications for the comet assay in human biomonitoring studies. *Archives of Toxicology 2024*, 1–10. https://doi.org/10.1007/S00204-024-03823-1

Matković, K., Jurič, A., Jakovljević, I., Kazensky, L., Milić, M., Kašuba, V., Davila, S., Pehnec, G., Brčić Karačonji, I., Cvitković, A., Wild, P., Guseva Canu, I., Hopf, N. B., Gajski, G., and Gerić, M. (2025). Evaluating air pollution and BTEX exposure effects on DNA damage: A human biomonitoring study in Zagreb, Croatia. *Atmospheric Environment*, *343*, 121004. https://doi.org/10.1016/J.ATMOSENV.2024.121004

Matthaios, V. N., Holland, I., Kang, C. M., Hart, J. E., Hauptman, M., Wolfson, J. M., Gaffin, J. M., Phipatanakul, W., Gold, D. R., and Koutrakis, P. (2024). The effects of urban green space and road proximity to indoor traffic-related PM2.5, NO2, and BC exposure in inner-city schools. *Journal of Exposure Science & Environmental Epidemiology 2024*, 1–8. https://doi.org/10.1038/s41370-024-00669-8

Meeker, J. D., Barr, D. B., Serdar, B., Rappaport, S. M., and Hauser, R. (2007). Utility of urinary 1-naphthol and 2-naphthol levels to assess environmental carbaryl and naphthalene exposure in an epidemiology study. *Journal of Exposure Science and Environmental Epidemiology*, *17*(4), 314–320. https://doi.org/10.1038/SJ.JES.7500502;KWRD=MEDICINE

Mejino-López, J., and Oliu-Barton, M. (2024). How much does Europe pay for clean air? In *Working Paper*.

Mengelers, M., van den Brand, A., Picavet, S., Visser, W., and Bogaardt, L. (2024). *Biomonitoring of cadmium and lead in adults*. https://doi.org/10.21945/RIVM-2024-0141

Mesnage, R. (2025). Environmental Health Is Overlooked in Longevity Research. *Antioxidants 2025, Vol. 14, Page 421*, *14*(4), 421. https://doi.org/10.3390/ANTIOX14040421

Michael, S., Montag, M., and Dott, W. (2013). Pro-inflammatory effects and oxidative stress in lung macrophages and epithelial cells induced by ambient particulate matter. *Environmental Pollution*, *183*, 19–29. https://doi.org/10.1016/J.ENVPOL.2013.01.026

Milić, M., Ceppi, M., Bruzzone, M., Azqueta, A., Brunborg, G., Godschalk, R., Koppen, G., Langie, S., Møller, P., Teixeira, J. P., Alija, A., Anderson, D., Andrade, V., Andreoli, C., Asllani, F., Bangkoglu, E. E., Barančoková, M., Basaran, N., Boutet-Robinet, E., … Bonassi, S. (2021). The hCOMET project: International database comparison of results with the comet assay in human biomonitoring. Baseline frequency of DNA damage and effect of main confounders. *Mutation Research/Reviews in Mutation Research*, *787*, 108371. https://doi.org/10.1016/J.MRREV.2021.108371

Milić, M., Gerić, M., Nodilo, M., Ranogajec-Komor, M., Milković, Đ., and Gajski, G. (2020). Application of the buccal micronucleus cytome assay on child population exposed to sinus X-ray. *European Journal of Radiology*, *129*, 109143. https://doi.org/10.1016/J.EJRAD.2020.109143

Misiukiewicz-Stepien, P., and Paplinska-Goryca, M. (2021). Biological effect of PM10 on airway epithelium-focus on obstructive lung diseases. *Clinical Immunology*, *227*, 108754. https://doi.org/10.1016/J.CLIM.2021.108754

Møller, P. (2018). The comet assay: ready for 30 more years. *Mutagenesis*, *33*(1), 1–7. https://doi.org/10.1093/MUTAGE/GEX046

Møller, P., Azqueta, A., Boutet-Robinet, E., Koppen, G., Bonassi, S., Milić, M., Gajski, G., Costa, S., Teixeira, J. P., Costa Pereira, C., Dusinska, M., Godschalk, R., Brunborg, G., Gutzkow, K. B., Giovannelli, L., Cooke, M. S., Richling, E., Laffon, B., Valdiglesias, V., … Langie, S. A. S. (2020). Minimum Information for Reporting on the Comet Assay (MIRCA): recommendations for describing comet assay procedures and results. *Nature Protocols 2020 15:12*, *15*(12), 3817–3826. https://doi.org/10.1038/s41596-020-0398-1

Møller, P., Bankoglu, E. E., Stopper, H., Giovannelli, L., Ladeira, C., Koppen, G., Gajski, G., Collins, A., Valdiglesias, V., Laffon, B., Boutet-Robinet, E., Perdry, H., Del Bo', C., Langie, S. A. S., Dusinska, M., and Azqueta, A. (2021). Collection and storage of human white blood cells for analysis of DNA damage and repair activity using the comet assay in molecular epidemiology studies. *Mutagenesis*, *36*(3), 193–212. https://doi.org/10.1093/MUTAGE/GEAB012

Møller, P., Loft, S., Ersson, C., Koppen, G., Dusinska, M., and Collins, A. (2014). On the search for an intelligible comet assay descriptor. *Frontiers in Genetics*, *5*(JUL), 217. https://doi.org/10.3389/FGENE.2014.00217

Morgan, J., Bell, R., and Jones, A. L. (2020). Endogenous doesn't always mean innocuous: a scoping review of iron toxicity by inhalation. *Journal of Toxicology and Environmental Health - Part B: Critical Reviews*, *23*(3), 107–136. https://doi.org/10.1080/10937404.2020.1731896;WGROUP:STRING:PUBLICATION

Mostafavi, N., Vermeulen, R., Ghantous, A., Hoek, G., Probst-Hensch, N., Herceg, Z., Tarallo, S., Naccarati, A., Kleinjans, J. C. S., Imboden, M., Jeong, A., Morley, D., Amaral, A. F. S., van Nunen, E., Gulliver, J., Chadeau-Hyam, M., Vineis, P., and Vlaanderen, J. (2018). Acute changes in DNA methylation in relation to 24 h personal air pollution exposure measurements: A panel study in four European countries. *Environment International*, *120*, 11–21. https://doi.org/10.1016/J.ENVINT.2018.07.026

Mukherjee, S., Dasgupta, S., Mishra, P. K., and Chaudhury, K. (2021). Air pollution-induced epigenetic changes: disease development and a possible link with hypersensitivity pneumonitis. *Environmental Science and Pollution Research International*, *28*(40), 55981. https://doi.org/10.1007/S11356-021-16056-X

Nagaraju, R., Kalahasthi, R., Balachandar, R., and Bagepally, B. S. (2022). Association between lead exposure and DNA damage (genotoxicity): systematic review and meta-analysis. *Archives of Toxicology*, *96*(11), 2899–2911. https://doi.org/10.1007/S00204-022-03352-9/METRICS

Nassikas, N. J., Luttmann-Gibson, H., Rifas-Shiman, S. L., Oken, E., Gold, D. R., and Rice, M. B. (2024). Acute exposure to pollen and airway inflammation in adolescents. *Pediatric Pulmonology*, *59*(5), 1313–1320. https://doi.org/10.1002/PPUL.26908

Nejad, M. T., Kamran, ·, Ghalehteimouri, J., Talkhabi, H., and Dolatshahi, Z. (2023). The relationship between atmospheric temperature inversion and urban air pollution characteristics: a case study of Tehran, Iran. *Discover Environment 2023 1:1*, *1*(1), 1–15. https://doi.org/10.1007/S44274-023-00018-W

Nersesyan, A., Fenech, M., Bolognesi, C., Mišík, M., Setayesh, T., Wultsch, G., Bonassi, S., Thomas, P., and Knasmüller, S. (2016). Use of the lymphocyte cytokinesis-block micronucleus assay in occupational biomonitoring of genome damage caused by in vivo exposure to chemical genotoxins: Past, present and future. *Mutation Research/Reviews in Mutation Research*, *770*, 1–11. https://doi.org/10.1016/J.MRREV.2016.05.003

Nersesyan, A., Proietti, S., Knasmueller, S., Bonassi, S., and Fenech, M. (2025). High correlation between micronuclei in lymphocytes and buccal cells in humans provides further validation of their use as biomarkers of DNA damage and cancer risks in vivo. *Mutagenesis*. https://doi.org/10.1093/MUTAGE/GEAF006

Nur Husna, S. M., Tan, H. T. T., Md Shukri, N., Mohd Ashari, N. S., and Wong, K. K. (2022). Allergic Rhinitis: A Clinical and Pathophysiological Overview. *Frontiers in Medicine*, *9*. https://doi.org/10.3389/FMED.2022.874114

OECD. (2023). *Test Guideline No. 487 In Vitro Mammalian Cell Micronucleus Test*. http://www.oecd.org/termsandconditions/

Olivieri, M., Marchetti, P., Murgia, N., Nicolis, M., Torroni, L., Spiteri, G., Ferrari, M., Marcon, A., and Verlato, G. (2022). Natural pollen exposure increases in a dose-dependent way Fraction of exhaled Nitric Oxide (FeNO) levels in patients sensitized to one or more pollen species. *Clinical and Translational Allergy*, *12*(2), e12096. https://doi.org/10.1002/CLT2.12096;PAGE:STRING:ARTICLE/CHAPTER

Padhi, S. K., and Gokhale, S. (2017). Treatment of gaseous volatile organic compounds using a rotating biological filter. *Bioresource Technology*, *244*(Pt 1), 270–280. https://doi.org/10.1016/J.BIORTECH.2017.07.112

Panchal, R., Panagi, M., May, H. R., Obszynska, J. A., Evans, M. S., Hansell, A. L., Gulliver, J., and Vande Hey, J. D. (2022). Personal air pollution exposure during morning commute car and active transport journeys. *Journal of Transport & Health*, *26*, 101365. https://doi.org/10.1016/J.JTH.2022.101365

Pandey, P., Patel, D. K., Khan, A. H., Barman, S. C., Murthy, R. C., and Kisku, G. C. (2013). Temporal distribution of fine particulates (PM2.5, PM10), potentially toxic metals, PAHs and Metal-bound carcinogenic risk in the population of Lucknow City, India. *Journal of Environmental Science and Health, Part A*, *48*(7), 730–745. https://doi.org/10.1080/10934529.2013.744613

Pandics, T., Major, D., Fazekas-Pongor, V., Szarvas, Z., Peterfi, A., Mukli, P., Gulej, R., Ungvari, A., Fekete, M., Tompa, A., Tarantini, S., Yabluchanskiy, A., Conley, S., Csiszar, A., Tabak, A. G., Benyo, Z., Adany, R., Ungvari, Z., Fazekas-Pongor have equal contributions Pandics, V. T., … Ungvari, Z. (2023). Exposome and unhealthy aging: environmental drivers from air pollution to occupational exposures. *GeroScience 2023 45:6*, *45*(6), 3381–3408. https://doi.org/10.1007/S11357-023-00913-3

Panico, A., Grassi, T., Bagordo, F., Idolo, A., Serio, F., Tumolo, M. R., De Giorgi, M., Guido, M., Tutino, M., and De Donno, A. (2020). Micronucleus Frequency in Exfoliated Buccal Cells of Children Living in an Industrialized Area of Apulia (Italy). *International Journal of Environmental Research and Public Health*, *17*(4). https://doi.org/10.3390/IJERPH17041208

Panxhaj, D., Asllani, F., Alija, A., Dreshaj, S., and Bresgen, N. (2024). Genotoxic effects in the buccal cells of students exposed to season-associated increase of air pollution in Prishtina urban area: a preliminary study. *Genetics & Applications*, *8*(1). https://doi.org/10.31383/ga.vol8iss1ga02

Pa´, P., Pacher, P., Beckman, J. S., and Liaudet, L. (2007). *Nitric Oxide and Peroxynitrite in Health and Disease*. https://doi.org/10.1152/physrev.00029.2006.-The

Particulate matter - PM2.5 | European Environment Agency's home page. (n.d.). Retrieved May 19, 2025, from https://www.eea.europa.eu/en/analysis/publications/air-quality-status-report-2025/particulate-matter-pm2.5

Particulate Matter (PM2.5) Mega Guide – See The Air. (n.d.). Retrieved February 21, 2025, from https://seetheair.org/2022/05/16/particulate-matter-pm2-5-mega-guide/

Patel, A. B., Shaikh, S., Jain, K. R., Desai, C., and Madamwar, D. (2020). Polycyclic Aromatic Hydrocarbons: Sources, Toxicity, and Remediation Approaches. *Frontiers in Microbiology*, *11*, 562813. https://doi.org/10.3389/FMICB.2020.562813/BIBTEX

Payus, C. M., Jikilim, C., and Sentian, J. (2020). Rainwater chemistry of acid precipitation occurrences due to long-range transboundary haze pollution and prolonged drought events during southwest monsoon season: climate change driven. *Heliyon*, *6*(9), e04997. https://doi.org/10.1016/J.HELIYON.2020.E04997

Pedrete, T. de A., and Moreira, J. C. (2018). Biomarkers of Susceptibility for Human Exposure to Environmental Contaminants. *Ecotoxicology*, 252–280. https://doi.org/10.1201/B21896-13

Pehnec, G., and Jakovljević, I. (2018). Carcinogenic potency of airborne polycyclic aromatic hydrocarbons in relation to the particle fraction size. *International Journal of Environmental Research and Public Health*, *15*(11), 2485. https://doi.org/10.3390/ijerph15112485

Pehnec, G., Jakovljević, I., Godec, R., Sever Štrukil, Z., Žero, S., Huremović, J., and Džepina, K. (2020). Carcinogenic organic content of particulate matter at urban locations with different pollution sources. *Science of The Total Environment*, *734*, 139414. https://doi.org/10.1016/J.SCITOTENV.2020.139414

Pehnec, G., Vađić, V., Čačković, M., Žužul, S., and Šilović Hujić, M. (2011). *Trend koncentracija dušikovog dioksida u zraku Zagreba*. 66–67.

Peludna prognoza | NZJZ Andrija Štampar. (n.d.). Retrieved February 21, 2025, from https://www.stampar.hr/hr/peludna-prognoza

Peng, C., Chen, W., Liao, X., Wang, M., Ouyang, Z., Jiao, W., and Bai, Y. (2011). Polycyclic aromatic hydrocarbons in urban soils of Beijing: status, sources, distribution and potential risk. *Environmental Pollution (Barking, Essex : 1987)*, *159*(3), 802–808. https://doi.org/10.1016/J.ENVPOL.2010.11.003

Peng, Z., Zhang, B., Wang, D., Niu, X., Sun, J., Xu, H., Cao, J., and Shen, Z. (2024). Application of machine learning in atmospheric pollution research: A state-of-art review. *Science of The Total Environment*, *910*, 168588. https://doi.org/10.1016/J.SCITOTENV.2023.168588

Pinakana, S. D., Raysoni, A. U., Sayeed, A., Gonzalez, J. L., Temby, O., Wladyka, D., Sepielak, K., and Gupta, P. (2024). Review of agricultural biomass burning and its impact on air quality in the continental United States of America. *Environmental Advances*, *16*, 100546. https://doi.org/10.1016/J.ENVADV.2024.100546

Pinto, T. G., Avanci, L. da S., Renno, A. C. M., Hipolide, D. C., Santos, J. N. dos, Cury, P. R., Dedivitis, R. A., and Ribeiro, D. A. (2025). The Impact of Genetic Polymorphisms on Genotoxicity (DNA Damage) Induced by Cigarette Smoke in Humans: A Systematic Review. In *Journal of Applied Toxicology*. John Wiley and Sons Ltd. https://doi.org/10.1002/jat.4753

Piracha, A., and Chaudhary, M. T. (2022). Urban Air Pollution, Urban Heat Island and Human Health: A Review of the Literature. *Sustainability 2022, Vol. 14, Page 9234*, *14*(15), 9234. https://doi.org/10.3390/SU14159234

Pope, C. A., Burnett, R. T., Thun, M. J., Calle, E. E., Krewski, D., Ito, K., and Thurston, G. D. (2002). Lung Cancer, Cardiopulmonary Mortality, and Long-term Exposure to Fine Particulate Air Pollution. *JAMA*, *287*(9), 1132–1141. https://doi.org/10.1001/JAMA.287.9.1132

Powers, S. K., Deminice, R., Ozdemir, M., Yoshihara, T., Bomkamp, M. P., and Hyatt, H. (2020). Exercise-induced oxidative stress: Friend or foe? *Journal of Sport and Health Science*, *9*(5), 415–425. https://doi.org/10.1016/J.JSHS.2020.04.001

Prunicki, M., Cauwenberghs, N., Lee, J., Zhou, X., Movassagh, H., Noth, E., Lurmann, F., Hammond, S. K., Balmes, J. R., Desai, M., Wu, J. C., and Nadeau, K. C. (2021). Air pollution exposure is linked with methylation of immunoregulatory genes, altered immune cell profiles, and increased blood pressure in children. *Scientific Reports*, *11*(1). https://doi.org/10.1038/s41598-021-83577-3

Pujol, J., Fenoll, R., Macià, D., Martínez-Vilavella, G., Alvarez-Pedrerol, M., Rivas, I., Forns, J., Deus, J., Blanco-Hinojo, L., Querol, X., and Sunyer, J. (2016). Airborne copper exposure in

school environments associated with poorer motor performance and altered basal ganglia. *Brain and Behavior*, *6*(6), 467. https://doi.org/10.1002/BRB3.467

Qian, Z., Meng, Q., Chen, K., Zhang, Z., Liang, H., Yang, H., Huang, X., Zhong, W., Zhang, Y., Wei, Z., Zhang, B., Zhang, K., Chen, M., Zhang, Y., and Ge, X. (2023). Machine Learning Explains Long-Term Trend and Health Risk of Air Pollution during 2015–2022 in a Coastal City in Eastern China. *Toxics 2023, Vol. 11, Page 481*, *11*(6), 481. https://doi.org/10.3390/TOXICS11060481

Qu, F., and Zheng, W. (2024). Cadmium Exposure: Mechanisms and Pathways of Toxicity and Implications for Human Health. *Toxics 2024, Vol. 12, Page 388*, *12*(6), 388. https://doi.org/10.3390/TOXICS12060388

Račić, N., Pehnec, G., Jakovljević, I., Štrukil, Z. S., Mureddu, F., Forsmann, M., and Lovrić, M. (2025). Machine learning analysis of drivers of differences in PAH content between PM1 and PM10 in Zagreb, Croatia. *Atmospheric Pollution Research*, *16*(7), 102541. https://doi.org/10.1016/J.APR.2025.102541

Rasnick, E., Ryan, P. H., Bailer, A. J., Fisher, T., Parsons, P. J., Yolton, K., Newman, N. C., Lanphear, B. P., and Brokamp, C. (2021). Identifying sensitive windows of airborne lead exposure associated with behavioral outcomes at age 12. *Environmental Epidemiology*, *5*(2), E144. https://doi.org/10.1097/EE9.0000000000000144

Rider, C. F., and Carlsten, C. (2019). Air pollution and DNA methylation: Effects of exposure in humans. *Clinical Epigenetics*, *11*(1), 1–15. https://doi.org/10.1186/S13148-019-0713-2/TABLES/1

Robertson, K. D. (2005). DNA methylation and human disease. *Nature Reviews Genetics 2005 6:8*, *6*(8), 597–610. https://doi.org/10.1038/nrg1655

Rodríguez-Carrillo, A., Mustieles, V., Salamanca-Fernández, E., Olivas-Martínez, A., Suárez, B., Bajard, L., Baken, K., Blaha, L., Bonefeld-Jørgensen, E. C., Couderq, S., D'Cruz, S. C., Fini, J. B., Govarts, E., Gundacker, C., Hernández, A. F., Lacasaña, M., Laguzzi, F., Linderman, B., Long, M., … Fernández, M. F. (2023). Implementation of effect biomarkers in human biomonitoring studies: A systematic approach synergizing toxicological and epidemiological knowledge. *International Journal of Hygiene and Environmental Health*, *249*, 114140. https://doi.org/10.1016/J.IJHEH.2023.114140

Rossnerova, A., Spatova, M., Schunck, C., and Sram, R. J. (2011). Automated scoring of lymphocyte micronuclei by the MetaSystems Metafer image cytometry system and its application in studies of human mutagen sensitivity and biodosimetry of genotoxin exposure. In *Mutagenesis* (Vol. 26, Issue 1, pp. 169–175). https://doi.org/10.1093/mutage/geq057

Rousseeuw, P. J. (1987). Silhouettes: a graphical aid to the interpretation and validation of cluster analysis. In *Journal of Computational and Applied Mathematics* (Vol. 20).

Ryu, J. Y., and Hong, D. H. (2024). Association of mixed polycyclic aromatic hydrocarbons exposure with oxidative stress in Korean adults. *Scientific Reports*, *14*(1), 1–10. https://doi.org/10.1038/S41598-024-58263-9;SUBJMETA=172,174,308,4081,478,692,700,704;KWRD=ENVIRONMENTAL+IMPACT,EPIDEMIOLOGY,PUBLIC+HEALTH

Saenen, N. D., Martens, D. S., Neven, K. Y., Alfano, R., Bové, H., Janssen, B. G., Roels, H. A., Plusquin, M., Vrijens, K., and Nawrot, T. S. (2019). Air pollution-induced placental alterations: An interplay of oxidative stress, epigenetics, and the aging phenotype? *Clinical Epigenetics*, *11*(1), 1–14. https://doi.org/10.1186/S13148-019-0688-Z/FIGURES/2

Safieddine, S., Clerbaux, C., George, M., Hadji-Lazaro, J., Hurtmans, D., Coheur, P. F., Wespes, C., Loyola, D., Valks, P., and Hao, N. (2013). Tropospheric ozone and nitrogen dioxide measurements in urban and rural regions as seen by IASI and GOME-2. *Journal of Geophysical Research: Atmospheres*, *118*(18), 10,555-10,566. https://doi.org/10.1002/JGRD.50669

Santos, C. X. C., Anjos, E. I., and Augusto, O. (1999). Uric Acid Oxidation by Peroxynitrite: Multiple Reactions, Free Radical Formation, and Amplification of Lipid Oxidation. *Archives of Biochemistry and Biophysics*, *372*(2), 285–294. https://doi.org/10.1006/ABBI.1999.1491

Santovito, A., and Gendusa, C. (2020). Micronuclei frequency in peripheral blood lymphocytes of healthy subjects living in Turin (North-Italy): contribution of body mass index, age and sex. *Annals of Human Biology*, *47*(1), 48–54. https://doi.org/10.1080/03014460.2020.1714728

Sauvain, J. J., Wild, P., Charreau, T., Jouannique, V., Sakthithasan, K., Debatisse, A., Suárez, G., Hopf, N. B., and Guseva Canu, I. (2025). Are metals in exhaled breath condensate and urine associated with oxidative/nitrosative stress and metabolism-related biomarkers? Results from 303 randomly selected Parisian subway workers. *Environment International*, *196*. https://doi.org/10.1016/j.envint.2025.109325

Scholten, B., Vlaanderen, J., Stierum, R., Portengen, L., Rothman, N., Lan, Q., Pronk, A., and Vermeulen, R. (2020). A quantitative meta-analysis of the relation between occupational benzene exposure and biomarkers of cytogenetic damage. *Environmental Health Perspectives*, *128*(8), 1–7. https://doi.org/10.1289/EHP6404/SUPPL_FILE/EHP6404.S001.ACCO.PDF

Šega, K., and Hršak, J. (1995). Total suspended particulate matter concentrations in Zagreb during the 1975-1993 period. *Arhiv Za Higijenu Rada i Toksikologiju*, *46*(2), 217–224.

Sekar, A., Varghese, G. K., and Ravi Varma, M. K. (2019). Analysis of benzene air quality standards, monitoring methods and concentrations in indoor and outdoor environment. *Heliyon*, *5*(11), e02918. https://doi.org/10.1016/J.HELIYON.2019.E02918

Sekovanić, A., Jurasović, J., Piasek, M., Pašalić, D., Orct, T., Grgec, A. S., Stasenko, S., Čakanić, K. B., and Jazbec, A. (2018). Metallothionein 2A gene polymorphism and trace elements in mother-newborn pairs in the Croatian population. *Journal of Trace Elements in Medicine and Biology*, *45*, 163–170. https://doi.org/10.1016/J.JTEMB.2017.10.011

Serafini, M. M., Maddalon, A., Iulini, M., and Galbiati, V. (2022). Air Pollution: Possible Interaction between the Immune and Nervous System? *International Journal of Environmental Research and Public Health*, *19*(23), 16037. https://doi.org/10.3390/IJERPH192316037

Shangari, N., and O'Brien, P. J. (2006). Catalase Activity Assays. *Current Protocols in Toxicology*, *27*(1), 7.7.1-7.7.16. https://doi.org/10.1002/0471140856.TX0707S27

Shan, H., Li, X., Ouyang, C., Ke, H., Yu, X., Tan, J., Chen, J., Wang, C., Zhang, L., Tang, Y., Yu, L., and Li, W. (2022). Salidroside prevents PM2.5-induced BEAS-2B cell apoptosis via SIRT1-dependent regulation of ROS and mitochondrial function. *Ecotoxicology and Environmental Safety*, *231*, 113170. https://doi.org/10.1016/J.ECOENV.2022.113170

Shukla, S., Srivastava, J. K., Shankar, E., Kanwal, R., Nawab, A., Sharma, H., Bhaskaran, N., Ponsky, L. E., Fu, P., MacLennan, G. T., and Gupta, S. (2020). Oxidative Stress and Antioxidant Status in High-Risk Prostate Cancer Subjects. *Diagnostics 2020, Vol. 10, Page 126*, *10*(3), 126. https://doi.org/10.3390/DIAGNOSTICS10030126

Sies, H., and Jones, D. P. (2020). Reactive oxygen species (ROS) as pleiotropic physiological signalling agents. *Nature Reviews Molecular Cell Biology 2020 21:7*, *21*(7), 363–383. https://doi.org/10.1038/s41580-020-0230-3

Simoni, M., Baldacci, S., Maio, S., Cerrai, S., Sarno, G., and Viegi, G. (2015). Adverse effects of outdoor pollution in the elderly. *Journal of Thoracic Disease*, *7*(1), 34. https://doi.org/10.3978/J.ISSN.2072-1439.2014.12.10

Šišović, A., Pehnec, G., Jakovljević, I., Šilović Hujić, M., Vacrossed D Signić, V., and Bešlić, I. (2012). Polycyclic aromatic hydrocarbons at different crossroads in Zagreb, Croatia. *Bulletin of Environmental Contamination and Toxicology*, *88*(3), 438–442. https://doi.org/10.1007/S00128-011-0516-4

Sommer, S., Buraczewska, I., and Kruszewski, M. (2020). Micronucleus Assay: The State of Art, and Future Directions. *International Journal of Molecular Sciences 2020, Vol. 21, Page 1534*, *21*(4), 1534. https://doi.org/10.3390/IJMS21041534

Song, Y. R., Kim, J. K., Lee, H. S., Kim, S. G., and Choi, E. K. (2020). Serum levels of protein carbonyl, a marker of oxidative stress, are associated with overhydration, sarcopenia and mortality in hemodialysis patients. *BMC Nephrology*, *21*(1), 1–11. https://doi.org/10.1186/S12882-020-01937-Z/TABLES/5

Sopčić, S., Godec, R., Prskalo, H., and Pehnec, G. (2025). Impact of a Summer Wildfire Episode on Air Quality in a Rural Area Near the Adriatic Coast. *Fire 2025, Vol. 8, Page 299*, *8*(8), 299. https://doi.org/10.3390/FIRE8080299

Speer, R. M., Zhou, X., Volk, L. B., Liu, K. J., and Hudson, L. G. (2023). Arsenic and cancer: evidence and mechanisms. *Advances in Pharmacology (San Diego, Calif.), 96*, 151. https://doi.org/10.1016/BS.APHA.2022.08.001

Strimbu, K., and Tavel, J. A. (2010). What are Biomarkers? *Current Opinion in HIV and AIDS*, *5*(6), 463. https://doi.org/10.1097/COH.0B013E32833ED177

Taylor, A. A., Tsuji, J. S., Garry, M. R., McArdle, M. E., Goodfellow, W. L., Adams, W. J., and Menzie, C. A. (2020). Critical Review of Exposure and Effects: Implications for Setting Regulatory Health Criteria for Ingested Copper. *Environmental Management*, *65*(1), 131–159. https://doi.org/10.1007/S00267-019-01234-Y/TABLES/5

Thai, P. K., Banks, A. P. W., Toms, L. M. L., Choi, P. M., Wang, X., Hobson, P., and Mueller, J. F. (2020). Analysis of urinary metabolites of polycyclic aromatic hydrocarbons and cotinine in pooled urine samples to determine the exposure to PAHs in an Australian population. *Environmental Research*, *182*, 109048. https://doi.org/10.1016/J.ENVRES.2019.109048

Thangavel, P., Park, D., and Lee, Y. C. (2022). Recent Insights into Particulate Matter (PM2.5)-Mediated Toxicity in Humans: An Overview. *International Journal of Environmental Research and Public Health 2022, Vol. 19, Page 7511*, *19*(12), 7511. https://doi.org/10.3390/IJERPH19127511

The Index - AQLI. (n.d.). Retrieved June 10, 2025, from https://aqli.epic.uchicago.edu/the-index/

The Third Clean Air Outlook. (n.d.). Retrieved June 26, 2024, from https://europa.eu/eurobarometer/surveys/detail/2660

Thomas, P., Holland, N., Bolognesi, C., Kirsch-Volders, M., Bonassi, S., Zeiger, E., Knasmueller, S., and Fenech, M. (2009). Buccal micronucleus cytome assay. *Nature Protocols 2009 4:6*, *4*(6), 825–837. https://doi.org/10.1038/nprot.2009.53

Tian, X., Cui, K., Sheu, H. L., Hsieh, Y. K., and Yu, F. (2021). Effects of Rain and Snow on the Air Quality Index, PM2.5 Levels, and Dry Deposition Flux of PCDD/Fs. *Aerosol and Air Quality Research*, *21*(8), 210158. https://doi.org/10.4209/AAQR.210158

Tong, R., Yang, X., Su, H., Pan, Y., Zhang, Q., Wang, J., and Long, M. (2018). Levels, sources and probabilistic health risks of polycyclic aromatic hydrocarbons in the agricultural soils from sites neighboring suburban industries in Shanghai. *Science of The Total Environment*, *616–617*, 1365–1373. https://doi.org/10.1016/J.SCITOTENV.2017.10.179

Torrens-Mas, M., Pons, D. G., Sastre-Serra, J., Oliver, J., and Roca, P. (2020). Sexual hormones regulate the redox status and mitochondrial function in the brain. Pathological implications. *Redox Biology*, *31*, 101505. https://doi.org/10.1016/J.REDOX.2020.101505

Tuazon, J. A., Kilburg-Basnyat, B., Oldfield, L. M., Wiscovitch-Russo, R., Dunigan-Russell, K., Fedulov, A. V., Oestreich, K. J., and Gowdy, K. M. (2022). Emerging Insights into the Impact of Air Pollution on Immune-Mediated Asthma Pathogenesis. *Current Allergy and Asthma Reports*, *22*(7), 77. https://doi.org/10.1007/S11882-022-01034-1

Turner, M. C., Andersen, Z. J., Baccarelli, A., Diver, W. R., Gapstur, S. M., C. Arden Pope, I., Prada, D., Samet, J., Thurston, G., and Cohen, A. (2020). Outdoor Air Pollution and Cancer: An Overview of the Current Evidence and Public Health Recommendations. *CA: A Cancer Journal for Clinicians*, *70*(6), 460–479. https://doi.org/10.3322/CAAC.21632

Turner, M. C., Jerrett, M., Pope, C. A., Krewski, D., Gapstur, S. M., Diver, W. R., Beckerman, B. S., Marshall, J. D., Su, J., Crouse, D. L., and Burnett, R. T. (2016). Long-Term Ozone Exposure and Mortality in a Large Prospective Study. *American Journal of Respiratory and Critical Care Medicine*, *193*(10), 1134–1142. https://doi.org/10.1164/rccm.201508-1633OC

Tyutereva, E. V., Strizhenok, A. D., Kiseleva, E. I., and Voitsekhovskaja, O. V. (2024). Comet Assay: Multifaceted Options for Studies of Plant Stress Response. *Horticulturae*, *10*(2), 174. https://doi.org/10.3390/HORTICULTURAE10020174/S1

Uffelmann, E., Huang, Q. Q., Munung, N. S., de Vries, J., Okada, Y., Martin, A. R., Martin, H. C., Lappalainen, T., and Posthuma, D. (2021). Genome-wide association studies. *Nature Reviews Methods Primers 2021 1:1*, *1*(1), 1–21. https://doi.org/10.1038/s43586-021-00056-9

Union, P. O. of the E. (2021). *European Green Deal : research & innovation call.* https://doi.org/10.2777/33415

Ural, B. B., Caron, D. P., Dogra, P., Wells, S. B., Szabo, P. A., Granot, T., Senda, T., Poon, M. M. L., Lam, N., Thapa, P., Lee, Y. S., Kubota, M., Matsumoto, R., and Farber, D. L. (2022). Inhaled particulate accumulation with age impairs immune function and architecture in human lung lymph nodes. *Nature Medicine 2022 28:12*, *28*(12), 2622–2632. https://doi.org/10.1038/s41591-022-02073-x

Vađić, V., Žužul, S., Rinkovec, J., and Pehnec, G. (2013). METALI U SITNIM ČESTICAMA U ZRAKU ZAGREBA. *Sigurnost : Časopis Za Sigurnost u Radnoj i Životnoj Okolini*, *55*(1), 1–8.

Vadjić, V., Hršak, J., and Žužul, S. (2009). Trends of lead in suspended particulate matter in Zagreb air. *International Journal of Environment and Pollution*, *39*(3–4), 385–391. https://doi.org/10.1504/IJEP.2009.028699;PAGE:STRING:ARTICLE/CHAPTER

Valavanidis, A., Vlachogianni, T., and Fiotakis, C. (2009). 8-hydroxy-2’ -deoxyguanosine (8-OHdG): A critical biomarker of oxidative stress and carcinogenesis. *Journal of Environmental Science and Health. Part C, Environmental Carcinogenesis & Ecotoxicology Reviews*, *27*(2), 120–139. https://doi.org/10.1080/10590500902885684

Van Gestel, C. A. M., and Van Brummelen, T. C. (1996). Incorporation of the biomarker concept in ecotoxicology calls for a redefinition of terms. *Ecotoxicology (London, England)*, *5*(4), 217–225. https://doi.org/10.1007/BF00118992

Venkatesan, S., Zare, A., and Stevanovic, S. (2024). Pollen and sub-pollen particles: External interactions shaping the allergic potential of pollen. *Science of The Total Environment*, *926*, 171593. https://doi.org/10.1016/J.SCITOTENV.2024.171593

Vidaček, N. Š., Nanić, L., Ravlić, S., Sopta, M., Gerić, M., Gajski, G., Garaj-Vrhovac, V., and Rubelj, I. (2018). Telomeres, Nutrition, and Longevity: Can We Really Navigate Our Aging? *The Journals of Gerontology: Series A*, *73*(1), 39–47. https://doi.org/10.1093/GERONA/GLX082

Viegas, S., Ladeira, C., Costa-Veiga, A., Perelman, J., and Gajski, G. (2017). Forgotten public health impacts of cancer – An overview. In *Arhiv za Higijenu Rada i Toksikologiju* (Vol. 68, Issue 4, pp. 287–297). Institute for Medical Research and Occupational Health. https://doi.org/10.1515/aiht-2017-68-3005

Vujčić Bok, V., Gerić, M., Gajski, G., Gagić, S., and Domijan, A. M. (2023). Phytotoxicity of Bisphenol A to Allium cepa Root Cells Is Mediated through Growth Hormone Gibberellic Acid and Reactive Oxygen Species. *Molecules*, *28*(5), 2046. https://doi.org/10.3390/MOLECULES28052046/S1

Wang, J., Gao, J., Che, F., Yang, X., Yang, Y., Liu, L., Xiang, Y., and Li, H. (2023a). Summertime response of ozone and fine particulate matter to mixing layer meteorology over the North China Plain. *Atmospheric Chemistry and Physics*, *23*(23), 14715–14733. https://doi.org/10.5194/ACP-23-14715-2023

Wang, J., Lin, C., Chu, Y., Deng, H., and Shen, Z. (2023b). Association between long-term exposure to air pollution and the risk of incident laryngeal cancer: a longitudinal UK Biobank-based study. *Environmental Science and Pollution Research International*, *30*(20), 58295. https://doi.org/10.1007/S11356-023-26519-Y

Wang, R., Cui, K., Sheu, H. L., Wang, L. C., and Liu, X. (2023c). Effects of Precipitation on the Air Quality Index, PM2.5 Levels and on the Dry Deposition of PCDD/Fs in the Ambient Air. *Aerosol and Air Quality Research*, *23*(4), 220417. https://doi.org/10.4209/AAQR.220417

Wang, T., and Zang, R. (2023). Metabolism: A Determinant of Toxicity. In A. W. Hayes and T. Kobets (Eds.), *Hayes' Principles and Methods of Toxicology: Volume I, Seventh Edition* (Vol. 1, pp. 143–209). CRC Press. https://doi.org/10.1201/9781003390008-5/TOXICOKINETICS-HAYES-WALLACE-KOBETS-TETYANA

Wang, Y., Guo, Z., and Han, J. (2021a). The relationship between urban heat island and air pollutants and them with influencing factors in the Yangtze River Delta, China. *Ecological Indicators*, *129*, 107976. https://doi.org/10.1016/J.ECOLIND.2021.107976

Wang, Y., Huang, Y., and Li, C. (2023d). The Effects of Air Pollutants on Mortality in the Elderly at Different Ages: A Case of the Prefecture with Most Serious Aging in China. *Sustainability 2023, Vol. 15, Page 15821*, *15*(22), 15821. https://doi.org/10.3390/SU152215821

Wang, Y., Wang, T., Xu, M., Yu, H., Ding, C., Wang, Z., Pan, X., Li, Y., Niu, Y., Yan, R., Song, J., Yan, H., Dai, Y., Sun, Z., Su, W., and Duan, H. (2020). Independent effect of main components in particulate matter on DNA methylation and DNA methyltransferase: A

molecular epidemiology study. *Environment International*, *134*, 105296. https://doi.org/10.1016/J.ENVINT.2019.105296

Wang, Y., Zhong, Y., Liao, J., and Wang, G. (2021b). PM2.5-related cell death patterns. *International Journal of Medical Sciences*, *18*(4), 1024–1029. https://doi.org/10.7150/IJMS.46421

Wan, W., Peters, S., Portengen, L., Olsson, A., Schüz, J., Ahrens, W., Schejbalova, M., Boffetta, P., Behrens, T., Brüning, T., Kendzia, B., Consonni, D., Demers, P. A., Fabiánová, E., Fernández-Tardón, G., Field, J. K., Forastiere, F., Foretova, L., Guénel, P., … Vermeulen, R. (2024). Occupational Benzene Exposure and Lung Cancer Risk: A Pooled Analysis of 14 Case-Control Studies. *American Journal of Respiratory and Critical Care Medicine*, *209*(2), 185–196. https://doi.org/10.1164/RCCM.202306-0942OC/SUPPL_FILE/DISCLOSURES.PDF

Wecker, H., Tizek, L., Ziehfreund, S., Kain, A., Traidl-Hoffmann, C., Zimmermann, G. S., Scala, E., Elberling, J., Doll, A., Boffa, M. J., Schmidt, L., Sikora, M., Torres, T., Ballardini, N., Chernyshov, P. V., Buters, J., Biedermann, T., and Zink, A. (2023). Impact of asthma in Europe: A comparison of web search data in 21 European countries. *The World Allergy Organization Journal*, *16*(8), 100805. https://doi.org/10.1016/J.WAOJOU.2023.100805

Wen, J., Zhang, J., Zhang, H., Zhang, N., Lei, R., Deng, Y., Cheng, Q., Li, H., and Luo, P. (2024). Large-scale genome-wide association studies reveal the genetic causal etiology between air pollutants and autoimmune diseases. *Journal of Translational Medicine*, *22*(1), 392. https://doi.org/10.1186/S12967-024-04928-Y

What is Particle Pollution? | US EPA. (n.d.). Retrieved February 19, 2025, from https://www.epa.gov/pmcourse/what-particle-pollution

WHO. (2021). *Global air quality guidelines: Particulate matter (PM2.5 and PM10), ozone, nitrogen dioxide, sulfur dioxide and carbon monoxide*. https://www.who.int/publications/i/item/9789240034228

WHO, and IPCS. (2001). *Biomarkers in risk assessment : validity and validation.* https://iris.who.int/handle/10665/42363

Wild, C. P. (2025). The exposome at twenty: a personal account. *Exposome*, *5*(1). https://doi.org/10.1093/exposome/osaf003

Wiseman, C. L. S., Levesque, C., and Rasmussen, P. E. (2021). Characterizing the sources, concentrations and resuspension potential of metals and metalloids in the thoracic fraction of urban road dust. *Science of The Total Environment*, *786*, 147467. https://doi.org/10.1016/J.SCITOTENV.2021.147467

Wu, Y., Qie, R., Cheng, M., Zeng, Y., Huang, S., Guo, C., Zhou, Q., Li, Q., Tian, G., Han, M., Zhang, Y., Wu, X., Li, Y., Zhao, Y., Yang, X., Feng, Y., Liu, D., Qin, P., Hu, D., … Zhang, M. (2021). Air pollution and DNA methylation in adults: A systematic review and meta-

analysis of observational studies. *Environmental Pollution*, *284*, 117152. https://doi.org/10.1016/J.ENVPOL.2021.117152

Xie, J., Sun, T., Liu, C., Li, L., Xu, X., Miao, S., Lin, L., Chen, Y., and Fan, S. (2022). Quantitative evaluation of impacts of the steadiness and duration of urban surface wind patterns on air quality. *Science of The Total Environment*, *850*, 157957. https://doi.org/10.1016/J.SCITOTENV.2022.157957

Xue, W., and Warshawsky, D. (2005). Metabolic activation of polycyclic and heterocyclic aromatic hydrocarbons and DNA damage: A review. *Toxicology and Applied Pharmacology*, *206*(1), 73–93. https://doi.org/10.1016/J.TAAP.2004.11.006

Yan, F., Li, K., Xing, W., Dong, M., Yi, M., and Zhang, H. (2022). Role of Iron-Related Oxidative Stress and Mitochondrial Dysfunction in Cardiovascular Diseases. *Oxidative Medicine and Cellular Longevity*, *2022*. https://doi.org/10.1155/2022/5124553

Yang, Z., Guo, C., Li, Q., Zhong, Y., Ma, S., Zhou, J., Li, X., Huang, R., and Yu, Y. (2021). Human health risks estimations from polycyclic aromatic hydrocarbons in serum and their hydroxylated metabolites in paired urine samples. *Environmental Pollution*, *290*, 117975. https://doi.org/10.1016/J.ENVPOL.2021.117975

Yuan, L., Tao, J., Wang, J., She, W., Zou, Y., Li, R., Ma, Y., Sun, C., Bi, S., Wei, S., Chen, H., Guo, X., Tian, H., Xu, J., Dong, Y., Ma, Y., Sun, H., Lv, W., Shang, Z., … Zhang, M. (2025). Global, regional, national burden of asthma from 1990 to 2021, with projections of incidence to 2050: a systematic analysis of the global burden of disease study 2021. *EClinicalMedicine*, *80*. https://doi.org/10.1016/J.ECLINM.2024.103051

Zani, C., Donato, F., Ceretti, E., Pedrazzani, R., Zerbini, I., Gelatti, U., and Feretti, D. (2021). Genotoxic Activity of Particulate Matter and In Vivo Tests in Children Exposed to Air Pollution. *International Journal of Environmental Research and Public Health*, *18*(10), 5345. https://doi.org/10.3390/IJERPH18105345

Zare Jeddi, M., Hopf, N. B., Louro, H., Viegas, S., Galea, K. S., Pasanen-Kase, R., Santonen, T., Mustieles, V., Fernandez, M. F., Verhagen, H., Bopp, S. K., Antignac, J. P., David, A., Mol, H., Barouki, R., Audouze, K., Duca, R. C., Fantke, P., Scheepers, P., … Bessems, J. (2022). Developing human biomonitoring as a 21st century toolbox within the European exposure science strategy 2020–2030. *Environment International*, *168*, 107476. https://doi.org/10.1016/J.ENVINT.2022.107476

Zare Jeddi, M., Hopf, N. B., Viegas, S., Price, A. B., Paini, A., van Thriel, C., Benfenati, E., Ndaw, S., Bessems, J., Behnisch, P. A., Leng, G., Duca, R. C., Verhagen, H., Cubadda, F., Brennan, L., Ali, I., David, A., Mustieles, V., Fernandez, M. F., … Pasanen-Kase, R. (2021a). Towards a systematic use of effect biomarkers in population and occupational biomonitoring. *Environment International*, *146*, 106257. https://doi.org/10.1016/J.ENVINT.2020.106257

Zare Jeddi, M., Virgolino, A., Fantke, P., Hopf, N. B., Galea, K. S., Remy, S., Viegas, S., Mustieles, V., Fernandez, M. F., von Goetz, N., Vicente, J. L., Slobodnik, J., Rambaud, L., Denys, S., St-Amand, A., Nakayama, S. F., Santonen, T., Barouki, R., Pasanen-Kase, R., … Bessems, J. (2021b). A human biomonitoring (HBM) Global Registry Framework: Further advancement of HBM research following the FAIR principles. *International Journal of Hygiene and Environmental Health*, *238*, 113826. https://doi.org/10.1016/J.IJHEH.2021.113826

Zhang, J. J., Wei, Y., and Fang, Z. (2019). Ozone Pollution: A Major Health Hazard Worldwide. *Frontiers in Immunology*, *10*(OCT), 2518. https://doi.org/10.3389/FIMMU.2019.02518

Zhang, J., Zou, Y., Chen, L., Xu, Q., Wang, Y., Xie, M., Liu, X., Zhao, J., and Wang, C. Y. (2022). Regulatory T Cells, a Viable Target Against Airway Allergic Inflammatory Responses in Asthma. *Frontiers in Immunology*, *13*, 902318. https://doi.org/10.3389/FIMMU.2022.902318/XML/NLM

Zhang, X., Yang, L., Zhang, H., Xing, W., Wang, Y., Bai, P., Zhang, L., Hayakawa, K., Toriba, A., Wei, Y., and Tang, N. (2021a). Assessing Approaches of Human Inhalation Exposure to Polycyclic Aromatic Hydrocarbons: A Review. *International Journal of Environmental Research and Public Health 2021, Vol. 18, Page 3124*, *18*(6), 3124. https://doi.org/10.3390/IJERPH18063124

Zhang, Y., Eckel, S. P., Berhane, K., Garcia, E., Muchmore, P., Molshatzki, N. B. A., Rappaport, E. B., Linn, W. S., Habre, R., and Gilliland, F. D. (2021b). Long-term exposures to air pollutants affect FeNO in children: a longitudinal study. *European Respiratory Journal*, *58*(5). https://doi.org/10.1183/13993003.00705-2021

Zhang, Y., and Steiner, A. L. (2022). Projected climate-driven changes in pollen emission season length and magnitude over the continental United States. *Nature Communications 2022 13:1*, *13*(1), 1–10. https://doi.org/10.1038/s41467-022-28764-0

Zheng, K., Zeng, Z., Tian, Q., Huang, J., Zhong, Q., and Huo, X. (2023). Epidemiological evidence for the effect of environmental heavy metal exposure on the immune system in children. *Science of The Total Environment*, *868*, 161691. https://doi.org/10.1016/J.SCITOTENV.2023.161691

Zhou, X., Speer, R. M., Volk, L., Hudson, L. G., and Liu, K. J. (2021). Arsenic co-carcinogenesis: Inhibition of DNA repair and interaction with zinc finger proteins. *Seminars in Cancer Biology*, *76*, 86–98. https://doi.org/10.1016/J.SEMCANCER.2021.05.009

Zhou, Y., Wang, K., Wang, B., Pu, Y., and Zhang, J. (2020). Occupational benzene exposure and the risk of genetic damage: A systematic review and meta-analysis. *BMC Public Health*, *20*(1), 1–11. https://doi.org/10.1186/S12889-020-09215-1/TABLES/4

Zhu, G., Wen, Y., Cao, K., He, S., and Wang, T. (2024). A review of common statistical methods for dealing with multiple pollutant mixtures and multiple exposures. In *Frontiers in Public Health* (Vol. 12). Frontiers Media SA. https://doi.org/10.3389/fpubh.2024.1377685

Zhu, H., Martinez-Moral, M. P., and Kannan, K. (2021). Variability in urinary biomarkers of human exposure to polycyclic aromatic hydrocarbons and its association with oxidative stress. *Environment International*, *156*, 106720. https://doi.org/10.1016/J.ENVINT.2021.106720

Ziernicka-Wojtaszek, A., Zuśka, Z., and Kopcińska, J. (2024). Assessment of the Effect of Meteorological Conditions on the Concentration of Suspended PM2.5 Particulate Matter in Central Europe. *Sustainability (Switzerland) , 16*(11). https://doi.org/10.3390/su16114797

How air pollution affects our health | European Environment Agency's home page. (n.d.). Retrieved February 21, 2025, from https://www.eea.europa.eu/en/topics/in-depth/air-pollution/eow-it-affects-our-health

8. APPENDIX

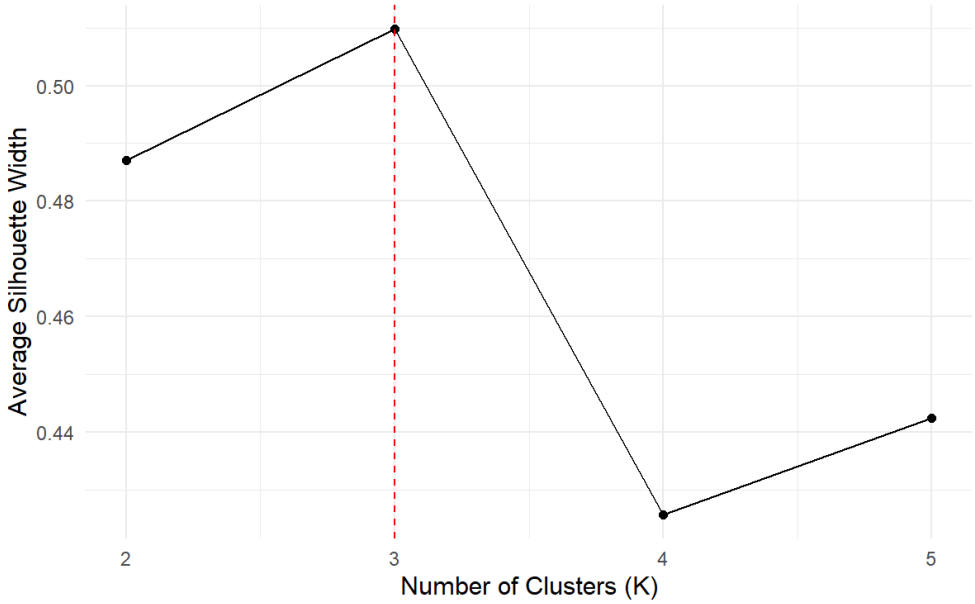

Supplementary Figure 1. Silhouette width across different cluster solutions for one-day average exposure variables. The plot displays average silhouette widths for cluster solutions ranging from 2 to 5 clusters. The maximum silhouette value indicates the optimal number of clusters (in this case, k =3), suggesting the most coherent grouping of variables. Higher silhouette values reflect greater intra-cluster similarity and inter-cluster dissimilarity.

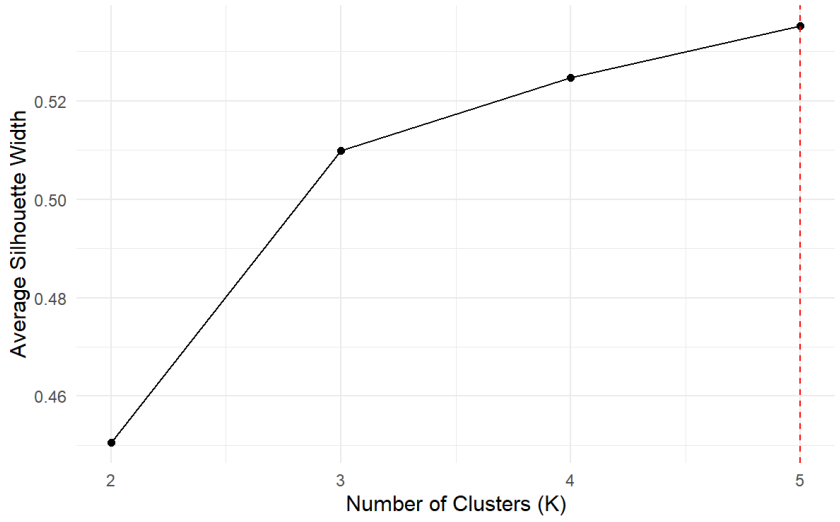

Supplementary Figure 2. Silhouette width across different cluster solutions for three-day average exposure variables. The plot displays average silhouette widths for cluster solutions ranging from 2 to 5 clusters. The maximum silhouette value indicates the optimal number of clusters (in this case, k =5), suggesting the most coherent grouping of variables. Higher silhouette values reflect greater intra-cluster similarity and inter-cluster dissimilarity.

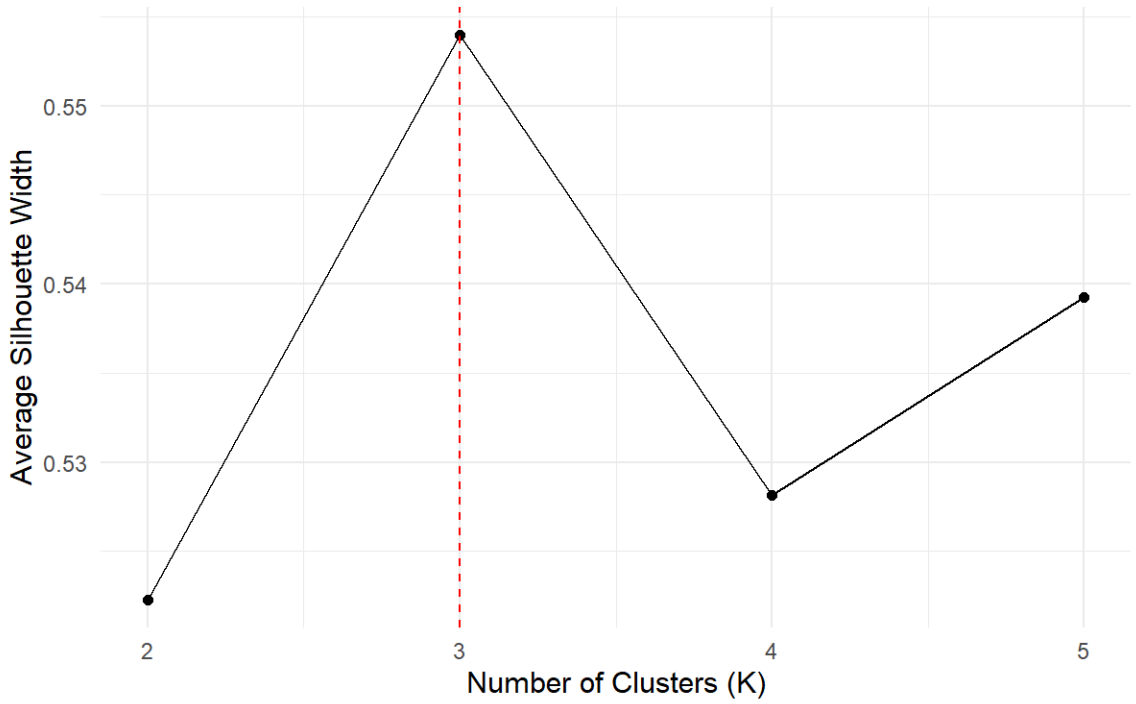

Supplementary Figure 3. Silhouette width across different cluster solutions for seven-day average exposure variables. The plot displays average silhouette widths for cluster solutions ranging from 2 to 5 clusters. The maximum silhouette value indicates the optimal number of clusters (in this case, k =3), suggesting the most coherent grouping of variables. Higher silhouette values reflect greater intra-cluster similarity and inter-cluster dissimilarity.

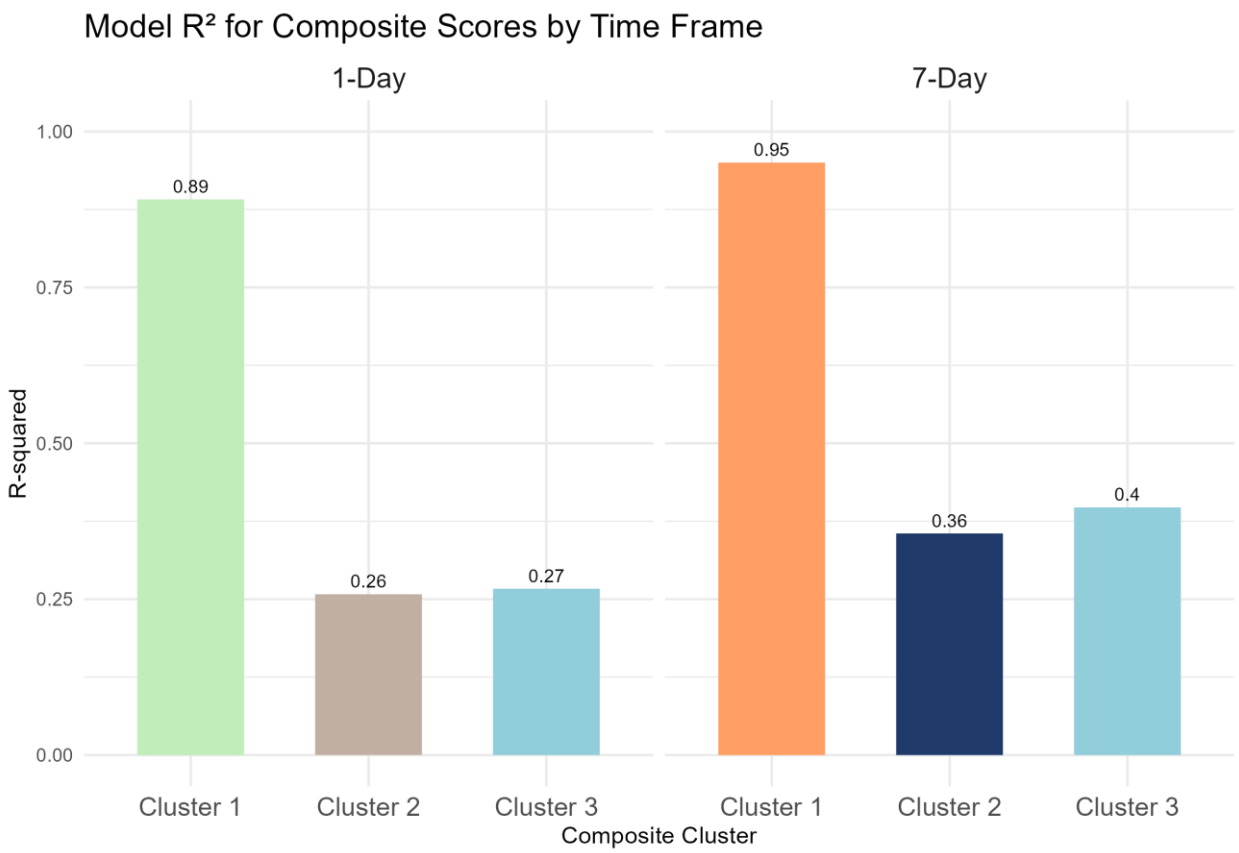

Supplementary Figure 4. Explained variance (R^2) of linear models predicting composite exposure clusters based on meteorological variables, stratified by time frame (one-day and seven-day averages). Each bar represents the proportion of variance in a cluster-specific composite score accounted for by temperature, pressure, humidity, wind, and UVB radiation. Cluster 1 shows consistently high predictive accuracy in both time frames, particularly in the seven-day model (R^2 = 0.95), while Clusters 2 and 3 show modest explanatory power. The stronger performance for Cluster 1 suggests that its underlying variables are more directly or consistently influenced by short- and mid-term meteorological conditions.

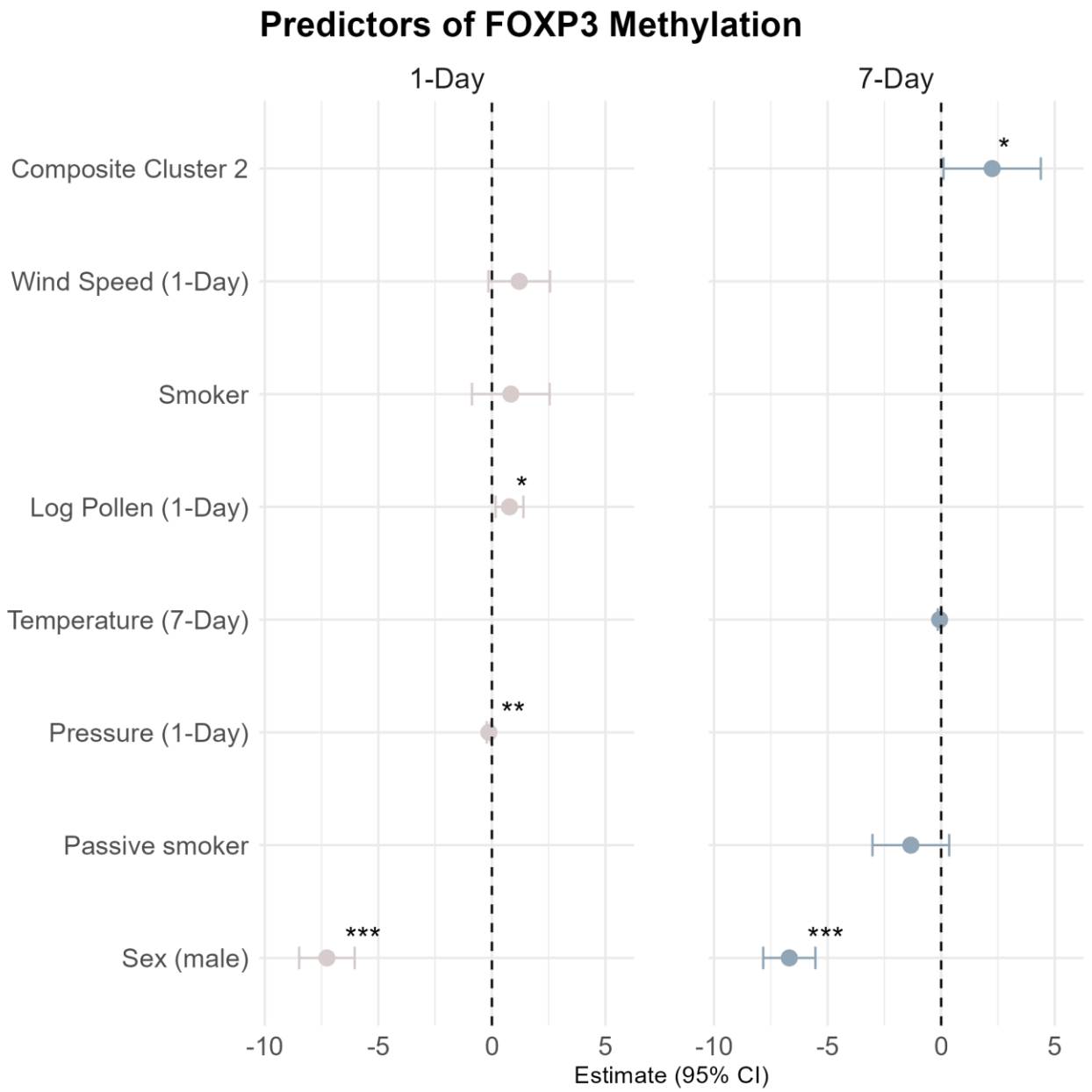

Supplementary Figure 5. Forest plot of predictors selected by best subset regression for FOXP3 gene methylation. The figure shows the estimated regression coefficients and 95% confidence intervals for variables retained in the best subset linear models predicting FOXP3 methylation, separately for the one-day and seven-day exposure windows. The one-day model included log-transformed pollen, sex, smoking status, atmospheric pressure, and wind speed as significant predictors. The seven-day model retained sex, passive smoking status, ambient temperature, and Composite Cluster 2. Effect sizes are displayed on the x-axis, stratified by time frame. Significant predictors are marked with * ($p < 0.05$), ** ($p < 0.01$), *** ($p < 0.001$).

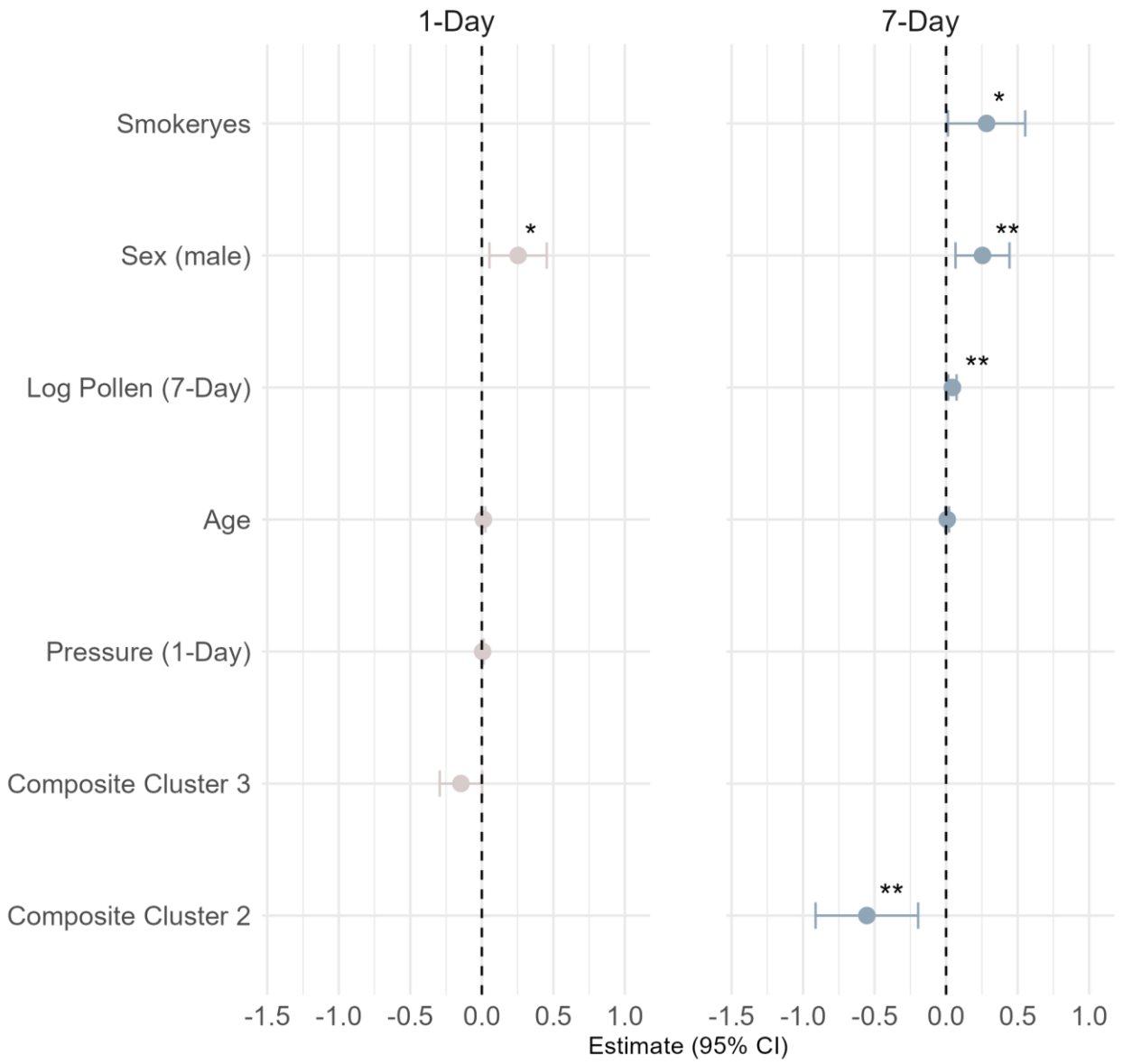

Supplementary Figure 6. Forest plot of predictors selected by best subset regression for log-transformed FeNO. This figure summarizes the results of best subset regression models identifying predictors of log-transformed FeNO levels. For the one-day exposure frame, the model included Composite Cluster 3, sex, age, and pressure. For the seven-day frame, the best-fitting model retained Composite Cluster 2, log-transformed pollen, sex, smoking status, and age. Coefficient estimates and 95% confidence intervals are shown. Significant predictors are marked with * ($p < 0.05$), ** ($p < 0.01$), *** ($p < 0.001$).

9. *CURRICULUM VITAE*

Katarina Matković, mag. biol. mol. has been employed at the Institute for Medical Research and Occupational Health since 2021 as a doctoral student in the field of genetic and environmental toxicology. Her academic training was completed at the Faculty of Science, University of Zagreb, where a bachelor's and master's degree in Molecular Biology were obtained, followed by enrollment in the doctoral program in Biology in 2021. A multidisciplinary research focus has been maintained on air pollution, genotoxicity, and human biomonitoring, with an emphasis on cytogenetic biomarkers.

Active contributions have been made to multiple national and European projects, including the Croatian Science Foundation-funded project *Air Pollution and Human Biomarkers of Effect* (HUMNap), and the Horizon Europe project *Evidence driven indoor air quality improvement* (EDIAQI). A project funded by the Croatian Academy of Sciences and Arts titled *Statistical tools for evaluating the impact of air pollution on cytogenotoxicity in human cells in vitro* was independently led as principal investigator and successfully completed. Multiple projects and doctoral research findings have been disseminated at over ten international and national conferences, including invited lecture at the 11th International Congress of the Turkish Society of Toxicology held in Antalya, Turkey.

Scientific productivity has been demonstrated through the authorship of peer-reviewed publications in international journals covering toxicology, environmental health, and molecular epidemiology, resulting in a Scopus *h*-index of 5. Recognition of scientific excellence has been received in the form of competitive travel grants from EEMGS, EUROTOX, and HGD. Technical proficiency has been developed in statistical programming, programming languages (R, C++), and bioanalytical techniques used in molecular toxicology. Professional engagement has also extended to science outreach, where mentorship has been provided in educational programs for primary school students.

Scientific Publications (Peer-Reviewed Journals)

1. **Matković, K.**, Jurič, A., Jakovljević, I., Kazensky, L., Milić, M., Kašuba, V., Davila, S., Pehnec, G., Brčić Karačonji, I., Cvitković, A., et al. Evaluating air pollution and BTEX exposure effects on DNA damage: A human biomonitoring study in Zagreb, Croatia. *Atmospheric Environment*, 343 (2025), 121004.

2. Kazensky, L., **Matković, K**., Gerić, M., Žegura, B., Pehnec, G., Gajski, G. Impact of indoor air pollution on DNA damage and chromosome stability: a systematic review. *Archives of Toxicology*, 98 (2024), 9, 2817–2841.

3. **Matković, K.**, Gerić, M., Kazensky, L., Milić, M., Kašuba, V., Cvitković, A., Sanković, M., Šumanovac, A., Møller, P., Gajski, G. Comparison of DNA damage in fresh and frozen blood samples: implications for the comet assay in human biomonitoring studies. *Archives of Toxicology*, 98 (2024), 9.

4. Gerić, M., Pehnec, G., **Matković, K.**, et al. Air Pollution and Primary DNA Damage among Zagreb (Croatia) Residents: A Cross-Sectional Study. *Journal of Xenobiotics*, 14 (2024), 1, 368–379.

5. Gajski, G., Kašuba, V., Milić, M., Gerić, M., **Matković, K.**, et al. Exploring cytokinesis block micronucleus assay in Croatia: A journey through the past, present, and future in biomonitoring of the general population. *Mutation Research*, 895 (2024), 503749.

6. Gajski, G., **Matković, K.**, et al. Evaluation of Primary DNA Damage in Young Healthy Females Based on Their Dietary Preferences. *Nutrients*, 15 (2023), 9, 2218.

7. Milić, M., **Matković, K.**, et al. Combined Approach: FFQ, DII, Anthropometric, Biochemical and DNA Damage Parameters in Obese with BMI ≥ 35kg/m². *Nutrients*, 15 (2023), 4, 899.

8. Gajski, G., Gerić, M., Pehnec, G., **Matković, K.**, et al. Associating Air Pollution with Cytokinesis-Block Micronucleus Assay Parameters in Lymphocytes of the General Population in Zagreb (Croatia). *International Journal of Molecular Sciences*, 23 (2022), 17, 10083.

9. Gerić, M., **Matković, K.**, et al. Adherence to Mediterranean Diet in Croatia: Lessons Learned Today for a Brighter Tomorrow. *Nutrients*, 14 (2022), 18, 3725.
10. Smodlaka Tanković, M., **Matković, K.**, et al. Characterisation and toxicological activity of three different *Pseudo-nitzschia* species from the northern Adriatic Sea (Croatia). *Environmental Research*, 214 (2022), 114108.
11. Lovrić, M., Gajski, G., Fernández-Agüera, J., Pöhlker, M., Gursch, H., The EDIAQI Consortium including **Matković, K.**, et al. Evidence-driven indoor air quality improvement: An innovative and interdisciplinary approach to improving indoor air quality. *Biofactors*, (2025).

Conference Abstracts (Active Participation)

1. **Matković, K.**, Kazensky, L., Rinkovec, J., Šišková, A., Jakovljević, I., Pehnec, G., Vodenková, S., Gajski, G., Gerić, M. *In vitro effect of airborne PAHs and metal mixture on viability and DNA damage in human peripheral blood cells.* Comfort At The Extremes, Sevilla, Spain, 2024.
2. **Matković, K.**, Jurič, A., Jakovljević, I., Kazensky, L., Kašuba, V., Milić, M., Davila, S., Pehnec, G., Brčić Karačonji, I., Hopf, N. B., et al. *Predictive modelling of genotoxicity biomarkers in response to air pollution exposure across seasons.* Arhiv za higijenu rada i toksikologiju, 75(Suppl. 1), 2024: 158.
3. **Matković, K.**, Delić, L., Jurič, A., Davila, S., Milić, M., Jakovljević, I., Kašuba, V., Pehnec, G., Hopf, N. B., Guseva Canu, I., et al. *Machine learning in predicting genotoxicity biomarkers based on the exposure to air pollutants in colder and warmer periods in the general population of Zagreb (Croatia).* Toxicology Letters, 384S1, 2023: S107.
4. **Matković, K.**, Jurič, A., Jakovljević, I., Davila, S., Milić, M., Kašuba, V., Pehnec, G., Brčić Karačonji, I., Gajski, G., Gerić, M. *The impact of different exposure time frames on the comet assay descriptors: A case of air pollution.* 13th Congress of the Serbian Society of Toxicology & 1st TOXSEE Regional Conference, 2023: 141–142.

5. **Matković, K.**, Delić, L., Jurič, A., Jakovljević, I., Davila, S., Milić, M., Kašuba, V., Pehnec, G., Brčić Karačonji, I., Gajski, G., Gerić, M. *Impact of air pollution on biomarkers of exposure and effect: human biomonitoring in city of Zagreb.* 4th International ZORH Conference, Split, 2023: 23.

6. **Matković, K.**, Jurič, A., Jakovljević, I., Davila, S., Milić, M., Kašuba, V., Pehnec, G., Brčić Karačonji, I., Gajski, G., Gerić, M. *Monitoring Air Pollution and The Health-Related Biomarkers: Lessons from HUMNap.* 11th International Congress of the Turkish Society of Toxicology, 2022: 9.

7. **Matković, K.**, Jurič, A., Jakovljević, I., Davila, S., Milić, M., Kašuba, V., Pehnec, G., Brčić Karačonji, I., Gajski, G., Gerić, M. *Does air pollution have an impact on our DNA? Measuring DNA damage by the comet assay and BTEX exposure in human blood cells.* ICAW & EEMGS Meeting, Maastricht, 2022: 26.